

ADDIS ABABA UNIVERSITY
ADDIS ABABA INSTITUTE OF TECHNOLOGY
SCHOOL OF CIVIL AND ENVIRONMENTAL ENGINEERING
GEOTECHNICAL ENGINEERING CHAIR



Site specific Ground Response Analysis at South - Western part
of Addis Ababa

By

Birkit Solomon

A Thesis Submitted to the School of Graduate studies of Addis Ababa
Institute of Technology in Partial Fulfillment of the Requirements for the
Degree of Master of Science in Civil Engineering (Geotechnical
Engineering).

Advisor

Dr. Tensay Gebremedhin

Addis Ababa, Ethiopia

December, 2024

The under signed have examined the thesis entitled “ **Site specific Ground Response Analysis at South - Western part of Addis Ababa**” prepared by **Birkit Solomon**, a candidate for the degree of Master of Science in geotechnical engineering and hereby certify that it is worthy acceptance.

Dr. Tensay Gebremedhin	_____	_____
Advisor Name	Signature	Date
_____	_____	_____
Internal Examiner	Signature	Date
_____	_____	_____
External Examiner	Signature	Date
_____	_____	_____
Chair person	Signature	Date

UNDERTAKING

I certify that I am the original writer of the research named " Site specific Ground Response Analysis at South - Western part of Addis Ababa." The work hasn't been submitted for assessment elsewhere else. Where material has been used from other sources, it has been properly referred.

Birkit Solomon

ACKNOWLEDGMENT

Above all, I am thankful to Saint Michael for supporting me during my life. I've seen his help to be quite valuable.

I would like to extend my heartfelt gratitude to Dr. Tensay Gebremedhin, for his unwavering support and guidance throughout my research. His insightful advice, constant encouragement, and expert knowledge have been vital in the successful completion of this work. I am deeply thankful for his mentorship and the invaluable contributions he has made to this study.

I would also like to express my gratitude to Prof. Atalay Ayele, who is the Director of Addis Ababa University's Institute of Geophysics Space Science and Astronomy (IGSSA), for agreeing to assist me with the field investigation. His assistance and crucial contributions to this study are greatly valued.

I would also like to thank the following consulting companies that provided me with all the necessary geotechnical data: ARCON Design Build PLC (Yared Tilahun, your support throughout the research is invaluable), Tracon Trading PLC, DMC real estate, AL EHWAN real estate, Limay real estate, SABA Engineering PLC, JDAW Consulting Architects & Engineers PLC, Ethiopian Construction Design and Supervision Works Corporation, JEROCCIA Geotechnical Services and Engineering PLC, BEST Consulting Engineers PLC, TURAB Geotechnical Engineering, and ADDIS GEOSYSTEMS PLC.

Last but not least, I would like to express my gratitude to my family, Kirubel Solomon, Genet Bekele, and Solomon Mamo, as well as to my friends Surafel Teferi, Bethemariam Getu, and Rediet Lemma. I also want to thank everyone else who supported me during this study but whose names I did not mention. Throughout the study, you really were my inspiration and support. I really want to thank you a lot.

ABSTRACT

Ethiopia's capital, Addis Ababa, is situated near the edge of the Ethiopian Rift System, an area with moderate seismic activity. The city is vulnerable to earthquakes due to its geographic location. Because the characteristics of soil affect seismic wave propagation, amplification and attenuation, studying site effect is crucial for earthquake investigations in a particular location. For this purpose, a two-dimensional ground response analysis is performed using soil data from geotechnical investigation reports and multi-channel analysis of surface waves (MASW) to characterize the soil profile of selected sites at five sub cities that are found on the South – Western part of Addis Ababa and to determine how these locations affected the input ground motions. Considering the local geology and tectonic circumstances, the input ground motions are selected from the PEER ground motion database. Ground response analysis is conducted using the input soil data and five ground motions at the ground surface in the PLAXIS 2D software. And based on the results and shape file of the study area, Seismic micro zonation map is produced. The results of the analyses indicate that the selected sites have a significant potential for amplifying ground motions. This amplification is notably higher than current local code specified predictions but near to NEHRP provisions. Therefore, it is recommended to revise the local code spectra and conduct a detailed investigation and mapping of the rest six sub cities of Addis Ababa to ensure accurate seismic risk assessment and improve safety measures.

TABLE OF CONTENTS

UNDERTAKING	II
ACKNOWLEDGMENT	III
ABSTRACT	IV
LIST OF TABLES	VIII
LIST OF FIGURES	IX
CHAPTER ONE	1
1. INTRODUCTION	1
1.1. Background	1
1.2. Objectives.....	2
1.2.1. General Objective	2
1.2.2. Specific Objectives	2
1.3. Scope of the study	2
1.4. Methodology	3
1.5. Outline of the study.....	3
CHAPTER TWO	4
2. LITERATURE REVIEW	4
2.1. Behavior of soils under cyclic loading.....	4
2.1.1. Shear modulus reduction curve	4
2.1.2. Damping curve.....	6
2.2. Ground Response Analysis	7
2.2.1. One Dimensional Ground Response Analysis.....	7
2.2.2. Two-Dimensional Ground Response Analysis.....	8
2.2.3. Three-Dimensional Ground Response Analysis.....	8
2.3. Finite Element Analysis	9
2.4. Constitutive Models	9
2.5. Dynamic Soil Property Measurement	10
2.5.1. Multi - channel Analysis of Surface Waves (MASW)	10
2.5.2. Seismic Refraction Surveys	11
2.6. Case Study.....	12
2.7. Limitations	13
CHAPTER THREE	14
3. LOCATION AND SEISMICITY OF THE STUDY AREA	14
3.1. Location and Topography	14

3.2.	Geology.....	15
3.3.	Seismic hazard of Addis Ababa.....	16
3.3.1.	Ethiopian Building Code Standard, EBCS 8: 1995.....	17
3.3.2.	Ethiopian Building Code Standard, ES EN 1998:2015.....	18
3.3.3.	Global Seismic Hazard Assessment Program (GSHAP).....	19
CHAPTER FOUR		21
4.	INPUT SOIL DATA AND METHODS.....	21
4.1.	Data collection	21
4.1.1.	Data from Geotechnical investigation reports	21
4.1.2.	Data from Geophysical investigation	27
4.2.	Site Response Analysis	34
4.3.	Soil Geometry and Properties	36
4.3.1.	Unit weight (γ).....	36
4.3.2.	Void ratio (e).....	36
4.3.3.	Cohesion (c).....	37
4.3.4.	Friction angle (ϕ).....	37
4.4.	Boundary condition.....	41
4.5.	Mesh.....	41
CHAPTER FIVE		43
5.	INPUT GROUND MOTIONS	43
5.1.	Introduction.....	43
5.2.	Input Motions from PEER Ground Motion Database.....	43
5.2.1.	Tectonic Regime.....	44
5.2.2.	Definition of Target Spectrum.....	44
5.2.3.	Moment magnitude Range.....	46
5.2.4.	Duration of Strong Motion	46
5.2.5.	Shear-wave velocity of uppermost 30 meters ($V_{S,30}$).....	47
5.2.6.	Time Series Scaling	48
5.2.7.	Collected input motions.....	49
CHAPTER SIX		53
6.	ANALYSIS AND DISCUSSION.....	53
6.1.	Analysis summary.....	53
6.2.	Comparison of Mean response spectra with code spectra	76
6.3.	Seismic micro zonation.....	84
6.3.1.	Geographic Information System (GIS) data	84

6.3.2. Shape file of Addis Ababa.....	85
6.3.3. Mapping two dimensional ground response analysis results.....	85
CHAPTER SEVEN	88
7. CONCLUSION AND RECOMMENDATION.....	88
7.1. Conclusion	88
7.2. Recommendation	89
REFERENCE.....	90
APPENDIX A.....	93
APPENDIX B.....	102
APPENDIX C.....	114
APPENDIX D.....	191
APPENDIX E.....	192

LIST OF TABLES

Table 3-1: Bedrock Acceleration Ratio, α_0 (EBCS-8, 1995)	18
Table 3-2: Bedrock Acceleration Ratio, α_0 (ES EN 1998:2015)	18
Table 4-1: Recommended SPT–stress– V_s correlation equations after (Wair et al., 2012)	23
Table 4-2: Summary of raw and adjusted SPT data and shear wave velocity profiles of the sites	24
Table 4-3: Summary of raw and adjusted SPT data and shear wave velocity profiles of the sites	25
Table 4-4: Summary of raw and adjusted SPT data and shear wave velocity profiles of the sites	26
Table 4-5: Location of all the sites selected for the study	33
Table 5-1: Values of the parameters describing the recommended Type 1 elastic response spectrum (ES EN 1998:2015).....	46
Table 5-2: Selected ground motions from PEER ground motion database	49
Table 6-1: Mean PGA values obtained from SPT data and Seismic survey	61
Table 6-2: Mean maximum response spectra obtained from SPT data and Seismic survey	75
Table D-1: Corrections to Field SPT-N Values (Martin, et al., 1999)	191
Table E-1: ES EN 1998:2015 site categories	192
Table E-2: Summary of site categories in NEHRP provisions.....	193

LIST OF FIGURES

Figure 2-1: Hysteresis loop showing Secant and Tangent shear modulus (Kramer, 1996)	4
Figure 2-2: (a) backbone curve. (b) modulus-reduction curve showing typical variations of G_{sec} with (Brinkegreve, 2005) shear strain (after Kramer 1996)	5
Figure 2-3: Variation of damping ratio of soils with cyclic shear strain and plasticity index (Dobry & Vucetic, 1987).	6
Figure 4-1: Hammer and strike plate	28
Figure 5-1: Recommended Type 1 elastic response spectrum for Type A ground condition (ES EN 1998:2015)	45
Figure 5-2: Comparison of empirical predictive models for significant duration (Bommer et al., 2009)	47
Figure 5-3: Chi chi Taiwan (Unscaled)	49
Figure 5-4: Chi chi Taiwan (Scaled to 0.11g)	50
Figure 5-5: Niigata Japan (Unscaled)	50
Figure 5-6: Niigata Japan (Scaled to 0.11g)	50
Figure 5-7: Northridge-06 (Unscaled)	51
Figure 5-8: Northridge-06 (Scaled to 0.11g)	51
Figure 5-9: San fernando (Unscaled)	51
Figure 5-10: San fernando (Scaled to 0.11g)	52
Figure 5-11: Whittier (Unscaled)	52
Figure 5-12: Whittier (Scaled to 0.11g)	52
Figure 6-1: Mean PGA chart obtained from SPT data: (a) Akaki kality:	54
Figure 6-2: Mean PGA chart obtained from SPT data: (b) Kirkos and (c) Kolfe keranyo	55
Figure 6-3: Mean PGA chart obtained from SPT data: (d) Lafto-1 and (e) Lafto-2	56
Figure 6-4: Mean PGA chart obtained from SPT data: (f) Lafto-3 and (g) Lideta-1	57
Figure 6-5: Mean PGA chart obtained from SPT data: (h) Lideta-2	58
Figure 6-6: Mean PGA chart obtained from Seismic survey data: (a) Akaki kality, and (b) Kirkos	59
Figure 6-7: Mean PGA chart obtained from Seismic survey data: (c) Lafto, and (d) Lideta	60
Figure 6-8: Mean one dimensional response spectra obtained from SPT data: (a) Akaki kality, and (b) Kirkos	63
Figure 6-9: Mean one dimensional response spectra obtained from SPT data: (c) Kolfe keranyo, and (d) Lafto-1	64
Figure 6-10: Mean one dimensional response spectra obtained from SPT data: (e) Lafto-2, and (f) Lafto-3	65
Figure 6-11: Mean one dimensional response spectra obtained from SPT data: (g) Lideta-1, and (h) Lideta-2	66
Figure 6-12: Mean two dimensional response spectra obtained from SPT data: (a) Akaki kality, and (b) Kirkos	67
Figure 6-13: Mean two dimensional response spectra obtained from SPT data: (c) Kolfe keranyo, and (d) Lafto-1	68
Figure 6-14: Mean two dimensional response spectra obtained from SPT data: (e) Lafto-2, and (f) Lafto-3	69

Figure 6-15: Mean two dimensional response spectra obtained from SPT data: (g) Lideta-1, and (h) Lideta-2.....	70
Figure 6-16: Mean one dimensional response spectra obtained from Seismic survey: (a) Akaki Kality.....	71
Figure 6-17: Mean one dimensional response spectra obtained from Seismic survey: (b) Kirkos, and (c) Lafto.....	72
Figure 6-18: Mean one dimensional response spectra obtained from Seismic survey: (d) Lideta	73
Figure 6-19: Mean two dimensional response spectra obtained from Seismic survey: (a) Akaki kality	73
Figure 6-20: Mean two dimensional response spectra obtained from Seismic survey: (b) Kirkos, and (c) Lafto.....	74
Figure 6-21: Mean two dimensional response spectra obtained from Seismic survey: (d) Lideta	75
Figure 6-22: Comparison of mean response spectra from SPT data with code spectra: (a) Akaki kality	77
Figure 6-23: Comparison of mean response spectra from SPT data with code spectra: (b) Kirkos, and (c) Kolfe keranyo	78
Figure 6-24: Comparison of mean response spectra from SPT data with code spectra: (d) Lafto-1, and (e) Lafto-2	79
Figure 6-25: Comparison of mean response spectra from SPT data with code spectra: (f) Lafto-3, and (g) Lideta-1	80
Figure 6-26: Comparison of mean response spectra from SPT data with code spectra: (h) Lideta-2.....	81
Figure 6-27: Comparison of mean response spectra from Seismic survey with code spectra: (a) Akaki kality, and (b) Kirkos	82
Figure 6-28: Comparison of mean response spectra from Seismic survey with code spectra: (c) Lafto, and (d) Lideta	83
Figure 6-29: Seismic micro zonation map.....	86
Figure A- 1: PGA results from SPT data: a) Akaki kality, and (b) Kirkos	93
Figure A- 2: PGA results from SPT data: (c) Kolfe keranyo, and (d) Lafto-1	94
Figure A- 3: PGA results from SPT data: (e) Lafto-2, and (f) Lafto-3	95
Figure A- 4: PGA results from SPT data: (g) Lideta-1, and (h) Lideta-2	96
Figure A- 5: PGA results from Seismic survey data: (a) Akaki Kality, and (b) Kirkos... ..	97
Figure A- 6: PGA results from Seismic survey data: (c) Lafto, and (d) Lideta	98
Figure A- 7: Comparison of PGA results with the input motion: (a) Akaki kality, and (b) Kirkos	99
Figure A- 8: Comparison of PGA results with the input motion: (c) Kolfe keranyo, and (d) Lafto	100
Figure A- 9: Comparison of PGA results with the input motion: (e) Lideta	101
Figure B- 1: One dimensional response spectra from SPT data : (a) Akaki kality, and (b) Kirkos	102
Figure B- 2: One dimensional response spectra from SPT data : (c) Kolfe keranyo, and (d) Lafto-1.....	103
Figure B- 3: One dimensional response spectra from SPT data : (e) Lafto-2, and (f) Lafto-3	104

Figure B- 4: One dimensional response spectra from SPT data : (g) Lideta-1, and (h) Lideta-2.....	105
Figure B- 5: Two dimensional response spectra from SPT data : (a) Akaki kality, and (b) Kirkos	106
Figure B- 6: Two dimensional response spectra from SPT data : (c) Kolfe keranyo, and (d) Lafto-1.....	107
Figure B- 7: Two dimensional response spectra from SPT data : (e) Lafto-2, and (f) Lafto-3	108
Figure B- 8: Two dimensional response spectra from SPT data : (g) Lideta-1, and (h) Lideta-2.....	109
Figure B- 9: One dimensional response spectra from Seismic survey data : (a) Akaki kality, and (b) Kirkos	110
Figure B- 10: One dimensional response spectra from Seismic survey data : (c) Lafto, and (d) Lideta.....	111
Figure B- 11: Two dimensional response spectra from Seismic survey data : (a) Akaki kality, and (b) Kirkos	112
Figure B- 12: Two dimensional response spectra from Seismic survey data : (c) Lafto, and (d) Lideta.....	113
Figure C- 1: Akaki Kality borehole logs	131
Figure C- 2:Kirkos borehole logs	156
Figure C- 3:Kolfe keranyo borehole logs	164
Figure C- 4:Lafto-1 borehole logs	166
Figure C- 5: Lafto-2 borehole logs	172
Figure C- 6: Lafto-3 borehole logs	178
Figure C- 7: Lideta-1 borehole logs.....	180
Figure C- 8: Lideta-2 borehole logs.....	190

CHAPTER ONE

1. INTRODUCTION

1.1. Background

Studying site effect is essential for earthquake studies in a specific area because soil properties influence seismic wave propagation, amplification, and attenuation. Site effect has emerged as a major concern in geotechnical earthquake engineering among all the parameters that influence strong earthquake ground motions. These variables include the earthquake's size, its distance from the epicenter, the length of the ground motion, the wave path's geology, its frequency, and the region's soil characteristics (Getu, 2022). As a result, the site has a visible impact on either amplifying or attenuating the ground response when an earth quake happens at the site.

Ethiopia's capital, Addis Ababa, is situated near the edge of the Ethiopian Rift System, an area with moderate seismic activity. Because of its location, the city is susceptible to earthquakes. It is essential to comprehend and get ready for the seismic dangers if Addis Ababa's population and infrastructure are to be secure and resilient. In the recent past, it has had several earthquakes with magnitudes up to MS 6.8. There have already been several destructive earthquakes in the area. On certain cases, a handful of the city's engineering structures suffered minor damage as a result of these earthquakes. Among the notable earthquakes that occurred within that period were the 1906, 1960, and 1961 earthquakes, with respective magnitudes of 6.8, 6.3, and 6.7 (Mammo, 2005).

If an earthquake were to strike a city like Addis Ababa, the consequences could be significant and wide-ranging. The seismic forces could cause substantial structural damage, leading to the collapse or severe damage of buildings and infrastructure across the entire city. Such destruction would not only result in the loss of homes and businesses but also disrupt critical services like transportation, water, and electricity. The impact on human lives would be significant, with potential injuries and losses.

Depending on the level of detail being studied and the complexity of the study, one, two, or three-dimensional methods can be used to represent the site conditions and conduct ground response analysis.

1.2. Objectives

1.2.1. General Objective

The general objective of this study is to investigate the ground response analysis in the selected South - Western part of Addis Ababa.

1.2.2. Specific Objectives

The following specific objectives are comprised:

- Characterizing selected sites in South - Western part of Addis Ababa by the integration of geotechnical investigations and geophysical techniques.
- Investigating whether the chosen sites have the ability to amplify or attenuate the input seismic ground motions;
- Determining mean response spectra of the sites and making comparison with code-specified spectra.

1.3. Scope of the study

In order to conduct a large-scale investigation into the ground amplification or attenuation potential of the soil in Addis Ababa, a complete site characterization of the entire city is required. However, such an investigation would involve significant time and financial resources, which are beyond the scope of this particular study.

Instead, this study takes a narrower approach by focusing specifically on the South - Western part of Addis Ababa specially five sub cities with in the region. This particular section is of special interest due to its significance and potential vulnerability to seismic events. Within this scope, the study collects and examine existing geotechnical investigation reports to obtain essential soil data. Additionally, geophysical tests are conducted in selected areas. These reports serve as valuable sources of information which is used as input for the ground response analysis.

The analysis method of this study is two-dimensional ground response analysis, as it provides a detailed representation of the selected sites, which optimizes the accuracy of the ground response analysis.

1.4. Methodology

Two-dimensional ground response analysis is performed on selected sites in the South - Western part of Addis Ababa to examine their potential for amplifying or attenuating earthquake ground motions. To conduct the study, geotechnical and geophysical data is collected from construction companies in the area and through Multi-Channel Analysis of Surface Waves (MASW) tests in selected areas respectively, offering valuable insights into subsurface conditions and seismic characteristics down to a minimum depth of 30 meters.

After collecting data from both geotechnical and geophysical tests, the ground motions used as input are sourced from the PEER ground motion database, taking into account the geological and tectonic conditions specific to the study area, and the ground motion analyses have been carried out using PLAXIS 2D software, as two-dimensional analysis necessitates finite element software. Chapter four provides comprehensive details on the procedures, methods, and input parameters employed in this study.

Based on the analysis results collected from the PLAXIS 2D software, a seismic micro zonation map of the five sub cities in the South - Western part of Addis Ababa is produced using Geographic information system (GIS) software.

1.5. Outline of the study

There are seven chapters in this study. Chapter 1 introduces the study's objective, scope, and methodology. Chapter 2 provides a literature review of previous research on how soil responds to cyclic loading and presents techniques for analyzing ground response analysis. Chapter 3 describes the location, topography, geology, and seismic hazards of the study area. Chapter 4 focuses on data collection, processing, and the methodologies employed in geotechnical and geophysical methods, Chapter 5, describes the ground motions used as input for the analysis. In Chapter 6, the findings of the ground response analyses and micro zonation map are presented. Finally, Chapter 7 summarizes the conclusions drawn from the analysis results and provides recommendations based on those conclusions.

CHAPTER TWO

2. LITERATURE REVIEW

2.1. Behavior of soils under cyclic loading

The hysteresis loop shown in Figure 2-1 might be seen in a typical soil that is under a flat ground surface, distant from surrounding structures, and exposed to symmetric cyclic stress as one might expect. There are two approaches to characterize this hysteresis loop: first, by looking at the loop's actual route. Secondly, by characteristics that depict its overall form. Generally speaking, the inclination and width of a hysteresis loop are two crucial aspects of its shape (Kramer, 1996).

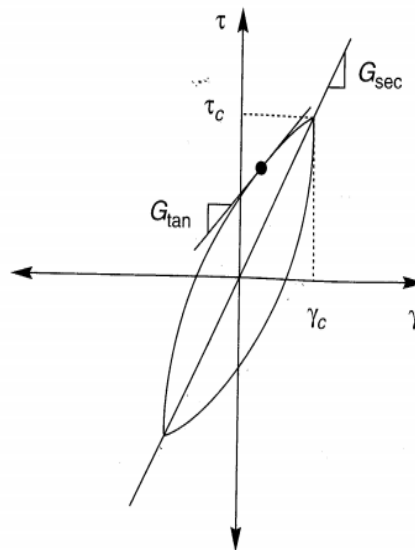


Figure 2-1: Hysteresis loop showing Secant and Tangent shear modulus (Kramer, 1996)

The tangent shear modulus G_{tan} can be used to characterize the soil's stiffness at any stage of the loading process, which determines the loop's inclination. And, G_{tan} fluctuates over a loading cycle, but the secant shear modulus can roughly represent its average value across the whole loop (Kramer, 1996).

2.1.1. Shear modulus reduction curve

The shear modulus is one of the most important soil parameters used for the dynamic response analysis of the soil. The determination of these parameters at low strain level is done by geophysical technique. This parameter's key benefit is that it may be utilized to vary in response to strain, allowing the soil reaction to accurately reflect the modulus of

degradation in the behavior of the soil. The stiffness matrices for the finite element analysis of foundation soils and earth structures are defined using this parameter (Luna & Jadi, 2000).

The shear modulus reduction curve, or G/G_{max} curve, illustrates how the stiffness of a material decreases with increasing shear strains or cyclic loading. It shows the ratio of the current shear modulus (G) to the maximum shear modulus (G_{max}). This curve is crucial in understanding the material's behavior, energy dissipation, and potential for liquefaction or deformation under different loading conditions.

Maximum Shear modulus denoted as G_{max} , refers to the peak or maximum value of the shear modulus that a material can attain. The measured shear wave velocities can be used to compute G_{max} (Kramer, 1996).

$$G_{max} = \rho V_s^2 \quad (2.1)$$

The slope at the origin (zero cyclic strain amplitude) represents the largest value of the shear modulus, G_{max} (Kramer, 1996).

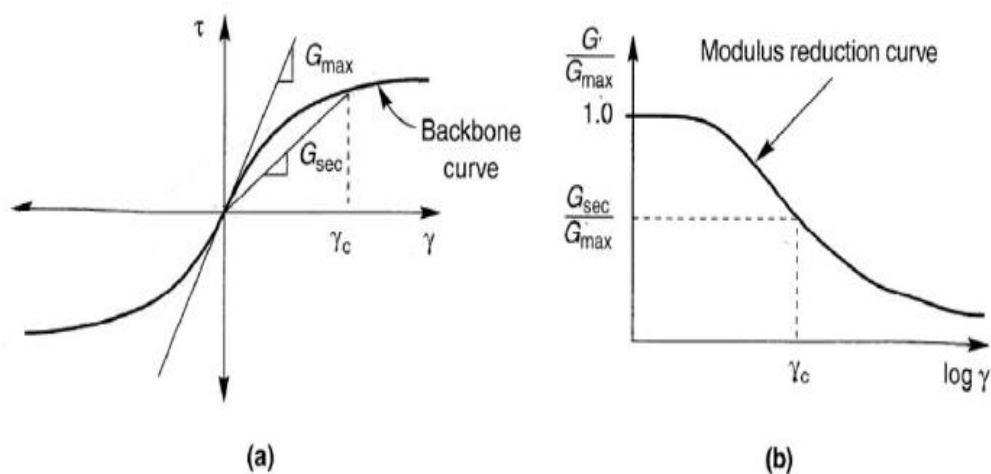


Figure 2-2: (a) backbone curve. (b) modulus-reduction curve showing typical variations of G_{sec} with (Brinkegreve, 2005) shear strain (after Kramer 1996)

2.1.2. Damping curve

The other material curves to consider are damping curves, which represent the breadth of a hysteresis loop. These curves signify the extent of energy dissipation caused by the movements of soil particles. Damping is the dissipation of energy within a system, which results in the gradual reduction of oscillations or vibrations over time. Different damping mechanisms are used to dissipate the kinetic and strain energy of a vibrating system (Chopra, 2012).

$$\xi = \frac{W_D}{4\pi W_S} = \frac{1}{2\pi} \frac{A_{loop}}{G_{sec} \gamma_c^2} \quad (2.2)$$

Where: W_D is the dissipated energy,

W_S is the maximum strain energy and

A_{loop} is the area of the hysteresis loop

G_{sec} is the secant shear modulus

γ_c is the shear strain

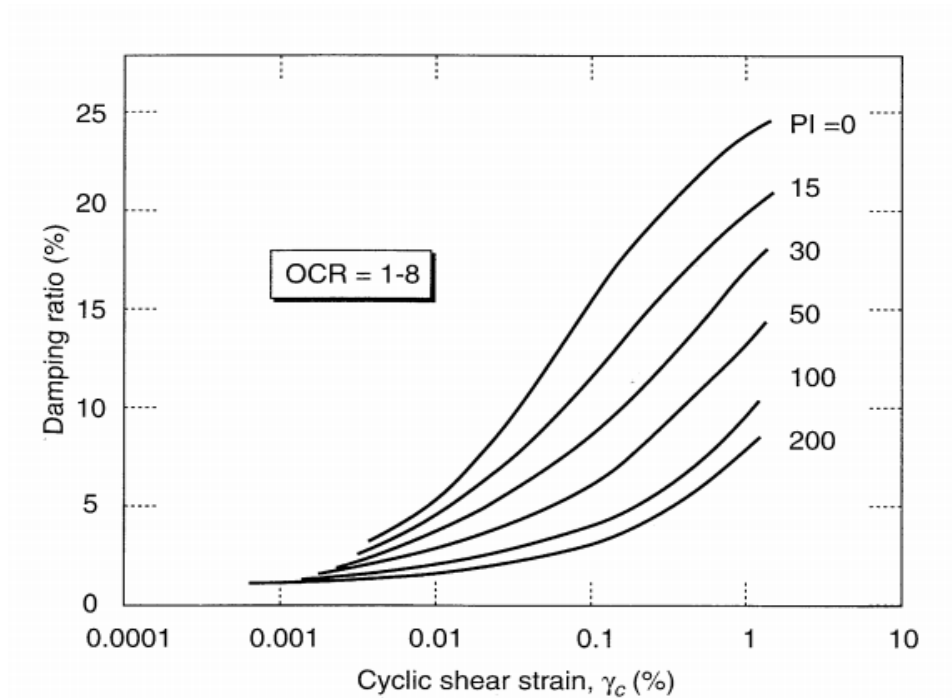


Figure 2-3: Variation of damping ratio of soils with cyclic shear strain and plasticity index (Dobry & Vucetic, 1987).

2.2. Ground Response Analysis

Ground response analysis is a computational method used to evaluate the behavior of soil layers during seismic events. The analysis aims to understand how the ground motion is modified as it propagates through different soil layers at a specific location. Ground response analyses (GRA) need to be performed for obtaining ground motions at surface level for a chosen bed rock motion (Kumar & Krishna, 2013). GRA is used to predict ground surface motions for different purpose. These include development design response spectrum, evaluation of dynamic strain and stresses and for liquefaction hazard analysis and determination of earthquake induced forces that can lead to instability of geotechnical structures (Kramer, 1996). So that conducting a ground response analysis is essential when evaluating the behavior of the ground surface during an earthquake event.

Ground response analysis can be executed by either one-dimensional, two-dimensional, or three-dimensional methods. These include the complexity of the geological conditions, the accuracy required for the study, the computational resources available, and the specific objectives of the analysis. Each method offers different levels of detail and precision, with three-dimensional methods providing the most comprehensive results.

2.2.1. One Dimensional Ground Response Analysis

Considering the presumption that all boundaries are horizontal and that SH-waves propagating vertically from underlying bedrock are the primary cause of a soil deposit's response, one-dimensional ground response analysis is conducted. The horizontal direction of the soil and bedrock surface is assumed to be limitless in one-dimensional ground response analysis (Kramer, 1996).

In this analysis method, the ground is typically idealized as a series of horizontally layered soil or rock strata. Each layer is characterized by its mechanical properties, such as shear modulus, damping ratio, and density. The analysis assumes that the ground motion is vertically propagating and that the soil layers are laterally homogeneous. This analysis method can effectively evaluate the response of levelled or gently sloping grounds. In the context of ground response analysis, the 1-D analysis is helpful for sites that are flat or gently sloping and have parallel material limits (Arjuna et al., 2021).

One-dimensional ground response analysis can be conducted using three different methods. These methods vary in simplicity and accuracy of representation. The methods

include linear analysis, which is the simplest, equivalent linear analysis, and non-linear analysis, which provides the detailed representation of the analysis. Each method offers a different balance between complexity and accuracy.

2.2.2. Two-Dimensional Ground Response Analysis

Two-dimensional ground response analysis refers to the analysis and modeling of soil behavior and ground motion in two dimensions. Techniques for the solution of such problems have been developed using both frequency domain (complex response) methods and time domain (direct integration) methods. It involves considering the vertical and horizontal responses of the soil to dynamic loading, such as seismic waves or vibrations from structures. Sloping or irregular ground surfaces, the presence of heavy structures or stiff, embedded structures, or walls and tunnels all require two-dimensional analysis (Kramer, 1996).

The presence of a soft soil valley and/or a hill are considered to contribute to the acceptance of 2-D numerical schematizations due to the focalization of seismic waves at the valley's ground surface and at the crest, respectively (Arjuna et al., 2021). The inherent complexity of sites, characterized by varying soil properties and topographical features, necessitates a two-dimensional ground response analysis.

This method enables a more accurate representation of spatial variability and boundary effects, providing crucial insights into seismic response across diverse geological settings and aiding in effective engineering design and risk mitigation.

2.2.3. Three-Dimensional Ground Response Analysis

In some instances, two-dimensional idealizations might not be able to capture the actual features and hence, three-dimensional analysis may be necessary. With this three-dimensional analysis it is possible to investigate the amplification and damping in earthquake wave amplitudes considering the actual prevailing conditions at a site (Dogan, 2023). Even though the analysis approach is sophisticated, it will be necessary to analyze the site in three dimensions due to the level of heterogeneous environment present in the area.

If soil conditions exhibit three-dimensional variability, if problem boundaries vary in three dimensions, and if the response of three-dimensional structures is of concern, conducting

three-dimensional analysis is essential for the specific project. Three-dimensional dynamic response problems are treated in much the same way as two-dimensional problems (Kramer, 1996). These analysis methods remain largely consistent; however, three-dimensional analysis necessitates the inclusion of complex geometries and loading conditions.

The dynamic response and soil-structure interaction problems for the higher dimensions are often solved using dynamic finite element analysis (Kramer, 1996). Different finite element methods can be used to carry out this ground response analysis.

2.3. Finite Element Analysis

Finite element method has proven to be very effective in solving problems with bounded domains, particularly when inhomogeneities and nonlinear effects should be treated (Kamalian et al., 2006). The region to be analyzed is discretized into several elements in this method of analysis. Using this finite element method, the responses at each nodal point in each stage of the analysis can be investigated (Arjuna et al., 2021). Conducting finite element analysis for each element helps combine the nodes, representing the entire ground response. This method ensures an accurate representation of the ground's behavior.

Several finite element software are capable of modelling geotechnical engineering problems (Arjuna et al., 2021). These commonly used soft wares include PLAXIS 2D, PLAXIS 3D, FLAC 3D, and ABAQUS. Choosing the appropriate software depends on available resources, and specific features offered by each software.

2.4. Constitutive Models

Constitutive models form the qualitative description of material behavior; whereas the model parameters further quantify the soil's behavior (Brinkgreve, 2005). These models vary from simple linear elastic to intricate nonlinear advanced formulations depending on the complexity of the soil behavior being analyzed. The Mohr-Coulomb model is one of the most commonly used constitutive models in geotechnical engineering.

The Mohr- Coulomb model involving five parameters, namely the two elastic parameters from Hooke's law (Young's modulus, E , and Poisson's ratio, ν), the two parameters from coulomb's failure criterion (the friction angle, ϕ and cohesion, c) and dilatancy angle, ψ

is used. The Mohr-Coulomb failure contour's hexagonal shape closely matches the stress combinations that lead to failure in actual soil samples. As a result, this model works well for analyzing the stability of geotechnical structures (Brinkgreve, 2005).

2.5. Dynamic Soil Property Measurement

The evaluation of dynamic soil properties is one important task while solving geotechnical earthquake engineering problems (Kramer, 1996). The test provides valuable understandings into subsurface conditions, enabling a more accurate representation of site-specific characteristics. They play a significant role in characterizing soil properties, assessing seismic hazards, and contributing to geological and geotechnical mapping.

To characterize the properties of soil, there are a number of laboratory and field tests. Laboratory tests are typically conducted on relatively small samples that are thought to be indicative of a larger body of soil. The ability of laboratory tests to accurately evaluate soil properties depends on their capacity to duplicate the initial conditions and the loading conditions of the problem of interest, whereas field testing enables in-situ measurements of soil parameters. Sampling is not necessary for field tests, as it can change the stress, chemical, thermal, and structural properties of the soil samples. Therefore, it is beneficial to apply field testing to interesting problems (Getu, 2023). To be ready for the field test, a few more tests must be conducted. When choosing testing procedures to quantify dynamic soil properties, careful consideration and understanding of the specific problem at hand are necessary (Kramer, 1996).

The next section describes the two field test methods that are currently in use: Multi – Channel Analysis of surface waves (MASW) and seismic refraction survey.

2.5.1. Multi - channel Analysis of Surface Waves (MASW)

Multi - channel Analysis of Surface Waves (MASW) is a geophysical method used for the characterization of subsurface materials and the determination of shear wave velocity profiles. The MASW technique offers several notable advantages, making it an excellent choice for site characterization. One such advantage is its capacity to provide a substantial investigation depth of approximately 30 meters. Recently, MASW has been created as an alternative to conventional high-resolution seismic methods. It operates at comparatively lower frequencies and shallower study depth ranges (Ark et al., 2007). This depth range

allows for a comprehensive understanding of subsurface conditions, enabling effective site assessment and characterization.

Three steps are involved in the process of producing a shear wave profile through spectral analysis of surface waves: obtaining ground roll, creating a dispersion curve (a plot of phase velocity versus f), and then inverting the calculated dispersion curve to calculate the shear wave profile (V_s). To precisely calculate the V_s profile, broadband ground roll must be generated and captured with the least amount of noise (Park et al., 1999). Combining dispersion images processed from active and passive data sets is frequently helpful or required for two reasons: (1) to increase the depth range of dispersion that can be studied, and (2) to more clearly define the modal character of dispersion patterns (Ark et al., 2007).

The entire wave field is inverted to get the shear wave velocities. Body waves, higher-mode surface waves, and scattered, non-source generated surface waves are examples of these nonplanar, non-fundamental mode Rayleigh waves (noise). Both frequency and distance from the source affect how much each of these noise types impact the dispersion curve and, eventually, the inverted shear wave velocity profile (Park et al., 1999). In order to conduct a more detailed geotechnical studies, the inverted shear wave velocity collected from the MASW test is commonly used.

2.5.2. Seismic Refraction Surveys

A seismic refraction survey is a geophysical technique used to investigate subsurface properties and determine the shear wave velocity and depth of different geological layers. The method depends upon Seismic waves travel through different material at different velocities and measuring the time taken for a seismic wave to travel from one point to another (Ayolabi, Adeoti, , Oshinlaja, Adeosun, & Idowu, 2009). The major drawbacks of the seismic refraction test from a geotechnical point of view are the inability to detect low velocity layers between high velocity layers and the fact that it samples only a portion of the material in a thick soil layer (Luna & Jadi, 2000).

It is important to note that the choice between a seismic refraction survey and MASW depends on various factors, including the specific objectives of the investigation, the depth range of interest, and the geological complexity of the site.

2.6. Case Study

Site-specific ground motion simulation and seismic response analysis at the proposed bridge sites within the city of Addis Ababa, Ethiopia was done by (Mammo, 2005). Theoretical ground motion modeling is used in this work to determine ground motions and their spectral responses at five different sites proposed for bridge constructions in connection with the Addis Ababa ring road project. The analysis method for this study is one – dimensional and the geophysical investigation used for the study was seismic refraction surveys, which have inherent limitations. These limitations include depth constraints, assumptions of layer homogeneity, limited resolution for small scale features, and sensitivity to near surface conditions.

Ground Response Analysis of Selected Sites in Hawassa Area was done by (Eshetu, 2017). Primary data from seismic refraction tests and secondary data from available geotechnical reports were collected from different locations of the city so as to model respective soil profiles. This study focused on an earthquake prone area, which is of significant importance. However, the analysis method for this study is one – dimensional and the data used in the study lacked sufficient support, as the geophysical test relied on seismic refraction surveys, which are subject to depth limitations.

An investigation into the ground motion amplification potential of selected sites of Addis Ababa city was done by (Gashaye, 2018). In the study, specific site characterization and one-dimensional ground response analysis were performed using seismic refraction data and geotechnical data. This study is conducted using seismic refraction surveys, which are subject to depth limitations. And also, the one-dimensional ground response analysis method has limitations in representing the study area.

Site Response Analysis of Selected Sites of Adama City was done by (Abiy, 2021). One-dimensional equivalent linear and nonlinear site response analyses have been conducted at nine sites in Adama. The shear wave profiles of the sites were obtained using a geophysical test called Multi - channel Analysis of Surface Waves (MASW). This test offers a significant investigation depth of around 30 meters, which is representative of the area. However, the one-dimensional ground response analysis method has limitations.

Nonlinear Ground Response Analysis of Selected Sites of Addis Ababa using Geotechnical and Seismic data was done by (Getu, 2022). Geotechnical investigation test results are collected, and geophysical tests are directly conducted for the purpose of site characterization. The study employed both primary and secondary data to characterize the site. Primary data was collected using Multi-Channel Analysis of Surface Waves (MASW), revealing a high susceptibility to seismic waves in the area and recommending a seismic micro zonation, which sparked further interest in conducting additional investigations and map the recommended study area. This study was conducted using one-dimensional ground response analysis, which has limitations affecting its accuracy in certain conditions.

2.7.Limitations

Due to limited secondary data and the high expense of geophysical testing, finer classifications at the woreda level or smaller scales were not pursued in this study. The produced map is also categorized by sub cities only, acknowledging potential differences in soil types within each sub city.

CHAPTER THREE

3. Location and Seismicity of the study area

3.1. Location and Topography

Addis Ababa, the capital of Ethiopia, serves as a diplomatic hub for Africa and hosts various international programs. It is situated in the central highlands of the country, positioned at an elevation of 2,355 meters. Located at coordinates $9^{\circ}1'48''\text{N}$ $38^{\circ}44'24''\text{E}$.

Addis Ababa is divided into eleven sub cities, which are Addis Ketema, Akaki Kality, Arada, Bole, Gulele, Kirkos, Kolfe keranyo, Lideta, Nifas silk Lafto, Yeka, and the recently added Lemi Kura sub cities. Out of which, five sub cities, which are Akaki Kality, Kirkos, Kolfe Keranyo, Lideta, and Nifas Silk Lafto sub cities, are selected for this study since they are located in the South - Western part of Addis Ababa. The Addis Ababa and South – Western part of Addis Ababa map is presented in Figure 3-1.

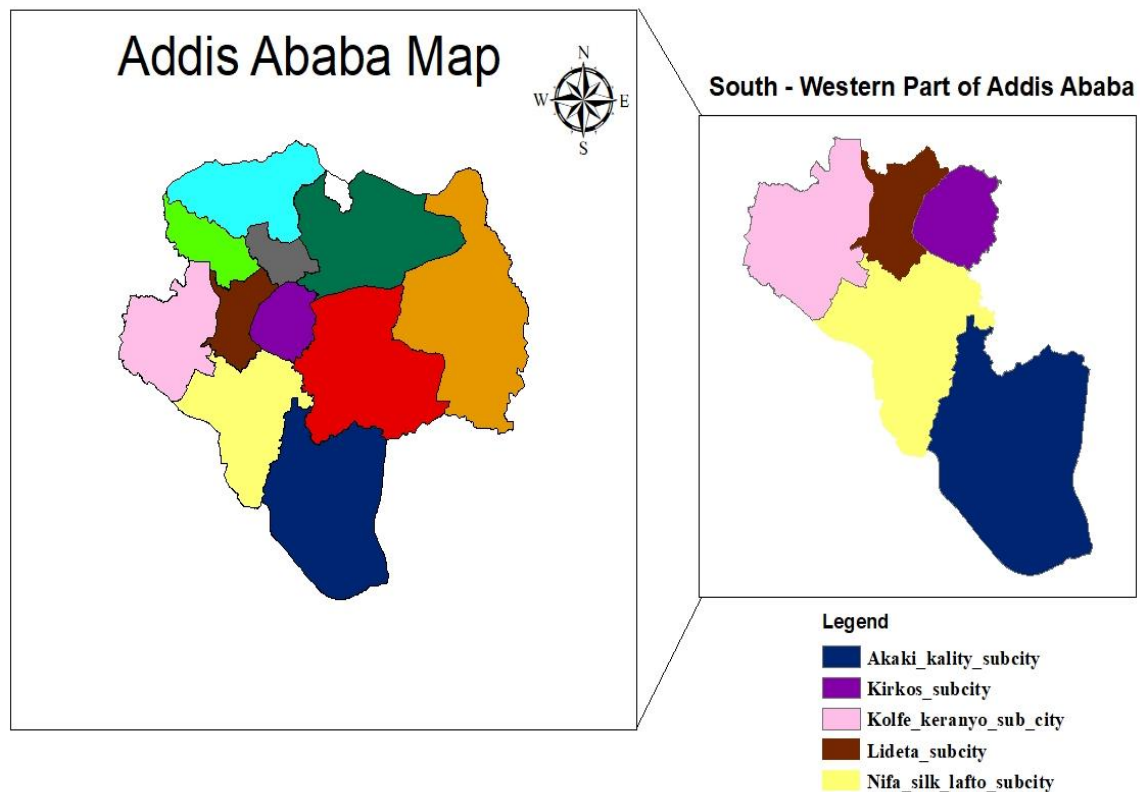


Figure 3-1: South – Western part of Addis Ababa map

The South - Western region of Addis Ababa presents a diverse topography, characterized by irregular shapes and slopes. This distinctive terrain creates a unique urban landscape with varying elevations and gradients throughout. Additionally, the irregular landforms add character to the area, contributing to its dynamic responses.

3.2. Geology

Addis Ababa is situated on the edge of the active East African Rift System, which includes the Main Ethiopian Rift. Therefore, the geology and structural components of the city and its surroundings are impacted by each stage involved in the formation and subsequent extension of the Rift System (Mammo, 2005).

The city is surrounded by volcanic mountains, which include Mount Furi to the east, the Wechecha range to the southwest, Entoto Chain Mountain to the north, and Mount Yerer to the southeast. Rocks from the Lower Miocene to the Quaternary make up the geology of the city of Addis Ababa. (Engidasew & Abay, 2016). Aphanitic basalt, rhyolite, ignimbrite, tuff-agglomerate, trachyte, scoriaceous basalt, and alluvium are among the rock units. On the northern and southern portions, newer volcanic rocks from the recent volcanism of Wechecha, Furi, and Yerer are underlain by thick basalt units (Engidasew & Abay, 2016).

The entire area to the south, east, and west of the city is covered by the Younger Volcanics. The oldest aphanitic basalts, the middle-aged porphyritic feldspar basalts, and the youngest porphyritic olivine basalts are all defined as being Pliocene in age. The youngest volcanic rocks in the Addis Ababa region are the Pliocene - Pleistocene Younger Volcanics. These are the olivine basalts and silicic lavas and pyroclastics (Balchi rhyolites). Tuffs, ignimbrites, rhyolites, and trachytes are among the Balchi. They are vulnerable in the city's east and south, as well as outside of it (Mammo, 2005).

As indicated on the Modified geological map of Addis Ababa city the South - Western part of Addis Ababa is covered by volcanic features named Scoraea cones of Quaternary Younger Basaltic lavas, Cinder cones, Quaternary Alluvial soils, Upper Miocene Addis Ababa porphyritic Olivine Basalt, Ignimbrite of Pliocene to Quaternary Young Volcanics, and Trachy basalt of Pliocene to Quaternary Young volcanics.

The geological arrangement of Addis Ababa city (after SEURECA SOACE & BCEOM, 1996) is generalized on the Figure 3-2.

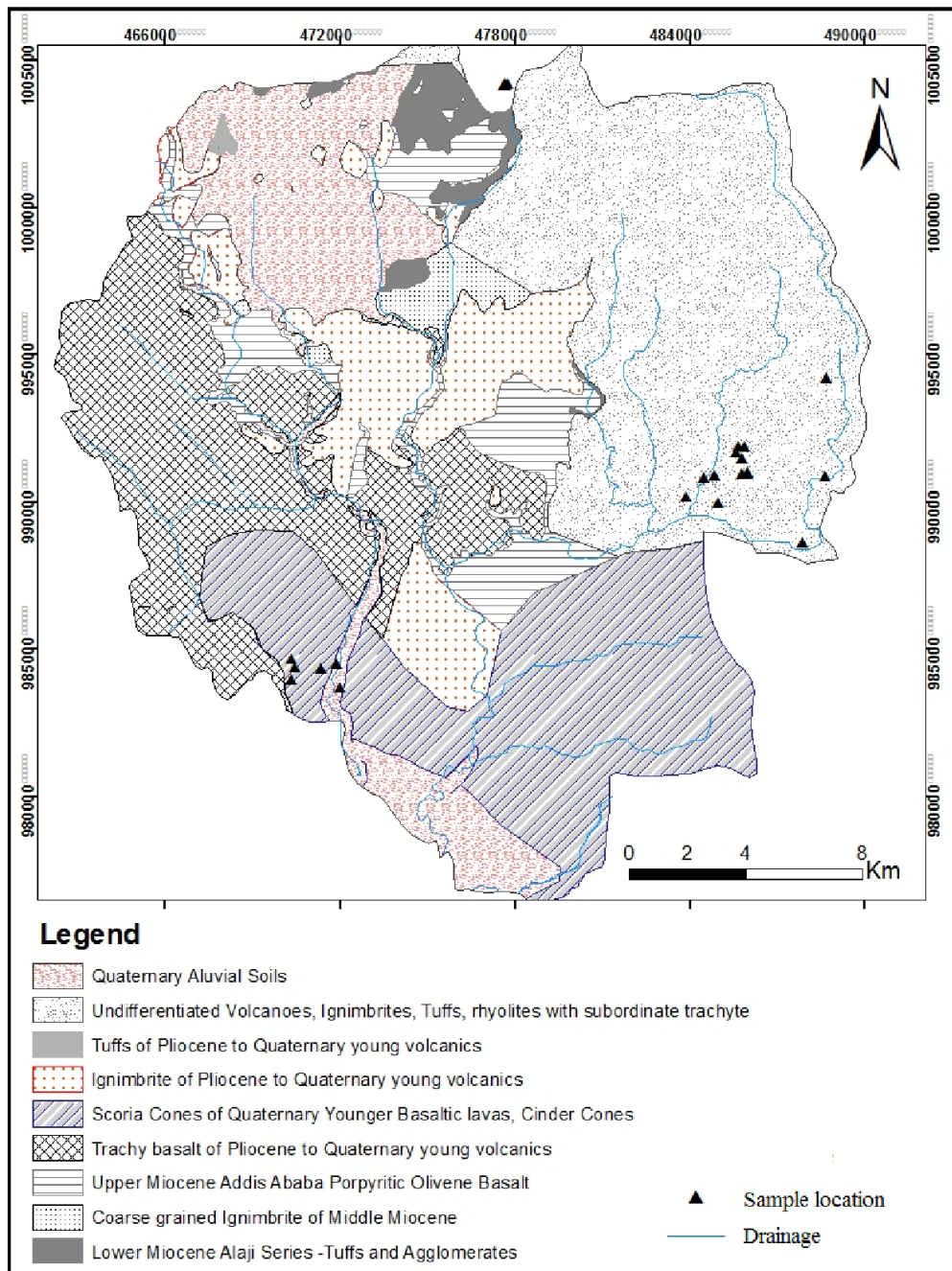


Figure 3-2: Modified geological map of Addis Ababa city (after SEURECA SOACE & BCEOM, 1996)

3.3. Seismic hazard of Addis Ababa

Addis Ababa, positioned at the margin of East African Rift Valley, faces potential earthquake hazards owing to the geological dynamics of the region. The city's proximity to the Rift Valley necessitates readiness for seismic occurrences and the adoption of suitable safety protocols.

At an epicentral distance of roughly 120 km south of Addis Ababa, a large earthquake with a magnitude of 6.8 struck this zone in 1906. The greatest earthquake to ever be recorded in Ethiopia was this one. In Addis Ababa, it had a widespread impact. The 6.3 magnitude earthquake that occurred in 1960 and the 6.2 magnitude earthquake that occurred in 1987 are two more notable earthquakes in this zone (Mammo, 2005).

The seismicity of Addis Ababa has been studied both locally and globally, providing valuable insights into earthquake activity in the region.

3.3.1. Ethiopian Building Code Standard, EBCS 8: 1995

The Ethiopian Building Code Standard, EBCS 8: 1995, regulates building safety and integrity in Ethiopia. Enacted in 1995, it covers design, materials, and construction methods. Assuming the hazard within each zone is constant, the local hazard within the country has been divided into seismic zones. For application of this standard, the hazard was described in terms of a single parameter, i.e. the value of the effective peak ground acceleration in rock or firm soil, which was called “design ground acceleration”. The seismic hazard map of the country is presented in Figure 3-3.

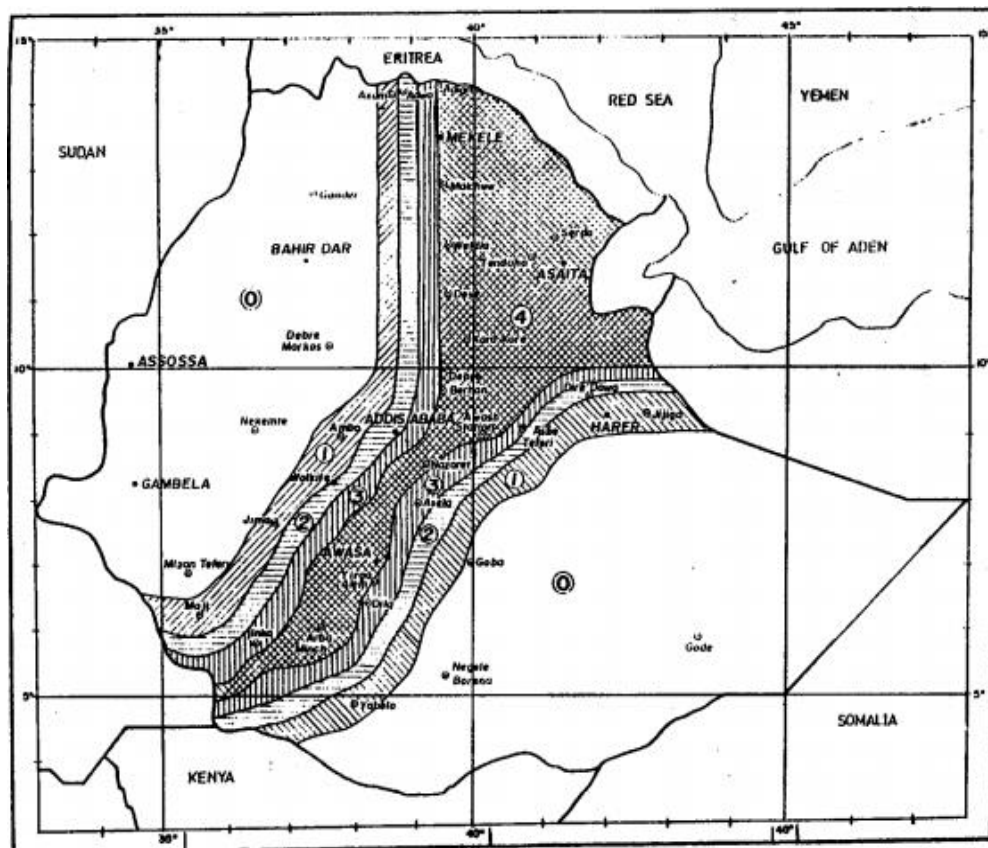


Figure 3-3: Seismic Hazard Map of Ethiopia

The code groups the country into four distinct seismic zones based on bedrock acceleration ratios as shown in Table 3-1.

Table 3-1: Bedrock Acceleration Ratio, α_0 (EBCS-8, 1995)

zone	4	3	2	1
α_0	0.10	0.07	0.05	0.03

Table 3-1 indicates that Addis Ababa's seismic hazard zone is 2, with a maximal ground acceleration of 0.05g (EBCS-8, 1995). And currently, the code is out of service and has been replaced by the Ethiopian Building Code Standard, ES EN 1998:2015.

3.3.2. Ethiopian Building Code Standard, ES EN 1998:2015

The Ethiopian Building Code Standard ES EN 1998:2015, provides seismic design guidelines in Ethiopia. Adopted in 2015, it ensures structural safety against earthquakes. The code has grouped the ground type in to 5 types relating to $V_{s,30}$ (m/s). The area will be considered ground type A if the $V_{s,30}$ is >800 m/s, ground type B if it is 360 m/s–800 m/s, ground type C if it is 180 m/s–360 m/s, ground type D <180 m/s, and ground type E if the soil profile consists of a surface alluvium layer with $V_{s,30}$ values of type C and D and thickness varying between about 5m and 20m.

Depending on the local hazard the country has been subdivided into seismic zones. The seismic zone corresponds to a reference return period of 475 years (10% probability of exceedance in 50 years). The Seismic Hazard of Ethiopia earthquake database, which is processed from instrumentation records, is the source of the preliminary hazard map displayed in Figures 3-4. And in Table 3-2, Addis Ababa, having a PGA of 0.1 g, is allocated to zone 3.

The code groups the country into five distinct seismic zones based on bedrock acceleration ratios as shown in Table 3-2.

Table 3-2: Bedrock Acceleration Ratio, α_0 (ES EN 1998:2015)

Zone	5	4	3	2	1
α_0	0.2	0.15	0.1	0.07	0.04

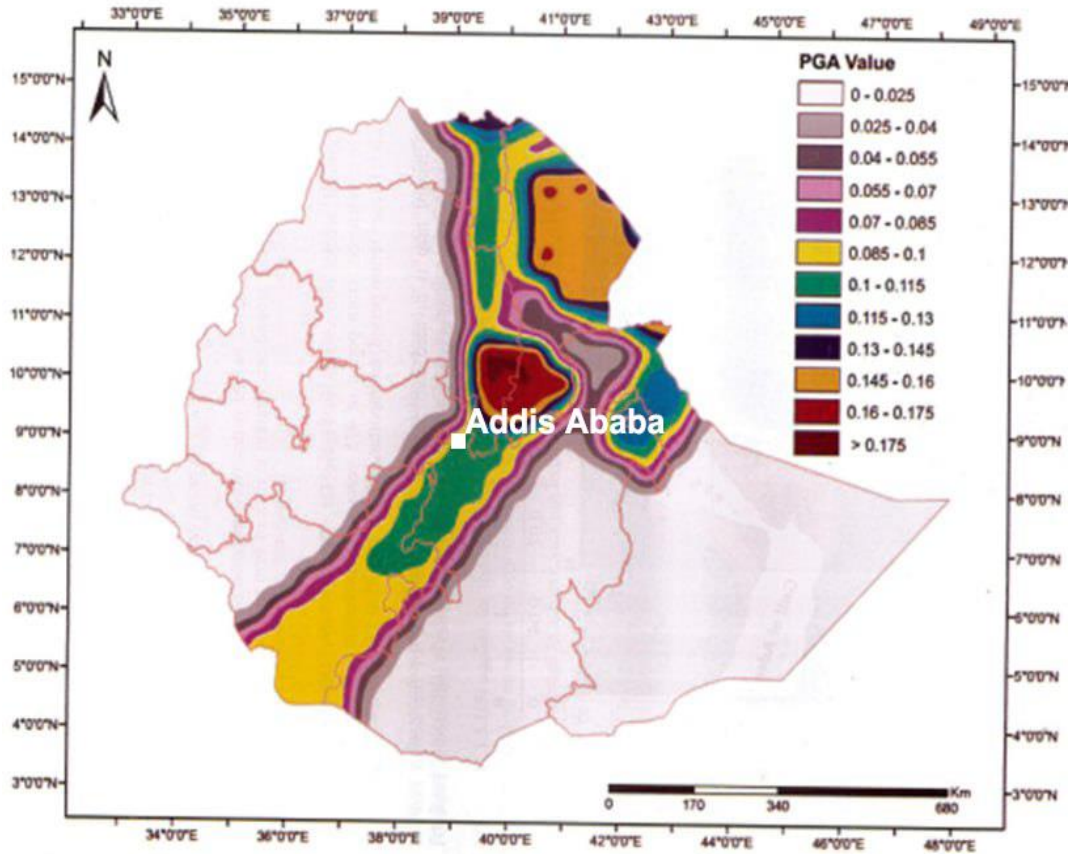


Figure 3-4: Seismic Hazard Map of Ethiopia (ES-EN 1998, 2015)

3.3.3. Global Seismic Hazard Assessment Program (GSHAP)

The Global Seismic Hazard Assessment Program (GSHAP) is an international initiative launched in the early 1990s to evaluate seismic hazards globally. It aims to develop standardized methodologies for seismic hazard assessment. GSHAP estimates the likelihood of future earthquakes using a probabilistic method that takes into account geological features and previous seismicity. A global seismic hazard map defined in terms of PGA values, assuming a 10% risk of exceedance in 50 years (return period of 475 years), was one of the initiative's primary deliverables, which was widely acknowledged (Giardini, Domenico , Grunthal Gottfried, n.d., 1999).

These hazard maps inform decision making processes related to land use planning, building codes, and infrastructure development. Figure 3-5 shows the seismic hazard map from GSHAP for the region containing Ethiopia.

The PGA value for the city, extracted from the widely acknowledged GSHAP Seismic Hazard Map shown in Figure 3-5, stands at 0.11 g, serving as the basis for this study.

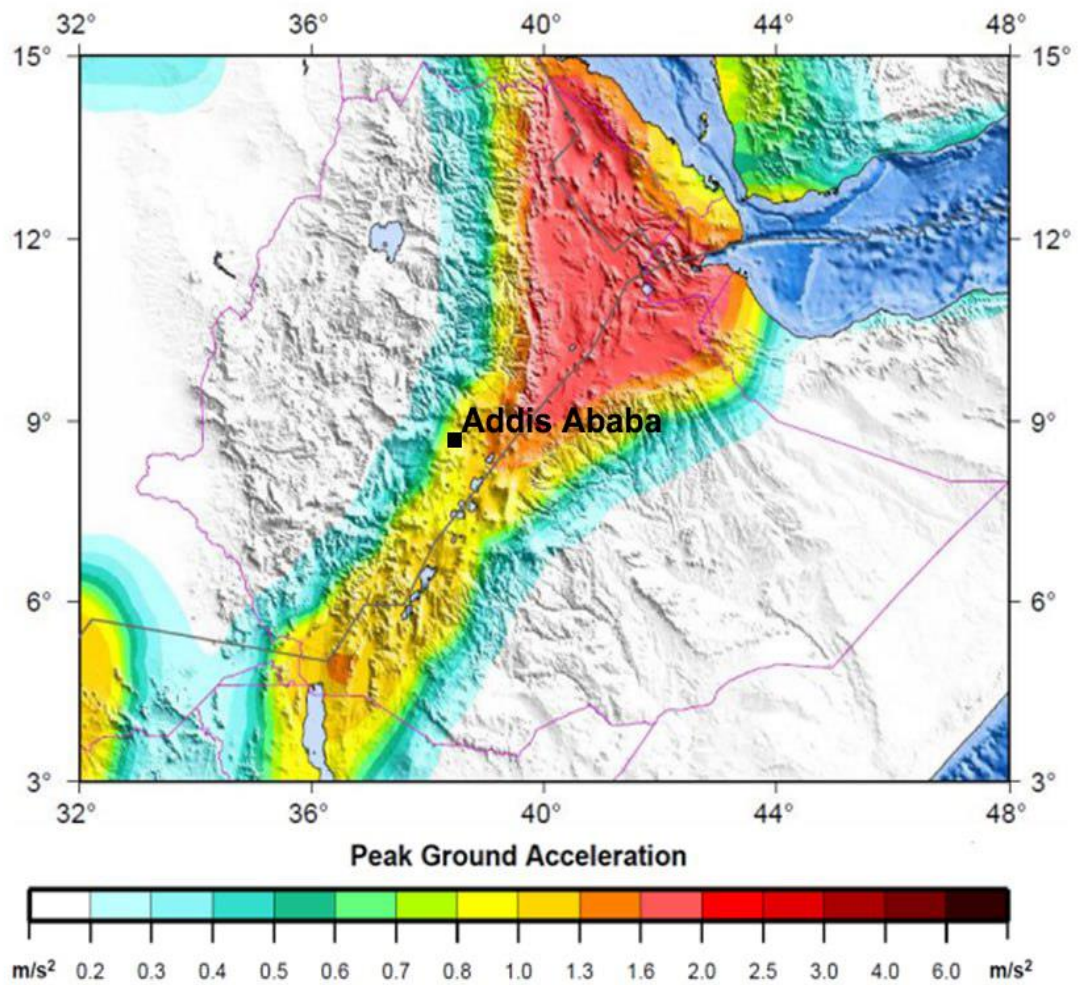


Figure 3-5: Seismic hazard map of Ethiopia based on the GSHAP data

CHAPTER FOUR

4. INPUT SOIL DATA AND METHODS

Input soil data for dynamic analysis is essential for representing soil behavior under seismic conditions. Shear wave velocity (V_s) is a valuable indicator of the dynamic properties of a soil due to its inherent relationship with low strain level stiffness of the soil (G_{max}). There are numerous field and laboratory tests available to characterizing the behavior of soils under stress and strain in ground response analysis (Gashaye, 2018). This study uses shear wave velocity and representative input soil data for two - dimensional ground response analysis.

Two different methods have been used to ascertain the shear wave velocity profiles of the sites selected for this indicative study. These are correlations between standard penetration tests from geotechnical testing and multi-channel analysis of surface waves from geophysical tests.

4.1.Data collection

Geotechnical investigation reports and geophysical survey data are sources of crucial information required for the ground response studies. The geotechnical data comes from different consulting firms that have carried out geotechnical studies for various projects in South – Western part of Addis Ababa. And the author performs the geophysical tests in order to gather the necessary soil characteristics.

4.1.1. Data from Geotechnical investigation reports

For this study, geotechnical investigation reports are gathered from both governmental institutions and private companies, covering project sites spanning various sectors within the study area. Selection criteria are carefully applied, considering factors such as investigation depth, soil thickness above underlying rock formations, and suitability for seismic surveys. The chosen sites are characterized by investigation depths exceeding 30 meters, ensuring sufficient data acquisition for comprehensive analysis. By incorporating reports from diverse sources and adhering to precise selection criteria, the study aims to obtain a holistic understanding of subsurface conditions and seismic response across the study area. This approach ensures that the resulting findings are robust and reflective of the geological variability present within the region.

The geotechnical report has been collected from ARCON Design Build PLC, Tracon Trading PLC, DMC real estate, AL EHWAN real estate, Limay real estate, SABA Engineering PLC, JDAW Consulting Architects & Engineers PLC, Ethiopian Construction Design and Supervision Works Corporation, JEROCCIA Geotechnical Services and Engineering PLC., BEST Consulting Engineers PLC, TURAB Geotechnical Engineering, and ADDIS GEOSYSTEMS PLC.

The corrected Standard Penetration Test (SPT) values are used to correlate shear wave velocity (V_s) with the number of blows obtained during the test. This correlation allows for estimating V_s profiles in the subsurface based on SPT data, providing valuable information for seismic site characterization and geotechnical engineering analyses. (Bowles, 1996). Equipment from different manufacturers has a large variety of drilling rigs in current use. By adjusting SPT values to account for factors such as energy efficiency, rod friction, and hammer efficiency, the corrected SPT values improve the accuracy of V_s predictions and enhance the reliability of seismic hazard assessments.

In accordance with the guidelines provided by ES EN 1998: 2015 regulation, SPT data are adjusted to a 60% reference energy ratio. Factors requiring correction include energy ratio, rod length, borehole diameter, and sample procedure (Getu, 2023).

The following equation was proposed by (Martin & Lew, 1999) for the SPT-N values correction.

$$N_{60} = N_m C_N C_E C_B C_R C_S \quad (4.1)$$

Where:

N_{60} = corrected SPT-N value

N_m = measured standard penetration resistance

C_N = overburden pressure correction factor

C_E = hammer energy ratio (ER) correction factor

C_B = borehole diameter correction factor

C_R = rod length correction factor

C_S = sampling method correction factor

Shear wave velocity is correlated using the corrected SPT-N measurements. Table 4-1 provides suggested correlation equations by (Wair et al., 2012) for various soil types, clays and silts, sands, and gravels.

The equations are typically written as follows:

$$V_s = aN_{60}^b(\sigma_v')^c \quad (4.2)$$

Where;

a, b and c are regression coefficients,

N_{60} is corrected SPT value and σ_v' is effective overburden stress.

Table 4-1: Recommended SPT–stress– V_s correlation equations after (Wair et al., 2012)

Soil Type	Shear Wave Velocity, v_s (m/s)
All soils	$30N_{60}^{0.215}(\sigma_v')^{0.275}$
Clays and Silts	$26N_{60}^{0.17}(\sigma_v')^{0.32}$
Sands	$30N_{60}^{0.23}(\sigma_v')^{0.23}$
Gravels-Holocene	$53N_{60}^{0.19}(\sigma_v')^{0.18}$
Gravels-Pleistocene	$115N_{60}^{0.17}(\sigma_v')^{0.12}$

In order to estimate the shear wave velocities, all adjustments and correlations are carefully applied to the SPT data of the chosen sites. The correlation equation used for this study is $30N_{60}^{0.215}(\sigma_v')^{0.275}$, since it governs all types of soil. Table 4-2, Table 4-3 and Table 4-4 provide an overview of the shear wave velocity profiles that are computed for this study.

Site specific Ground Response Analysis at South - Western part of Addis Ababa

Table 4-2: Summary of raw and adjusted SPT data and shear wave velocity profiles of the sites

Akaki Kality sub city				Kirkos sub city				Kolfe Keranyo sub city			
Depth (m)	SPT-N values	corrected SPT-N values	V _s (m/s)	Depth (m)	SPT-N values	corrected SPT-N values	V _s (m/s)	Depth (m)	SPT-N values	corrected SPT-N values	V _s (m/s)
2	22	15	144	2	23	16	148	2	6	4	109
4	22	17	178	4	27	21	190	4	6	5	134
6	10	9	173	6	21	18	206	6	19	17	199
8	9	8	183	8	17	15	210	8	21	18	220
10	9	8	194	10	19	17	233	10	36	33	261
12	9	8	207	12	25	23	262	12	45	41	293
14	6	6	198	14	24	22	271	14	46	42	307
16	9	8	226	16	39	36	314	16	42	39	314
18	15	14	262	18	33	30	311	18	43	39	329
20	11	10	249	20	37	34	330	20	48	44	342
22	10	9	246	22	46	42	358	22	50	46	348
24	23	21	307	24	50	46	373	24	50	46	362
26	27	25	324	26	50	46	381	26	50	46	370
28	36	33	347	28	50	46	389	28	50	46	372
30	50	46	385	30	50	46	397	30	50	46	385

Table 4-3: Summary of raw and adjusted SPT data and shear wave velocity profiles of the sites

Nifas silk lafto sub city - 1				Nifas silk lafto sub city - 2				Nifas silk lafto sub city - 3			
Depth (m)	SPT-N values	corrected SPT-N values	V _s (m/s)	Depth (m)	SPT-N values	corrected SPT-N values	V _s (m/s)	Depth (m)	SPT-N values	corrected SPT-N values	V _s (m/s)
2	7	5	113	2	7	5	111	2	19	13	140
4	10	8	151	4	7	5	140	4	18	14	172
6	17	15	197	6	8	7	165	6	21	18	206
8	24	21	230	8	9	8	186	8	23	20	228
10	29	27	258	10	10	9	198	10	16	15	223
12	34	31	280	12	10	9	212	12	27	25	262
14	24	22	272	14	12	11	230	14	42	39	305
16	41	38	316	16	11	10	234	16	42	39	317
18	42	39	323	18	38	35	320	18	36	33	317
20	45	41	339	20	15	14	266	20	43	39	334
22	50	46	360	22	50	46	348	22	45	41	346
24	50	46	368	24	50	46	362	24	48	44	359
26	50	46	375	26	50	46	370	26	50	46	370
28	50	46	383	28	50	46	372	28	50	46	378
30	50	46	390	30	50	46	385	30	50	46	385

Table 4-4: Summary of raw and adjusted SPT data and shear wave velocity profiles of the sites

Lideta sub city-1				Lideta sub city-2			
Depth (m)	SPT-N values	corrected SPT-N values	V _s (m/s)	Depth (m)	SPT-N values	corrected SPT-N values	V _s (m/s)
2	11	8	124	2	7	5	103
4	13	10	161	4	17	13	158
6	14	12	190	6	18	16	182
8	9	8	184	8	17	15	192
10	10	9	202	10	10	9	201
12	10	9	215	12	10	9	209
14	30	28	286	14	16	15	243
16	30	28	296	16	19	17	265
18	32	29	310	18	50	46	335
20	32	29	313	20	42	39	337
22	20	18	291	22	38	35	338
24	23	21	308	24	50	46	363
26	50	46	379	26	50	46	370
28	50	46	387	28	50	46	378
30	37	34	368	30	50	46	385
32	37	34	375				
34	22	20	341				
36	25	23	357				
38	36	33	392				
40	37	34	400				

4.1.2. Data from Geophysical investigation

Geophysical investigations data is required to complement geotechnical data for a more comprehensive understanding of subsurface conditions. Geophysical methods can provide insights into soil and rock properties and potential geological hazards such as faults or voids. This information is valuable for site characterization, foundation design, and assessing the feasibility and risks of construction projects.

For both passive surveys made from natural waves with depth results and active surveys provided by the author, multi-channel analysis of surface waves (MASW) has been performed. Combining the results of both tests offers a more comprehensive characterization of the area's subsurface conditions. This integrated approach ensures a more accurate assessment of the geological and geotechnical properties, enhancing the overall understanding of the site.

4.1.2.1. Equipment used for the seismic survey

The seismic survey equipment for Multi-Channel Analysis of Surface Waves (MASW) includes a hammer and strike plate for generating seismic waves, geophones deployed in arrays or along spread cables to detect ground motion, a seismograph for recording seismic waves, and a laptop for data acquisition and control.

a. Hammer and strike plate

In a seismic survey, the hammer is utilized to strike the strike plate firmly, generating a seismic wave that travels through the subsurface layers. This wave progresses downward until encountering an interface between different geological materials.

The hammer and strike plate constitute integral elements of the seismic source, furnishing a controlled and replicable means of generating seismic waves. They are frequently employed alongside geophones to capture the arrival times of seismic waves, facilitating the determination of subsurface properties. The amount of energy that may be used is determined by skill, energy, and the state of the ground. More studies will require more effort to find a realistic representation of the site. Figure 4-1 shows hammer and strike plate respectively.



Figure 4-1: Hammer and strike plate

b. Geophones and spread cables

Geophones are sensors used in seismic surveys to detect ground vibrations caused by seismic waves. They typically consist of a coil of wire attached to a magnet, suspended in a magnetic field. When ground vibrations occur, the movement induces a current in the wire coil, which is then recorded by the seismograph. Spread cables are used to connect multiple geophones in an array, allowing for simultaneous recording of seismic data from different locations. This setup provides valuable information about the propagation of seismic waves through the subsurface and helps to create detailed images of the Earth's structure.

Seismographs and geophones are connected via spread cables as indicated in Figure 4-3. Electrical takeout, or connection points, are dispersed along the length of a standard telephone wire. To connect the geophones to the geophone cables at certain takeout points, the geophone cable must be deployed with a takeout positioned at the geophone location. One takeaway cable can be used to link geophones to the seismograph. The 24 take-outs on the cable can accommodate a maximum of 24 geophones at once. To increase reception, geophones must be firmly buried in the ground. Figure 4-2 is one of the 24 geophones used for the seismic survey.



Figure 4-2: Geophone



Figure 4-3: Geophone and spread cable

c. Seismograph

A seismograph is used to detect and record seismic waves from earthquakes and other ground motions. In the context of the Multichannel Analysis of Surface Waves (MASW), seismographs are crucial for capturing surface waves generated by passive and active seismic sources. Then the results are recorded on a computer. A geode, specific type of Seismograph is indicated in Figures 4-4.



Figure 4-4: Seismograph

4.1.2.2. Data from Multi channel Analysis of surface waves (MASW)

Data has been collected from four sites using multi-channel analysis of surface waves (MASW), both for active and passive surveys. The geophones, each with a natural frequency of 4.5 Hz, are positioned in various configurations across the test site to capture wave motion resulting from seismic activity. The geophones are arranged in a straight line for both active and passive surveys. And an L-shaped arrangement of geophones is employed for passive surveys.

These geophones are tasked with recording wave motion over time following the generation of waves at designated shot points along the lineup. The waves are induced using an impact load delivered by a 10 kg hammer. Through these setups, the geophones provide valuable data regarding the propagation and characteristics of seismic waves, enabling researchers to analyze subsurface structures and properties with precision.

The results from multi-channel analysis of surface waves (MASW) are extracted and inverted under the guidance and control of a crew of applied geophysicists and seismologists. The collected data are presented in Figure 4-5 and Figure 4-6.

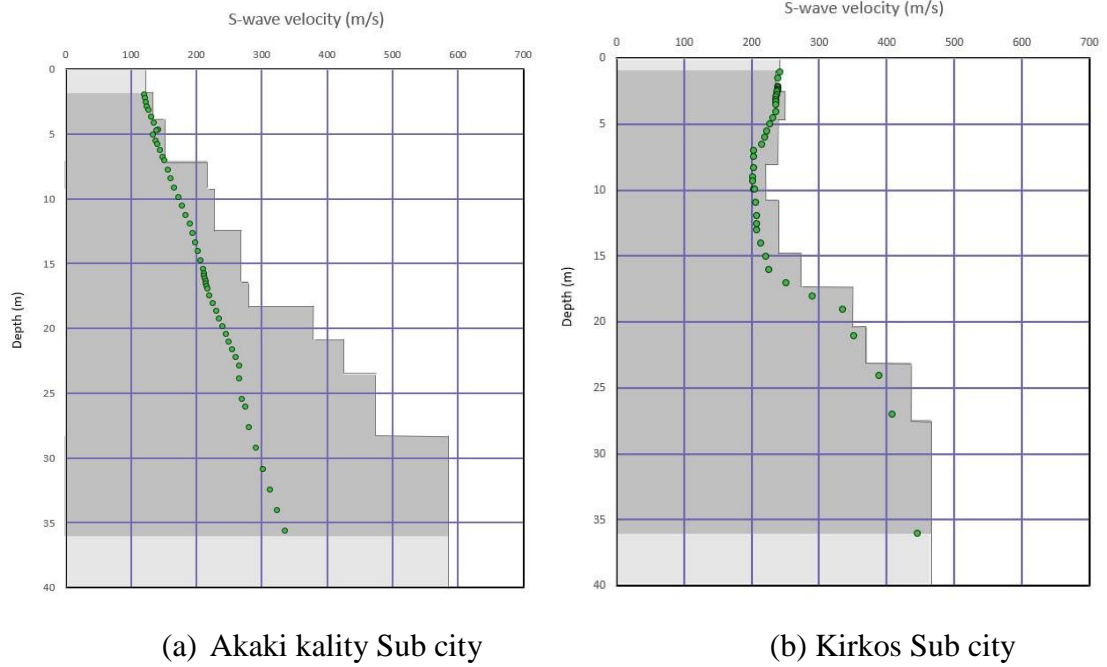


Figure 4-5: Shear wave velocity profiles obtained from the combined dispersion curves: (a) Akaki kality sub city, and (b) Kirkos sub city

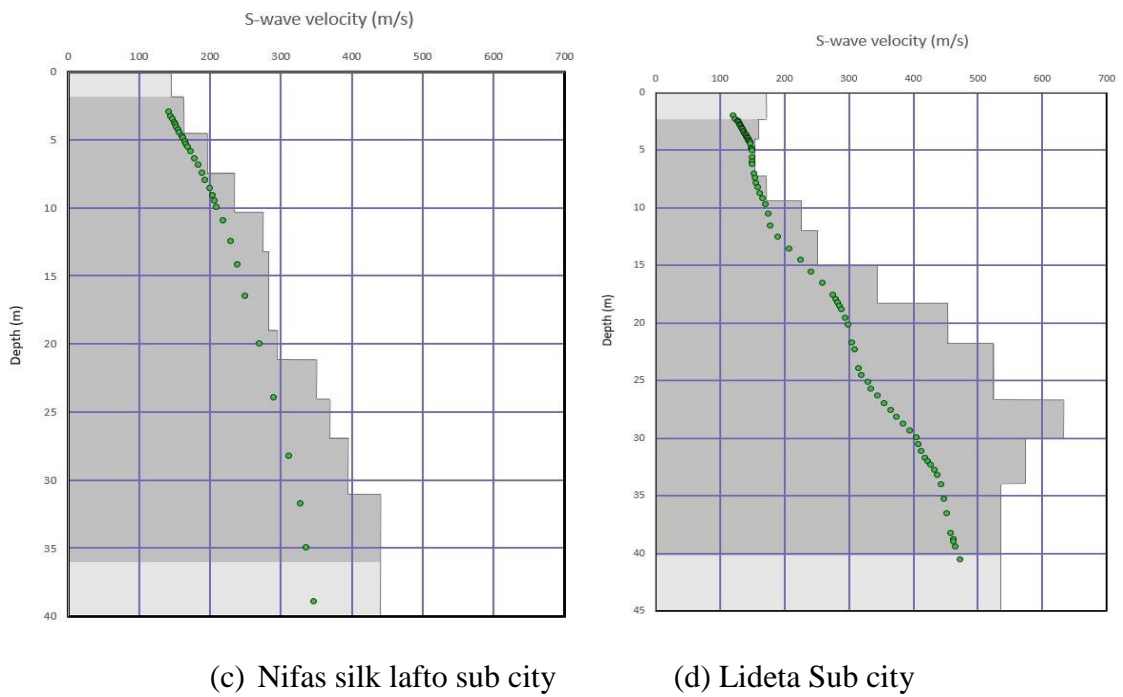


Figure 4-6: Shear wave velocity profiles obtained from the combined dispersion curves: (c) Nifas silk lafto sub city, and (d) Lideta Sub city

The locations of the sites for the SPT data in the South - Western part of Addis Ababa are presented in Figure 4-7.

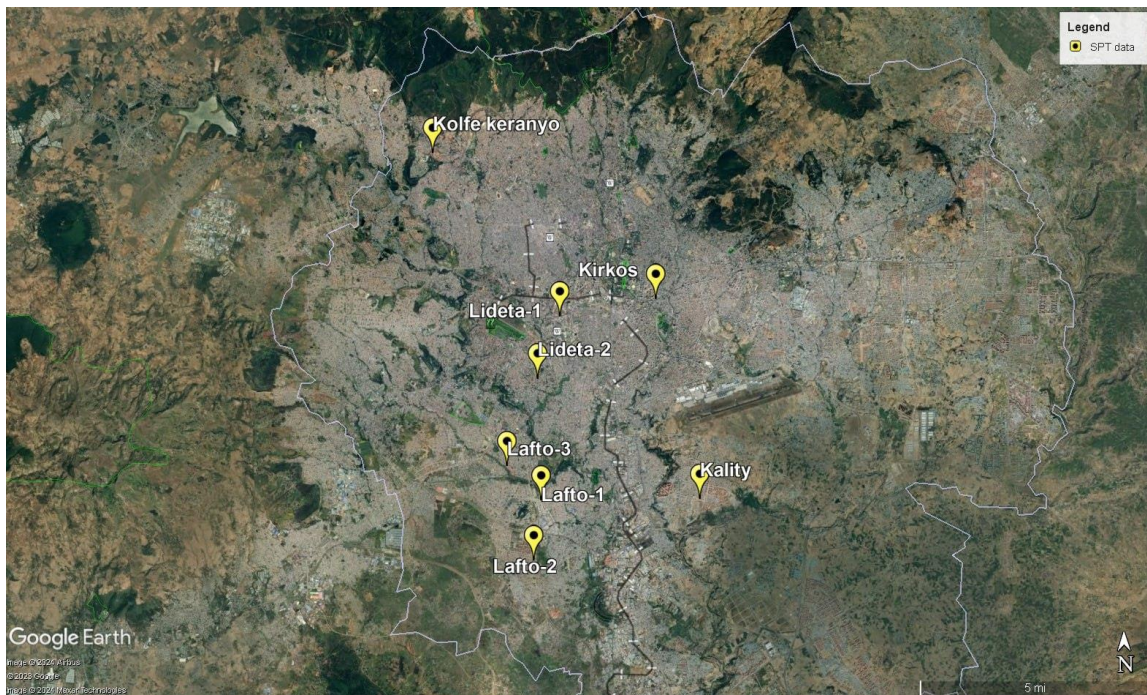


Figure 4-7: Locations of SPT data

The locations of the sites for the Seismic survey in the South - Western part of Addis Ababa are presented in Figure 4-8.

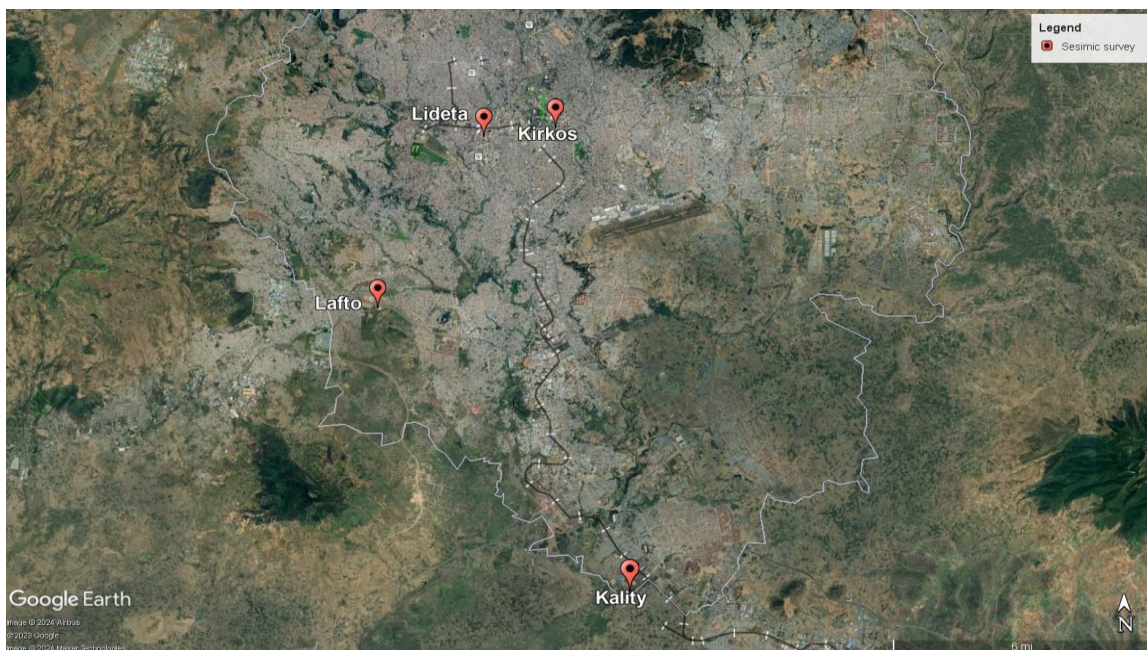


Figure 4-8: Locations of Seismic survey test

The Location of all the sites selected for the study are presented in Figure 4-9 and Table 4-5.

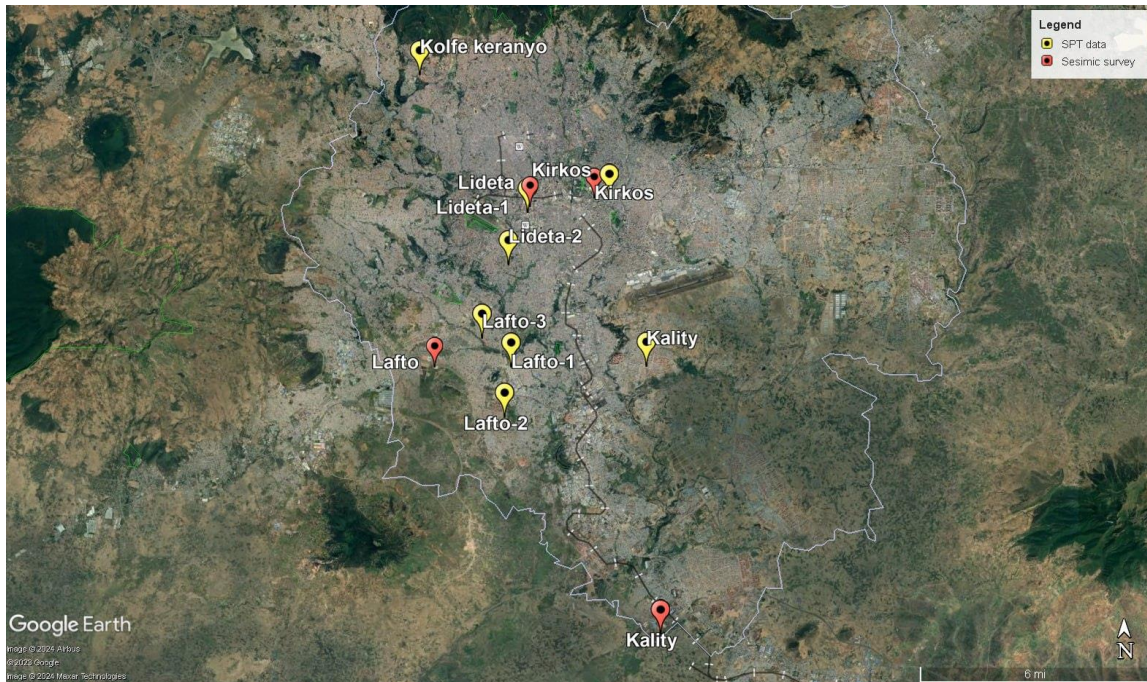


Figure 4-9: Location of all the sites selected for the study

Table 4-5: Location of all the sites selected for the study

Sub city	SPT-N data		Seismic survey	
	Easting	Northing	Easting	Northing
Akaki Kality	476535	989093	477030	977968
Kirkos	471641	995736	474453	996043
Kolfe Keranyo	467343	1000926		
Nifas silk Lafto-1	470988	989112	467857	989120
Nifas silk Lafto-2	470702	987042		
Nifas silk Lafto-3	471024	990105		
Lideta -1	471724	995473	471820	995649
Lideta-2	470831	993316		

4.2. Site Response Analysis

The one-dimensional approach to ground response analysis is helpful for flat or gently sloping sites with parallel material boundaries, as mentioned in Section 2.2.1. The study area contains various areas that are neither flat nor gently sloping.

One-dimensional analysis has limitations that are resolved by two-dimensional analysis, which provides a more realistic representation of the area. Dealing with sloping or uneven ground surfaces, walls and tunnels, and heavy or stiff embedded structures requires two-dimensional analysis (Kramer, 1996). And, three-dimensional analysis needs to be conducted for heavy structures with complex geometries and loading conditions. Since the site condition for this study varies moderately, it is sufficient to conduct two-dimensional ground response analysis. As a result, two-dimensional ground response analysis is employed for this study.

Two dimensional Ground Response Analysis

Two-dimensional ground response analysis uses the finite-element method, which treats a continuum as an assemblage of discrete elements whose boundaries are defined by nodal points and assumes that the response of the continuum can be described by the response of the nodal points.

The equations for the two dimensional ground response analysis are given by (Kramer, 1996) . Using the strain-displacement and stress- strain relationships, an element stiffness matrix can be written as follows:

$$[K_e] = \int_{-1}^1 \int_{-1}^1 [B]^T [D] [B] |J| d_s d_t \quad (4.3)$$

Where:

[B] is strain- displacement matrix,

[D] is stress-strain matrix

|J| is the Jacobian

The strain-displacement matrix [B], allows the strains to be determined from the nodal point displacements.

$$\{\varepsilon\} = [B] \{q\} \quad (4.4)$$

The stress-strain matrix, [D], relates stresses to strains:

$$\{\sigma\} = [D]\{\varepsilon\} \quad (4.5)$$

And the Jacobian |J|,

$$|J| = \sum_{i=1}^4 \sum_{j=1}^4 x_i \left(\frac{\partial N_i}{\partial S} \frac{\partial N_j}{\partial t} - \frac{\partial N_i}{\partial t} \frac{\partial N_j}{\partial S} \right) y_j \quad (4.6)$$

where:

[N] is the shape function

A consistent element mass matrix can be written, assuming constant density within the element, as:

$$[m_e] = \rho \int_{-1}^1 \int_{-1}^1 [N]^T [N] |J| d_s d_t \quad (4.7)$$

A consistent damping matrix can be obtained from:

$$[c_e] = \int_{-1}^1 \int_{-1}^1 [B]^T [\eta] [B] |J| d_s d_t \quad (4.8)$$

Where [\eta] is a matrix of damping terms

Then the equation of motion for the element can be written as:

$$[m_e]\{\ddot{q}\} + [c_e]\{\dot{q}\} + [k_e]\{q\} = \{Q(t)\} \quad (4.9)$$

The element force vector is given by:

$$\{Q(t)\} = \int_{-1}^1 \int_{-1}^1 [N]^T \{W\} |J| d_s d_t + \int_S [N]^T \{T\} d_s \quad (4.10)$$

Where:

\{W\} is the vector of prescribed body forces

\{T\} is a vector of external tractions that may be applied to some surface, S.

Once the equations of motion for each element are obtained, they are combined in a way that satisfies compatibility of displacements to obtain the global equations of motion.

$$[M]\{\ddot{u}\} + [C]\{\dot{u}\} + [K]\{u\} = \{R(t)\} \quad (4.11)$$

Where:

[M] is the global mass matrix,

[C] is the global damping matrix,

[K] is the global stiffness matrix,

{u} is the global nodal point displacement vector, and

{R(t)} is the global nodal point force vector.

For the case of loading induced by base motion, the global equation of motion is

$$[M]\{\ddot{u}\} + [C]\{\dot{u}\} + [K]\{u\} = -[M]\{1\}\ddot{u}_{b(t)} \quad (4.12)$$

4.3. Soil Geometry and Properties

The soil parameters employed in this study under the Mohr- Coulomb method are stated under the following sections.

4.3.1. Unit weight (γ)

A soil's unit weight, which is defined as its weight per unit volume, is frequently used to characterize a soil's density. When designing a foundation and determining the study area's load bearing capacity, it is helpful to use typical unit weights of soil. The unit weight of soil can be directly measured in the field using a nuclear densitometer, rubber balloon, or sand cone test. (Wondie, 2020). For this study, unit weight is taken from laboratory tests conducted on the secondary data.

4.3.2. Void ratio (e)

Void ratio of a soil is the ratio of the volume of voids (spaces filled with air or water) to the volume of solid particles in a soil mass. This dimensionless metric affects a soil's strength, permeability, and compressibility depending on how loosely or densely it is packed. Laboratory tests on soil samples are used to determine it. For this study the void ratio is taken from secondary data.

4.3.3. Cohesion (c)

Shear strength of the soil is influenced by its cohesiveness especially for clayey soils. Triaxial shear testing and unconfined compression testing are two common laboratory tests used to assess unconfined compressive strength. There are also correlations with shear strength as estimated from the field using vane shear tests (Wondie, 2020). For this study, the cohesion of the soil has already been determined from the secondary data collected from direct shear test and plastic index value. Correlation equation between cohesion and PI is given according to the equation determined by (Tchakalova & Ivanov, 2022).

$$C = 8.476 + (0.776 * PI)$$

Where: C is cohesion

PI is plastic index

4.3.4. Friction angle (ϕ)

The shear strength of soil caused by internal friction between particles is measured by the friction angle. The friction angle is influenced by the texture and composition of the soil; sandy and granular soils have higher values than clayey soils.

It is typically determined through laboratory tests like the direct shear test or triaxial test and is crucial for analyzing soil stability and load bearing capacity. For this study friction angle is taken from laboratory tests conducted on the secondary data and Correlating SPT data. Correlation equation between friction angle and SPT is given according to the equation determined by (Bowles, 1996).

$$\phi = 28 + 0.15 N$$

where: ϕ is friction angle

N is SPT data

The unit weight, cohesion, friction angle, and void ratio of the soil used for this study under each study area are stated from tables 4-6 to 4-8.

Site specific Ground Response Analysis at South - Western part of Addis Ababa

Table 4-6: Soil geometry and properties

Akaki Kality sub city					Kirkos sub city					Kolfe Keranyo sub city				
depth	unit weight	C	phi	e	depth	unit weight	C	phi	e	depth	unit weight	C	phi	e
2	19	18	25	0.69	2	18	29	23	0.64	2	17	25	30	0.60
4	19	18	25	0.69	4	21	29	23	0.64	4	18	25	31	0.60
6	19	37	30	0.69	6	18	31	25	0.65	6	18	22	32	0.59
8	20	32	30	0.70	8	18	29	24	0.63	8	19	28	36	0.63
10	20	25	30	0.70	10	17	39	33	0.70	10	17	29	37	0.64
12	17	21	32	0.70	12	20	39	33	0.70	12	18	30	38	0.64
14	17	40	31	0.70	14	20	32	32	0.65	14	18	26	36	0.61
16	20	32	32	0.65	16	18	23	21	0.60	16	18	33	39	0.66
18	20	40	33	0.70	18	18	23	21	0.60	18	19	30	39	0.64
20	17	40	33	0.70	20	18	27	22	0.62	20	18	22	40	0.59
22	17	33	32	0.66	22	18	27	22	0.62	22	17	23	40	0.60
24	17	33	35	0.66	24	18	27	22	0.62	24	18	22	40	0.59
26	18	28	37	0.63	26	17	36	38	0.68	26	18	22	40	0.59
28	18	32	38	0.65	28	18	33	37	0.66	28	17	22	40	0.59
30	18	32	39	0.65	30	18	33	37	0.66	30	18	22	40	0.59

Table 4-7: soil geometry and properties

Nifas silk lafto sub city - 1					Nifas silk lafto sub city - 2					Nifas silk lafto sub city - 3				
depth	unit weight	C	phi	e	depth	unit weight	C	phi	e	depth	unit weight	C	phi	e
2	18	20	25	0.66	2	17	24	23	0.60	2	18	22	28	0.59
4	18	25	31	0.70	4	18	24	23	0.60	4	18	22	28	0.59
6	19	24	25	0.60	6	18	22	21	0.59	6	19	22	28	0.59
8	19	24	25	0.60	8	19	19	21	0.57	8	19	8	20	0.50
10	19	24	25	0.60	10	17	20	20	0.58	10	18	8	20	0.50
12	19	28	27	0.63	12	18	22	21	0.59	12	18	8	20	0.50
14	19	28	27	0.63	14	18	16	20	0.55	14	19	8	20	0.50
16	19	20	38	0.58	16	18	22	38	0.59	16	19	8	20	0.50
18	18	28	38	0.63	18	19	18	38	0.56	18	19	8	20	0.50
20	18	25	39	0.61	20	18	28	39	0.63	20	18	29	25	0.64
22	19	24	39	0.60	22	17	29	39	0.64	22	18	29	38	0.63
24	19	24	39	0.60	24	18	29	39	0.63	24	18	29	39	0.63
26	19	26	39	0.61	26	18	28	39	0.63	26	18	29	39	0.63
28	19	26	39	0.61	28	17	29	39	0.63	28	18	29	39	0.63
30	19	26	39	0.61	30	18	29	39	0.63	30	18	29	39	0.63

Table 4-8: soil geometry and properties

Lideta sub city - 1					Lideta sub city -2				
depth	unit weight	C	phi	e	depth	unit weight	C	phi	e
2	18	25	21	0.61	2	13	11	25	0.65
4	18	23	21	0.59	4	14	11	27	0.58
6	19	23	21	0.61	6	14	12	25	0.56
8	18	23	23	0.61	8	13	12	26	0.56
10	18	23	25	0.61	10	18	17	35	0.56
12	19	23	25	0.61	12	17	18	33	0.63
14	19	37	31	0.55	14	18	28	33	0.67
16	19	37	31	0.55	16	18	34	33	0.67
18	19	37	33	0.55	18	18	35	35	0.68
20	18	43	33	0.69	20	19	36	34	0.63
22	18	43	32	0.69	22	19	28	35	0.61
24	18	43	32	0.69	24	18	26	38	0.61
26	20	43	36	0.58	26	18	26	38	0.61
28	20	37	36	0.58	28	18	26	38	0.61
30	19	37	34	0.63	30	18	26	38	0.61
32	19	46	34	0.63					
34	19	50	31	0.63					
36	20	50	31	0.61					
38	19	50	33	0.61					
40	19	50	35	0.61					

4.4. Boundary condition

In finite element analysis, boundary conditions have a significant role since they specify how the model interacts with its environment, guaranteeing that the simulation accurately represents the study area. And for many dynamic response problems, rigid or near rigid boundaries, such as bedrock, are located at considerable distances from the region of interest. This study also considers a representative boundary condition representing the study area.

In the dynamic analysis conducted using PLAXIS 2D, a combination of tied degrees of freedom and a compliant base was employed to simulate the realistic response of the soil under dynamic loading conditions. Tied degrees of freedom are utilized in the x-direction for x_{min} and x_{max} to connect adjacent soil elements and ensure compatibility of displacements, allowing for the accurate representation of soil behavior and interaction between soil layers.

Compliant base was implemented to simulate the influence of the underlying soil strata and boundary conditions on the dynamic response of the system. For the y_{min} , compliant base boundary requirements are taken into account. For earthquake analysis, where the dynamic input is applied at the bottom of the model, this boundary condition is recommended (Edition & Manual, 2021). y_{max} is located at the ground surface, where it remains unconfined. There are no boundaries restricting it at this level. Consequently, the boundary condition is considered to be none.

Incorporating these boundary conditions into the analysis enhances the assessment of seismic performance. Ultimately, this improves the overall understanding and resilience of a site during seismic events.

4.5. Mesh

In order to provide a thorough examination of the stress, strain, or displacement across the soil mass, mesh divides a complex shape into smaller, more manageable components. The accuracy and effectiveness of the simulation are directly impacted by the mesh's quality.

Selecting the appropriate element size for the finite elements is crucial for effectively capturing wave motion in seismic analysis, hence elements sizes are chosen with great

care. The shortest wave length of the element is computed using shear wave velocity and excitation frequency of the soil. The excitation frequency used for this study is according to (Ayele, 2021), which is 45 m/s.

$$\lambda_s = \frac{V_s}{f}$$

Where: V_s , is the shear wave velocity

f , is excitation frequency

λ_s , is the shortest wavelength

To attain the necessary accuracy, the maximum element size for soil was kept at a value smaller than one-fifth to one-eighth of the shortest wavelength (λ_s)(Ayele, 2021). The average element size used for this study is summarized in Table 4-9.

Table 4-9: Average element size

	Title	V_s	λ_s	h_{max}	h_{min}	h_{avg}
1	Akaki Kality secondary (S)	144	3.2	0.64	0.4	0.52
2	Akaki Kality Primary (P)	138	3.06	0.6	0.38	0.5
3	Kirkos S.	146	3.24	0.65	0.41	0.53
4	Kirkos P.	201	4.46	0.89	0.56	0.73
5	Kolfe Keranyo S.	109	2.42	0.48	0.3	0.4
6	Nifas silk lafto S-1	113	2.51	0.5	0.31	0.41
7	Nifas silk lafto S-2	111	2.47	0.49	0.31	0.4
8	Nifas silk lafto S-3	140	3.11	0.62	0.38	0.5
9	Nifas silk lafto P.	147	3.27	0.65	0.41	0.53
10	Lideta S-1	124	2.76	0.55	0.34	0.45
11	Lideta S-2	143	3.18	0.64	0.39	0.52
12	Lideta P.	170	3.78	0.76	0.47	0.62

The mesh size is selected by averaging one-fifth and one-eighth of the shortest wavelength at each site. This ensures that wave behavior is accurately captured while maintaining computational efficiency in the analysis.

CHAPTER FIVE

5. Input Ground Motions

5.1. Introduction

Ground response analysis is not only determined by geotechnical and geophysical results but it needs to have a representative input ground motions. These motions, typically obtained from historical earthquake records or simulated scenarios, offer essential insights into the behavior of the ground during seismic events. Studies recommend using motions recorded at other sites under comparable circumstances to those of the site of interest in the absence of representative ground motions using appropriate filtering mechanisms (Kramer, 1996).

A comprehensive ground motion database that has been collecting, processing, and archiving ground motion data for more than 20 years is the Pacific Earthquake Engineering Research (PEER) database (Kramer, 1996). A variety of appropriate ground motions are selected for this study based on filtering conditions from this data base.

5.2. Input Motions from PEER Ground Motion Database

Using a responsive web tool, it is possible to choose sets of strong ground motion acceleration time series that are typical of design ground motions using the PEER Ground Motion Database (PEER, 2010). It is crucial to apply appropriate filtering criteria for choosing relevant input motion time histories from a pool of available data for ground response investigations since Ethiopia lacks strong ground motion records.

When filtering an input ground motions, some factors to take into account are the magnitude of an earthquake, the geology of the seismic waves' travel path from the source to the site, the site's distance from the causative fault, the fault mechanism, and the local soil conditions at the site (Kramer, 1996).

The appropriate filtering criteria are comprehensively outlined, providing clear guidelines for selecting ground motion data that meet these study needs.

5.2.1. Tectonic Regime

Selecting an appropriate tectonic regime is a fundamental criterion for screening out representative input motions. The process involves choosing records from the same tectonic regime as the area of interest, as employed in this study. Shallow crustal earthquakes are the type of earthquakes that are representative of the Middle Ethiopian Rift (Kebede & Van Eck, 1997). An extensive collection of ground movements from shallow crustal earthquakes in active tectonic regimes around the world are documented in the Next Generation Attenuation (NGA) West 2 ground motion database. Thus, it's determined that this database is suitable for choosing the ground motion in this study.

5.2.2. Definition of Target Spectrum

The response spectrum is also considered in this study to filter a representative input ground motion. ES EN 1998:2015 gives two distinct kinds of reaction spectrum based on the features of the largest earthquake that increased the local threat. When the surface wave magnitude, M_s , of the earthquakes that most significantly contribute to the probabilistic seismic hazard assessment for the site is larger than 5.5, Type 1 reaction spectra are employed; Type 2 response spectra are used when M_s is not greater than 5.5.

There are several intermediate sized ($5.5 < M_s < 6.5$) earthquakes that are characteristic of the seismic activity of the Red Sea, the Ethiopian rift system, and the Gulf of Aden (Kebede & Van Eck, 1997). Since Ethiopia rift system has M_s larger than 5.5 this study uses Type 1 reaction spectra for the ground motion selection.

According to the ES EN 1998:2015, the elastic response spectrum $S_e(T)$ is defined by the following expressions for 5% damping:

$$0 \leq T \leq T_B: \quad S_e(T) = a_g \cdot S \cdot \left[1 + \frac{T}{T_B} \cdot (\eta \cdot 2.5 - 1) \right]$$

$$T_B \leq T \leq T_C: \quad S_e(T) = a_g \cdot S \cdot \eta \cdot 2.5$$

$$T_C \leq T \leq T_D: \quad S_e(T) = a_g \cdot S \cdot \eta \cdot 2.5 \left[\frac{T_C}{T} \right]$$

$$T_D \leq T \leq 4s: \quad S_e(T) = a_g \cdot S \cdot \eta \cdot 2.5 \left[\frac{T_C T_D}{T^2} \right]$$

Where:

$S_e(T)$ is the elastic response spectrum

T is the vibration period of a linear single-degree-of-freedom system;

a_g is the design ground acceleration;

T_B is the lower limit of the period of the constant spectral acceleration branch;

T_C is the upper limit of the period of the constant spectral acceleration branch;

T_D is the value defining the beginning of the constant displacement response range of the spectrum;

S is the soil factor and

η is the damping correction factor with a reference value of $\eta = 1$ for 5% viscous damping

The user defined response spectrum is developed using the peak ground acceleration of 0.11 g for a 475-year return period (10% likelihood of being exceeded in 50 years), as retrieved from GSHAP. The target spectrum is created for ground Type A because rock conditions are frequently used to represent reference site conditions.

For the type A ground condition, the parameters used for the response spectrum are chosen as indicated in Figure 5-1 and Table 5-1.

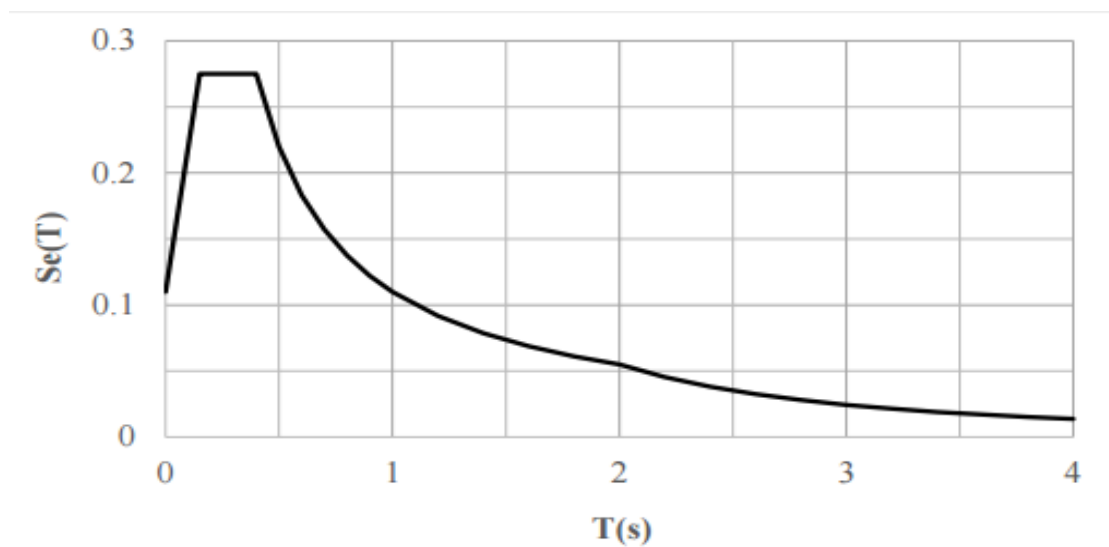


Figure 5-1: Recommended Type 1 elastic response spectrum for Type A ground condition (ES EN 1998:2015)

Table 5-1: Values of the parameters describing the recommended Type 1 elastic response spectrum (ES EN 1998:2015).

Ground type	S	T_B (S)	T_C (S)	T_D (S)
A	1.0	0.05	0.25	1.2
B	1.35	0.05	0.25	1.2
C	1.5	0.10	0.25	1.2
D	1.8	0.10	0.30	1.2
E	1.6	0.05	0.25	1.2

5.2.3. Moment magnitude Range

The moment magnitude range is also selection criteria to select appropriate input ground motion for the seismic analysis. It represents the magnitude of an earthquake event and provides valuable information about the level of ground shaking. Various major zones of seismicity and crustal deformation contributing to seismic hazard exist in Ethiopia and the neighboring countries. Eight seismic source zones can be used to identify the region as the primary source of destructive earthquakes. The observed seismicity and currently understood tectonic properties of each seismic source zone define the seismic hazard of a site (Kebede & Van Eck, 1997).

According to Kebede & Van Eck, 1997, Zone 2 refers to the main Ethiopian rift and the southernmost rifts in Ethiopia. Since this magnitude reflects zone 2, this analysis adopts the upper bound magnitude M_{max} of 7.0 and the lower bound magnitude M_o of 4.0 for the seismic source zone. The PEER database system's ground motion filtering rules have been directly applied to this magnitude range.

5.2.4. Duration of Strong Motion

The duration of the ground motion, or more precisely, the length of the signal's strong portion, must be measured in order to fully characterize the motion (Salmon & Short, 1992). The duration of strong motion provides valuable information about the temporal characteristics of ground shaking during earthquakes, which is essential for assessing structural response and potential damage.

From the moment seismic waves arrive until surrounding waves are restored, a significant portion of the ground motion duration occurs at relatively low shaking levels (Salmon & Short, 1992).

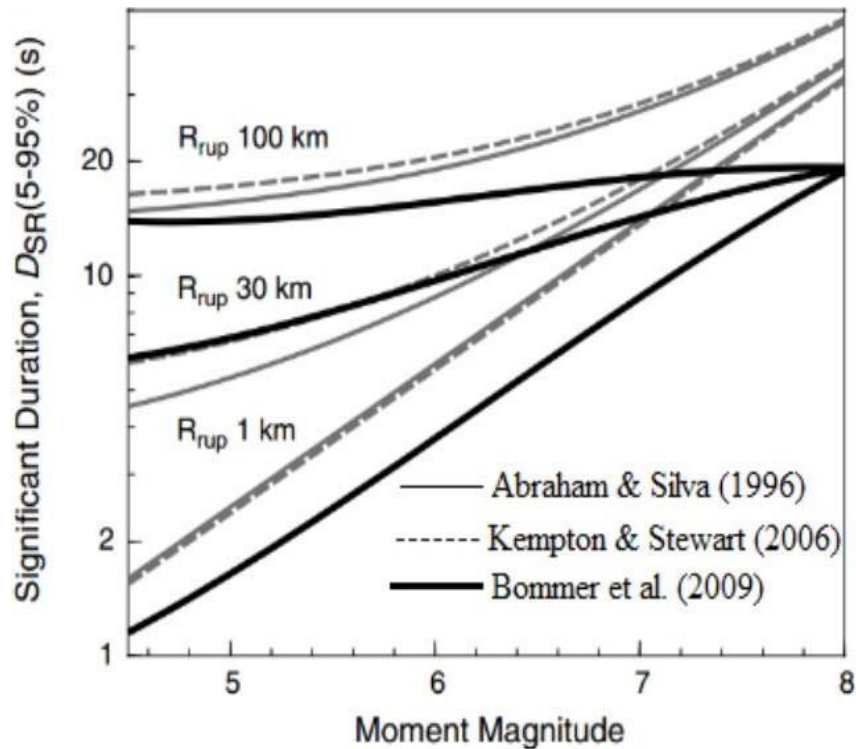


Figure 5-2: Comparison of empirical predictive models for significant duration (Bommer et al., 2009)

Bommer et al., 2009 conducted a brief review of prior studies and, using data from the NGA database, produced a new empirical predictive equation for the significant duration. This relation is used to estimate the duration of shallow crustal earthquakes up to 100 km from the source. Based on this relationship, a shallow crustal earthquake with a minimum magnitude (M_w) of 4 and a maximum magnitude (M_w) of 7 for the seismic source zone is estimated to have a relevant time frame of 17 seconds.

5.2.5. Shear-wave velocity of uppermost 30 meters ($V_{s,30}$)

The shear-wave velocity of the uppermost 30 meters ($V_{s,30}$) is a crucial parameter used in selecting appropriate input ground motion for seismic analysis. It provides valuable information about the stiffness and mechanical properties of the near surface soil layers, which significantly influence the propagation and amplification of seismic waves.

According to ES EN 1998:2015, the reference site condition is represented by rock conditions, ground type A, which has a range of shear wave velocities of 800-1500 m/s. This range is applied as a filtering criterion in the process of input motion selection.

5.2.6. Time Series Scaling

Time series scaling also used to screen the input ground motions by adjusting recorded ground motion time series to match a target response spectrum or ground motion parameters, making it a valuable tool for selecting appropriate input ground motion in seismic analysis.

Two approaches for the coupled tasks of ground motion selection and scaling are considered to be suitable for GRA applications. The first is to match the target spectrum across a certain period range with the spectral ordinates of ground motions. The target spectrum corresponds to the time interval of the buildings that are expected to experience ground motion. The second method considers ground movements according to their spectral shape and scales them so that their pseudo spectral acceleration (PSA) coincides with the required spectrum at a specific period (Stewart, 2014). When a response analysis of a certain structure over a predetermined time frame is required, this method should be applied.

The elastic first mode period (T) of a structure is used to determine the period range, which is $0.2T-2.0T$. Similar ranges dependent on the duration of the structural system under investigation in the overall ground motion analysis will typically be significant in ground response applications (Stewart, 2014). So that this study considered $0.2T-2.0T$ for time series scaling.

According to ES EN 1998:2015, the fundamental periods of vibration T_1 of buildings whose response is not significantly affected by higher modes of vibration is given by:

$$T_1 = \begin{cases} 4T_c \\ 2.0s \end{cases}$$

Where:

T_c is the upper limit of the period of the constant spectral acceleration branch

T_c equals 0.4 seconds for Type 1 response spectrum of ground type A. Hence;

$$T_1 = \begin{cases} 1.6s \\ 2.0s \end{cases}$$

The fundamental period, T_1 , is computed to be 1.6 s and applying the range from $0.2T-2.0T$, a period ranges of 0.32 - 3.2 is taken as a filtering criterion to select the input ground motions.

5.2.7. Collected input motions

As per the criteria explained in this study, five particular ground motions have been selected from the PEER ground motion database for further analysis. The motions are stated in Table 5-2.

Table 5-2: Selected ground motions from PEER ground motion database

5-95% Duration (sec)	EarthquakeName	Year	Station Name	Magnitude	V _{S30} (m/sec)
13.3	Chi-Chi_ Taiwan-02	1999	ILA001	5.9	909.09
16.7	Niigata Japan	2004	FKSH07	6.63	828.95
11.4	Northridge-06	1994	LA - Griffith Park Observatory	5.28	1015.88
10.4	San Fernando	1971	Cedar Springs_ Allen Ranch	6.61	813.48
9.2	Whittier Narrows- 01	1987	Vasquez Rocks Park	5.99	996.43

The acceleration time history plot of each of the five selected ground motions for unscaled and scaled to 0.11g motion is given in Figure 5-3 to Figure 5-12.

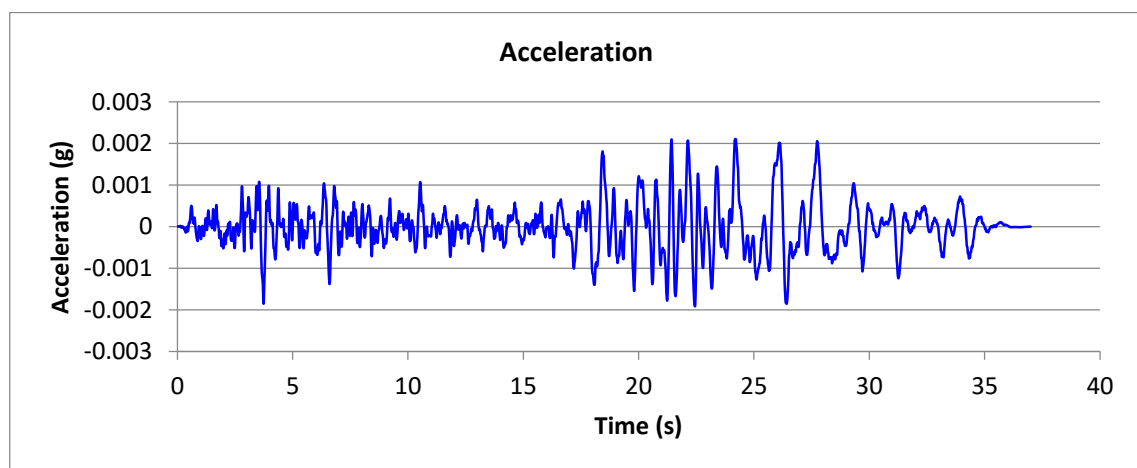


Figure 5-3: Chi chi Taiwan (Unscaled)

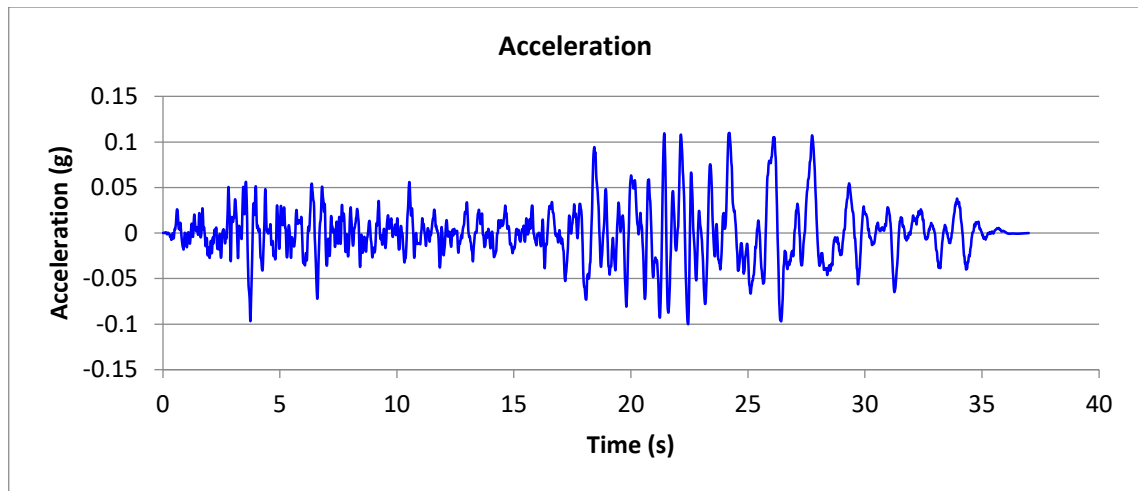


Figure 5-4: Chi chi Taiwan (Scaled to 0.11g)

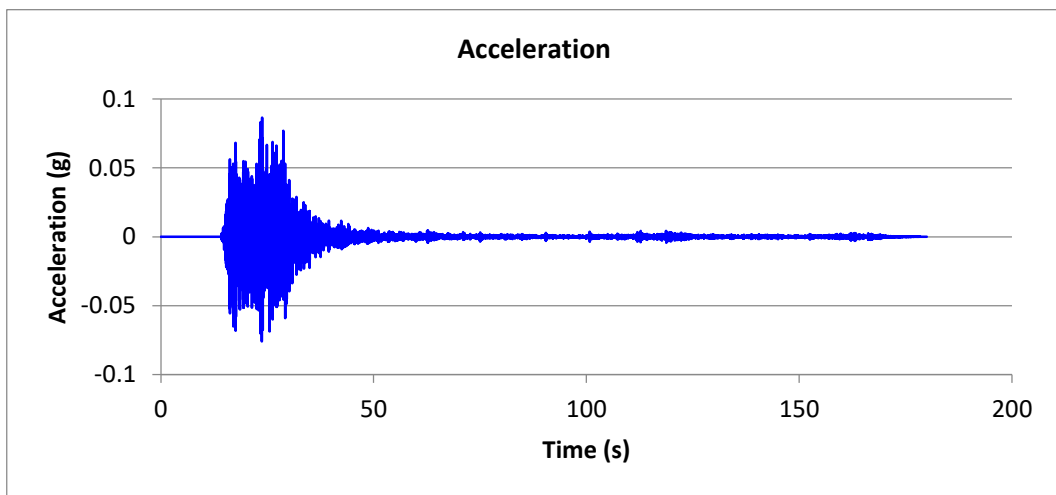


Figure 5-5: Niigata Japan (Unscaled)

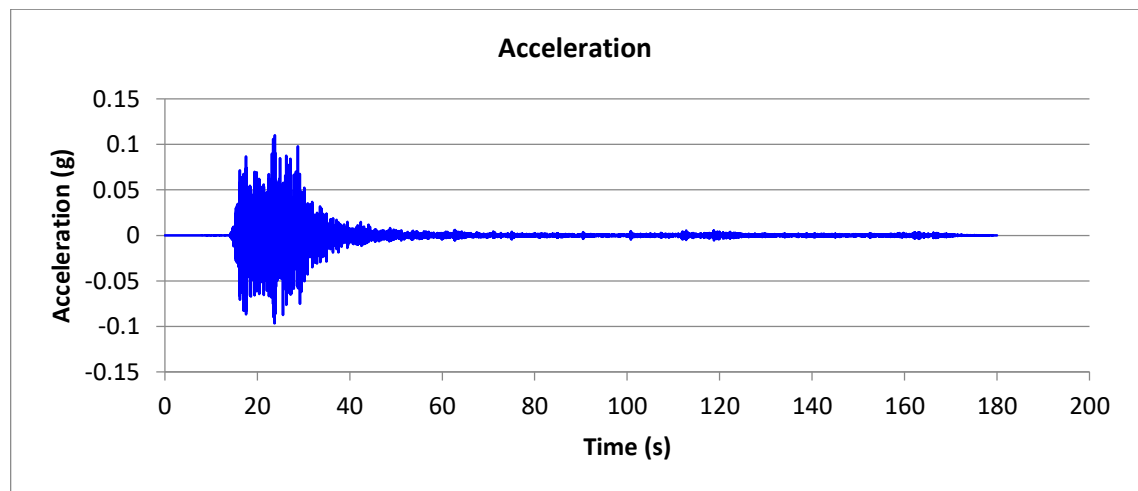


Figure 5-6: Niigata Japan (Scaled to 0.11g)

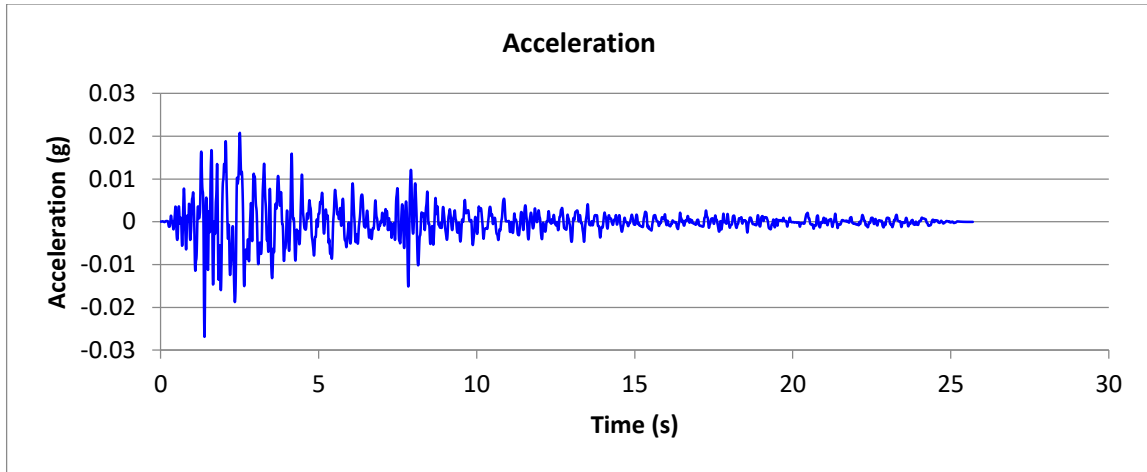


Figure 5-7: Northridge-06 (Unscaled)

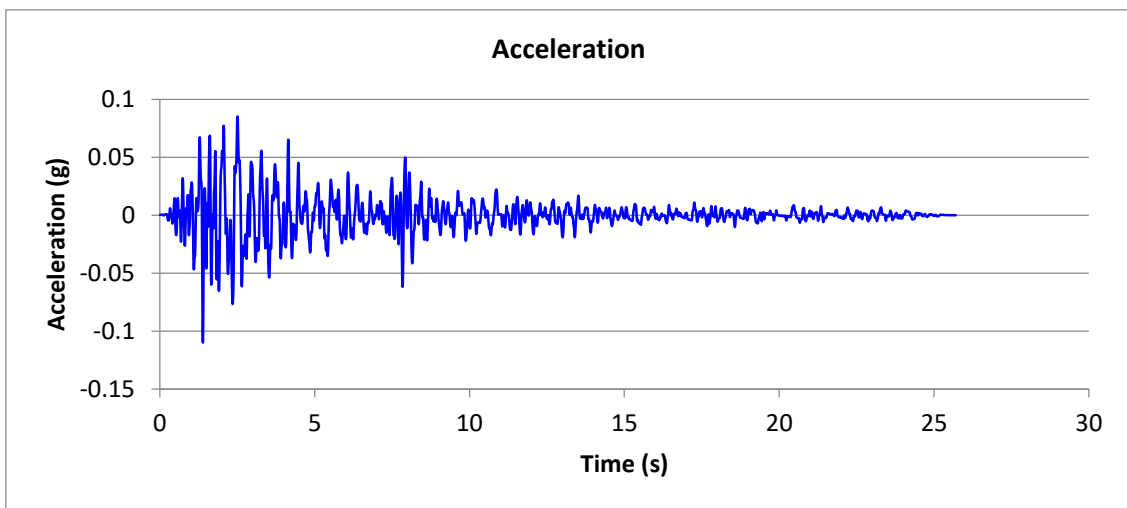


Figure 5-8: Northridge-06 (Scaled to 0.11g)

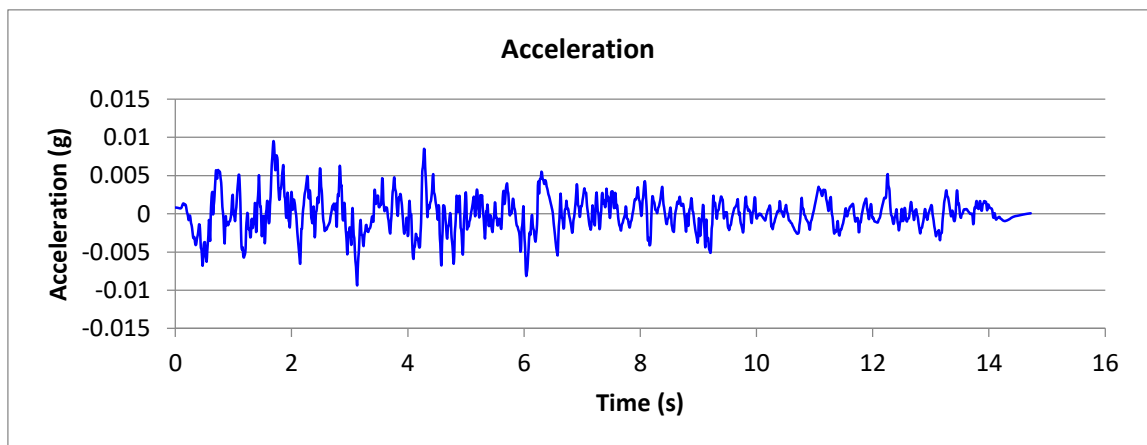


Figure 5-9: San fernando (Unscaled)

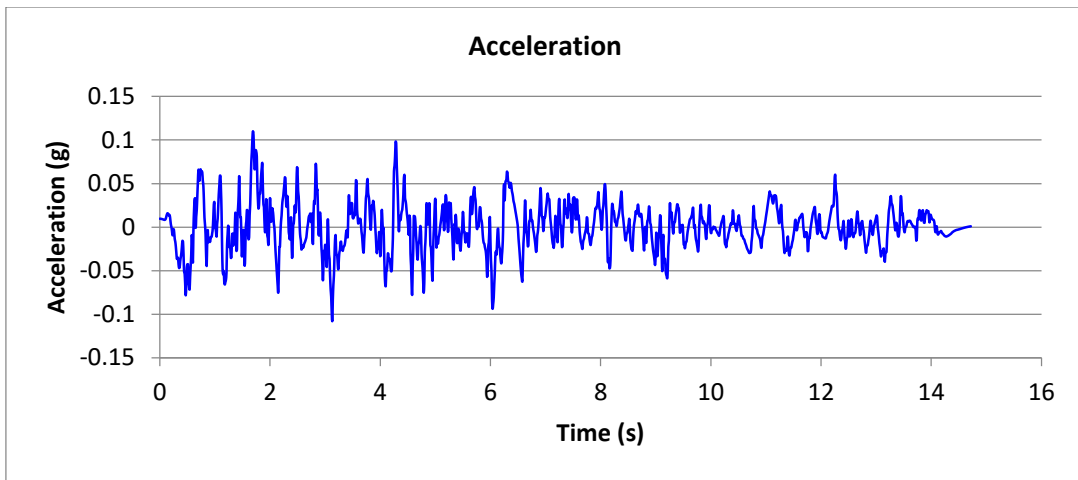


Figure 5-10: San fernando (Scaled to 0.11g)

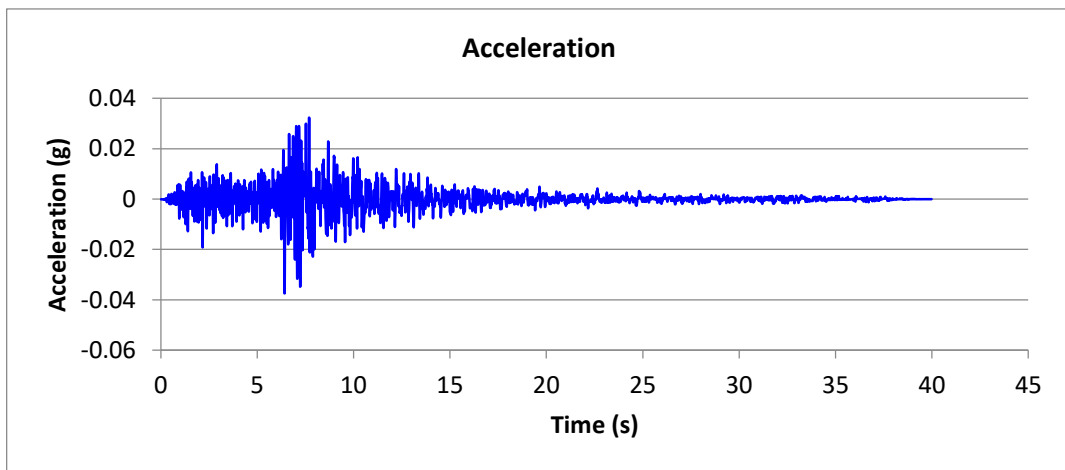


Figure 5-11: Whittier (Unscaled)

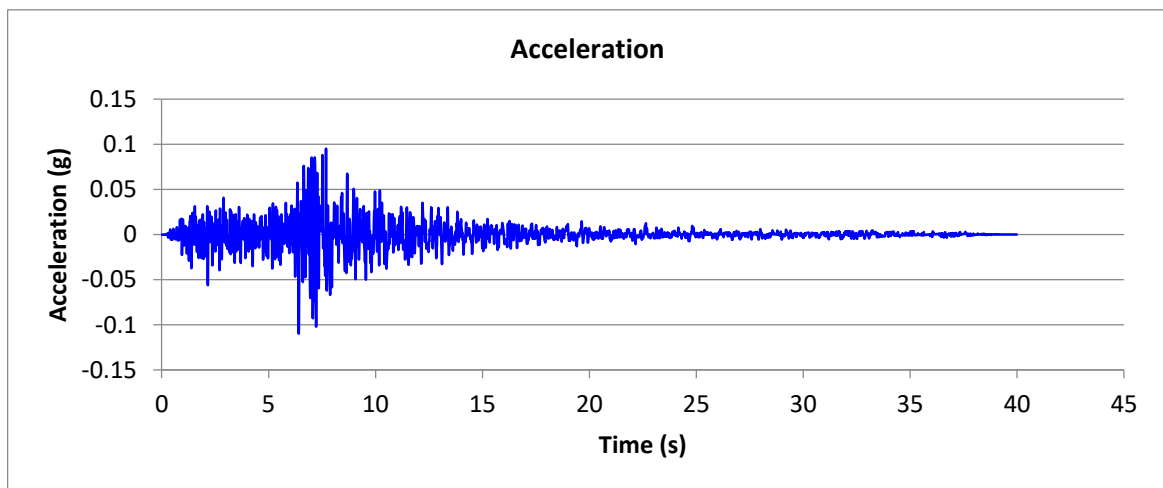


Figure 5-12: Whittier (Scaled to 0.11g)

CHAPTER SIX

6. Analysis and Discussion

After collecting crucial input parameters and input motions, the analysis is conducted using finite element software. Options include FLAC 3D, PLAXIS 2D, PLAXIS 3D, and ABAQUS. For this study, PLAXIS 2D is selected due to its suitability for two-dimensional analysis. This choice ensures accurate and reliable results particularly effective for the study's specific requirements.

The soil model employed in the analysis was the Mohr-Coulomb model, which is commonly used to simulate the nonlinear behavior of soils under dynamic loading conditions. Through the analysis, peak ground acceleration (PGA) and response spectra are generated, providing crucial insights into the soil's response to seismic excitation. Depending on the PGA results obtained, the micro zonation map of the study area is also produced.

6.1. Analysis summary

6.1.1. Peak Ground Acceleration (PGA) results

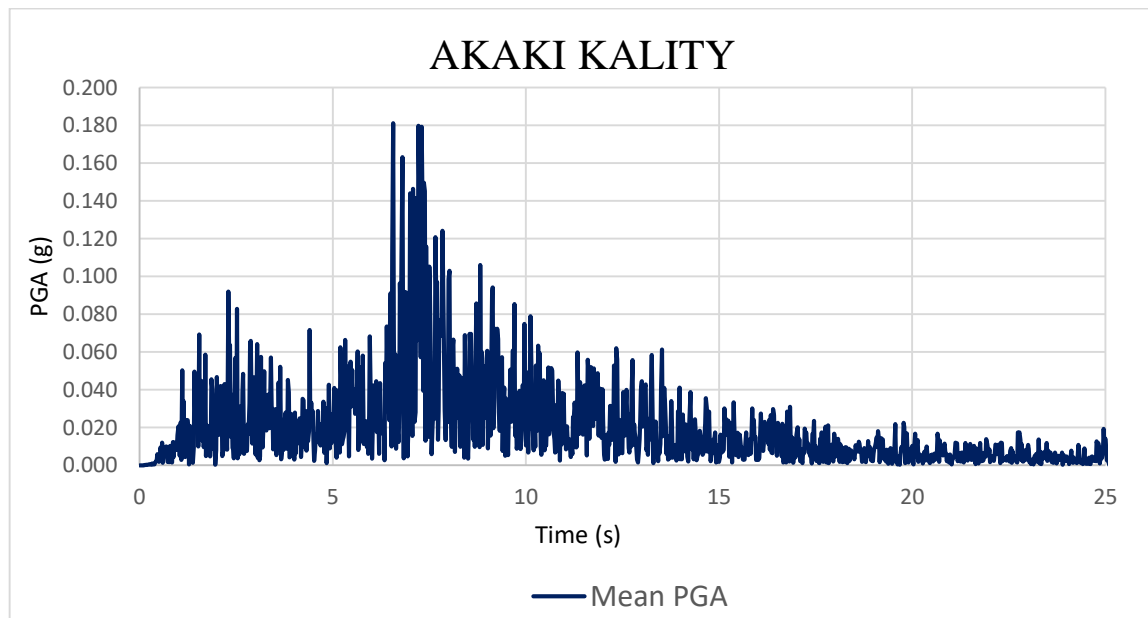
The Peak Ground Acceleration (PGA) distribution at the site's surface over time is analyzed using data from Standard Penetration Test (SPT) and Multi-Channel Analysis of Surface Waves (MASW). In all sites, it is observed that the given input earthquake ground motion, which is scaled to 0.11g, is amplified near the ground surface. This amplification results in surface PGA values varying between 0.14g to 0.29g. The analysis shows an increase in PGA values from the initial ground motion input to the surface. The variation in ground surface PGA indicates the influence of local soil conditions on seismic wave amplification.

For the SPT and MASW tests, the PGA analysis is conducted using five different input motions, as selected in Section 5.2. Each motion's PGA distribution over time is derived from geotechnical and geophysical data. The results of all five motions for each SPT and seismic survey data are comprehensively presented in Appendix A. This approach ensures a detailed analysis of the PGA variations.

PGA results based on SPT data

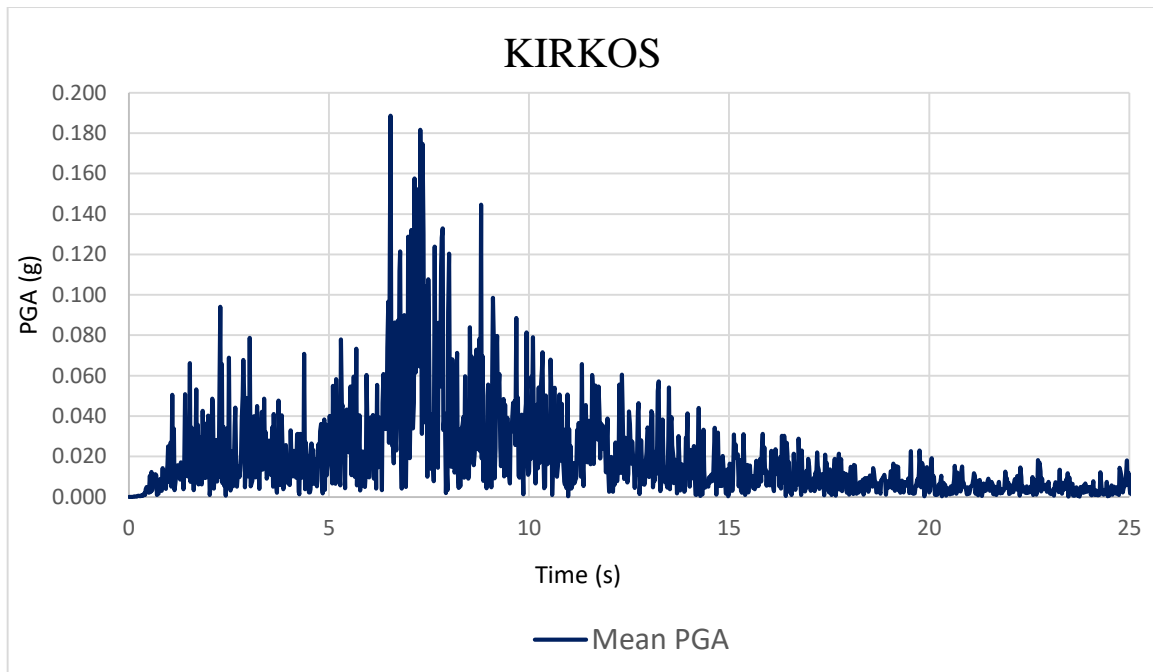
The geotechnical data reveals that the peak ground acceleration (PGA) distribution over time for five different motions shows amplification near the ground surface. Specifically, the absolute PGA value is 0.28g for the Whittier motion analyzed at Kolfe keranyo sub city. The lowest PGA value recorded is 0.17 g for the Northridge-06 motion, observed at Akaki kality sub city. These variations in PGA values highlight the dependence on the input motion considered. The data underscores the variability and amplification of seismic motions as they approach the ground surface, emphasizing the critical nature of site-specific analysis in understanding seismic impacts.

Precise seismic risk assessment requires detailed geotechnical evaluations because different motions and sites produce different PGA values. Figures 6-1 to 6-5 display the mean PGA values, which are obtained by averaging the PGA results of the five earthquake input motions for the site. Appendix A contains the full PGA distribution. The relevant values are shown in Table 6-1.

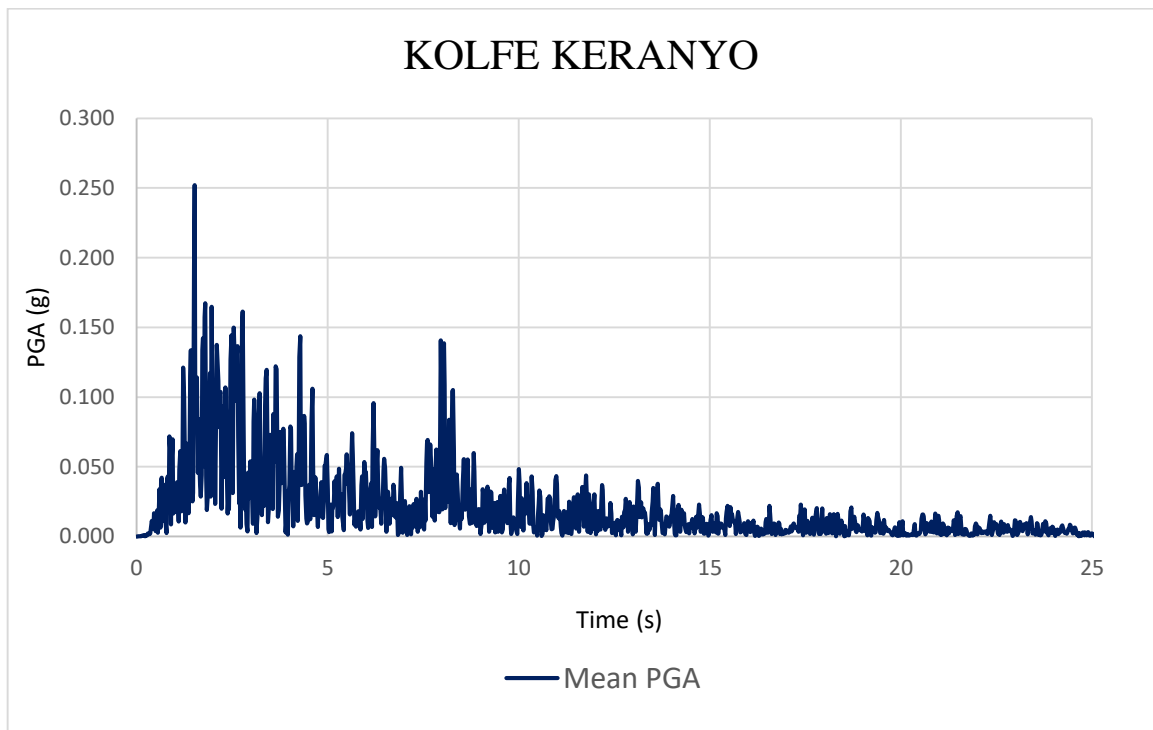


(a)

Figure 6-1: Mean PGA chart obtained from SPT data: (a) Akaki kality:

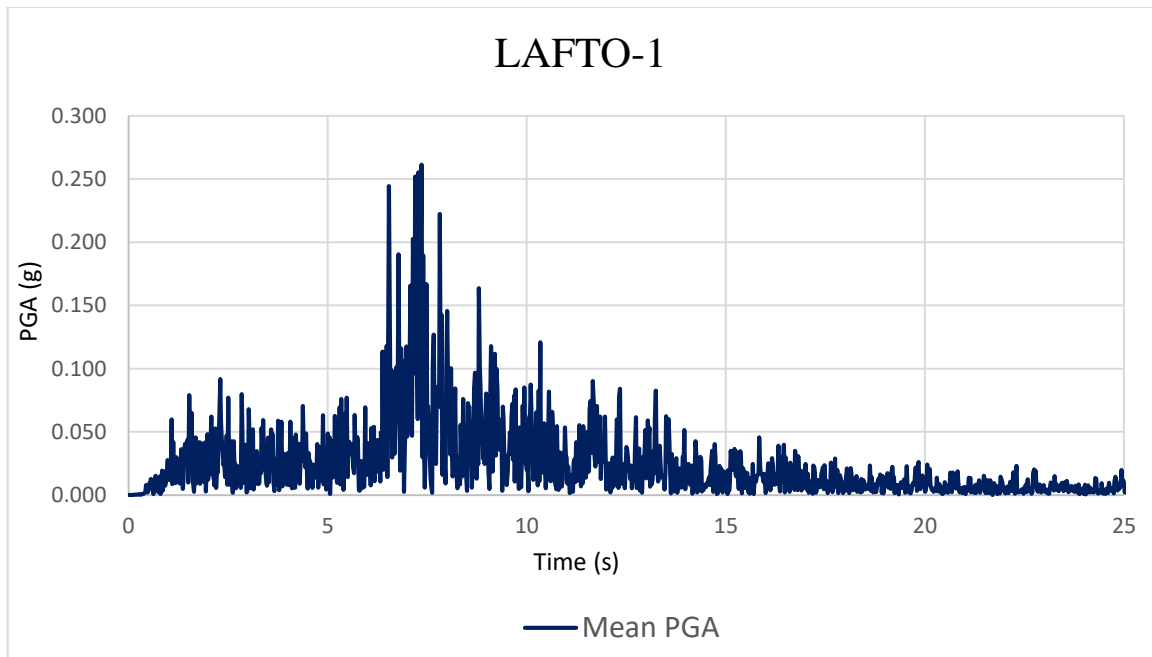


(b)

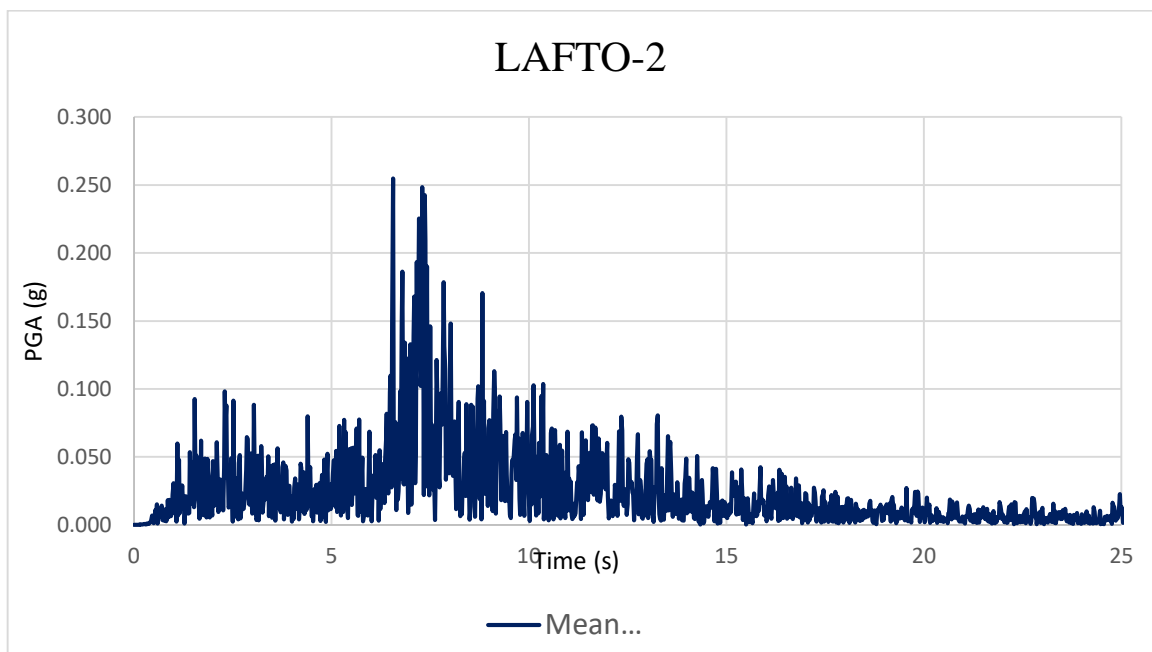


(c)

Figure 6-2: Mean PGA chart obtained from SPT data: (b) Kirkos and (c) Kolfe keranyo

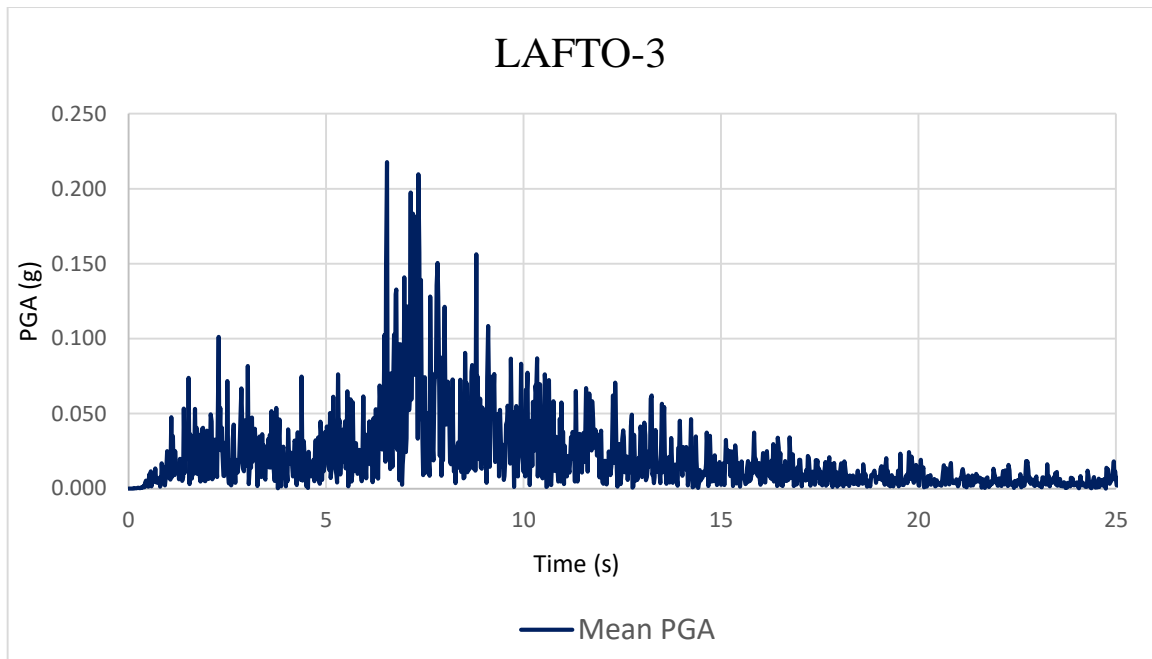


(d)

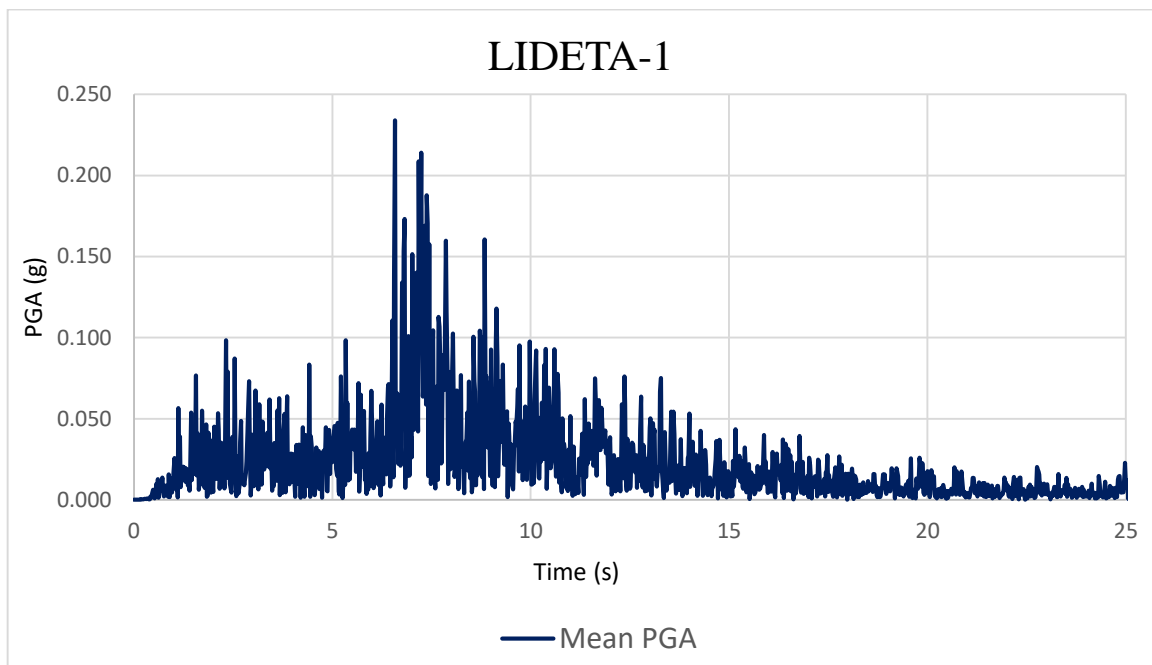


(e)

Figure 6-3: Mean PGA chart obtained from SPT data: (d) Lafto-1 and (e) Lafto-2

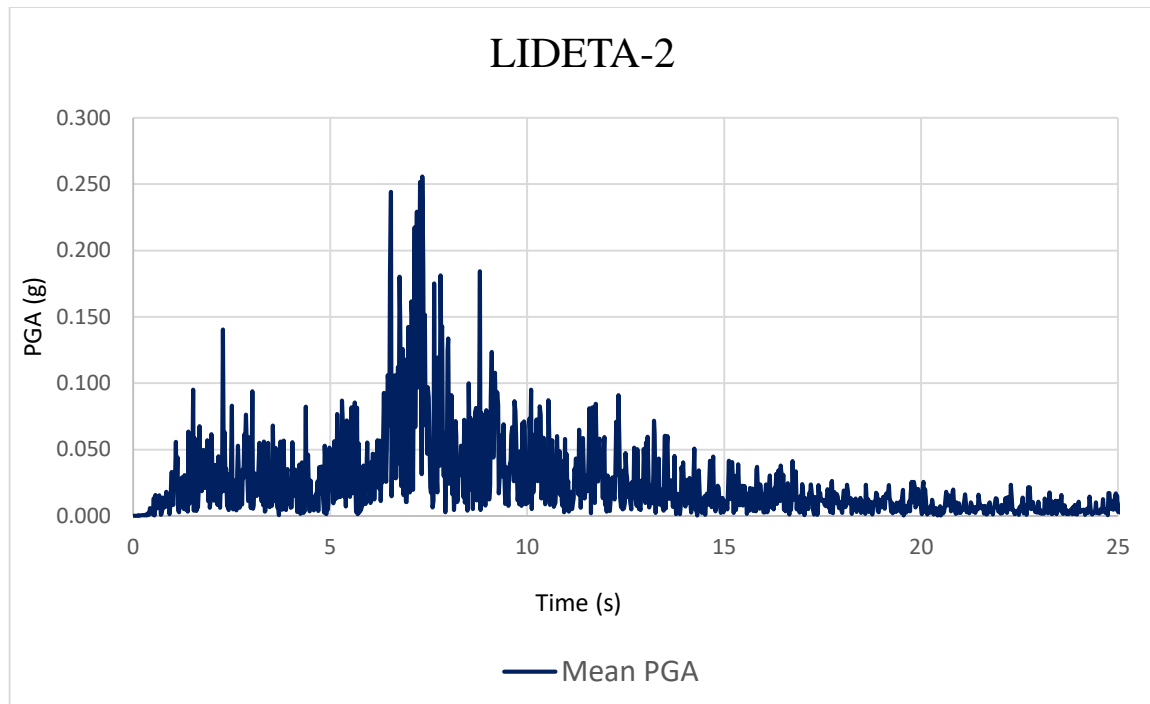


(f)



(g)

Figure 6-4: Mean PGA chart obtained from SPT data: (f) Lafto-3 and (g) Lideta-1



(h)

Figure 6-5: Mean PGA chart obtained from SPT data: (h) Lideta-2

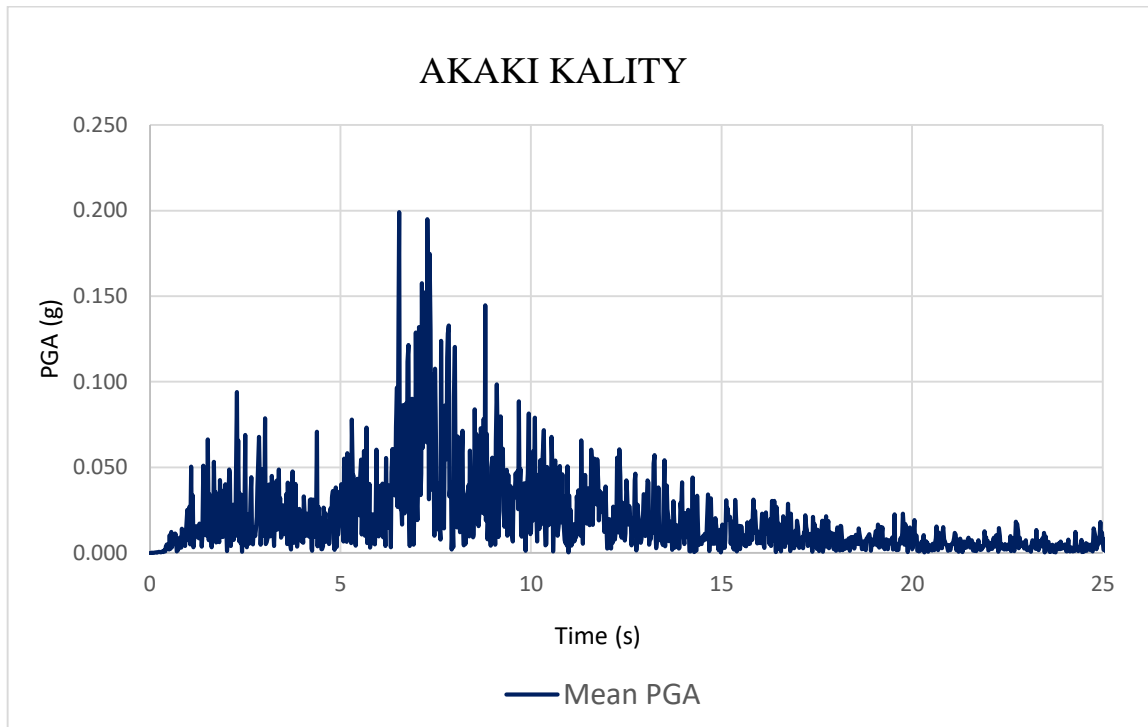
PGA results based on seismic survey data

Each seismic survey dataset indicates that input motions are amplified near the surface, with values ranging between 0.14g and 0.29g. The highest PGA value recorded is 0.29g for the Chi- Chi Taiwan earthquake ground motion at the Lideta sub city, while the lowest is 0.14g for the Whittier earthquake ground motion observed at the Kirkos sub city. These findings underscore the significant amplification of seismic motions near the ground surface and highlight the variability across different sites and input motions.

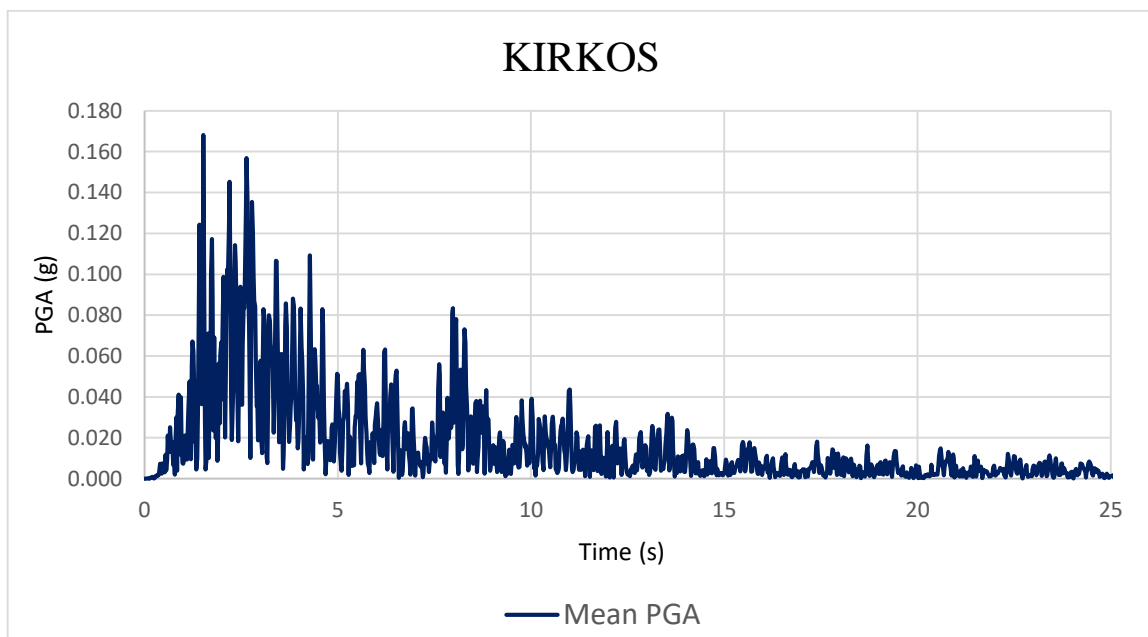
The maximum PGA records obtained in most cases where soft soil is at shallower depth and the lower PGA records obtained where the soil is stiff. The maximum amplification potential is reached between 5 and 10 seconds in most analyses, as this timeframe aligns closely with the motion's predominant period. This underscores the critical influence of timing on seismic response.

Table 6-1 displays the summary of mean PGA values, obtained by averaging the PGA results of the five earthquake input motions for the site, while Figures 6-6 to 6-7 illustrate

the corresponding mean PGA charts. The complete PGA distribution is accessible in Appendix A.

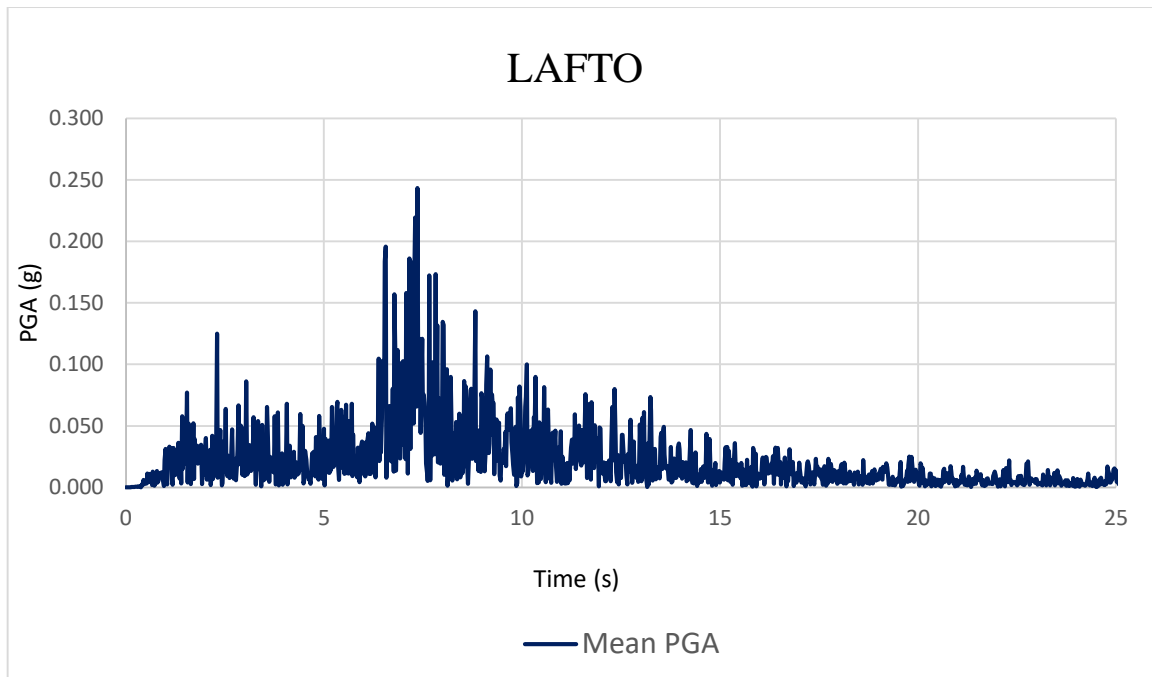


(a)

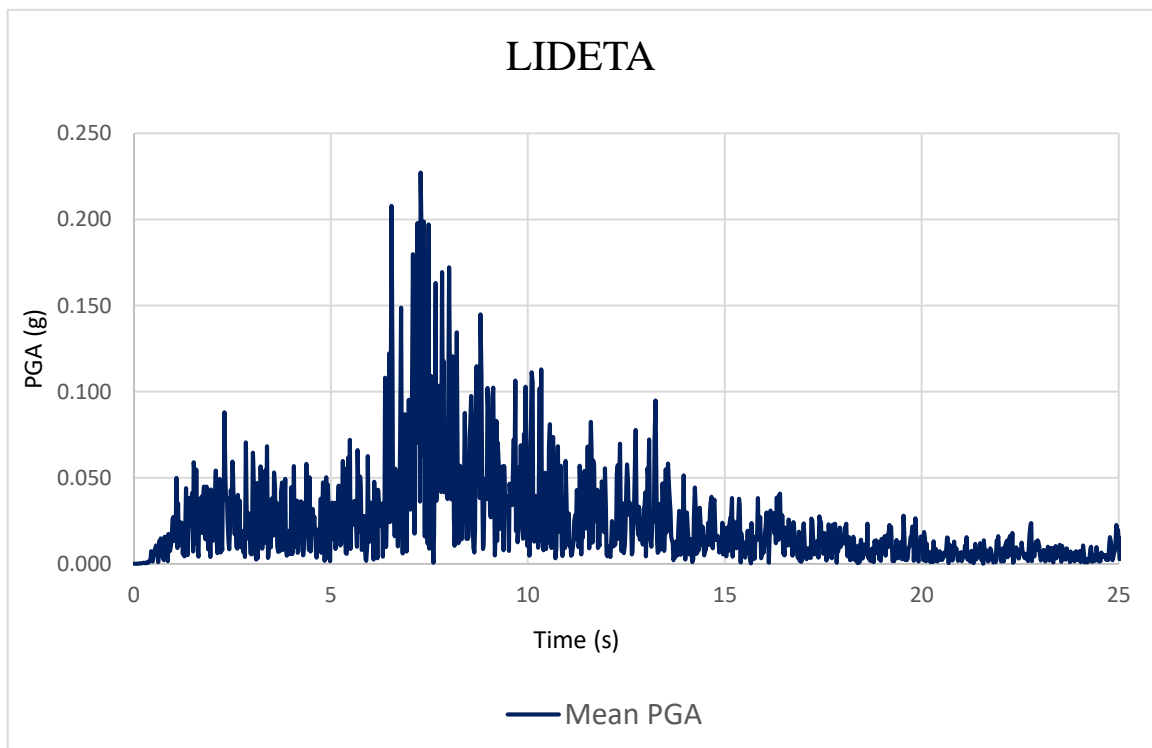


(b)

Figure 6-6: Mean PGA chart obtained from Seismic survey data: (a) Akaki kality, and (b) Kirkos



(c)



(d)

Figure 6-7: Mean PGA chart obtained from Seismic survey data: (c) Lafto, and (d) Lideta

Table 6-1: Mean PGA values obtained from SPT data and Seismic survey

PGA		
Sub city	SPT data	Seismic survey
Akaki Kality	0.18	0.2
Kirkos	0.19	0.17
Kolfe keranyo	0.26	
Nifas silk lafto-1	0.26	0.24
Nifas silk lafto-2	0.26	
Nifas silk lafto-3	0.22	
Lideta-1	0.23	0.23
Lideta-2	0.26	

Seismic survey data for Akaki kality, Kirkos, Lafto, and Lideta sites reveals PGA values closely resembling those obtained from SPT data, as depicted in Table 6-1. This combined approach enhances the characterization of these sites, offering more realistic data. Conversely, Kolfe keranyo site is characterized solely using SPT data. This diverse methodology is invaluable for site characterization based on available data sources.

The PGA results obtained from both SPT and seismic surveys amplify the input earthquake ground motion. A comparison of these PGA results with the input motion is provided in Appendix A.

From the latest previous work, which was conducted by Getu (2023), three of the study areas used are in the selected sub cities of this study, which are Mexico, Jemo, and Genet Hotel area. The PGA results from the previous study for non-linear analysis and the average PGA results of this study show 0.01 g to 0.07 g differences for both geotechnical and geophysical studies, which are factored due to the soil properties considered and analysis method used. The previous study uses one-dimensional ground response analysis, whereas this study uses two-dimensional ground response analysis. The PGA results are under estimated on the previous study as it is stated on the Table 6-2.

Table 6-2: Comparison of PGA results of previous study with this study

Sub city	(Getu, 2023)		This study	
	PGA results		PGA results	
	Geotechnical	Geophysical	Geotechnical	Geophysical
Lideta sub city (Mexico)	0.23		0.25	0.23
Lafto subcity (Jemo)	0.21	0.24	0.26	0.24
Kirkos Sub city (Genet Hotel)	0.18		0.19	0.17

6.1.2. Response spectra

With 5% structural damping, response spectra are used to determine attenuation or amplification. It is found that the mean response spectra vary between 0.3g and 1.37g, and that all of the study sites increase the input motions provided during periods between 0.05 seconds and 0.5 seconds.

Significant amplification and similar patterns are observed in nearly all curves, and the input ground motions are heavily influenced by the selected sites. Both one-dimensional and two-dimensional analyses generally indicate substantial amplifications, with a mean PSA of up to 0.7g.

Comparison of response spectra derived from one- and two-dimensional analyses reveals noticeable variation in representing the required response spectra. One-dimensional analysis tends to overestimate site response spectra due to its focus solely on spectral acceleration along one axis, limiting its ability to accurately represent the site's response. In reality, acceleration dissipates in all directions, which is inadequately captured by the one-dimensional approach. This variance highlights the importance of employing comprehensive, multi-dimensional analyses for more accurate characterization of site response and seismic behavior.

For the SPT data and MASW tests, response spectra are performed for five different input motions for both one- and two-dimensional analyses. Based on geotechnical and geophysical data, Appendix B shows the spectral distribution over period for each of the five motions.

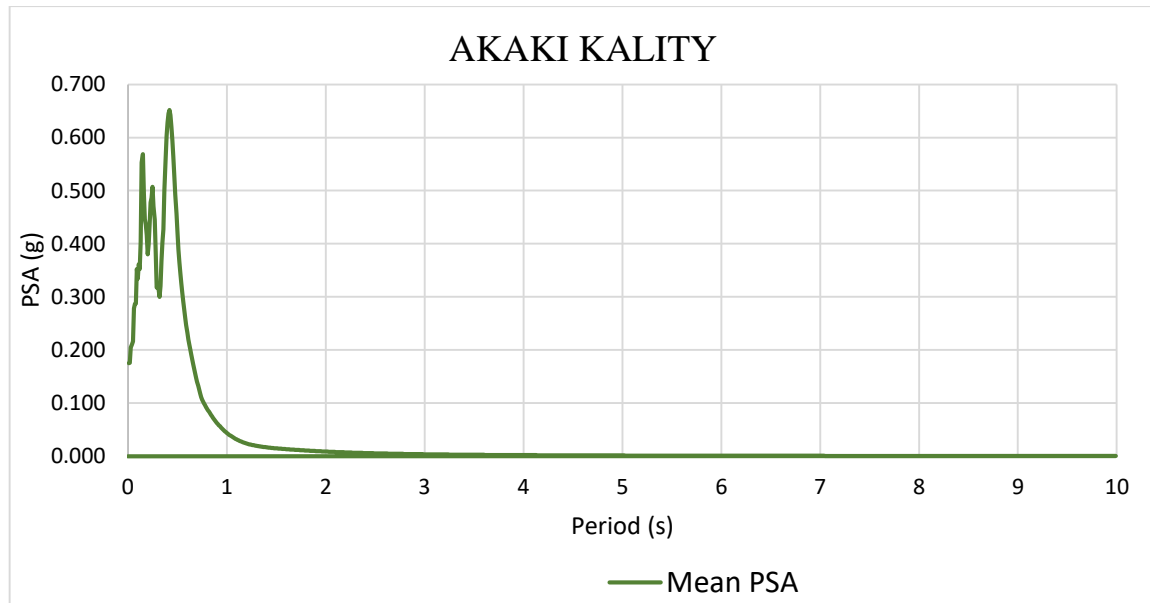
Response spectra based on SPT data

In the one-dimensional analysis, the absolute response spectra at the Lafto sub city site-1 for the Whittier earthquake ground motion is recorded at 1.23g. Conversely, the lowest absolute response spectra are observed at Lafto sub city site -3 and Kirkos sub city, where both measures 0.5g for the San fernando earthquake ground motion. This highlights the variability in response spectra between different sites and earthquake events.

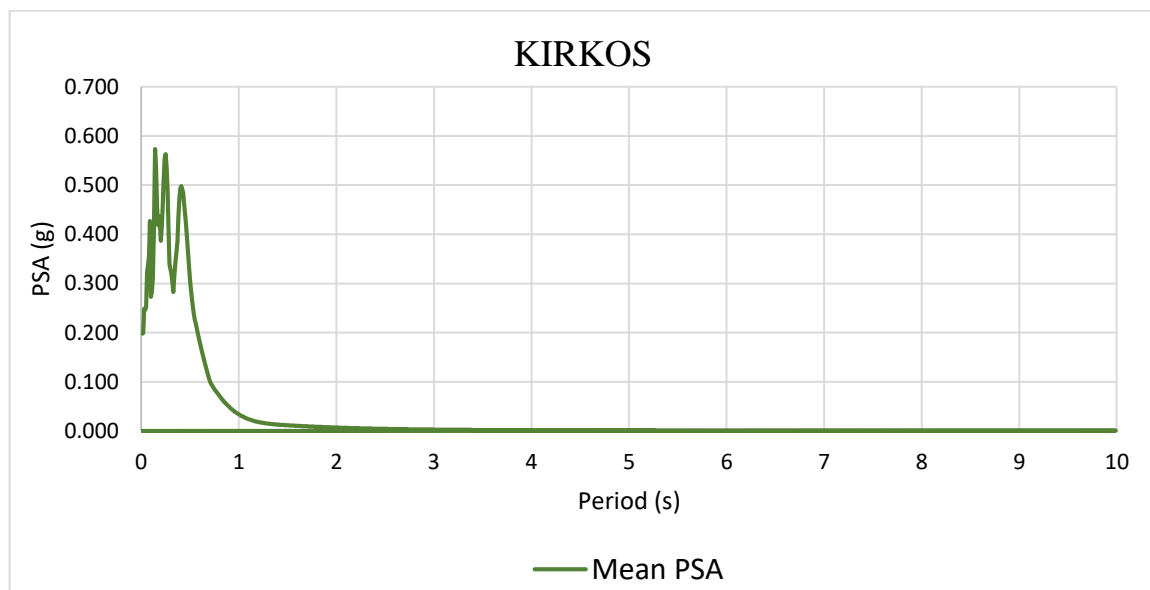
For the Whittier earthquake at Lideta sub city site-2, two-dimensional analysis obtained an absolute response spectrum of 0.67g. Meanwhile, Kirkos sub city recorded the lowest absolute response spectrum, measuring 0.36g for the San fernando earthquake ground

motion. Table 6-2 summarizes the mean response spectra obtained by averaging the PSA results of the five earthquake input motions for the site at the ground surface, while Figures 6-8 to 6-15 illustrate the corresponding mean response spectra charts for both one- and two-dimensional response spectra. The response spectra for each input ground motion is stated in Appendix B.

- **One dimensional response spectra**

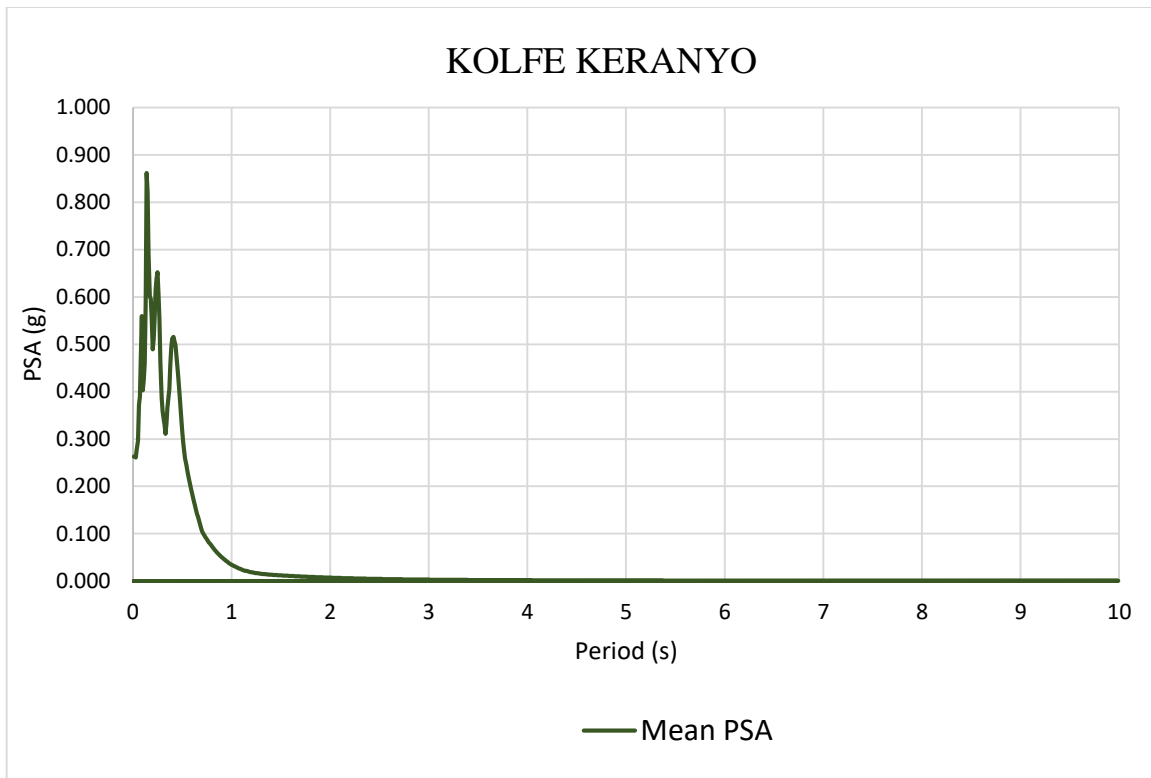


(a)

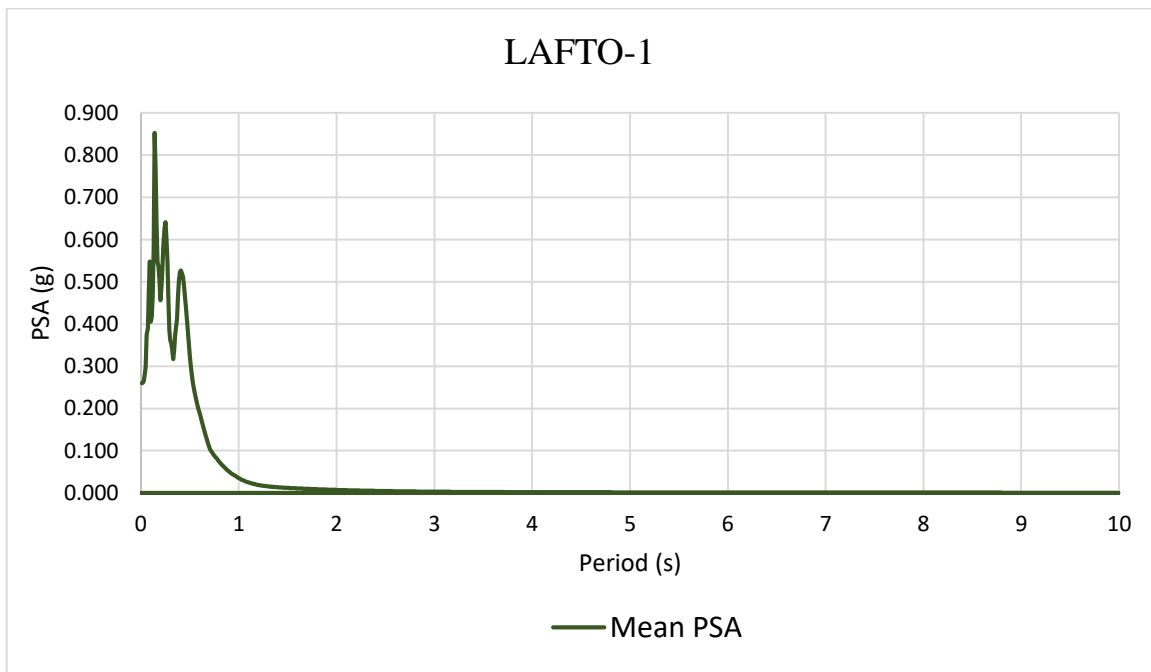


(b)

Figure 6-8: Mean one dimensional response spectra obtained from SPT data: (a) Akaki kality, and (b) Kirkos

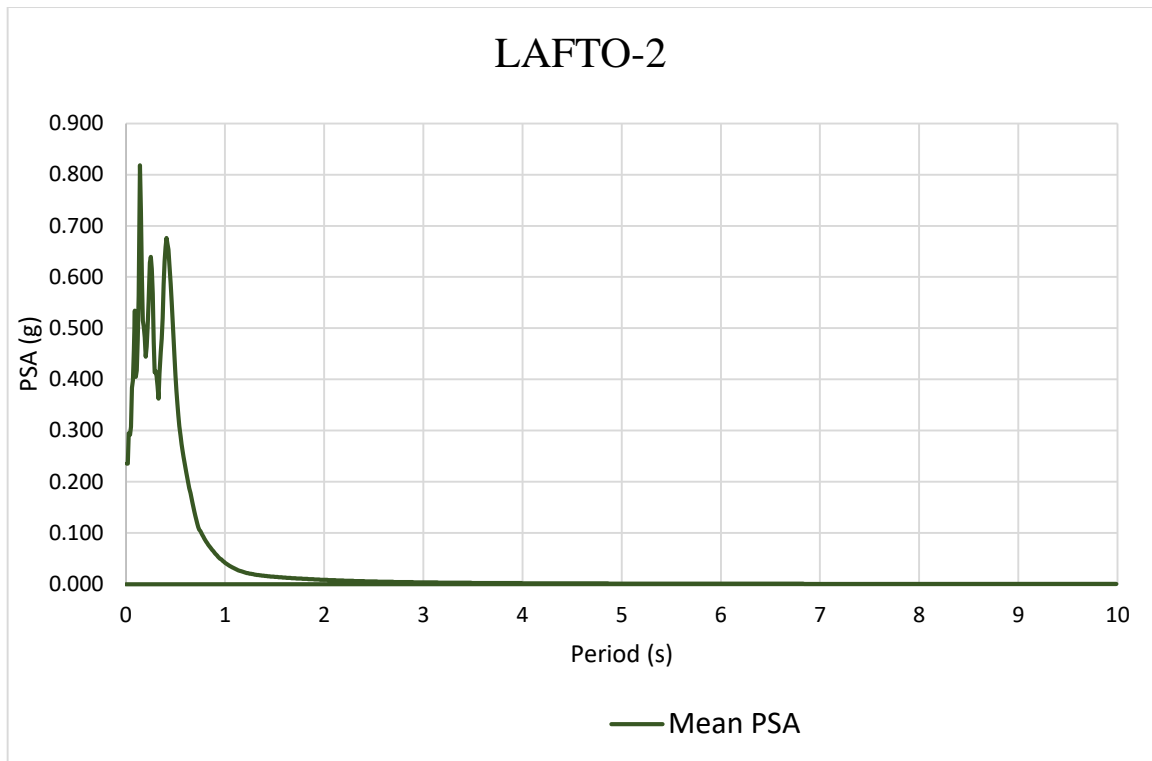


(c)

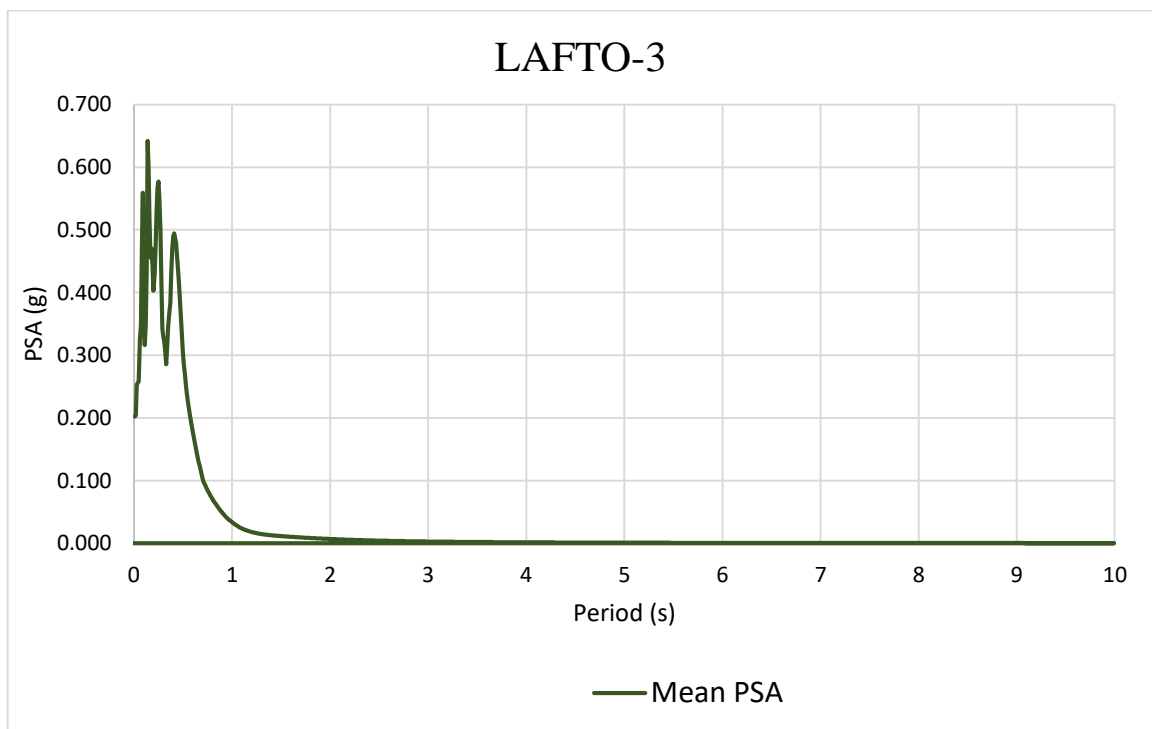


(d)

Figure 6-9: Mean one dimensional response spectra obtained from SPT data: (c) Kolfe keranyo, and (d) Lafto-1

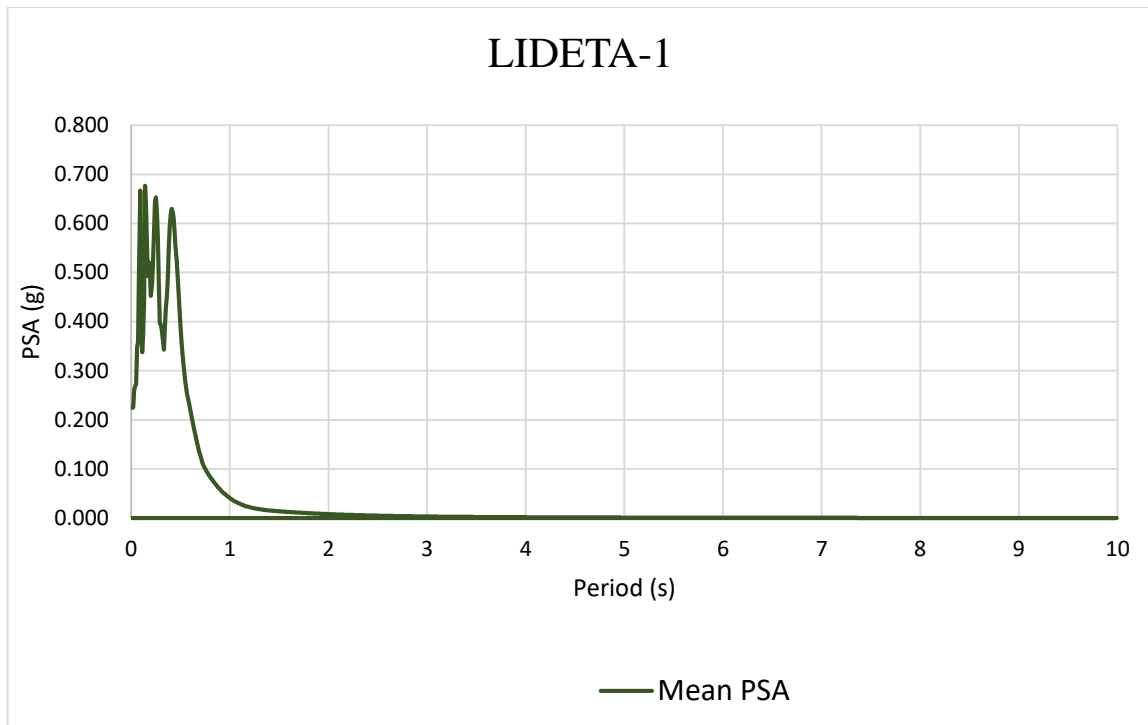


(e)

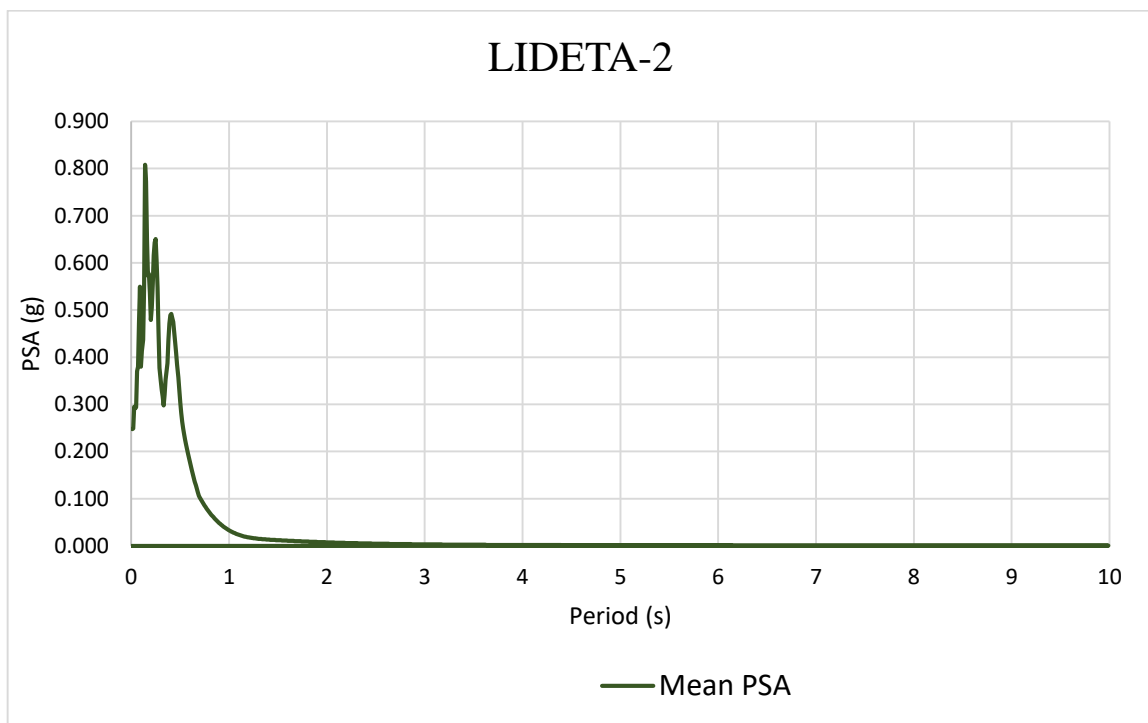


(f)

Figure 6-10: Mean one dimensional response spectra obtained from SPT data: (e) Lafto-2, and (f) Lafto-3



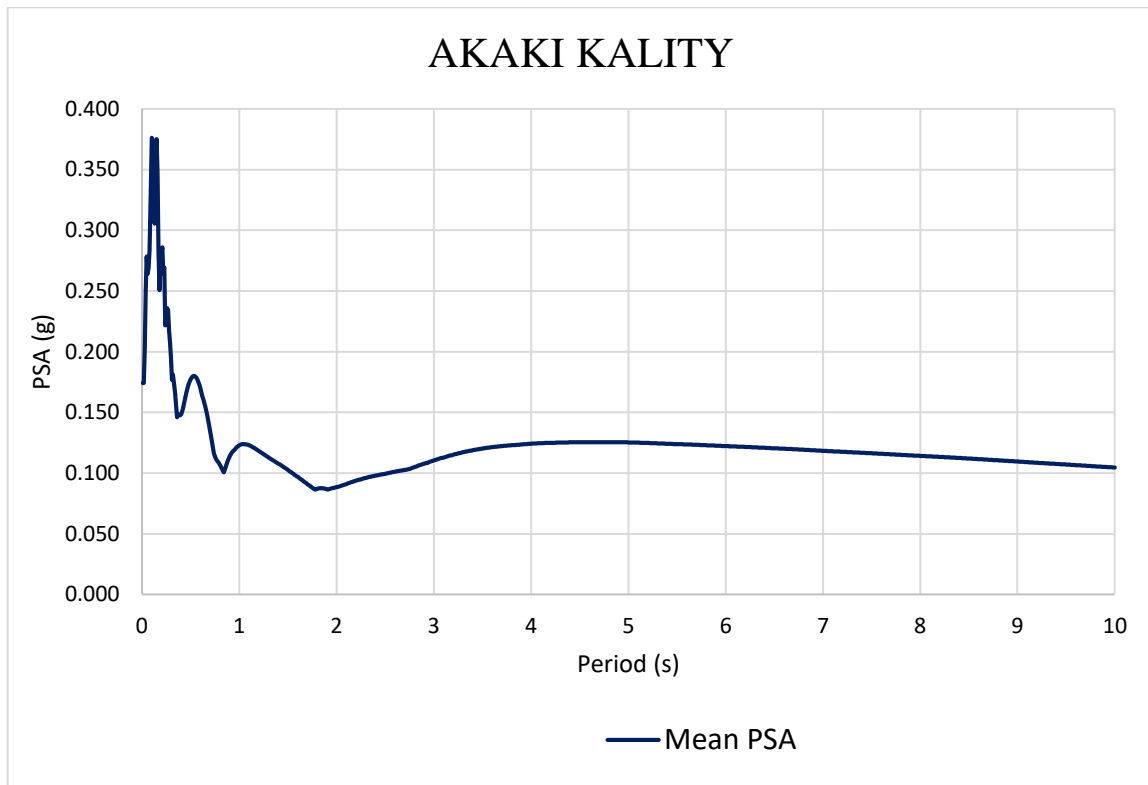
(g)



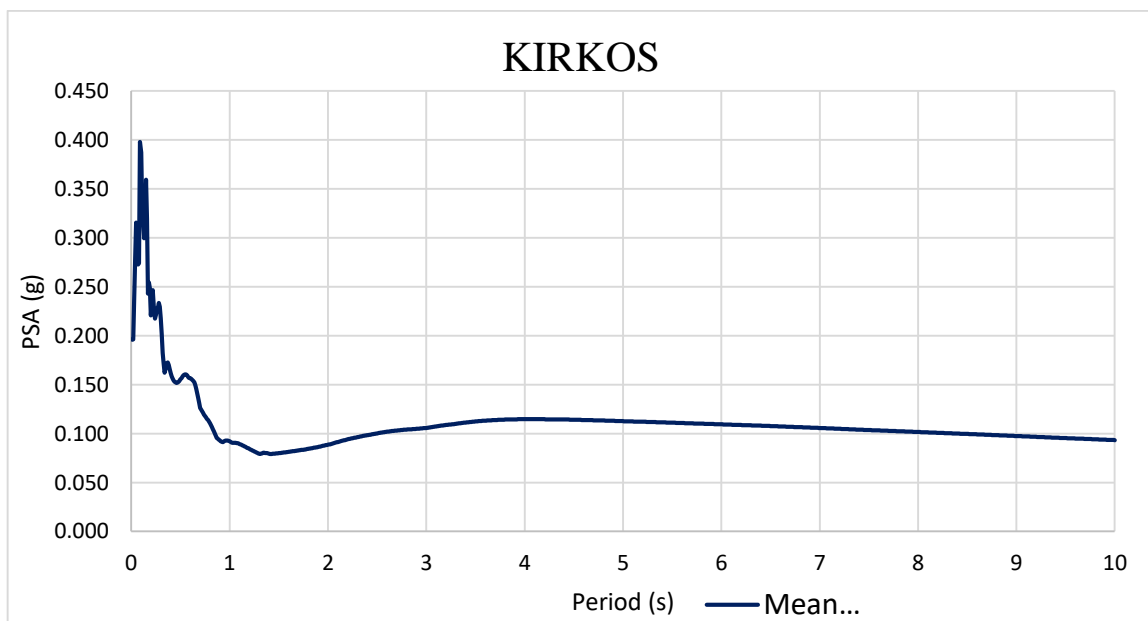
(h)

Figure 6-11: Mean one dimensional response spectra obtained from SPT data: (g) Lideta-1, and (h) Lideta-2

- Two dimensional response spectra

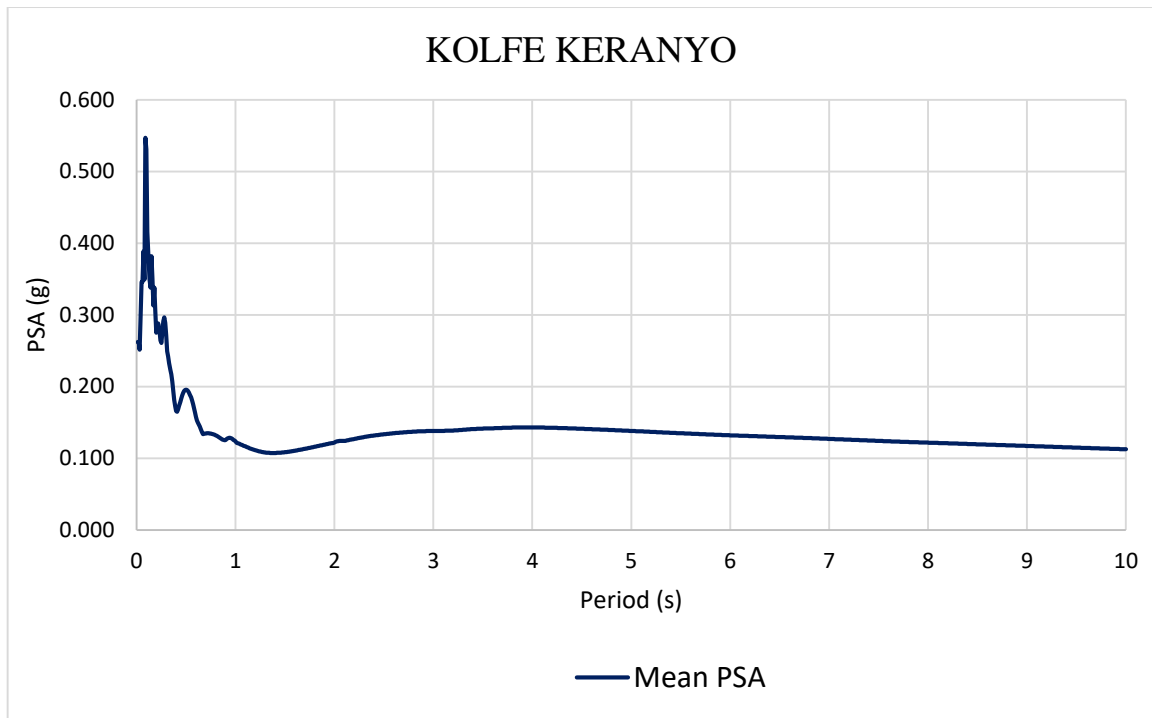


(a)

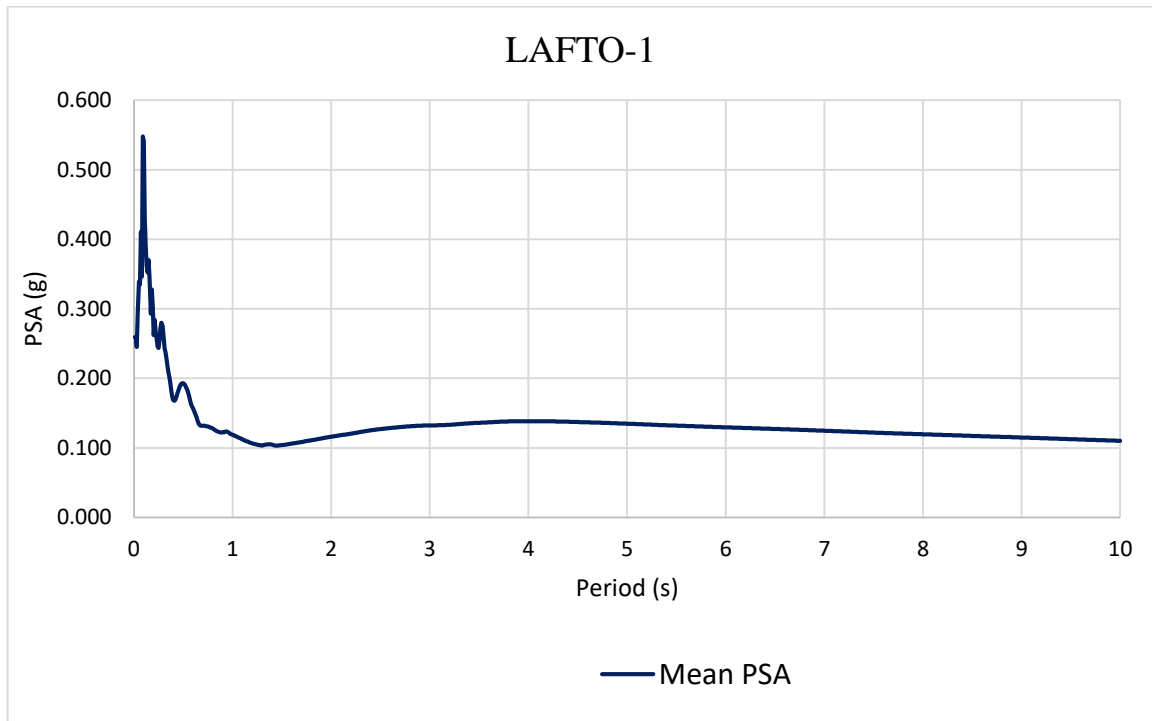


(b)

Figure 6-12: Mean two dimensional response spectra obtained from SPT data: (a) Akaki kality, and (b) Kirkos

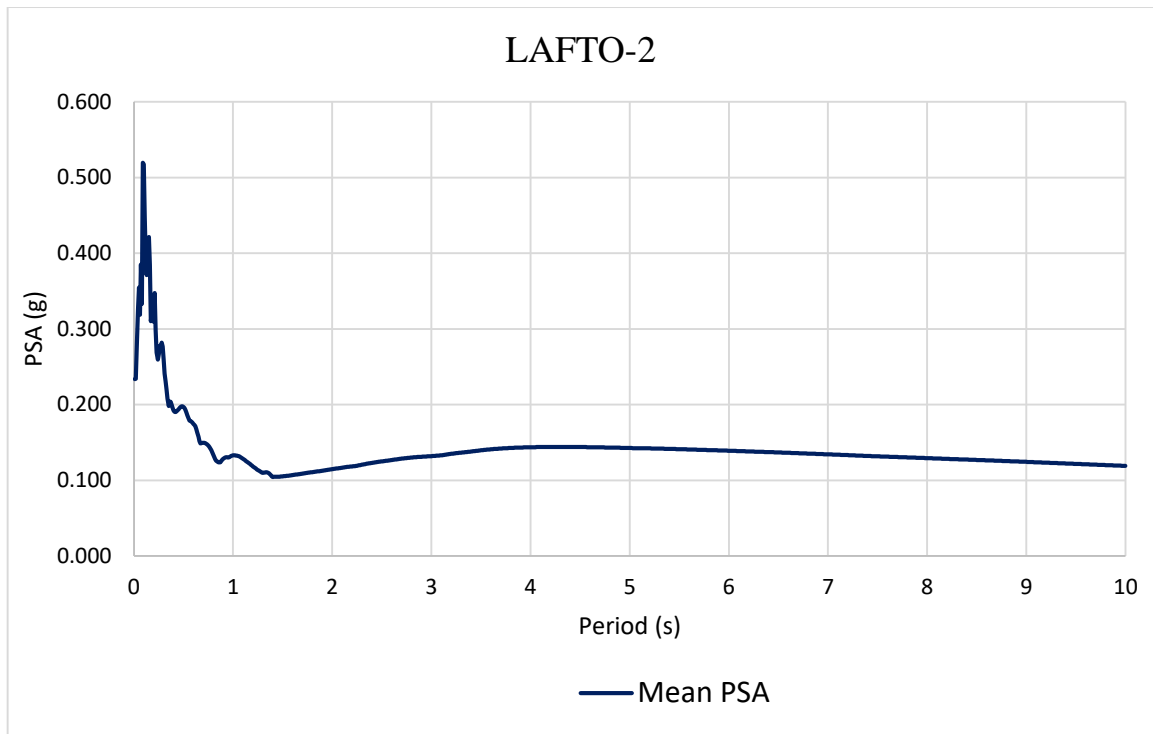


(c)

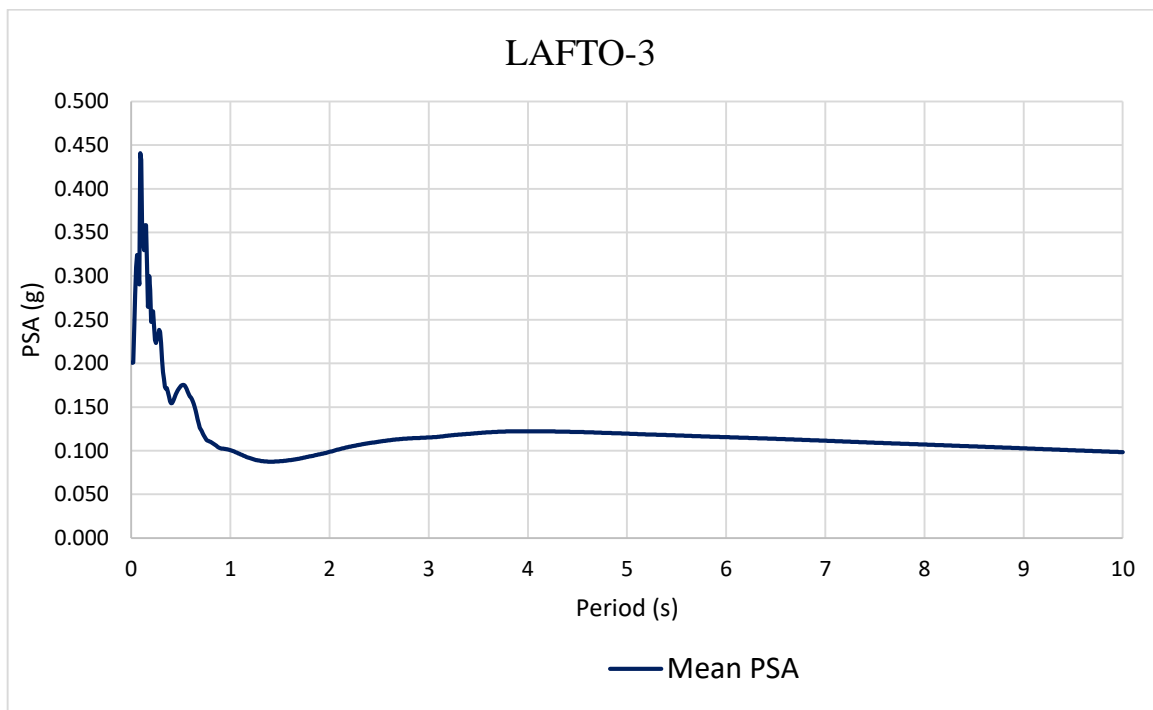


(d)

Figure 6-13: Mean two dimensional response spectra obtained from SPT data: (c) Kolfe keranyo, and (d) Lafto-1

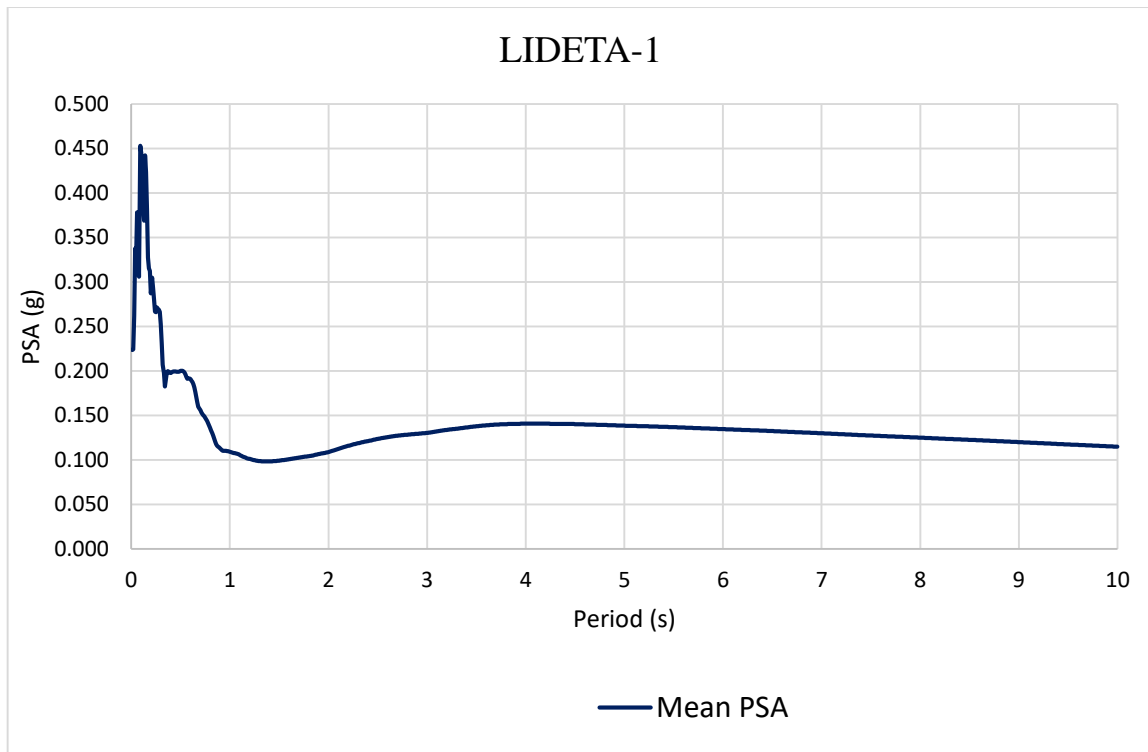


(e)

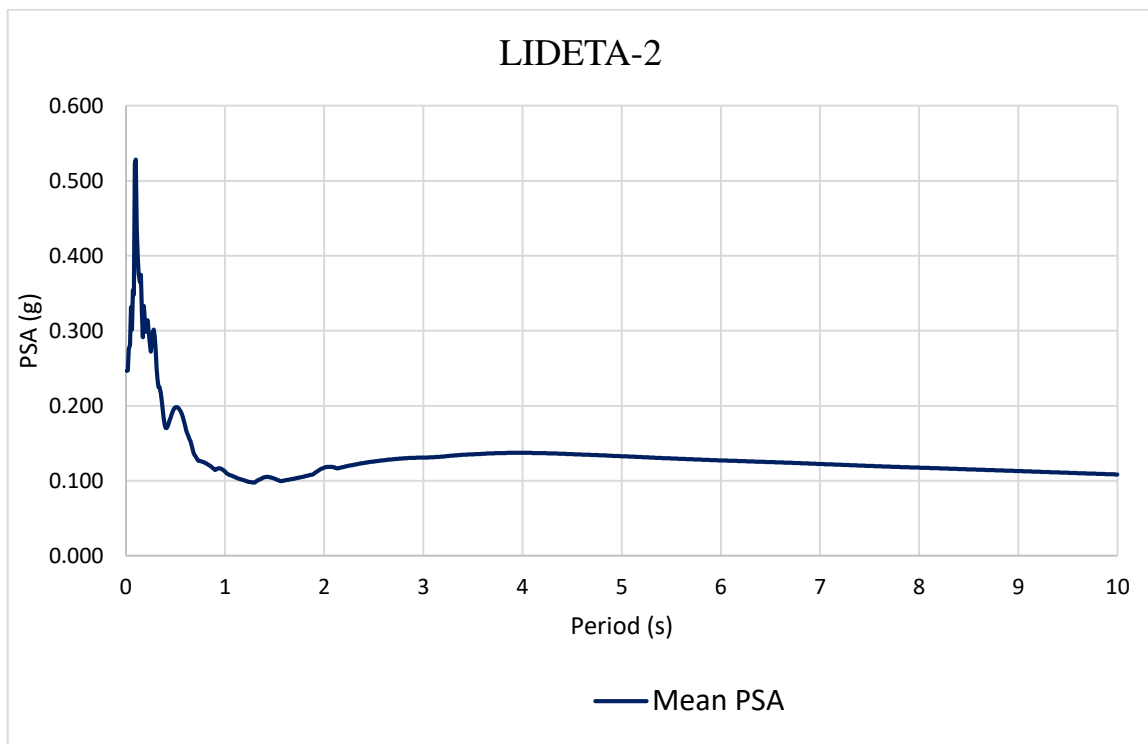


(f)

Figure 6-14: Mean two dimensional response spectra obtained from SPT data: (e) Lafto-2, and (f) Lafto-3



(g)



(h)

Figure 6-15: Mean two dimensional response spectra obtained from SPT data: (g) Lideta-1, and (h) Lideta-2

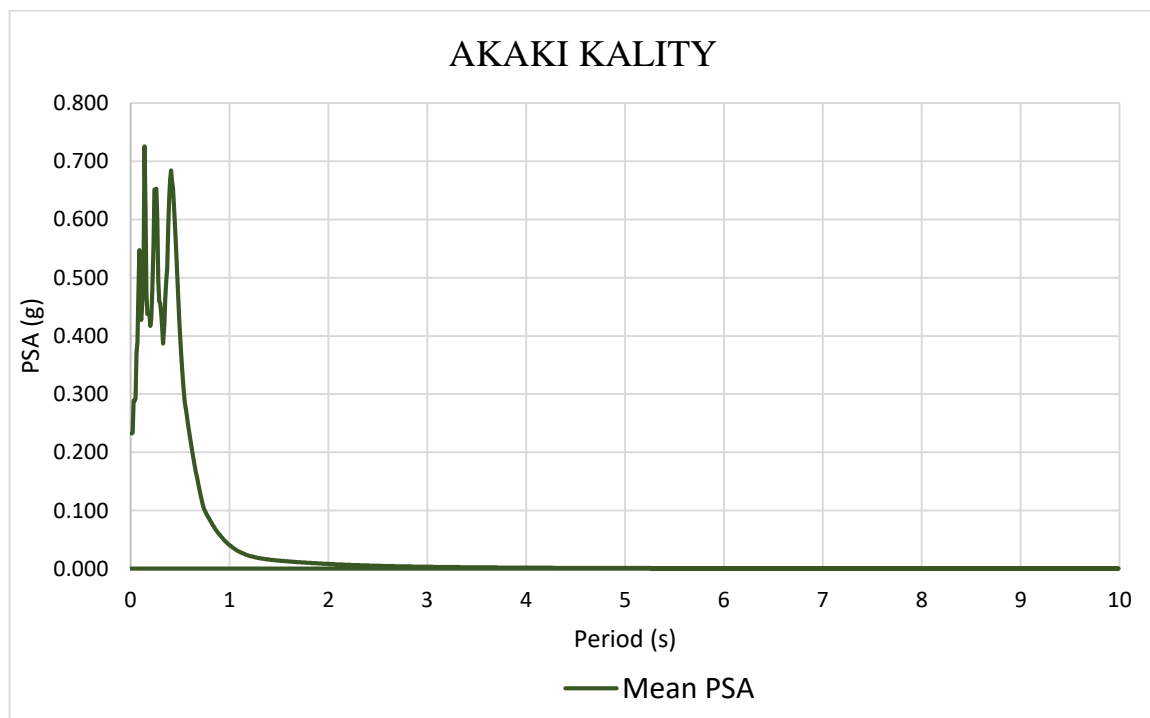
Response spectra based on seismic survey data

One-dimensional analysis finds that the absolute response spectrum for the ground motion of the chi-chi Taiwan earthquake in Lideta sub city is 1.37g. Conversely, the Kirkos sub city's ground motion recorded during the Niigata Japan earthquake yields the lowest absolute response spectrum, at 0.52g.

Two-dimensional analysis found an absolute response spectrum of 0.76g for the ground motion at Lideta sub city that corresponded to the ground motion caused by the chi-chi Taiwan earthquake. Meanwhile, ground motions associated with the Whittier earthquake showed 0.3g of the lowest absolute response spectra at the Kirkos sub city.

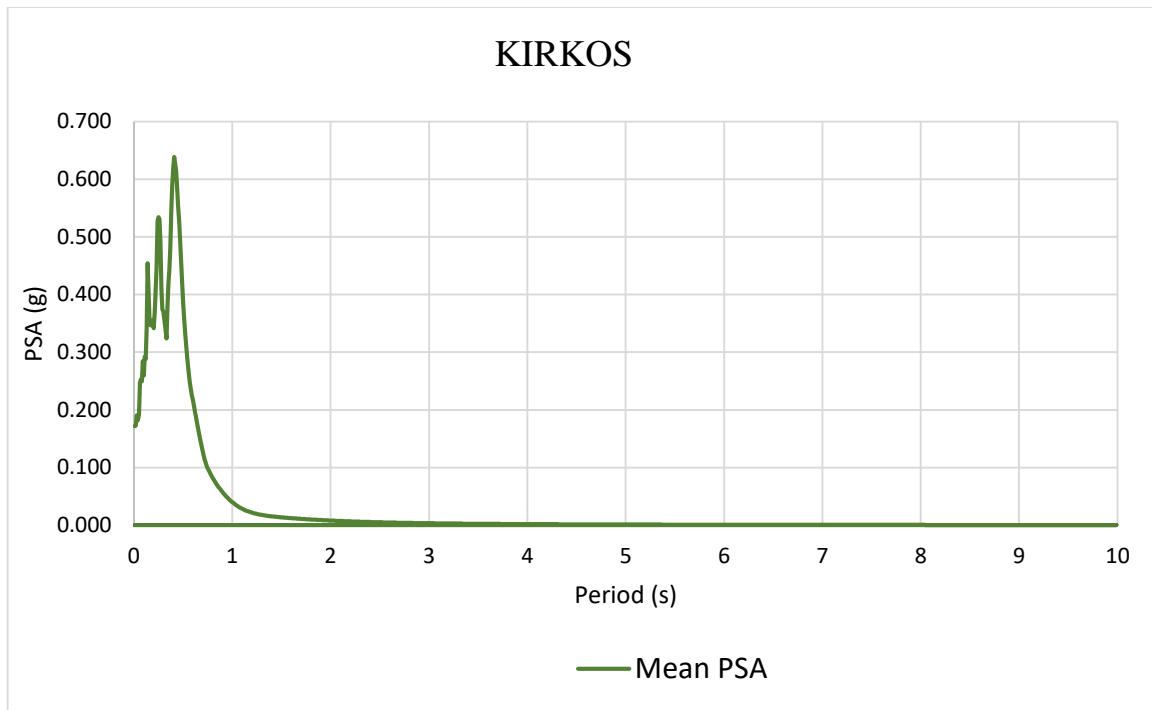
The mean response spectra obtained by averaging the PSA results of the five earthquake input motions for the site at the ground surface are summarized in Table 6-2, and the corresponding mean response spectra charts for one and two dimensional response spectra are shown in Figures 6-16 to Figure 6-21. Appendix B contains the response spectra in detail.

- **One dimensional response spectra**

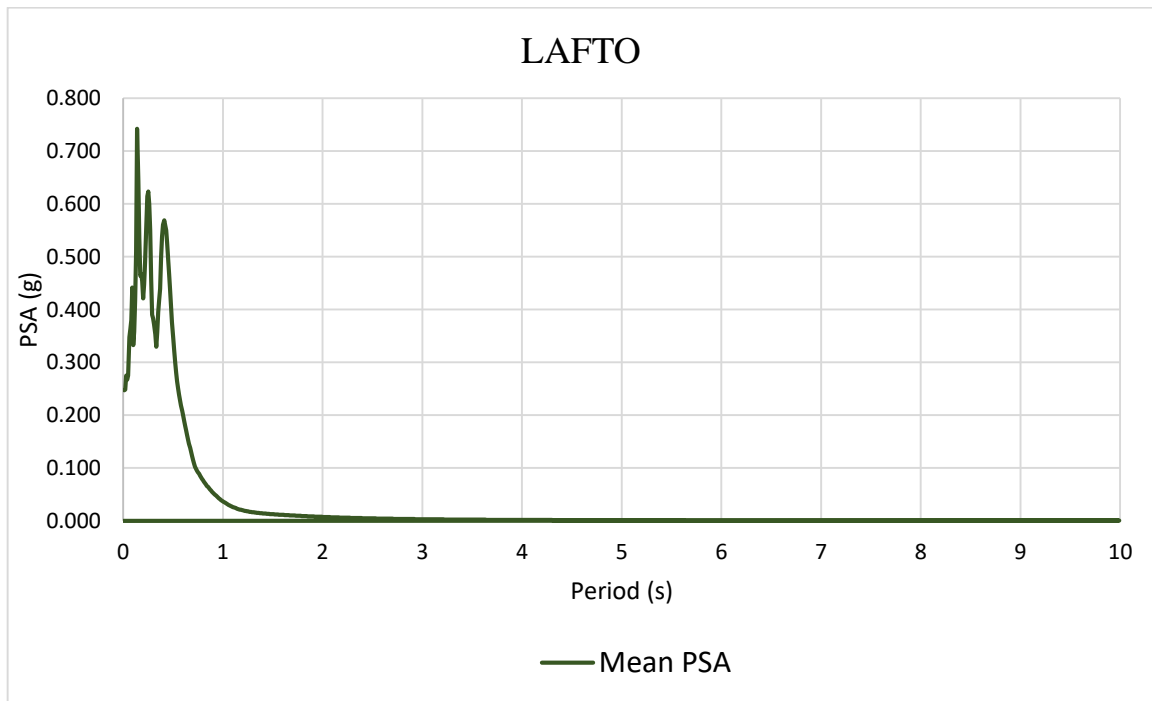


(a)

Figure 6-16: Mean one dimensional response spectra obtained from Seismic survey: (a) Akaki Kality

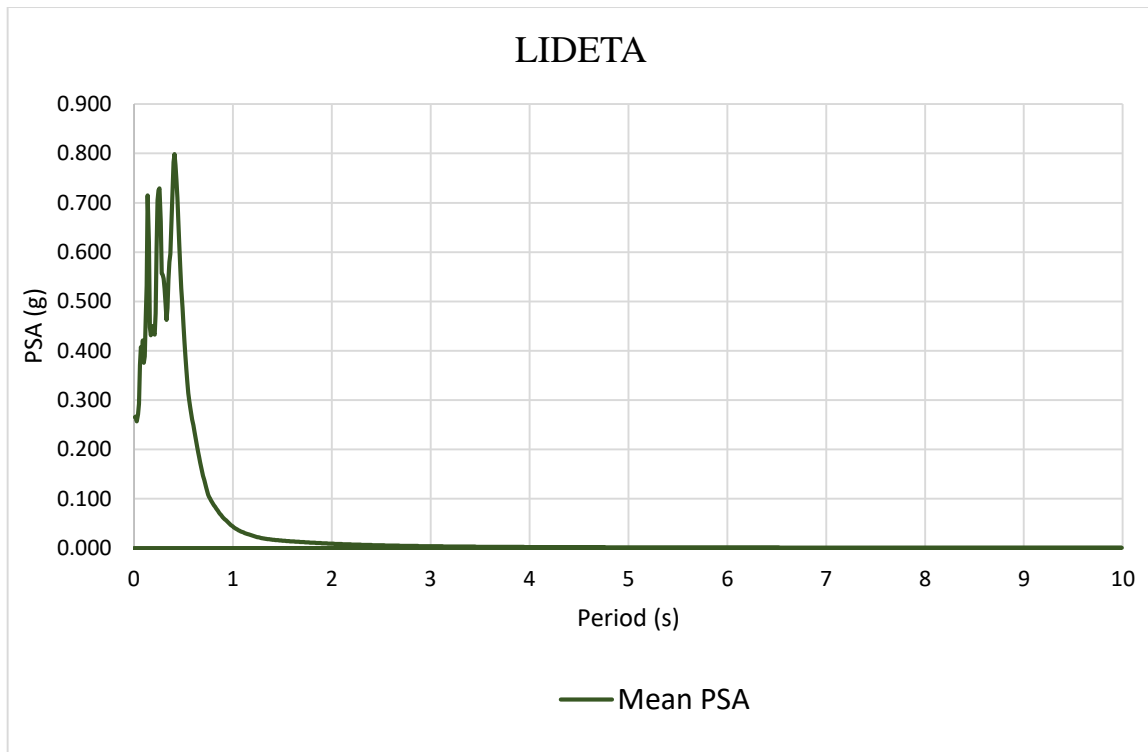


(b)



(c)

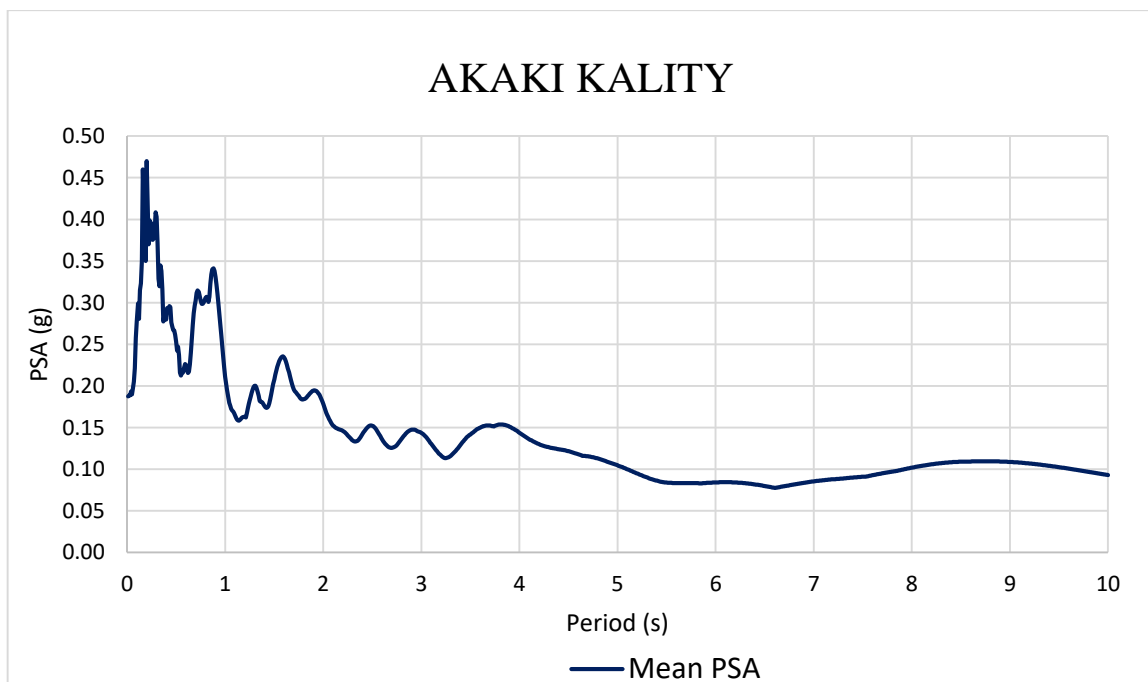
Figure 6-17: Mean one dimensional response spectra obtained from Seismic survey: (b) Kirkos, and (c) Lafto



(d)

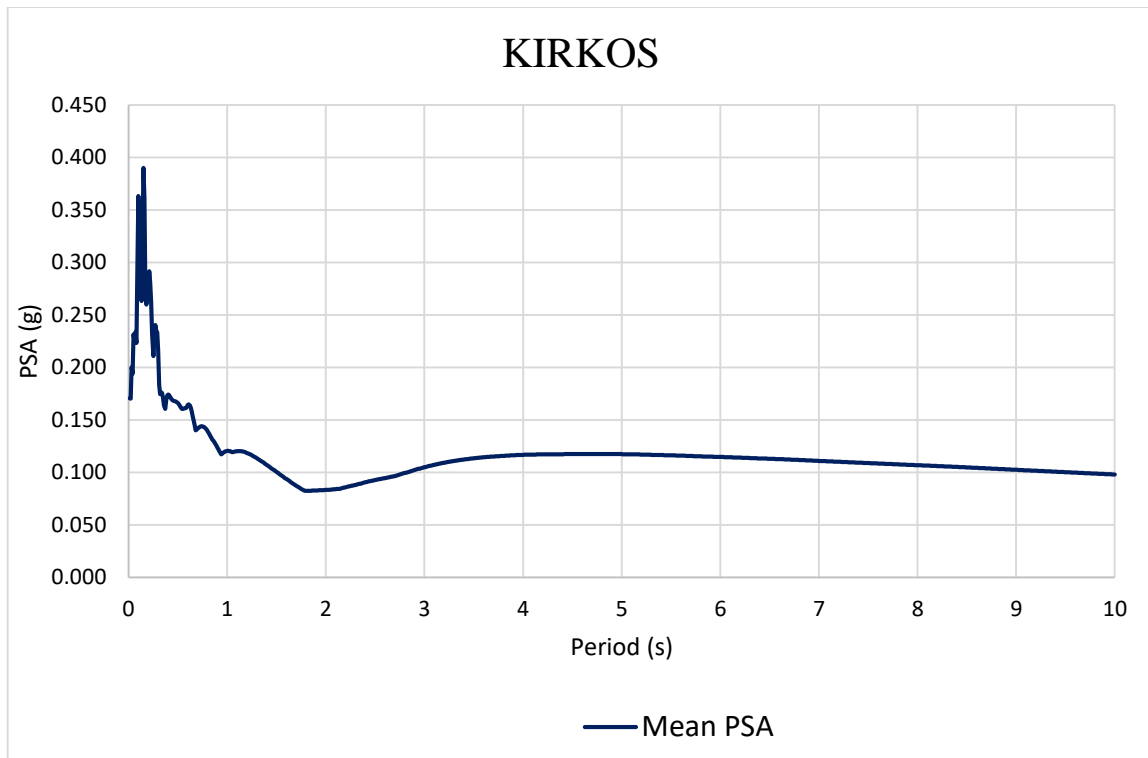
Figure 6-18: Mean one dimensional response spectra obtained from Seismic survey: (d) Lideta

• Two dimensional response spectra

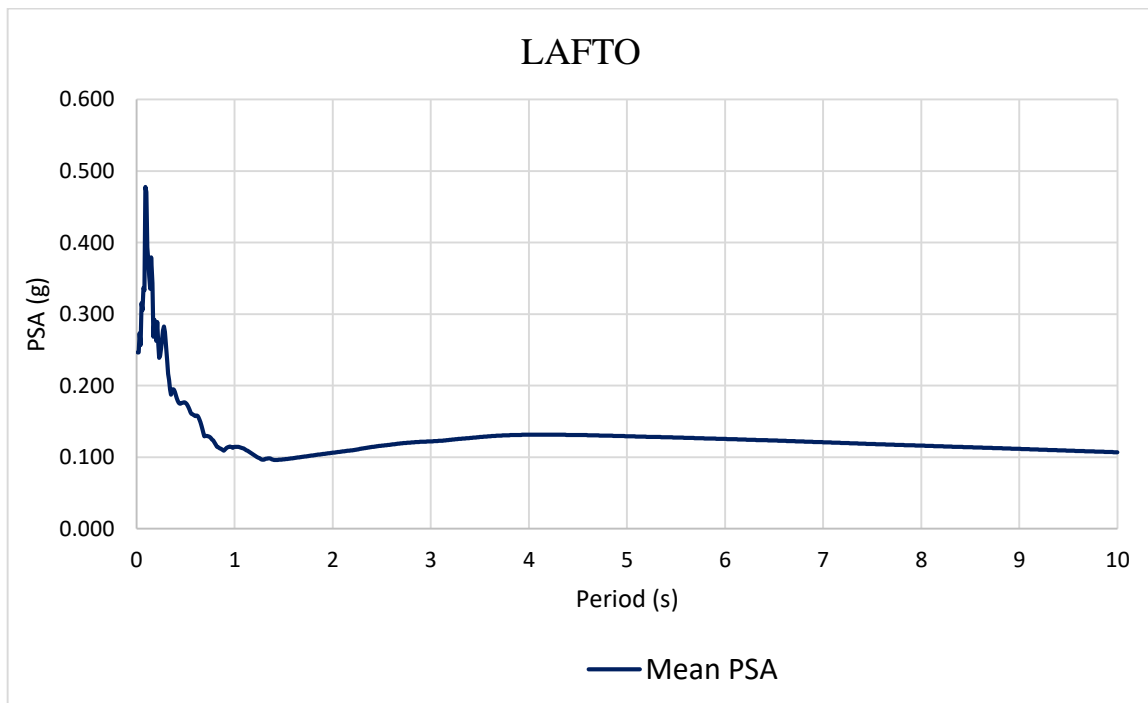


(a)

Figure 6-19: Mean two dimensional response spectra obtained from Seismic survey: (a) Akaki kality

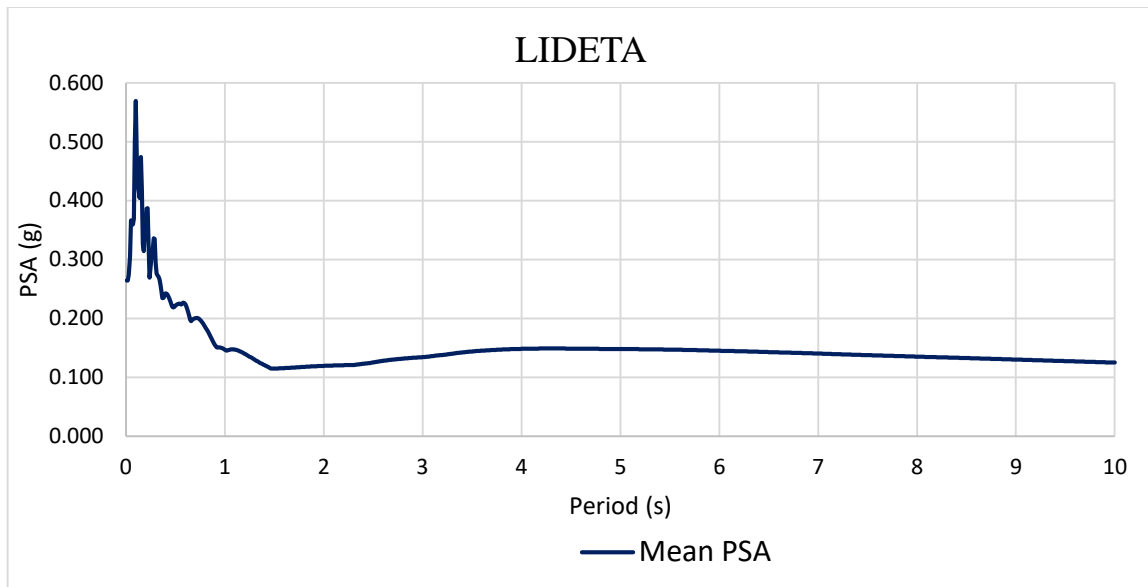


(b)



(c)

Figure 6-20: Mean two dimensional response spectra obtained from Seismic survey: (b) Kirkos, and (c) Lafto



(d)

Figure 6-21: Mean two dimensional response spectra obtained from Seismic survey: (d) Lideta
 As Table 6-2 indicates, the mean response spectra for seismic surveys and SPT data exhibit values that are nearly similar for both one- and two-dimensional analysis.

Table 6-2: Mean maximum response spectra obtained from SPT data and Seismic survey

Sub city	One dimensional response spectra		Two dimensional response spectra	
	SPT data	Seismic survey	SPT data	Seismic survey
Akaki Kality	0.68	0.72	0.38	0.46
Kirkos	0.57	0.64	0.4	0.39
Kolfe keranyo	0.86		0.55	
Nifas silk lafto-1	0.85	0.74	0.55	0.48
Nifas silk lafto-2	0.82		0.52	
Nifas silk lafto-3	0.64		0.44	
Lideta-1	0.69	0.8	0.46	0.57
Lideta-2	0.81		0.53	

Two-dimensional response spectra show less spectral acceleration than one-dimensional response spectra for each site and input ground motion. One-dimensional response spectra have an absolute value of 0.86g for SPT data and 0.8g for seismic survey data, whereas two-dimensional analysis has an absolute spectral acceleration of 0.55g for SPT data and 0.57g for seismic survey data.

The response spectra result from the previous study conducted by Getu (2023), for non-linear analysis and the average response spectra two dimensional results of this study show 0.04 g to 0.3 g differences for both geotechnical and geophysical studies, which are factored due to the difference of soil properties considered, the input ground motion and analysis method used. The previous study uses one-dimensional ground response analysis, whereas this study uses two-dimensional ground response analysis. The response spectra results are over estimated on the previous study as it is stated on the table 6-2.

Table 6-2: Comparison of PSA results of previous study with this study

Sub city	Getu		This study	
	Response spectra		Response spectra	
	Geotechnical	Geophysical	Geotechnical	Geophysical
Lideta sub city (Mexico)	0.79		0.5	0.57
Lafto subcity (Jemo)	0.54	0.51	0.5	0.48
Kirkos Sub city (Genet Hotel)	0.7		0.4	0.39

6.2. Comparison of Mean response spectra with code spectra

For both geotechnical and geophysical data, average shear wave velocity for the upper 30 meters ($V_{s, 30}$) was determined. For geotechnical data, $V_{s, 30}$ ranged from 290 m/s to 358 m/s. And geophysical data, $V_{s, 30}$ ranged from 299 m/s to 337 m/s. According to ES EN 2018:2015, these values fall under site class C. However, for NEHRP provisions, they fall under site class D. Therefore, the mean response spectra for one- and two-dimensional analyses are compared with the standards set by these two codes.

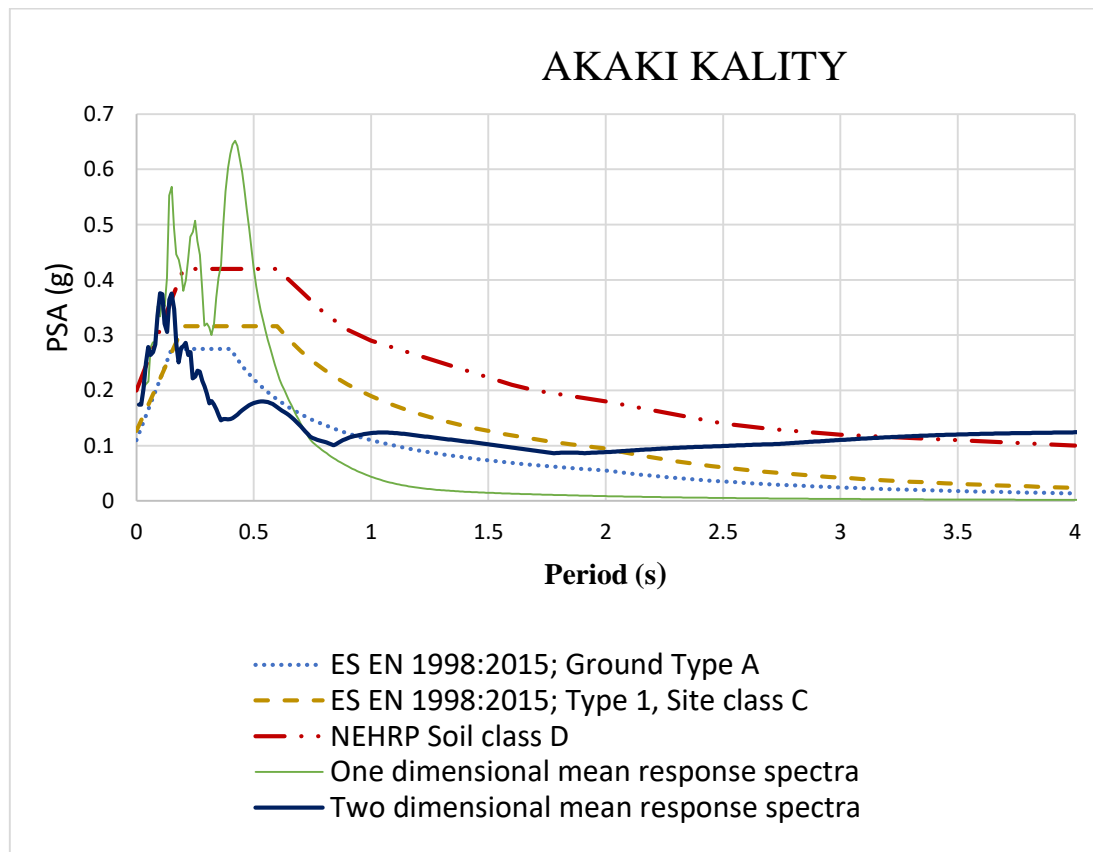
The comparison of mean response spectra with code spectra, shown in Figures 6-22 to 6-28, reveals that the one-dimensional response spectra overestimated the spectral acceleration. This overestimation is more than double the ES EN 1998:2015 standards and nearly double the NEHRP provisions.

The two-dimensional mean response spectra are relatively close to the code spectra for both ES EN 1998:2015 and NEHRP provisions. However, the local code still fails to accurately represent these sites. In most cases, the NEHRP provisions fit the study area better, while the ES EN 1998:2015 standards do not adequately represent these study sites.

Response spectra from SPT data

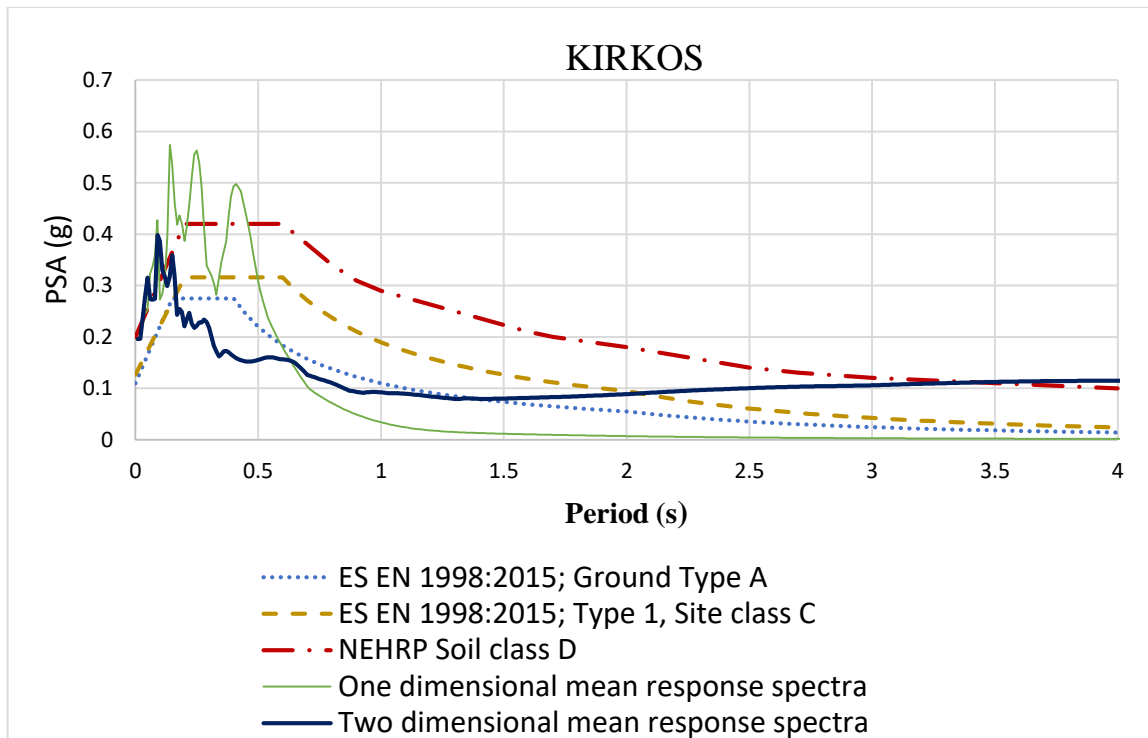
Comparing mean one- and two-dimensional response spectra with code spectra reveals significant spectral accelerations. In one-dimensional analysis, accelerations between 0.5g and 1.23g occur from 0.05 seconds to 0.5 seconds. Similarly, two-dimensional analysis shows accelerations ranging from 0.36g to 0.67g within the same timeframe. Notably, the response spectra in this study align closely with NEHRP provisions but underestimated by ES EN 1998:2015.

Between the time periods of 0.05 and 0.5 second, local code spectra tend to underestimate the spectral acceleration in most cases. However, between 0.5 second and 1.5 seconds, both code spectra overestimate the spectral acceleration in most cases. This discrepancy suggests a need for further examination and adjustment in code provisions to ensure more accurate estimations across various time intervals. Figures 6-22 to 6-26 indicate the comparison between the mean response spectra from SPT data and the code spectra.

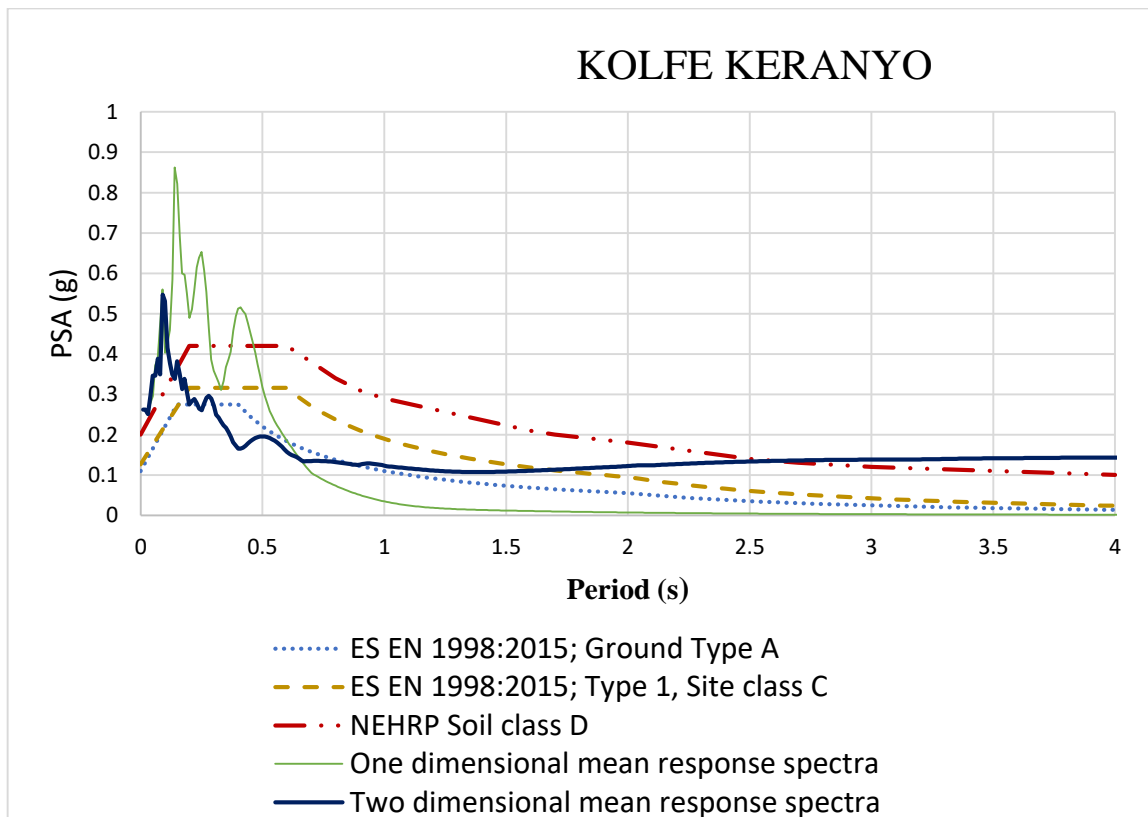


(a)

Figure 6-22: Comparison of mean response spectra from SPT data with code spectra: (a) Akaki kality

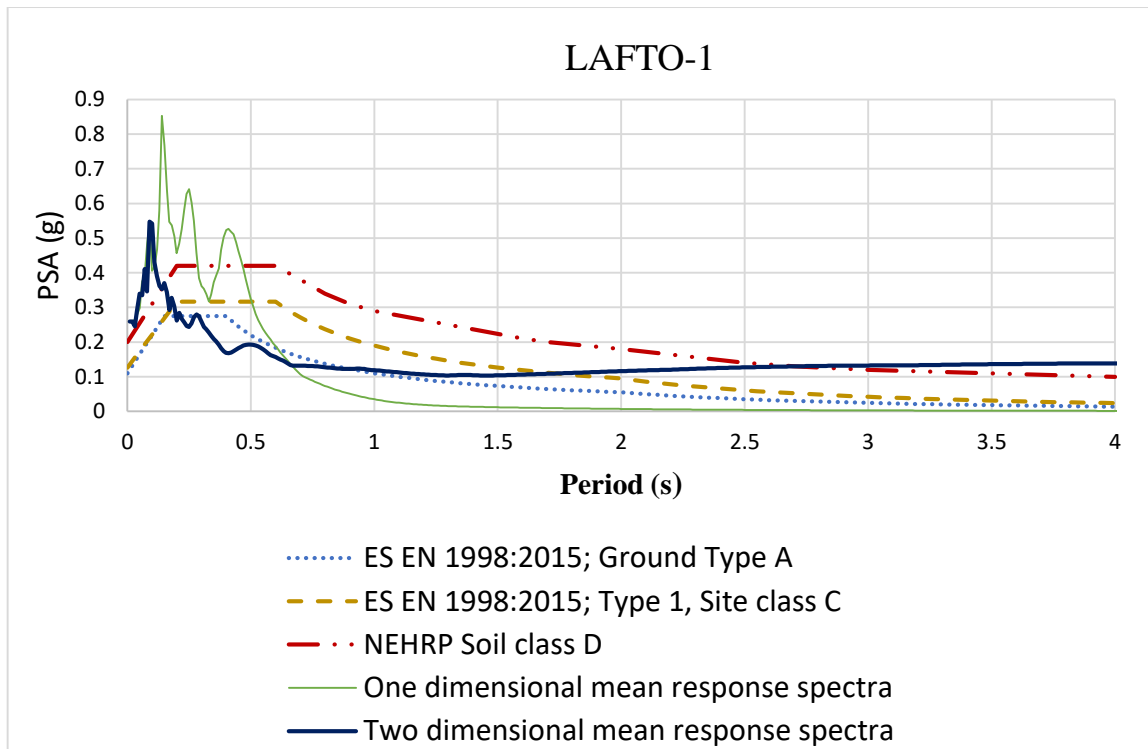


(b)

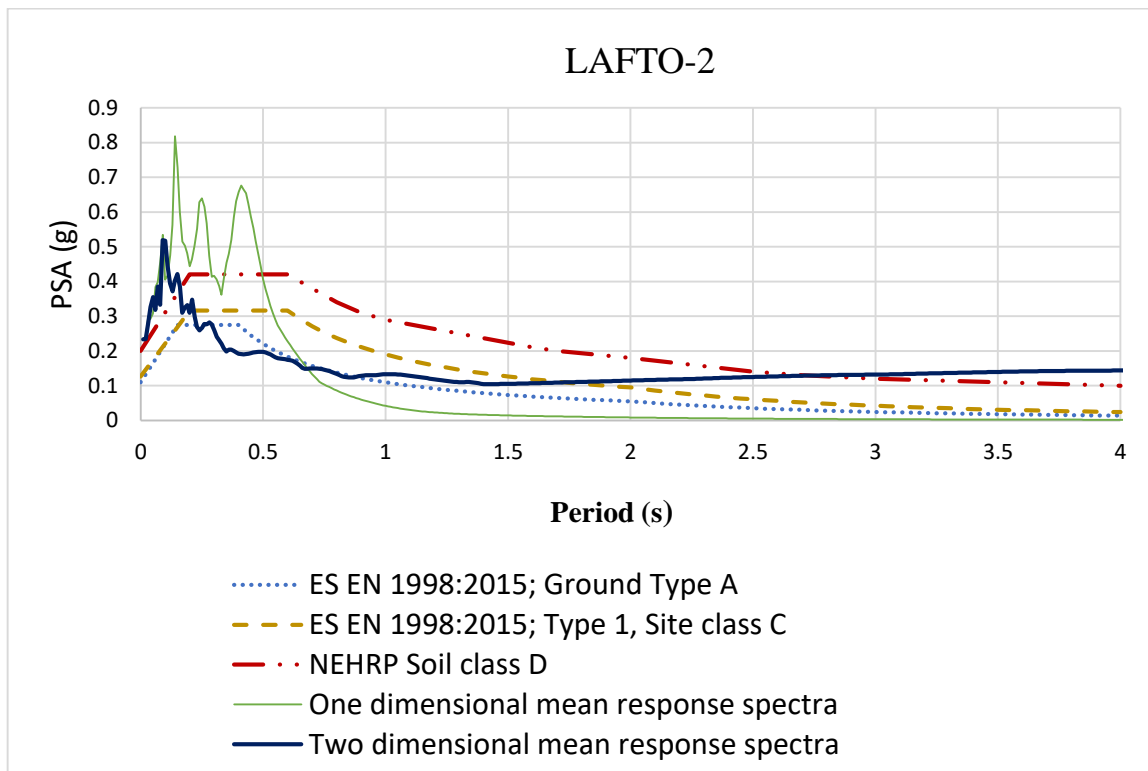


(c)

Figure 6-23: Comparison of mean response spectra from SPT data with code spectra: (b) Kirkos, and (c) Kolfe keranyo

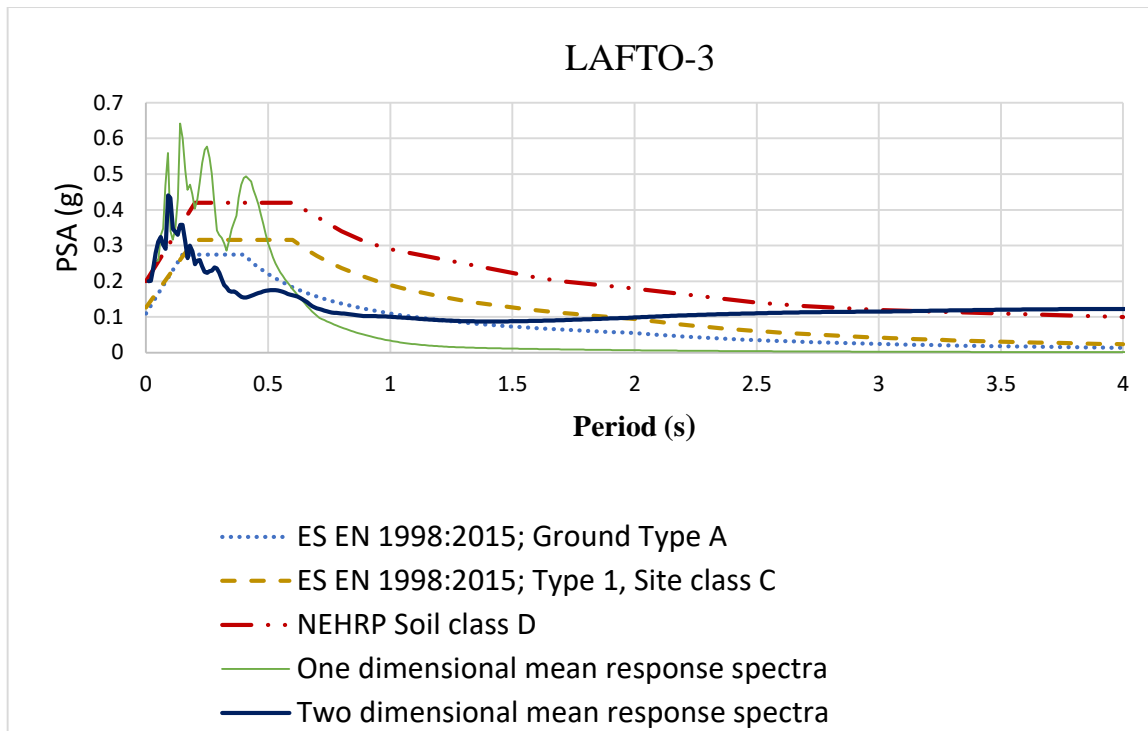


(d)

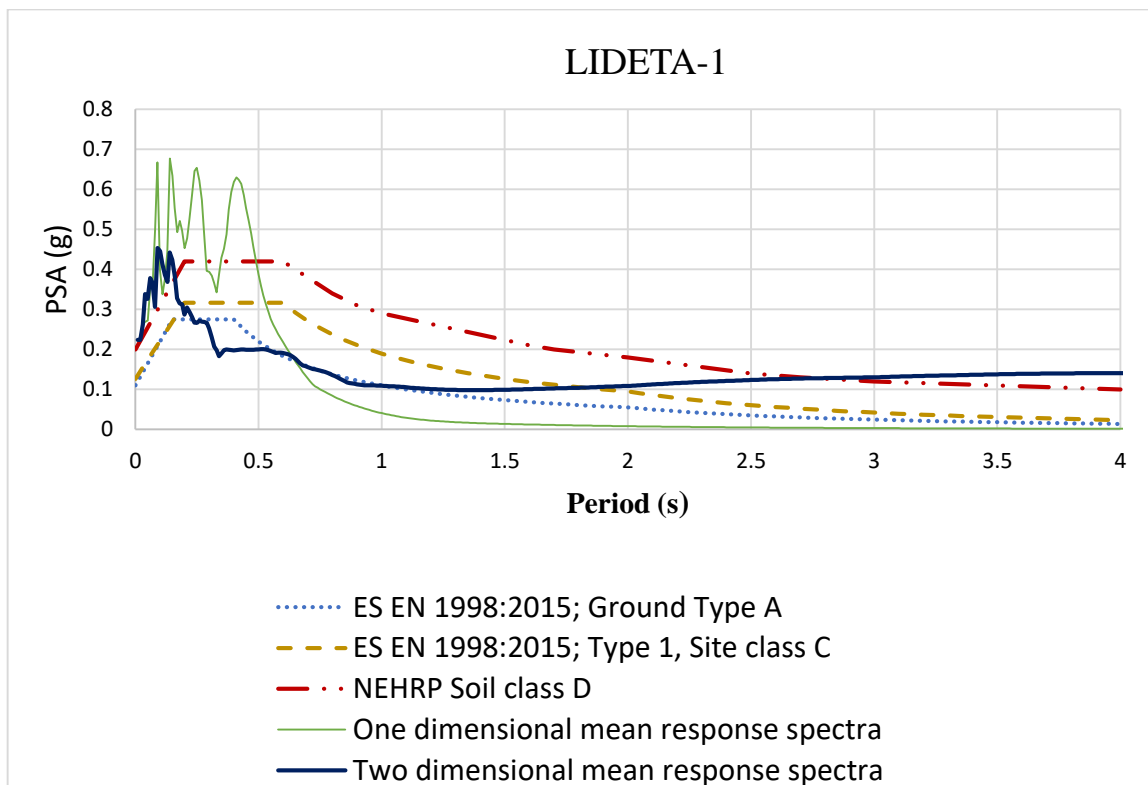


(e)

Figure 6-24: Comparison of mean response spectra from SPT data with code spectra: (d) Lafto-1, and (e) Lafto-2

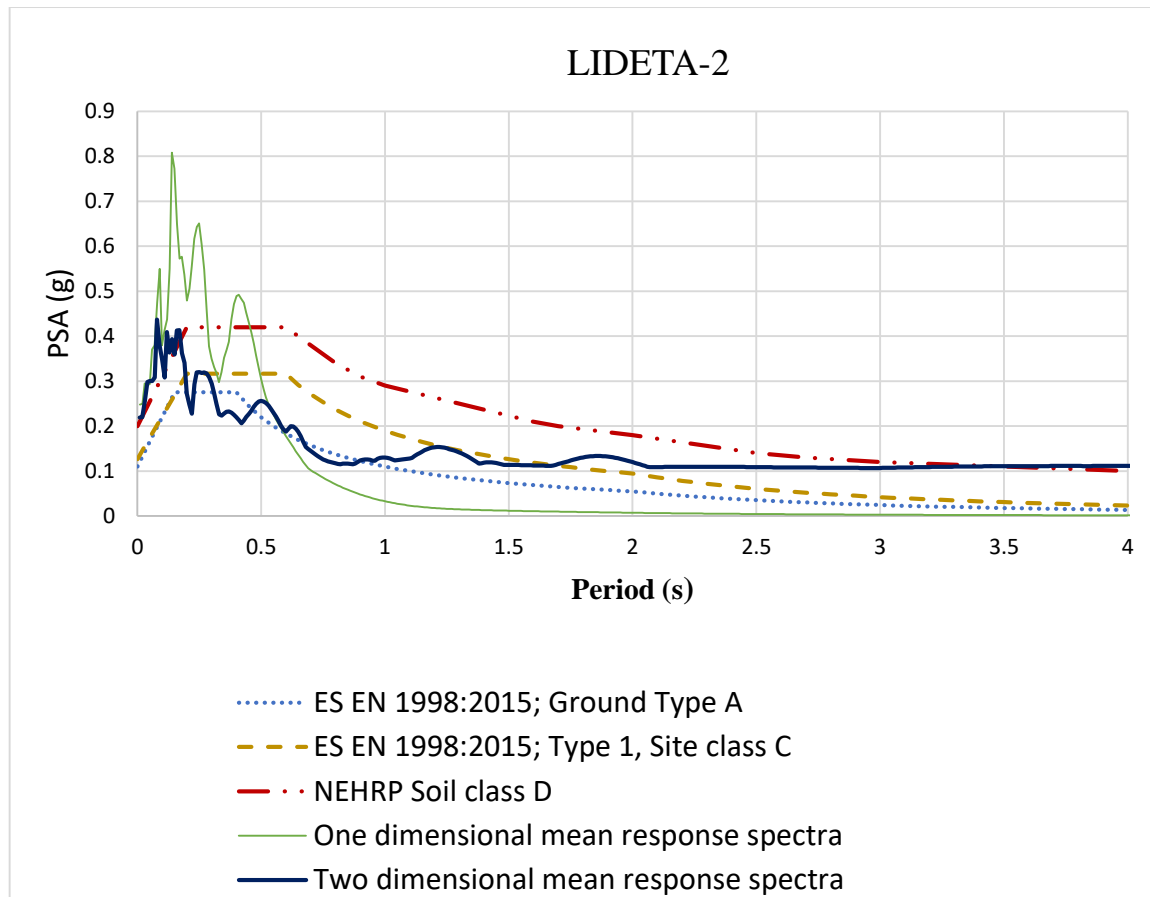


(f)



(g)

Figure 6-25: Comparison of mean response spectra from SPT data with code spectra: (f) Lafto-3, and (g) Lideta-1



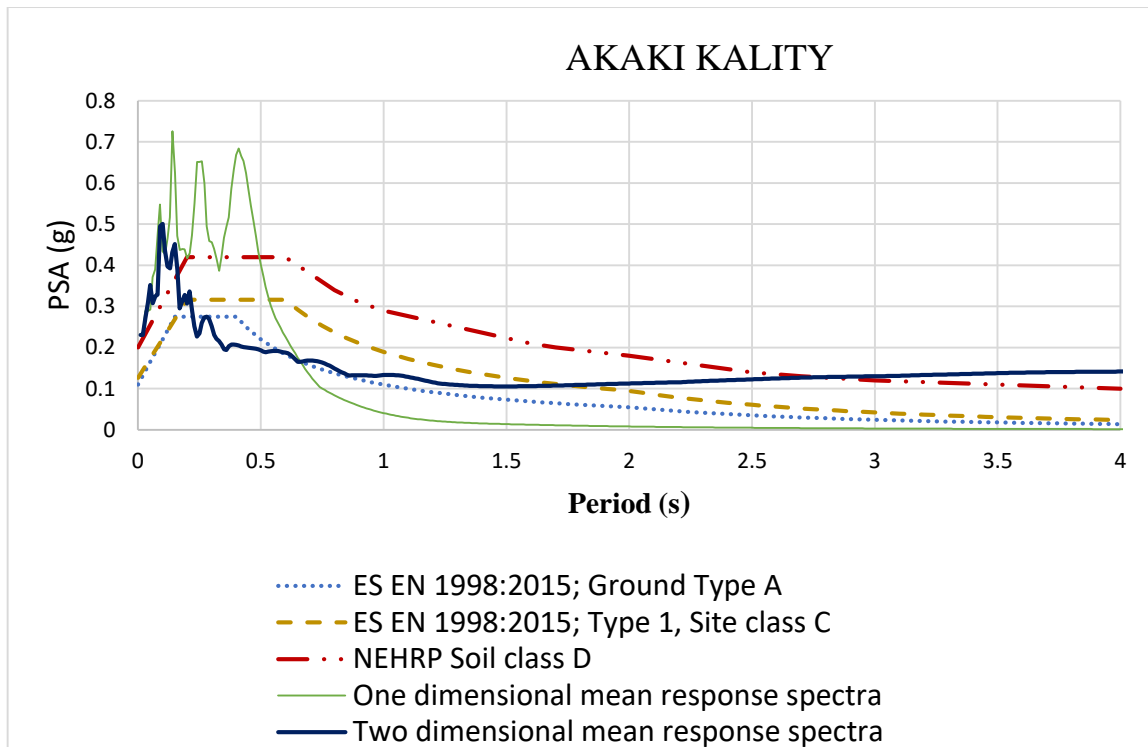
(h)

Figure 6-26: Comparison of mean response spectra from SPT data with code spectra: (h) Lideta-2

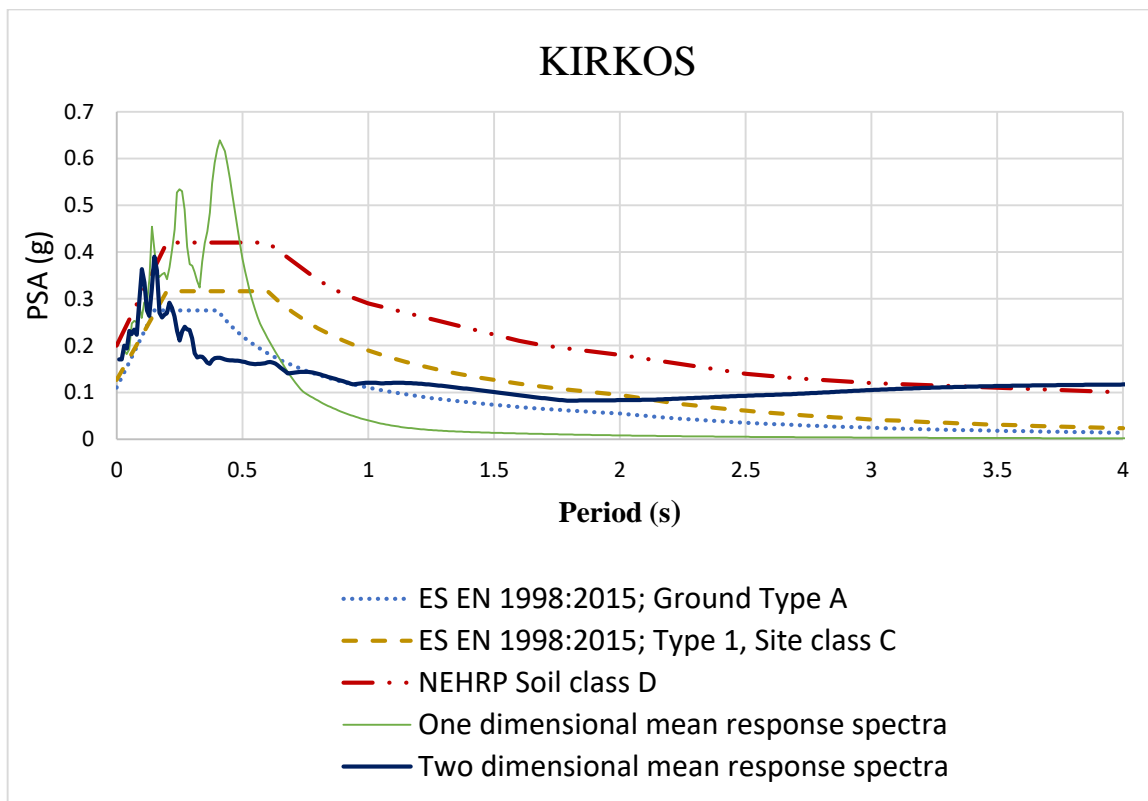
For Seismic survey data

Accelerations in one-dimensional analysis range from 0.52g to 1.37g and take place between 0.05 and 0.5 seconds. And, two-dimensional analysis reveals accelerations in the same time interval of 0.3g to 0.76g. Notably, this study's two-dimensional response spectra underestimated by ES EN 1998:2015 standards while nearly matching NEHRP requirements.

In nearly all cases, local code spectra underestimate the spectral acceleration between the time intervals of 0.05 and 0.5 second. Nevertheless, they typically overestimate the spectral acceleration between 0.5 and 1.5 seconds. This results indicates that additional research and modification of code provisions are necessary to provide more precise approximations over a range of time periods. The comparison of the code spectra and the mean response spectra from seismic survey data is shown in Figure 6-27 and Figure 6-28.

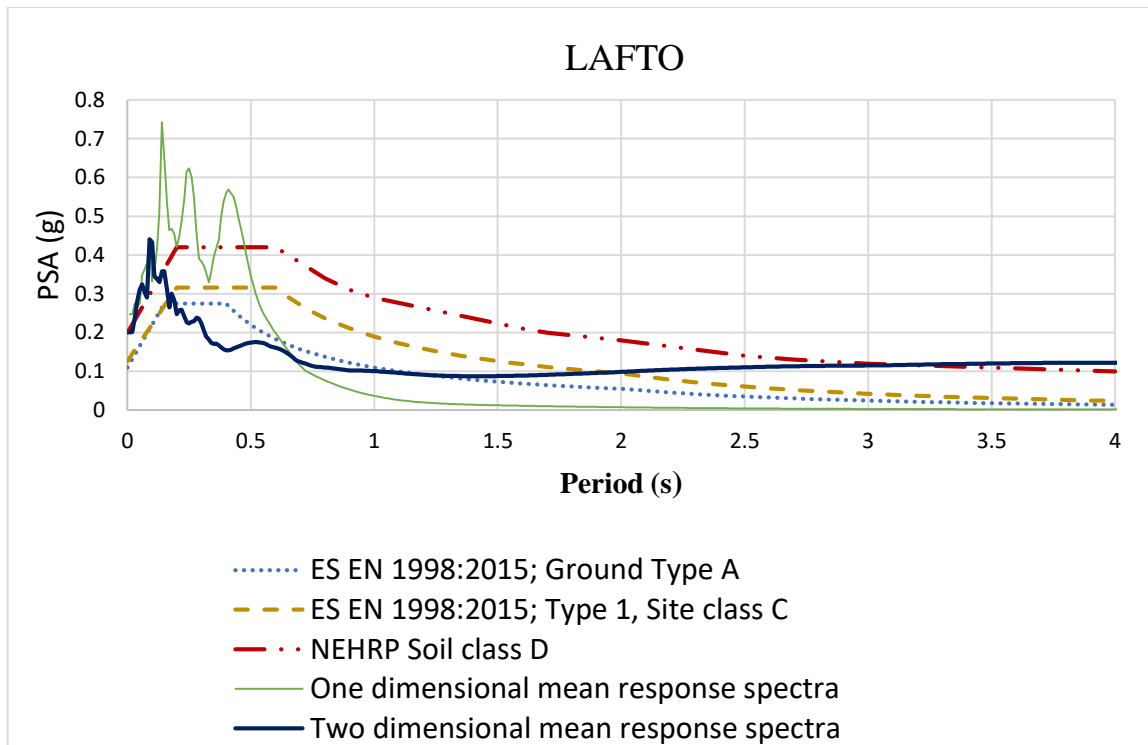


(a)

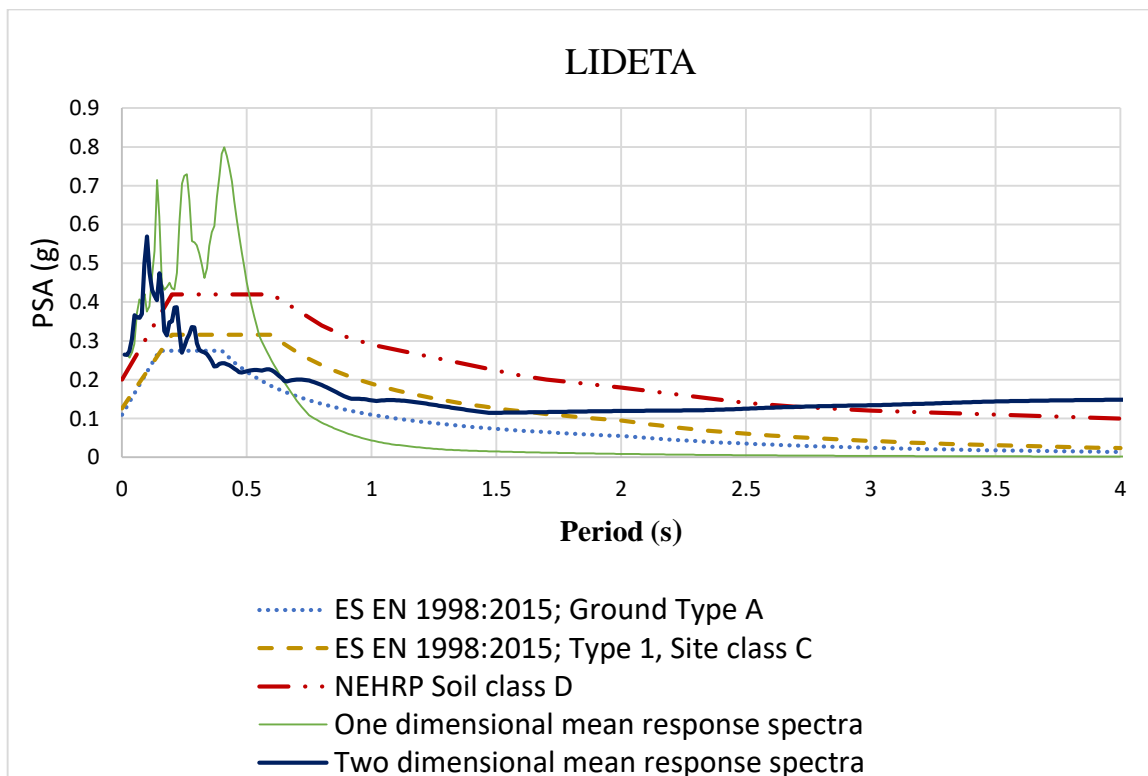


(b)

Figure 6-27: Comparison of mean response spectra from Seismic survey with code spectra: (a) Akaki kality, and (b) Kirkos



(c)



(d)

Figure 6-28: Comparison of mean response spectra from Seismic survey with code spectra: (c) Lafto, and (d) Lideta

6.3. Seismic micro zonation

Seismic micro zonation refers to the partitioning of an area with comparatively equal exposure to different types of earthquake related activity or the identification of specific locations with varying potential for seismic effects (Walling & Mohanty, 2009). It involves the assessment of local geological, geotechnical, and seismological conditions to evaluate factors such as soil behavior, ground shaking potential and liquefaction risk during an earthquake.

The purpose of micro zonation is to provide precise maps that identify regions with varying seismic risk, enabling more accurate planning and mitigation methods. Seismic micro zonation is necessary for areas of high seismic hazard, such as urban areas and areas that are soon to become urban, as well as for areas with moderate or low seismic hazard but where amplification is expected due to local geological conditions. The extent of the ground shaking during an earthquake is the most significant factor in determining the damage pattern caused by an earthquake (Walling & Mohanty, 2009). The results of micro zonation are crucial for urban planning, land use regulations, and designing earthquake resistant structures, as they help authorities and engineers understand and minimize the impact of seismic excitations.

Seismic micro zonation can be efficiently carried out with Geographic Information Systems (GIS). Strong tools are available in GIS for organizing, evaluating, and displaying many datasets such as seismicity, topography, and soil properties that are necessary for micro zonation.

6.3.1. Geographic Information System (GIS) data

Geographic Information System is a powerful tool used for capturing, storing, analyzing, and visualizing spatial and geographic data. It allows users to create detailed maps, perform spatial analysis, and model relationships between different geographical features. To create extensive spatial information, GIS software can incorporate a variety of data sources, including GPS coordinates, survey data, and satellite images.

GIS has numerous uses in the fields of land development, housing, transportation, land use, and the environment. Analyzing the suitability of the land and choosing a site are major examples (Yeh, 2005).

Some widely used GIS software includes ArcGIS, QGIS, and MapInfo, each offering features like data management, geo-processing, and advanced visualization tools. ArcGIS is used for this study since it is an advanced GIS tool due to its reliable capabilities for handling large datasets, performing complex spatial analysis, and producing high quality visualizations.

6.3.2. Shape file of Addis Ababa

Geometric data types, such as points, lines, and polygons, are stored in shape files along with a table of records that contains data attributes and properties. When combined with data properties, shapes (points, lines, and polygons) can form an endless number of representations for geographical data. (Shardul M. Chokshi, 2011). The shape file of countries can be obtained from several reliable sources, including GADM.org, DIVA-GIS, and Natural Earth, which offer free access to detailed administrative boundary data. For this study GADM.org is used for mapping in GIS.

The Global Administrative Areas (GADM) database offers comprehensive, accessible spatial data on administrative borders for every country worldwide. For usage with GIS software, it provides geographic data on numerous levels, including boundaries for countries, states, provinces, and districts. This data can be downloaded in a variety of forms, such as shape files and geo-packages. GADM is used since this study requires clearly defined administrative borders.

The GADM website is accessed, and a search for Ethiopia is done in order to obtain the Addis Ababa shape file. Based on the findings, Addis Ababa's administrative level is chosen. Then, after downloading the shape file in the proper format, it is imported into GIS software to be further processed. The South - Western part of Addis Ababa is then extracted from Addis Ababa's shape file using the attribute data earned from the shape file collected from GADM website.

6.3.3. Mapping two dimensional ground response analysis results

A comprehensive seismic hazard map is created for five specific sub cities inside the city using the shape file of Addis Ababa and the outcomes of the two-dimensional ground response analysis. The precise administrative boundaries provided by the shape file is utilized to determine the geographical limits of each sub city of the study.

The map illustrates zones of higher and lower seismic amplification by highlighting varying peak ground acceleration results. GIS data combined with ground response analysis provides a thorough visual illustration of the South – Western part of Addis Ababa's potential seismic response. Figure 6-29 illustrates the Seismic micro zonation map of the study area.

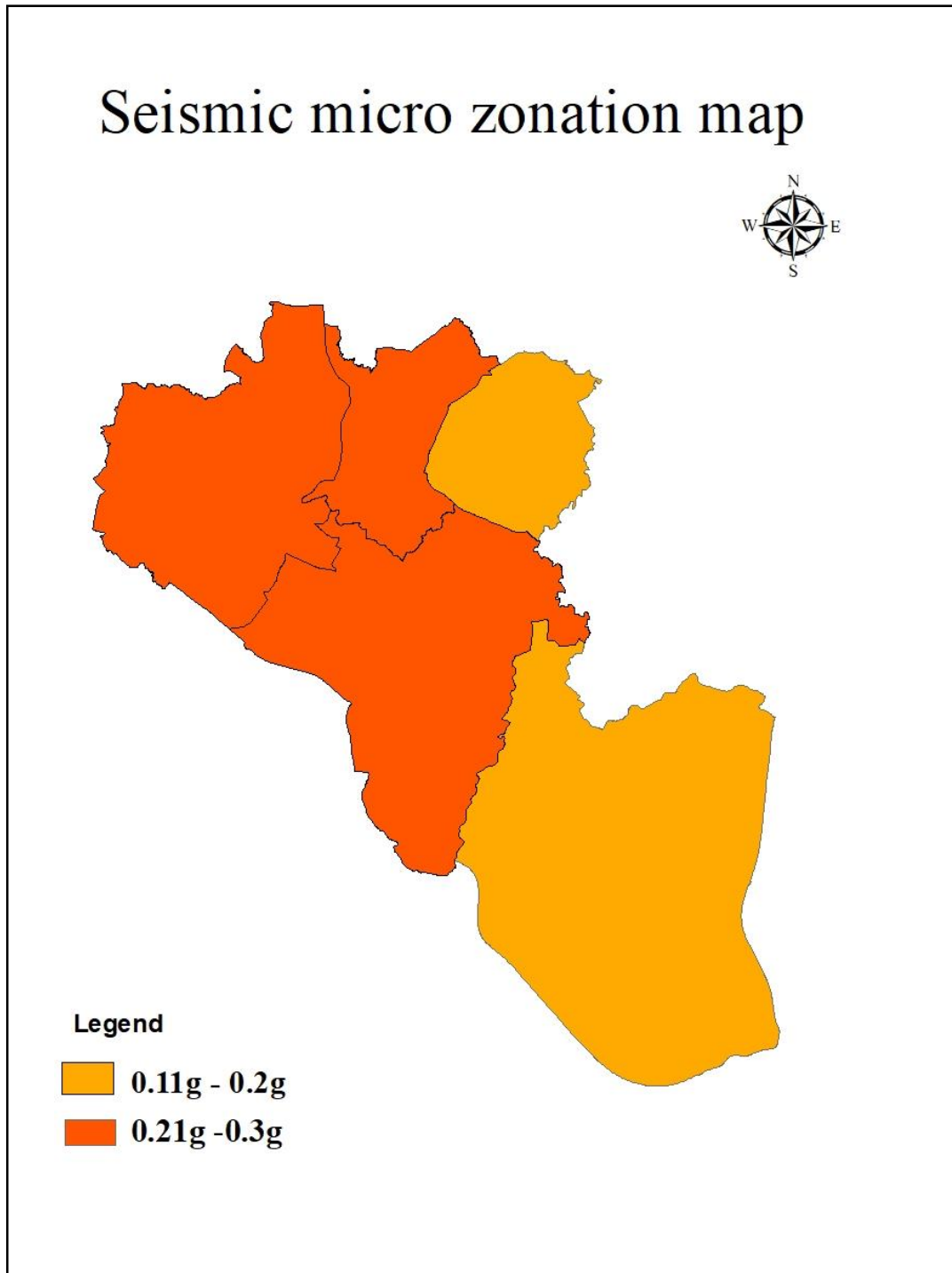


Figure 6-29: Seismic micro zonation map

The seismic micro zonation map indicated in Figure 6-29 shows that Kolfe keranyo, Lideta, and Nifas silk lafto sub cities from the study area have magnified the input ground motion between 0.21 g and 0.3 g, whereas Kirkos and Akaki kality sub cities have magnified the input ground motion between 0.11 g and 0.21 g, indicating relatively less susceptibility to earthquake-induced problems.

In the previous study by Getu (2023), the PGA results for the three study areas are as follows: Mexico (in Lideta sub city) recorded a PGA of 0.23g, Jemo (in Lafto sub city) recorded 0.21g, and Genet Hotel (in Kirkos sub city) recorded 0.18g. Comparing the previous study with this study's micro zonation map, I found that its results align closely and can be incorporated into this map, indicating strong agreement between the findings.

CHAPTER SEVEN

7. CONCLUSION AND RECOMMENDATION

7.1. Conclusion

To conduct two-dimensional ground response analysis in the South - Western part of Addis Ababa, representative geotechnical and geophysical data were collected from various sites within the study boundary. Based on the collected data, the sites are characterized accordingly. And this detailed characterization helps in understanding the diverse subsurface conditions.

Using the collected input data and earthquake motion, which is filtered from the PEER ground motion database, two-dimensional ground response analysis is conducted for each site using PLAXIS 2D software. The analysis provides detailed insights into site-specific responses. And the Seismic micro zonation map is produced combining shape files and peak ground response analysis results. Based on the results, the following conclusions are drawn.

- The range of the peak ground acceleration for two-dimensional analysis, as determined by geotechnical data, is 0.17 g to 0.28g, while for geophysical data, it is 0.14g to 0.29g. These PGA results show that the input ground motion is amplified by about 2.
- The mean response spectra from one-dimensional analysis range from 0.5g to 1.23g based on SPT data and from 0.52g to 1.37g based on seismic survey data. For two-dimensional analysis, the mean response spectra range from 0.36g to 0.67g based on SPT data and from 0.3g to 0.76g based on seismic survey data. These results indicate a significant difference between one-dimensional and two-dimensional analyses.
- The comparison between one-dimensional and two-dimensional mean response spectra with the code spectra reveals significant differences. Between the time periods of 0.05 and 0.5 seconds, local code ES EN 1998:2015 tend to underestimate the spectral acceleration in most cases but closer to NEHRP provisions.

Conversely, between 0.5 second and 1.5 seconds, they generally overestimate the spectral acceleration. Notably, the results from two-dimensional analysis align more closely with NEHRP provisions. This indicates a need to revise the local code design spectra, as it currently underestimates the mean response spectra for the entire study area.

- The seismic micro zonation indicated that Kolfe keranyo, Lideta, and Nifas silk lafto sub cities have magnified the input ground motion between 0.21g and 0.3g, whereas Kirkos and Akaki kality sub cities have magnified the input ground motion between 0.11g and 0.2g, indicating relatively less susceptibility to earthquake induced problems.
- In the previous study by Getu (2023), the PGA results for the three study areas are, Mexico (in Lideta sub city) recorded a PGA of 0.23g, Jemo (in Lafto sub city) recorded 0.21g, and Genet Hotel (in Kirkos sub city) recorded 0.18g. I found that its results align closely and can be incorporated into this micro zonation map, indicating strong agreement between the findings.

7.2. Recommendation

The study found that the selected sites in the South - Western part of Addis Ababa amplified the input ground motion more than the local code spectra estimates but near to the NEHRP provisions. Therefore, it is recommended to revise the local code spectra and conduct a detailed investigation and mapping of the rest six sub cities of Addis Ababa to ensure accurate seismic risk assessment and improve safety measures.

REFERENCE

- Abiy, B. T., & Ababa, A. (2021). *Site Response Analysis of Selected Sites of Adama City. September.*
- Arjuna, N., Adnan, A., Bakar, N. A., Aizon, N. H., Sheena, N., & Harith, H. (2021). *Malaysian Journal of Geosciences (MJG) 2-DIMENSIONAL GROUND RESPONSE ANALYSIS : A REVIEW. 01(1), 35–40.*
<https://doi.org/10.26480/mjg.01.2021.35.40>
- Ark, C. H. B. P., Iller, R. I. D. M., Ia, J. I. X., Vanov, J. U. I., & Survey, K. G. (2007). *Multichannel analysis of surface waves (MASW)— Figure 1, 60–64.*
- Ayele, H. (2021). *SIMULATION OF LOAD – DISPLACEMENT RESPONSE OF PILE FOUNDATION.*
- Ayolabi, E. A., Adeoti, L. and, & Oshinlaja, N. (n.d.). *Seismic Refraction and Resistivity Studies of part of Igbogbo Township , South- Seismic Refraction and Resistivity Studies of part of Igbogbo. February 2015.*
- Bommer, J. J., Stafford, P. J., & Alarcón, J. E. (2009). Empirical equations for the prediction of the significant, bracketed, and uniform duration of earthquake ground motion. *Bulletin of the Seismological Society of America, 99(6), 3217–3233.*
<https://doi.org/10.1785/0120080298>
- Bowles, J. E. (1996). Foundation Analysis and Design. In *Civil Engineering Materials.*
- Brinkgreve, B. J. R. (2005). *Copyright ASCE 2005 69 Soil Constitutive Models Evaluation, Selection, and Calibration. 69–98. doi*
- Chopra, A. K. (2012). *Dynamics of structures : theory and applications to earthquake engineering, 4/E.*
- Dogan, A. (2023). *Site Response Analysis by Generating a New 3-d Mesh Design With Surface Topography : a 3-d Site Response Analysis of Northwest Turkey.*
<https://doi.org/https://doi.org/10.21203/rs.3.rs-3163395/v1>
- EBCS-8. (1995). *Ethiopian Building code standard-8, Design of structures for earthquake resistance.* Urban, Ministry of Works & Development. Addis Ababa, Ethiopia.

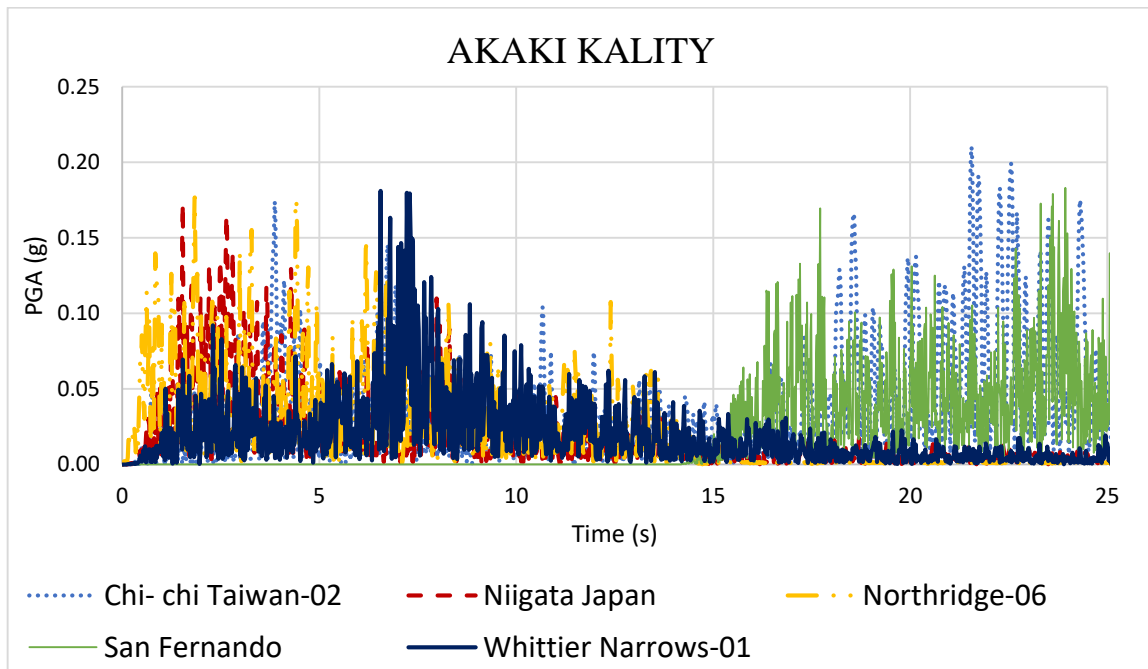
- Edition, C., & Manual, T. (2021). *CONNECT Edition V21.01 PLAXIS 2D - Tutorial Manual*. 1–255.
- Engidasew, T. A., & Abay, A. (2016). *Assessment and Evaluation of Volcanic Rocks Used as Construction Materials in the City of Addis Ababa*. 8(2), 193–212.
- Eshetu, B. (2017). *Ground Response Analysis of Selected Sites in Hawassa Area Addis Ababa Institute of Technology School of Civil and Environmental Engineering*.
- Gashaye, Z. (2018). An Investigation into the Ground Motion Amplification Potential of Selected Sites of Addis Ababa City. *Addis Ababa Institute of Technology School of Civil and Environmental Engineering, July*, 1–165.
- Getu, B. (2023). *Nonlinear Ground Response Analysis of Selected Sites of Addis Ababa using Geotechnical and Seismic data*. May.
- Giardini, Domenico , Grunthal Gottfried, S. M. K. and Z. P. (n.d.). *The_GSHAP_Global_Seismic_Hazard_Map.pdf*.
- Kamalian, M., Kazem, M., & Sohrabi-bidar, A. (2006). *Time-domain two-dimensional site response analysis of non-homogeneous topographic structures by a hybrid BE / FE method*. 26, 753–765. <https://doi.org/10.1016/j.soildyn.2005.12.008>
- Kebede, F., & Van Eck, K. (1997). *Probabilistic seismic hazard assessment for the Horn of Africa based on seismotectonic regionalisation*. 270, 221–237.
- Kumar, S. S., & Krishna, A. M. (2013). *Seismic Ground Response Analysis of Some Typical Sites of Guwahati City*. 4(June), 83–101.
<https://doi.org/10.4018/jgee.2013010106>
- Luna, R., & Jadi, H. (2000). *DETERMINATION OF DYNAMIC SOIL PROPERTIES USING GEOPHYSICAL METHODS*. December, 1–15.
- Mammo, T. (2005). Site-specific ground motion simulation and seismic response analysis at the proposed bridge sites within the city of Addis Ababa, Ethiopia. *Engineering Geology*, 79(3–4), 127–150.
<https://doi.org/10.1016/j.enggeo.2005.01.005>
- Martin, G., & Lew, M. (1999). Recommended procedures for implementation of DMG Special Publication 117, Guidelines for analyzing and mitigating liquefaction

- hazards in California. *University of Southern California*, 63.
<http://scholar.google.com/scholar?hl=en&btnG=Search&q=intitle:Recommended+Procedures+for+Implementation+of+DMG+Special+Publication+117+Guidelines+for+Analyzing+and+Mitigating+Liquefaction+Hazards+in+California#0>
- Park, C. B., Miller, R. D., & Xia, J. (1999). *Multichannel analysis of surface waves*. *64*(June), 800–808.
- PEER. (2010). *Users Manual for the PEER Ground Motion Database Web Application*.
- Salmon, M. W., & Short, S. A. (1992). *Strong Motion Duration and Earthquake Magnitude Relationships EQE Engineering Consultants Robert P. Kennedy RPK Structural Mechanics Consulting., ie 1992*.
- Shardul M. Chokshi. (2011). THE SHAPE FILE MANIPULATION TOOL. *Acta Universitatis Agriculturae et Silviculturae Mendelianae Brunensis*, *16*(2), 39–55.
- Stewart, J. P. (2014). *Guidelines for Performing Hazard-Consistent One-Dimensional Ground Response Analysis for Ground Motion Prediction*. October.
- Tchakalova, B., & Ivanov, P. (2022). *Correlation between effective cohesion and plasticity index of clay*. *51*(December), 45–49.
- Wair, B. R., Dejong, J. T., & Shantz, T. (2012). Guidelines for Estimation of Shear Wave Velocity Profiles. *Pacific Earthquake Engineering*, *8*(December), 68.
- Walling, M. Y., & Mohanty, W. K. (2009). Earth-Science Reviews An overview on the seismic zonation and microzonation studies in India. *Earth Science Reviews*, *96*(1–2), 67–91. <https://doi.org/10.1016/j.earscirev.2009.05.002>
- Wondie, Y. (2020). *No Title*. July.
- Yeh, A. G.-O. (2005). Urban planning and GIS. *Geographical Information Systems: Principles, Techniques, Management and Applications*, 404.
<http://masters.dgtu.donetsk.ua/2014/igg/gyulumyan/library/tem6.pdf>

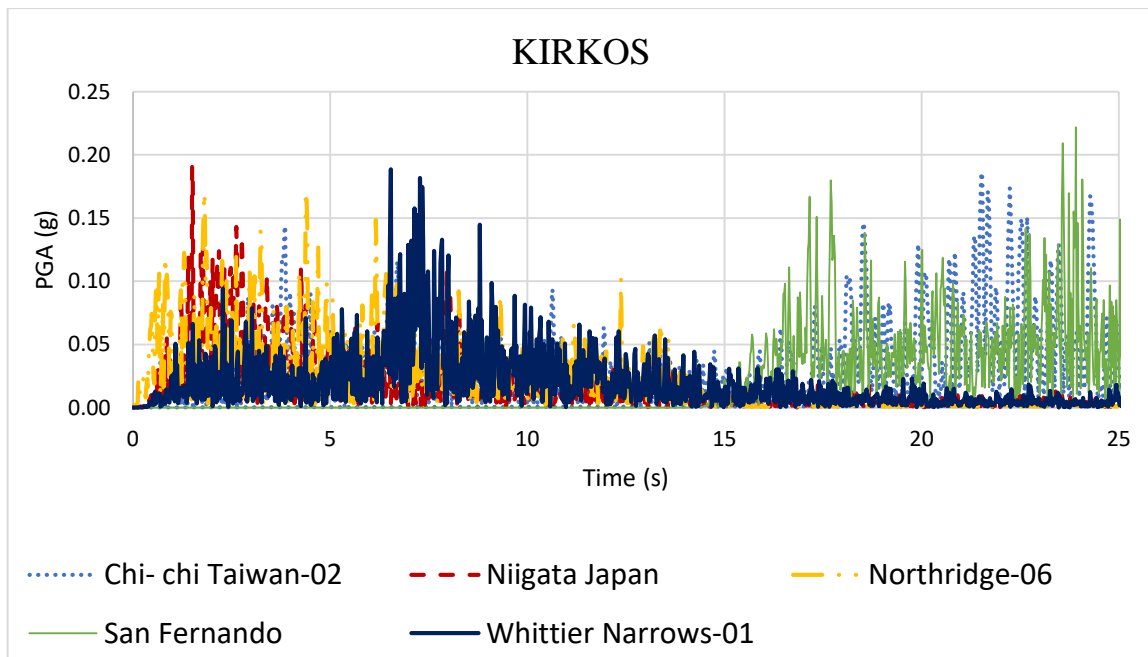
Appendix A

Peak Ground Acceleration (PGA)

a. Based on SPT data

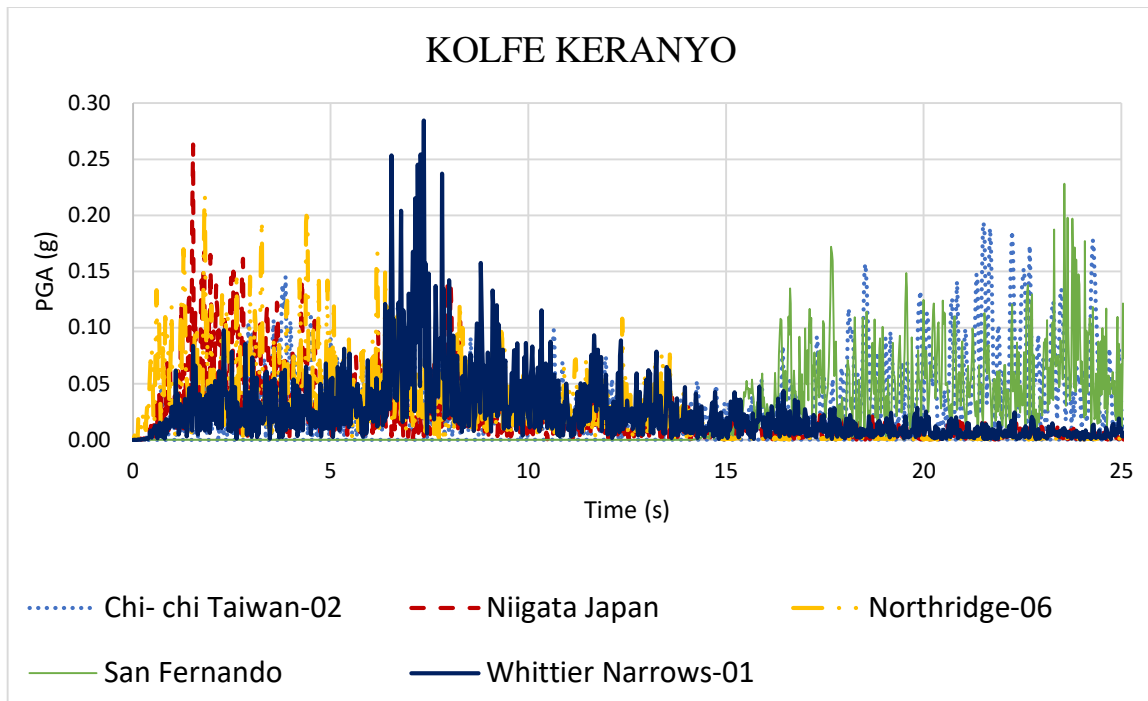


(a)

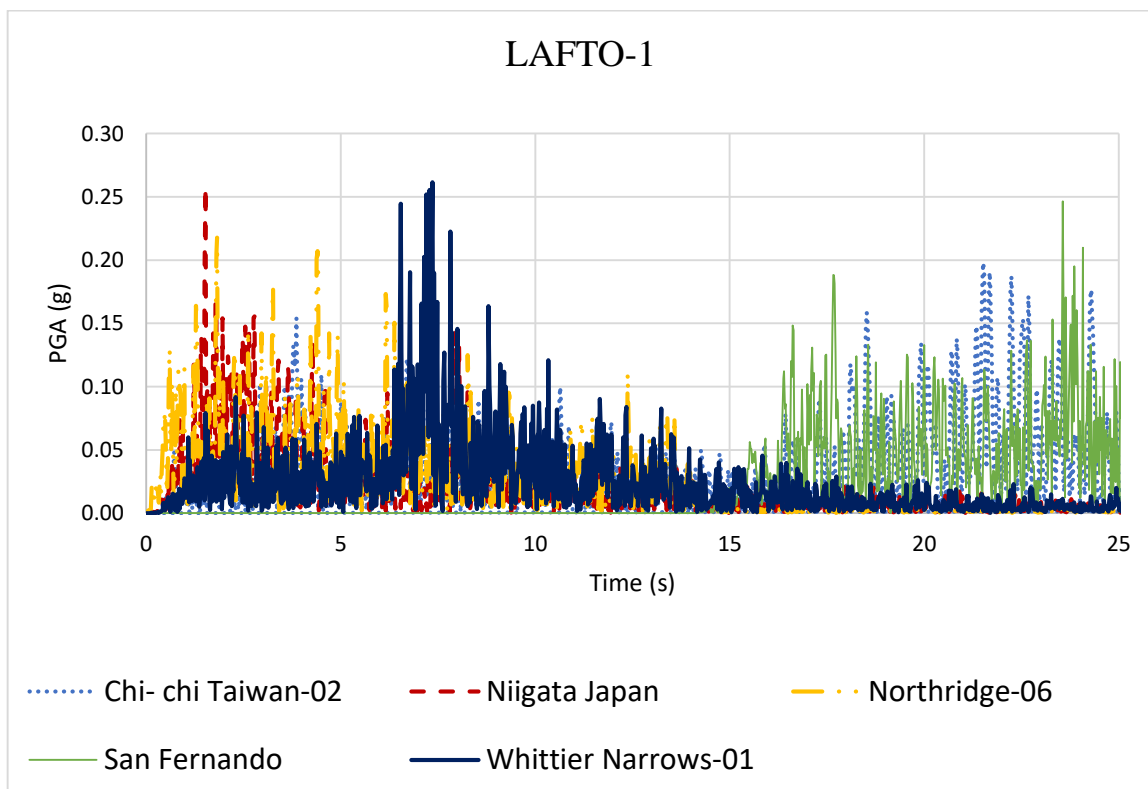


(b)

Figure A- 1: PGA results from SPT data: a) Akaki kality,and (b) Kirkos

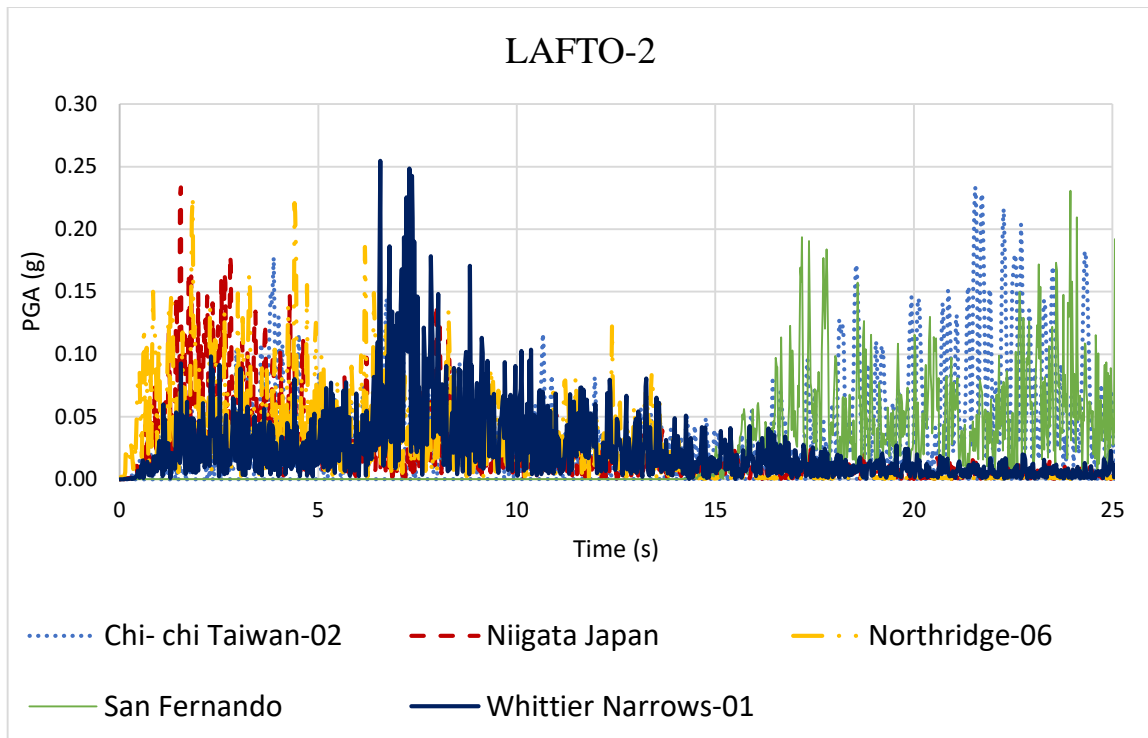


(c)

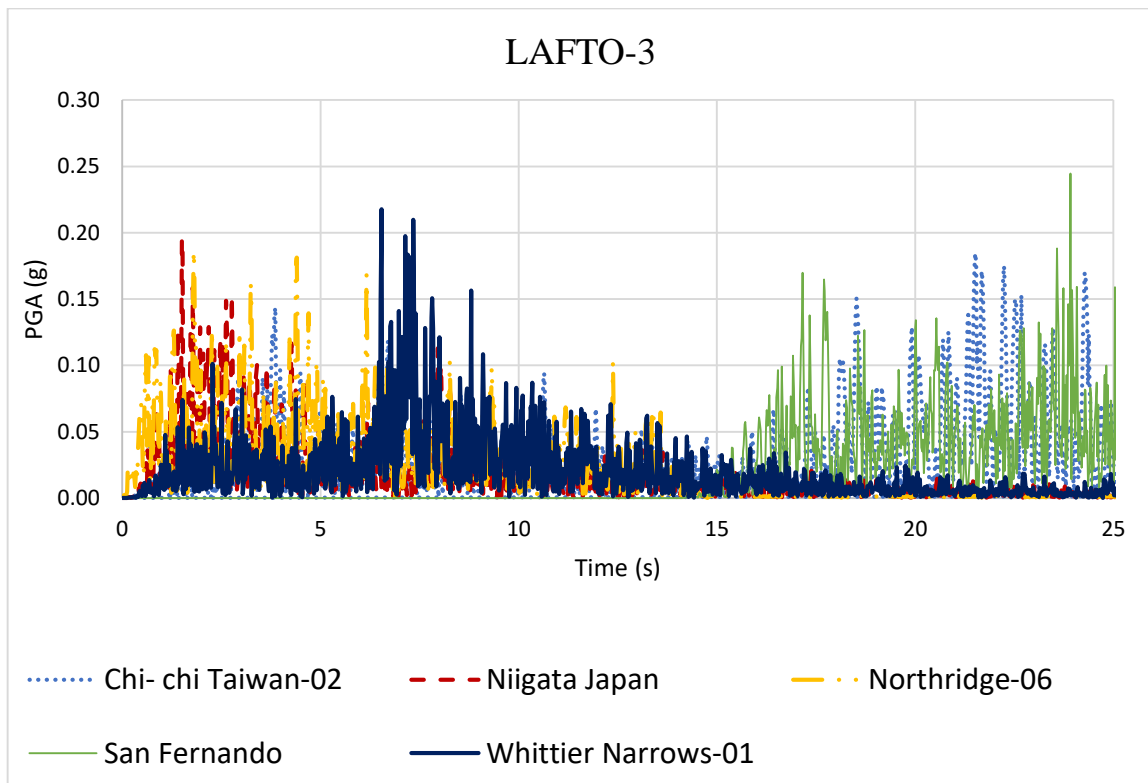


(d)

Figure A- 2: PGA results from SPT data: (c) Kolfe keranyo, and (d) Lafto-1

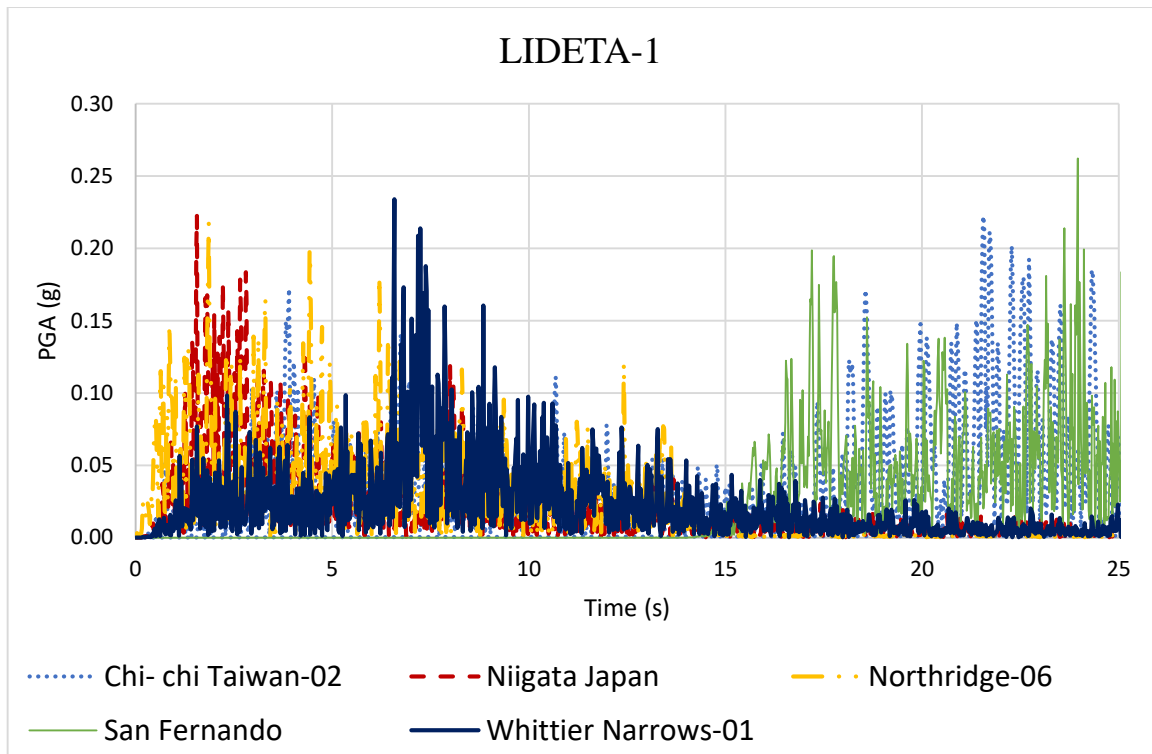


(e)

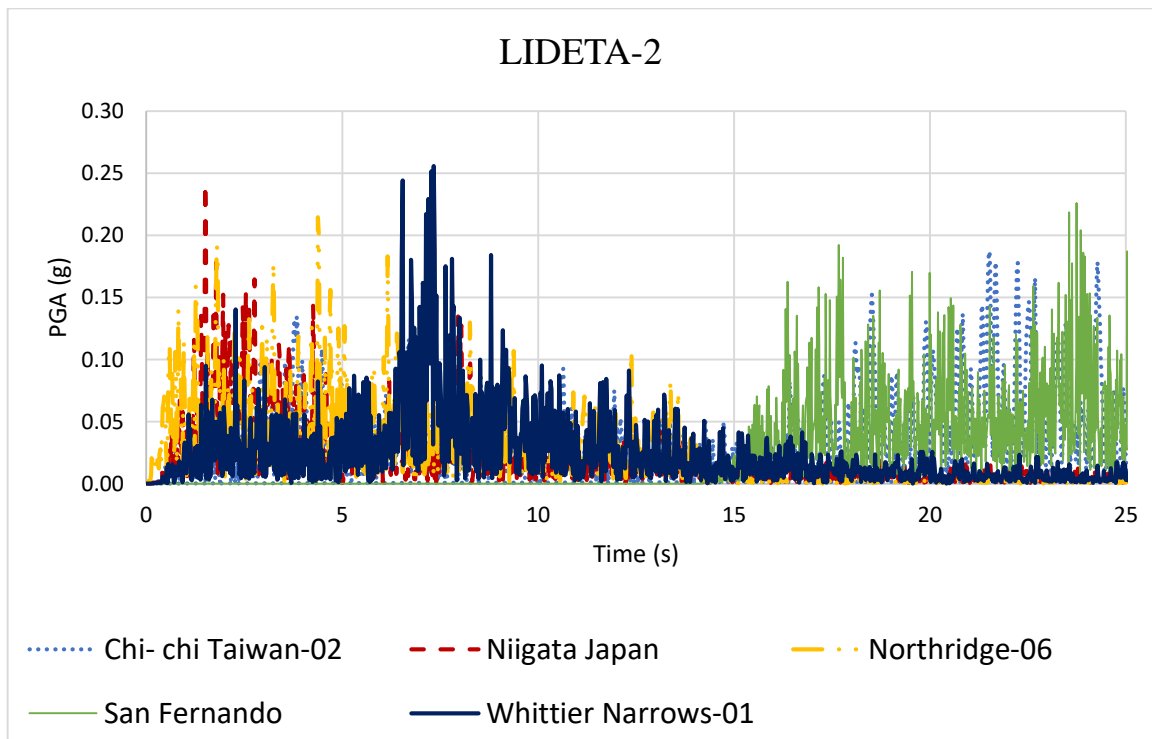


(f)

Figure A- 3: PGA results from SPT data: (e) Lafto-2,and (f) Lafto-3



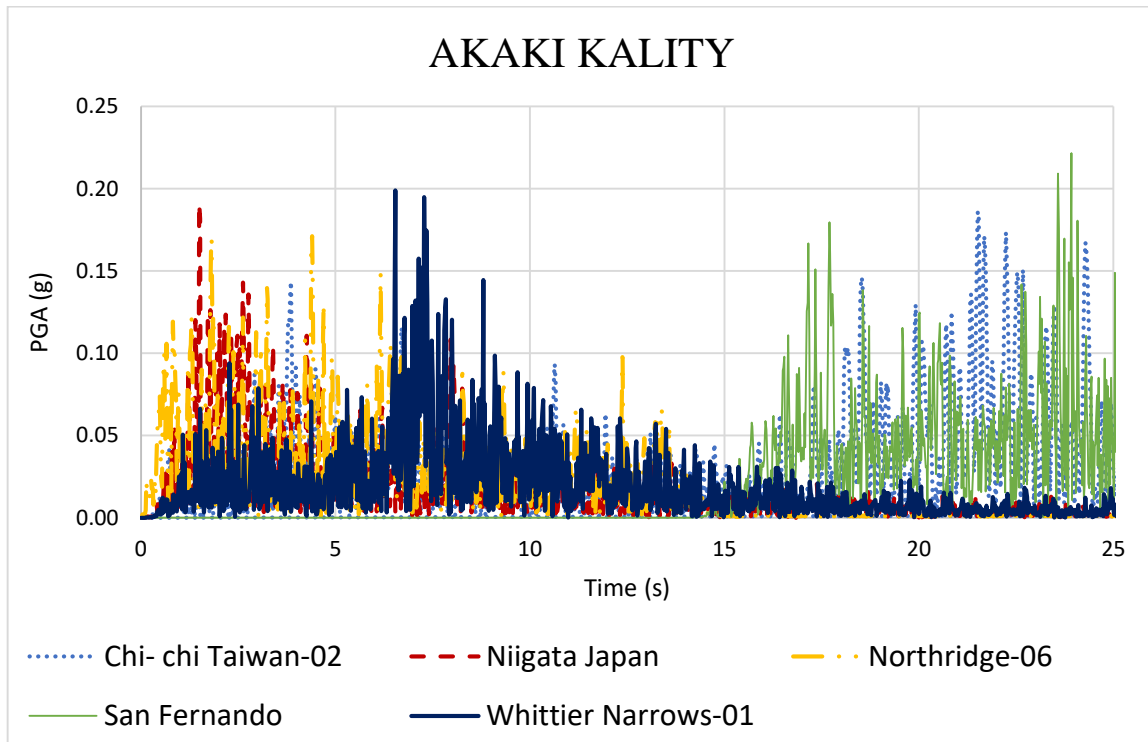
(g)



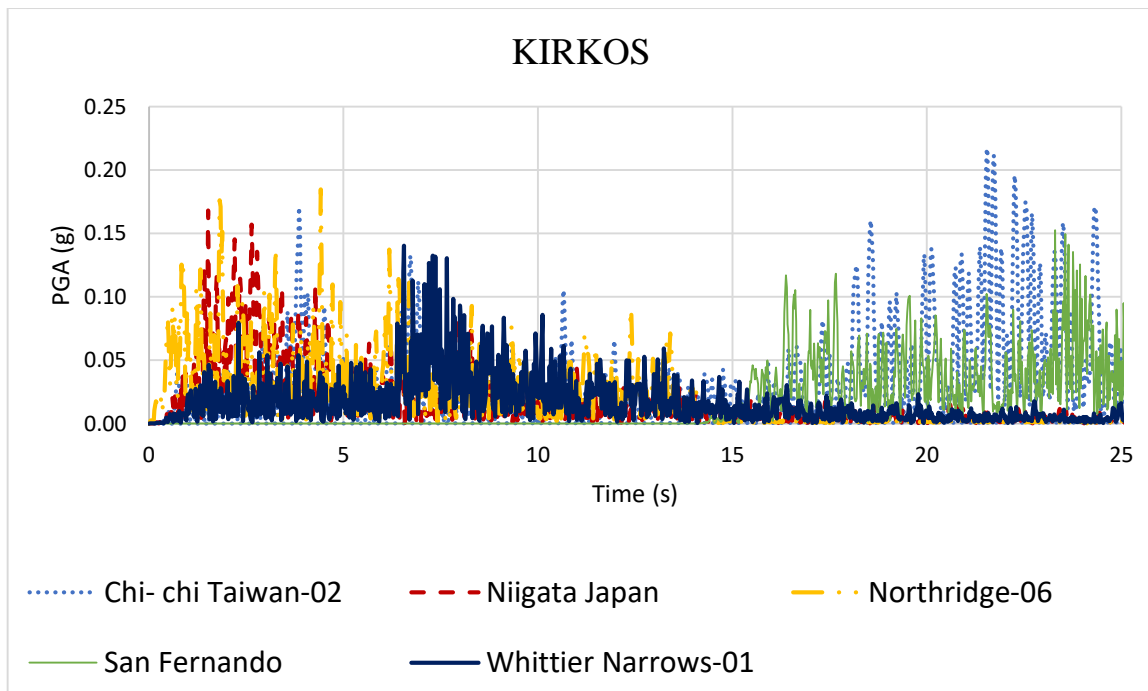
(h)

Figure A- 4: PGA results from SPT data: (g) Lideta-1, and (h) Lideta-2

b. Based on Seismic survey data

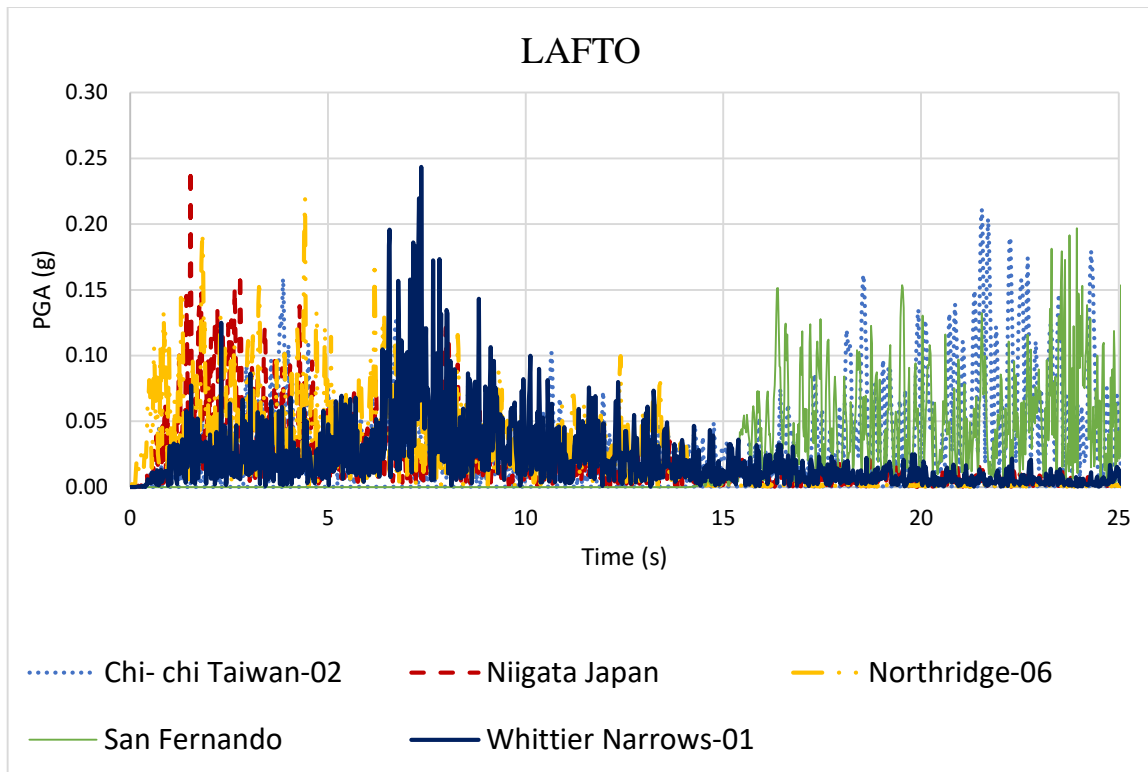


(a)

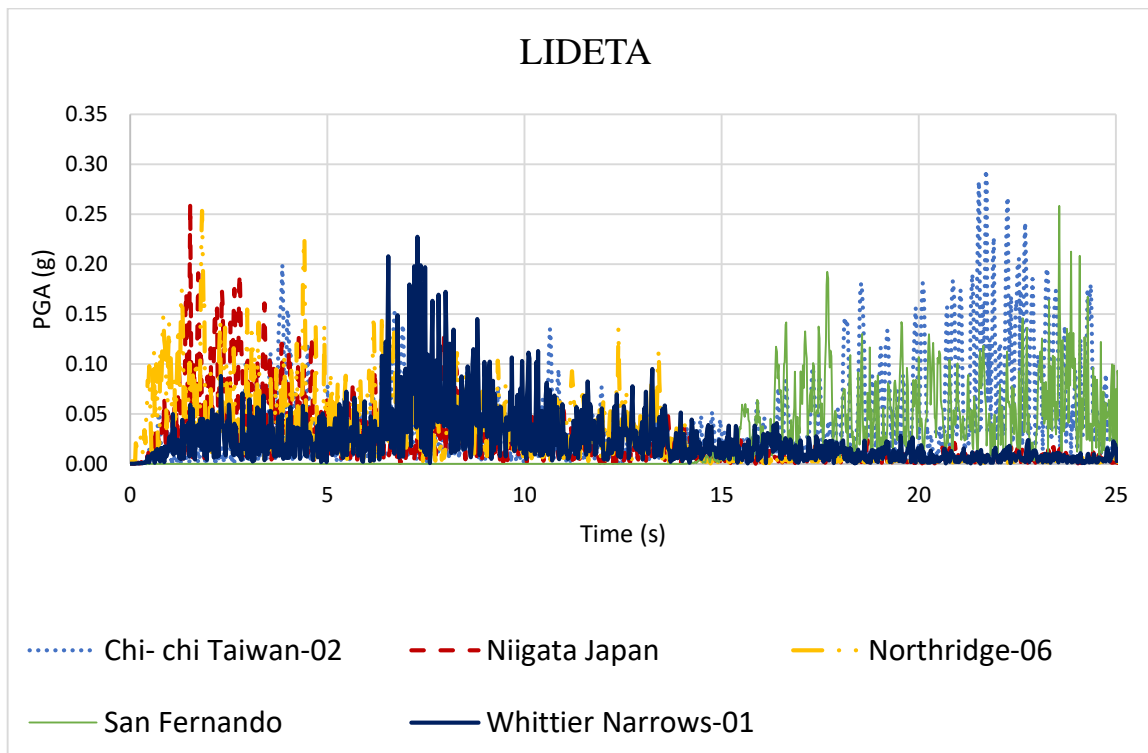


(b)

Figure A- 5: PGA results from Seismic survey data: (a) Akaki Kality, and (b) Kirkos



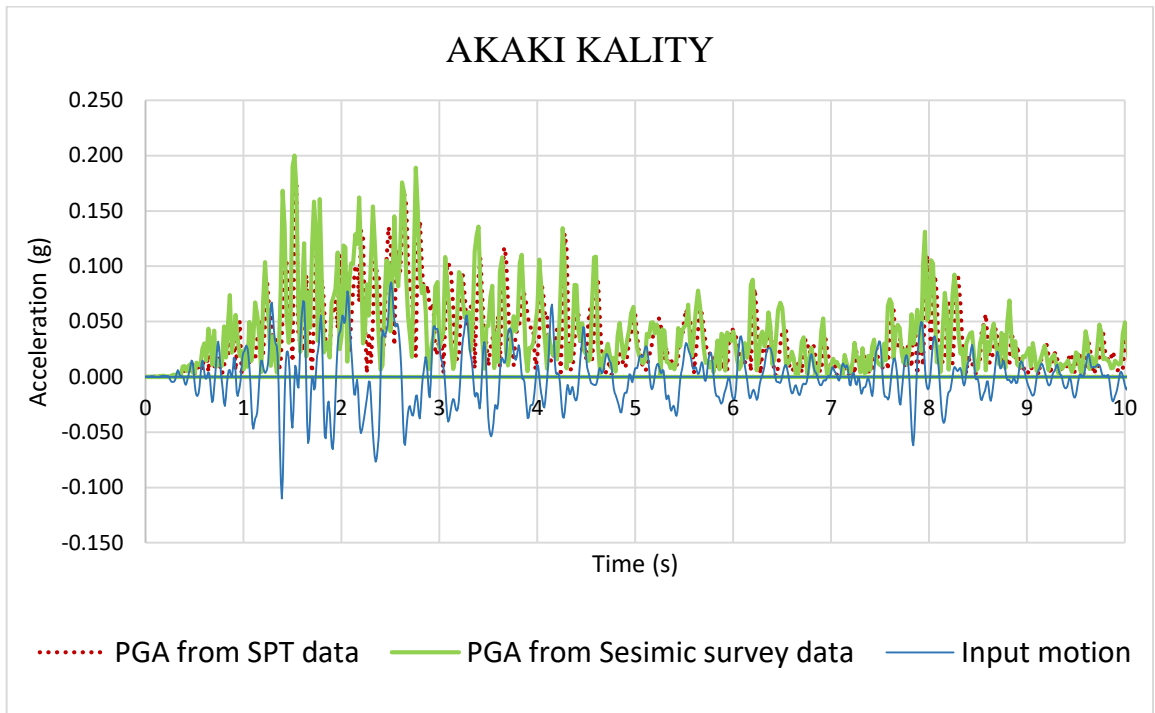
(c)



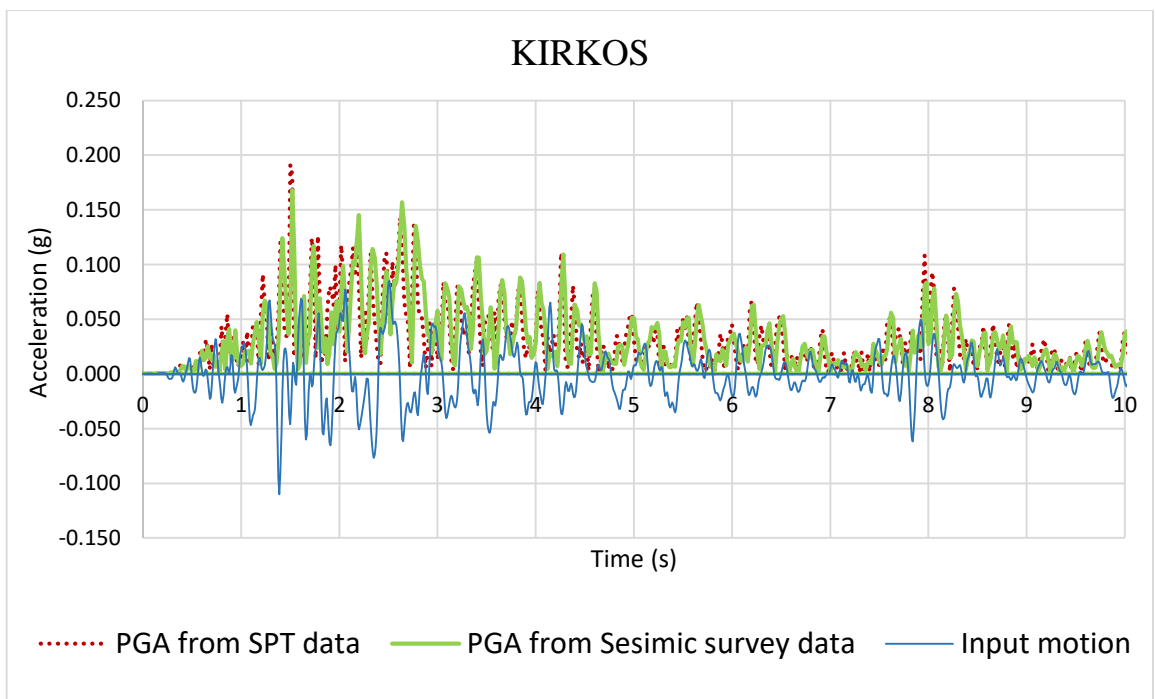
(d)

Figure A- 6: PGA results from Seismic survey data: (c) Lafto, and (d) Lideta

c. Comparison of PGA results with input motion

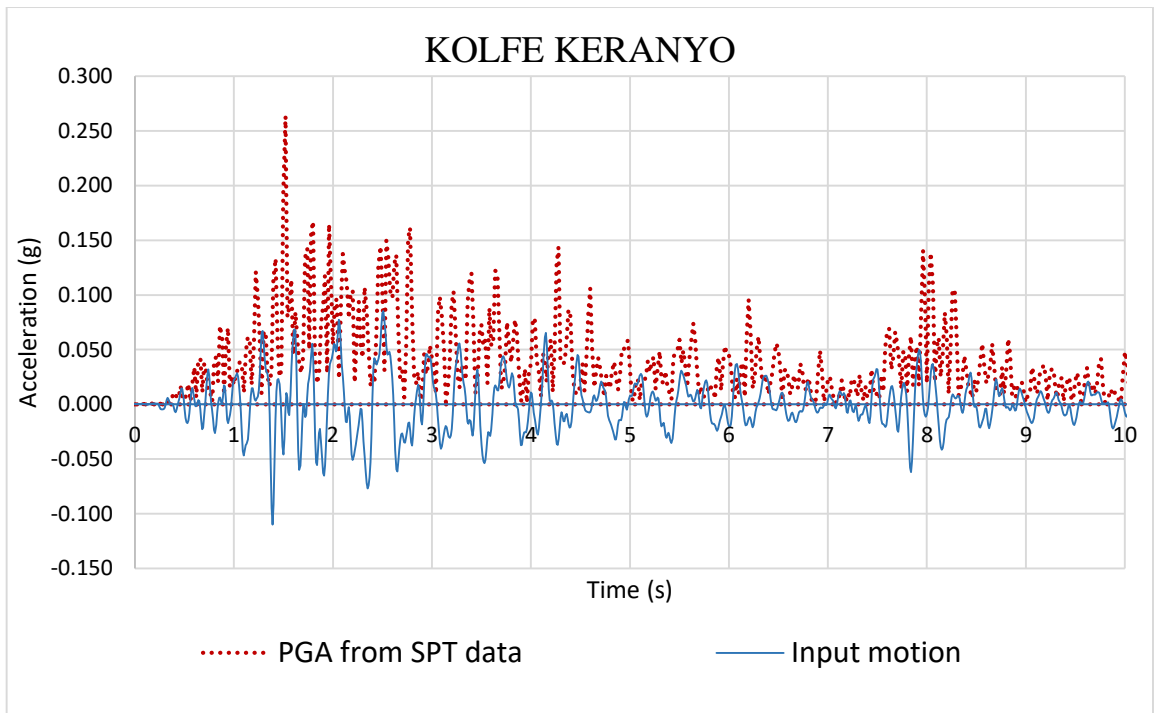


(a)

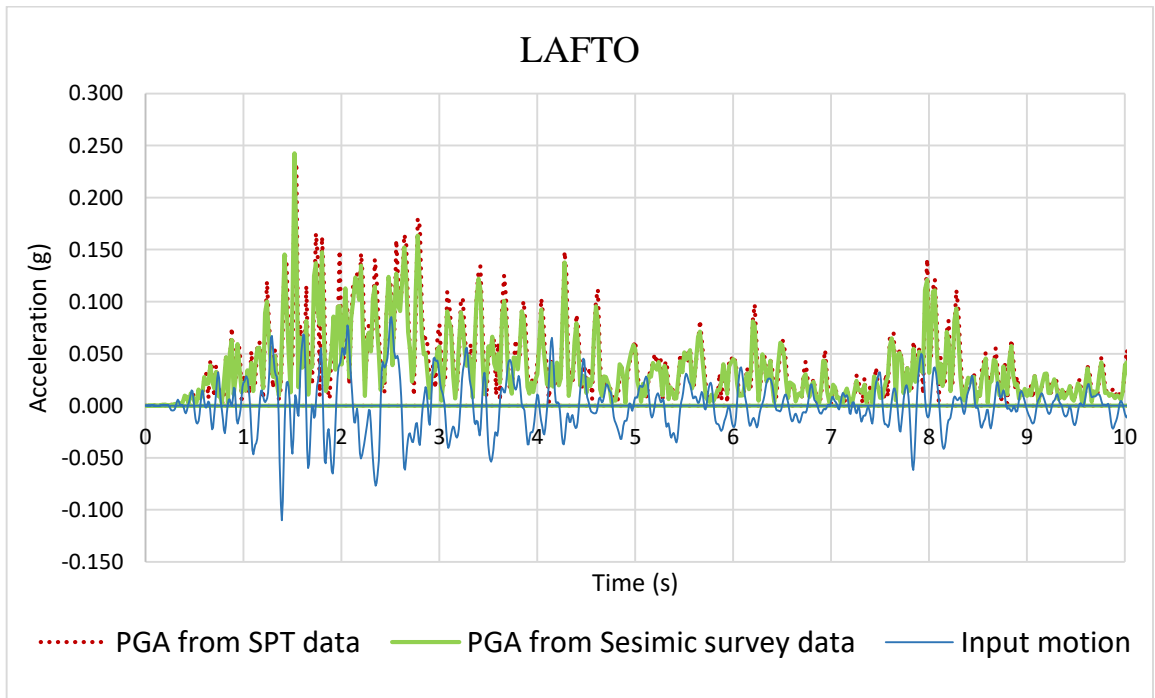


(b)

Figure A- 7: Comparison of PGA results with the input motion: (a) Akaki kality, and (b) Kirkos

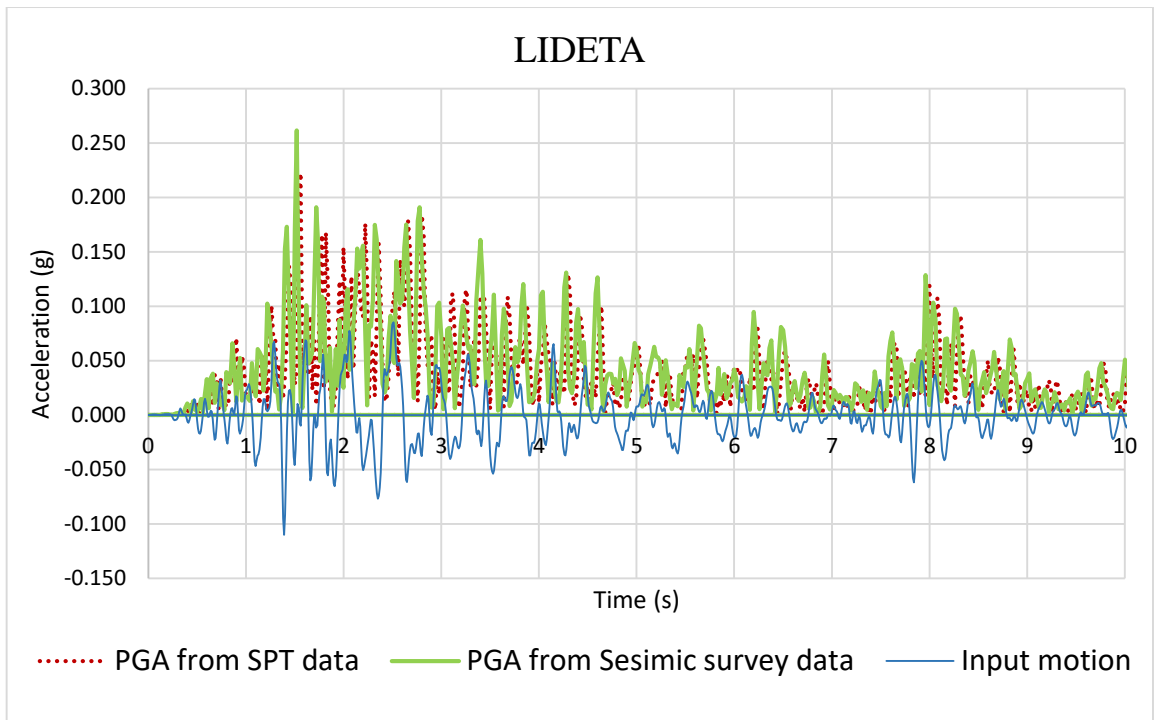


(c)



(d)

Figure A- 8: Comparison of PGA results with the input motion: (c) Kolfe keranyo, and (d) Lafto



(e)

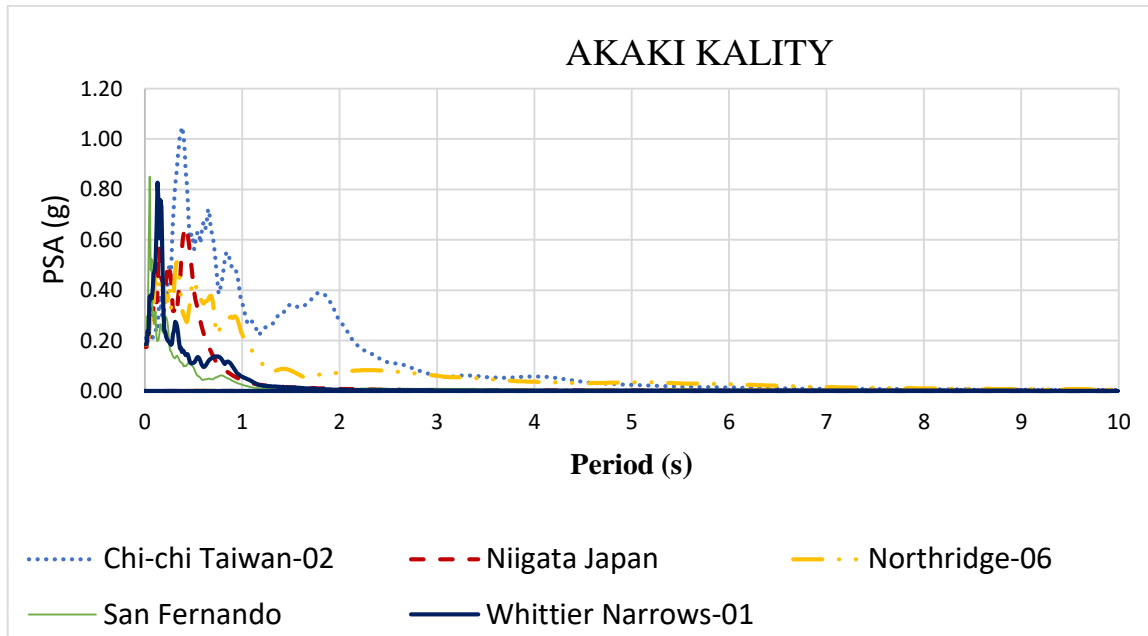
Figure A- 9: Comparison of PGA results with the input motion: (e) Lideta

Appendix B

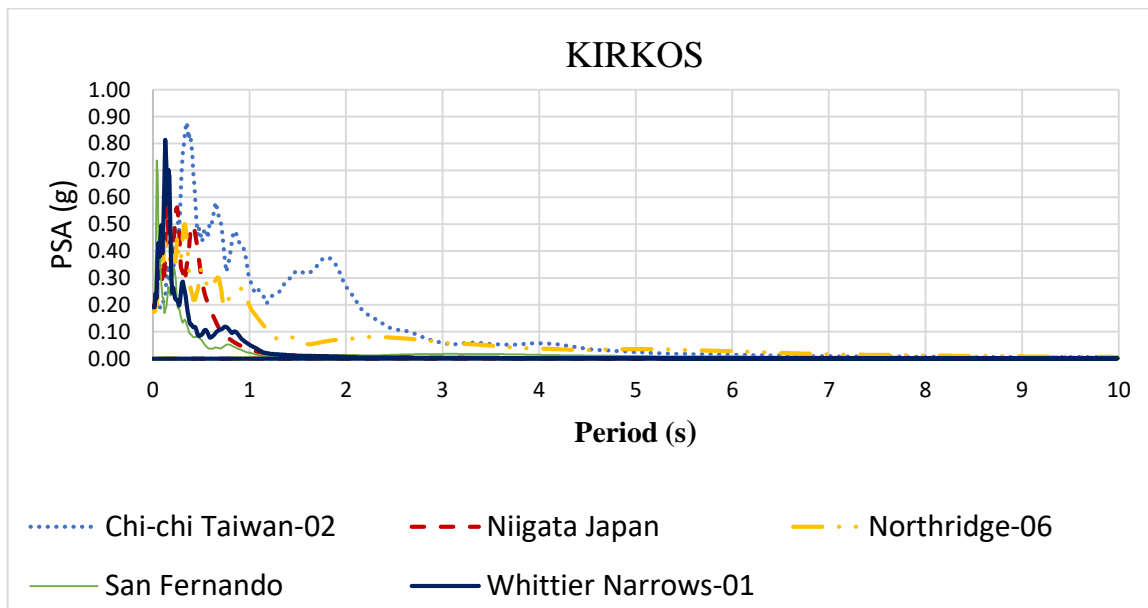
Response spectra

a. Based on SPT data

- one dimensional response spectra

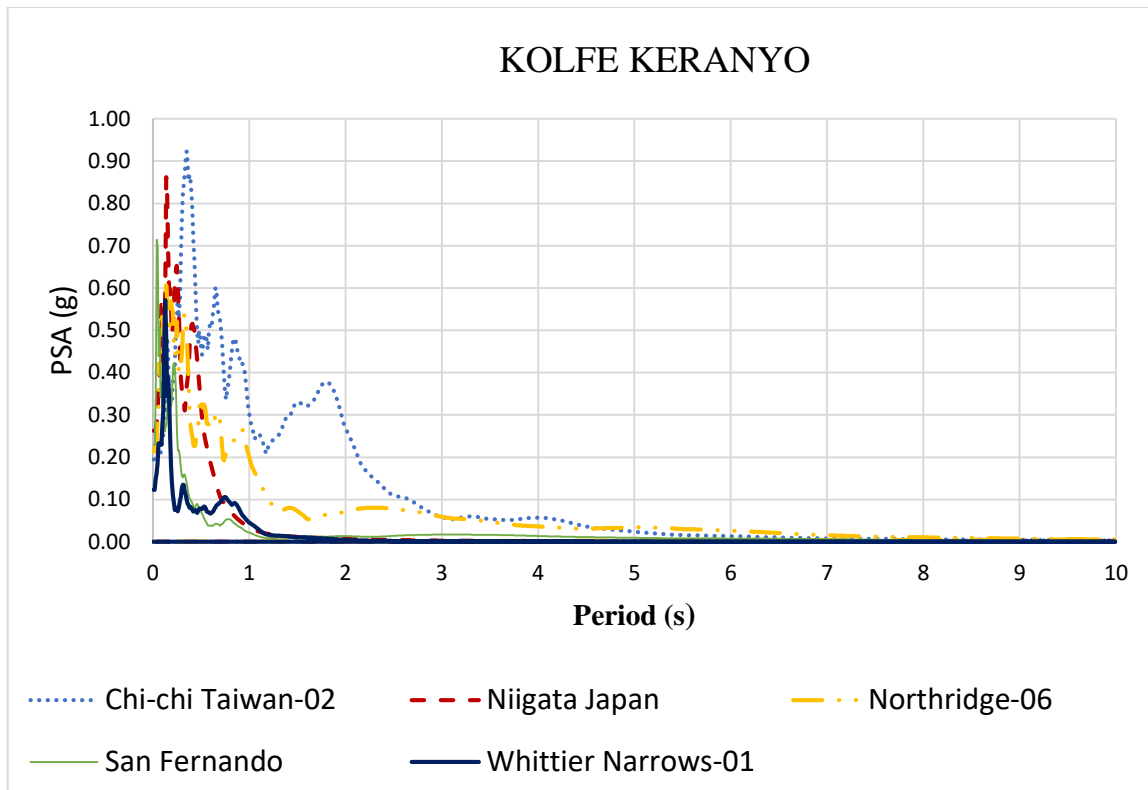


(a)

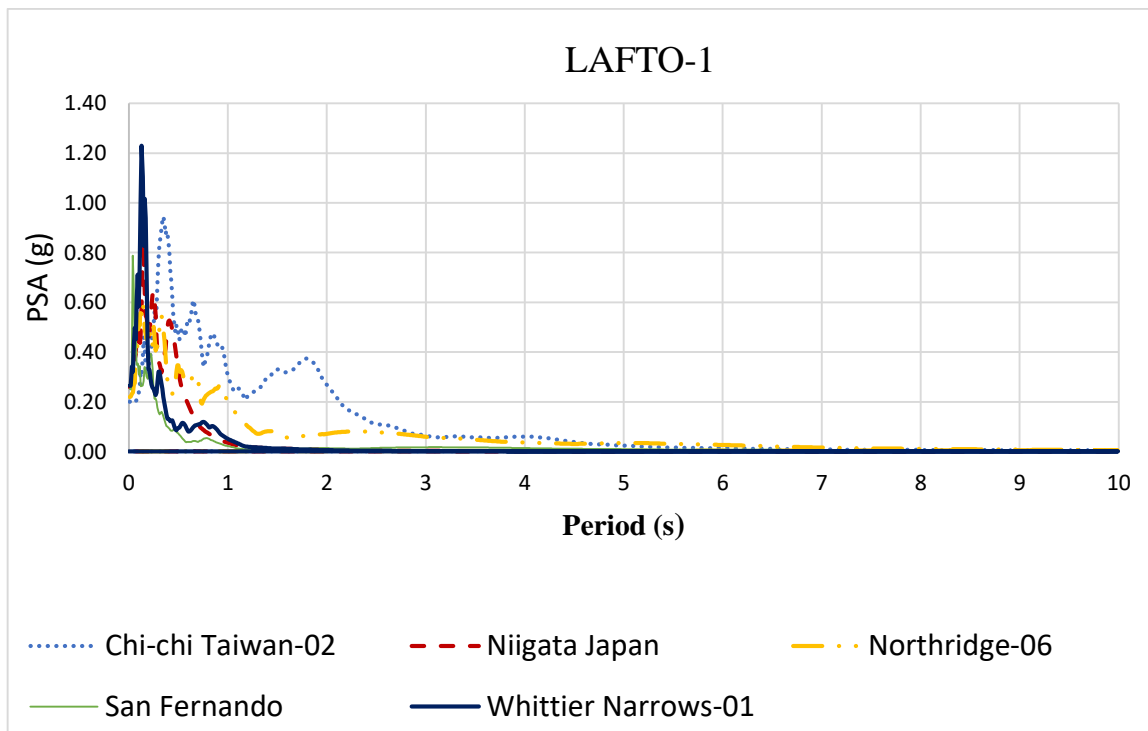


(b)

Figure B- 1: One dimensional response spectra from SPT data : (a) Akaki kality, and (b) Kirkos

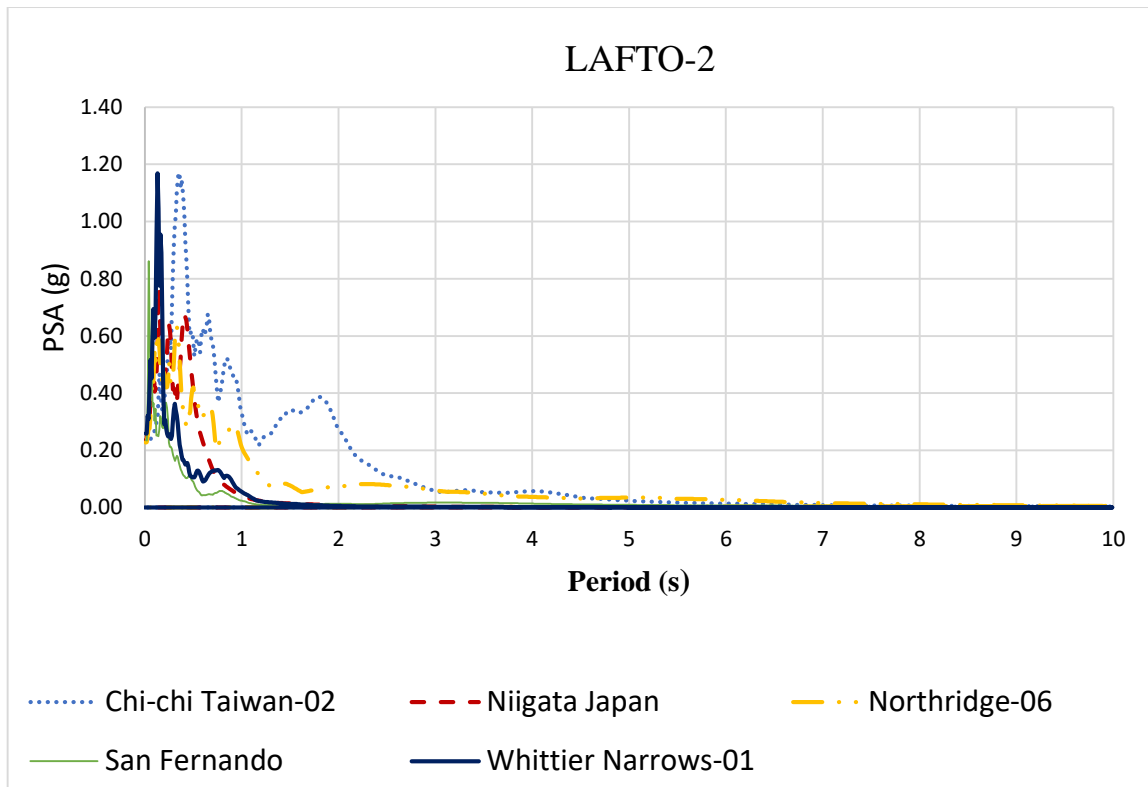


(c)

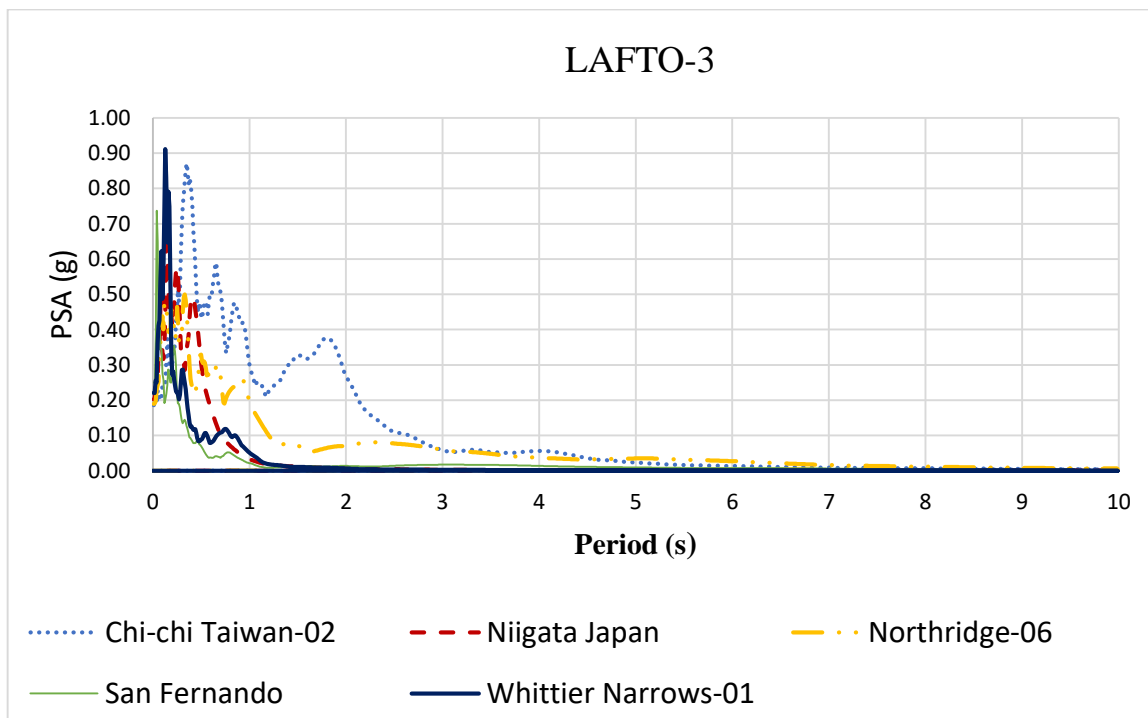


(d)

Figure B- 2: One dimensional response spectra from SPT data : (c) Kolfe keranyo, and (d) Lafto-1

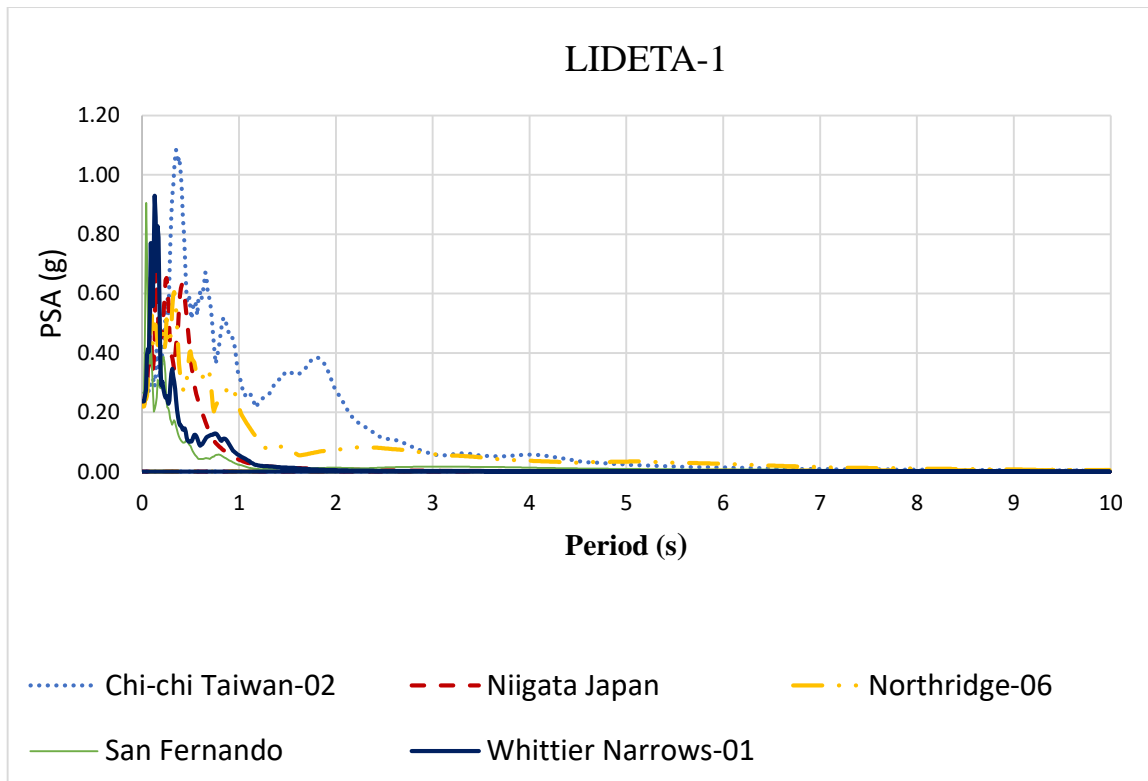


(e)

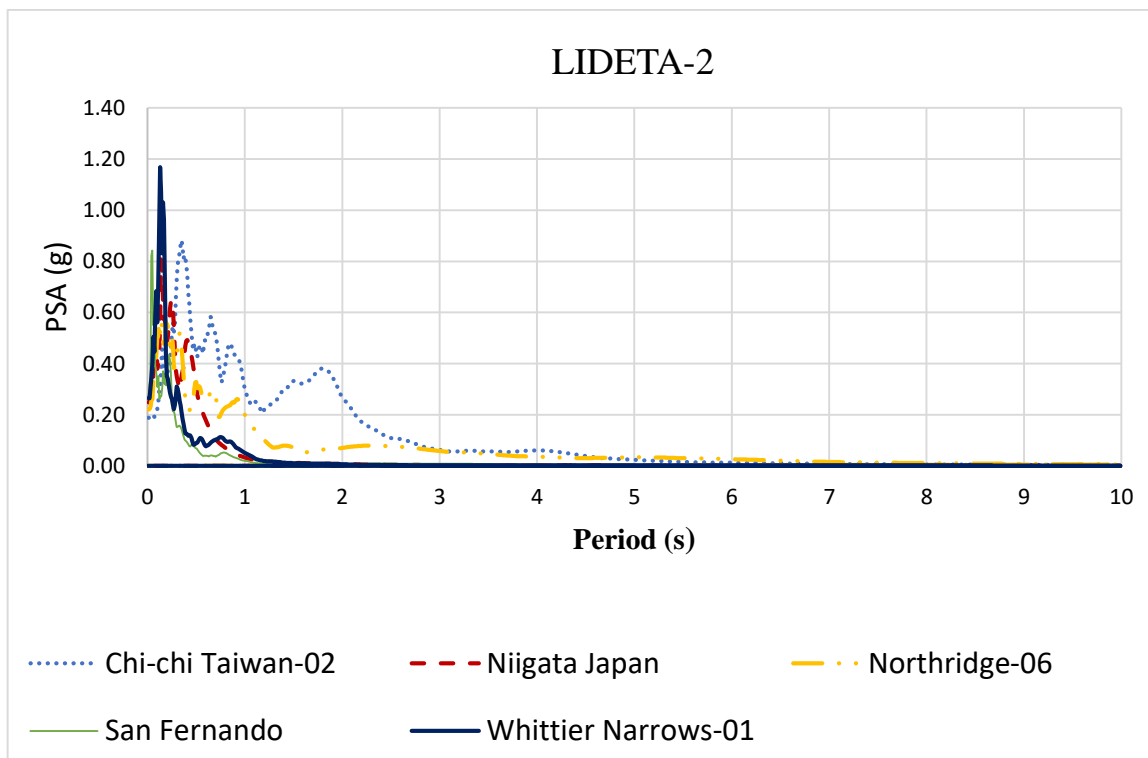


(f)

Figure B- 3: One dimensional response spectra from SPT data : (e) Lafto-2, and (f) Lafto-3



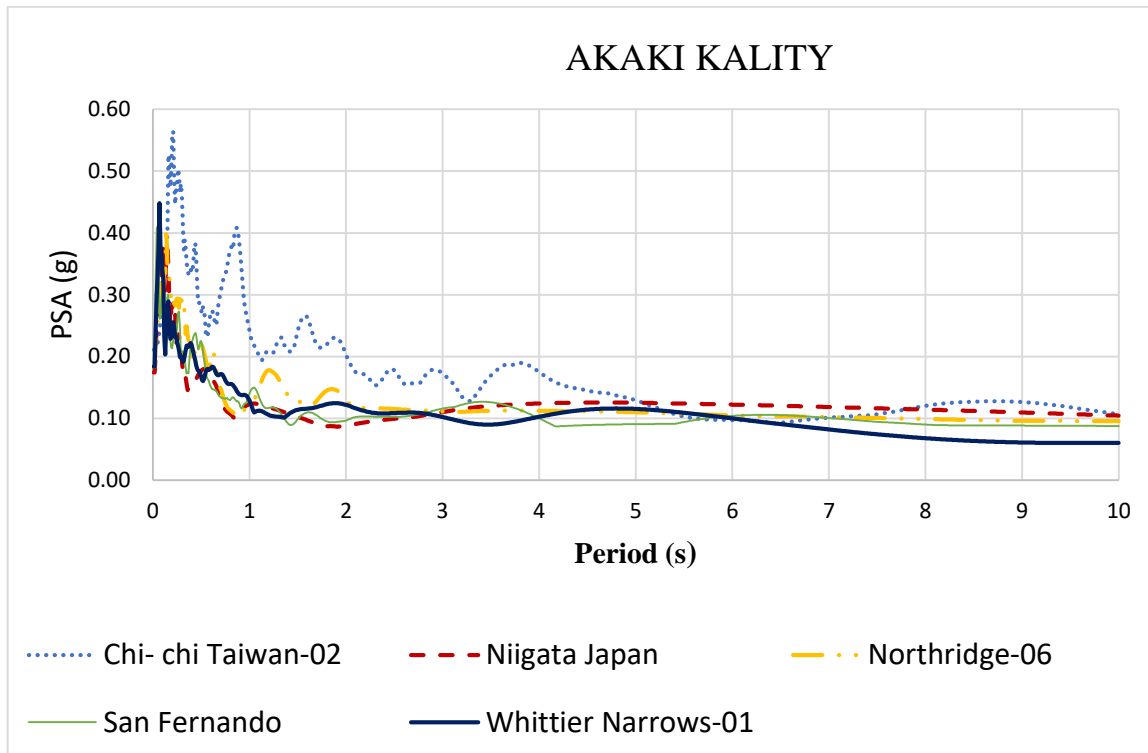
(g)



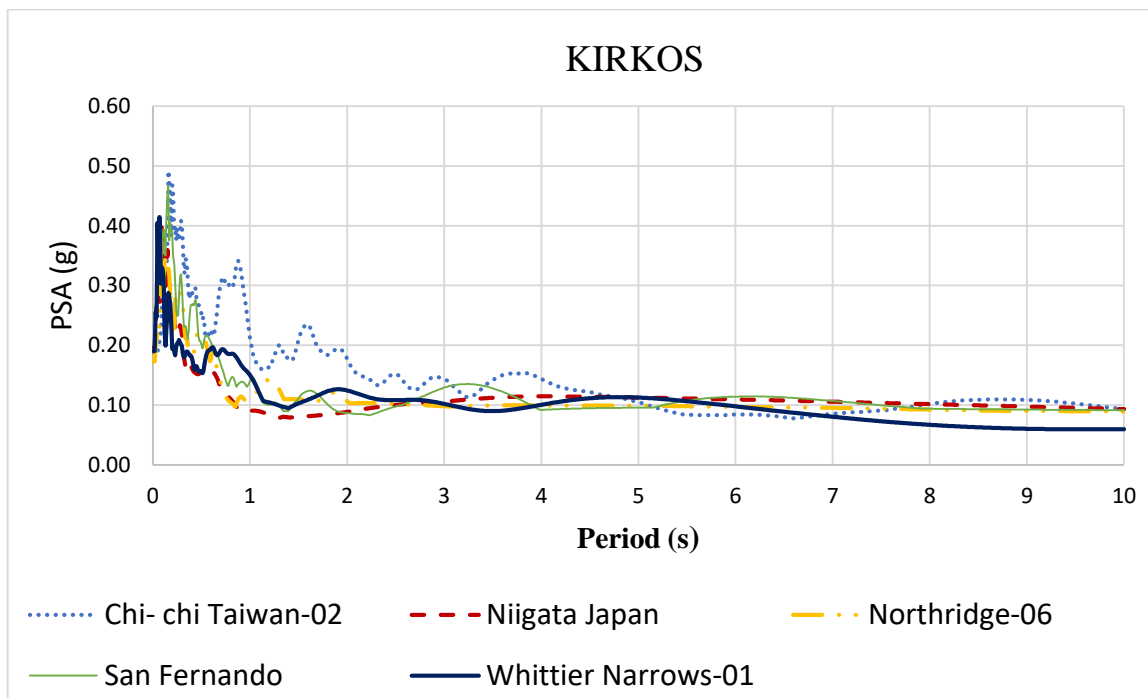
(h)

Figure B- 4: One dimensional response spectra from SPT data : (g) Lideta-1, and (h) Lideta-2

- Two dimensional response spectra

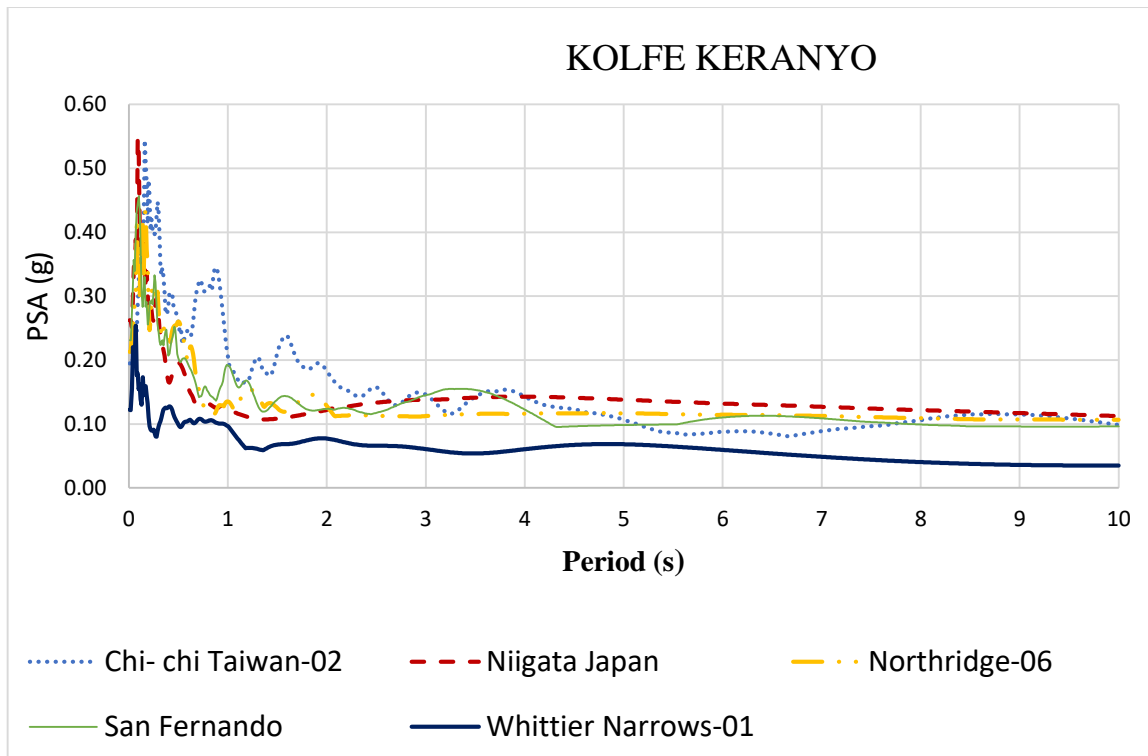


(a)

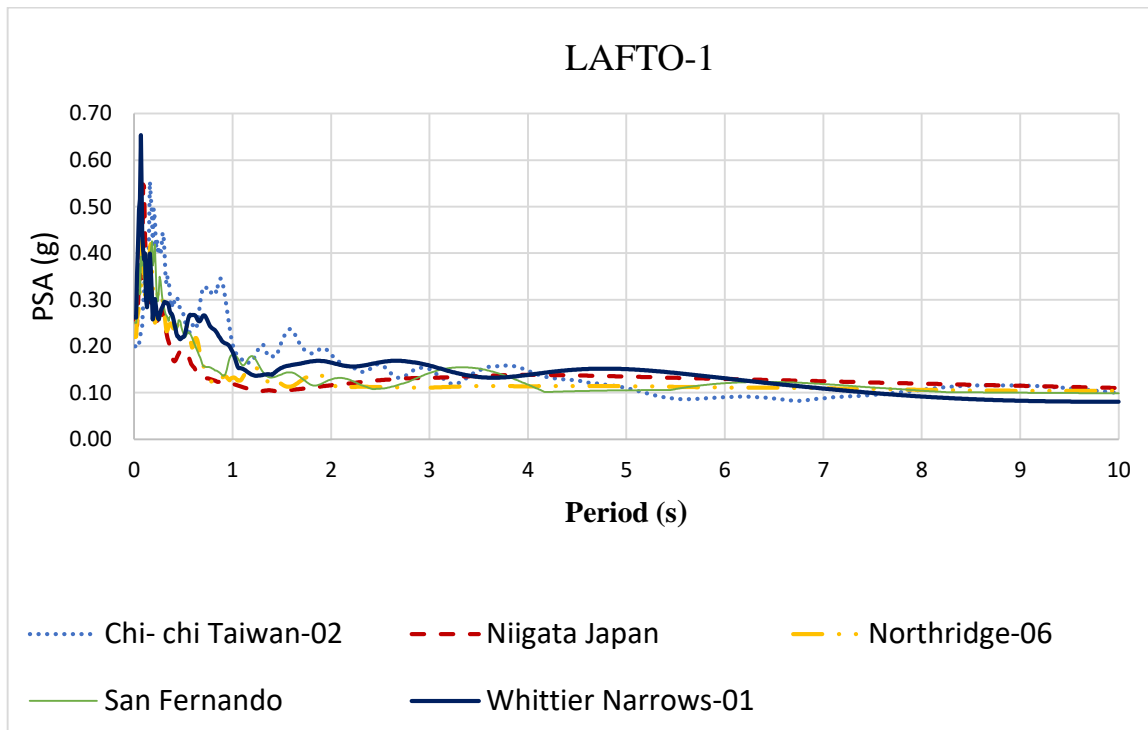


(b)

Figure B- 5: Two dimensional response spectra from SPT data : (a) Akaki kaliti, and (b) Kirkos

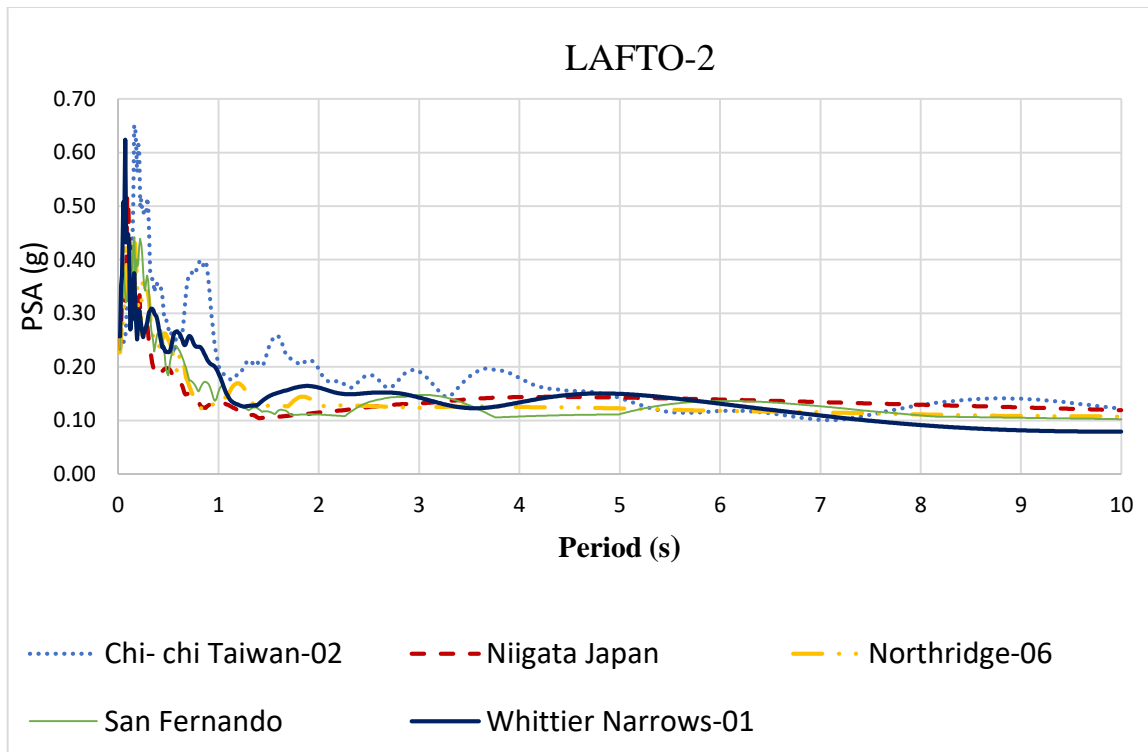


(c)

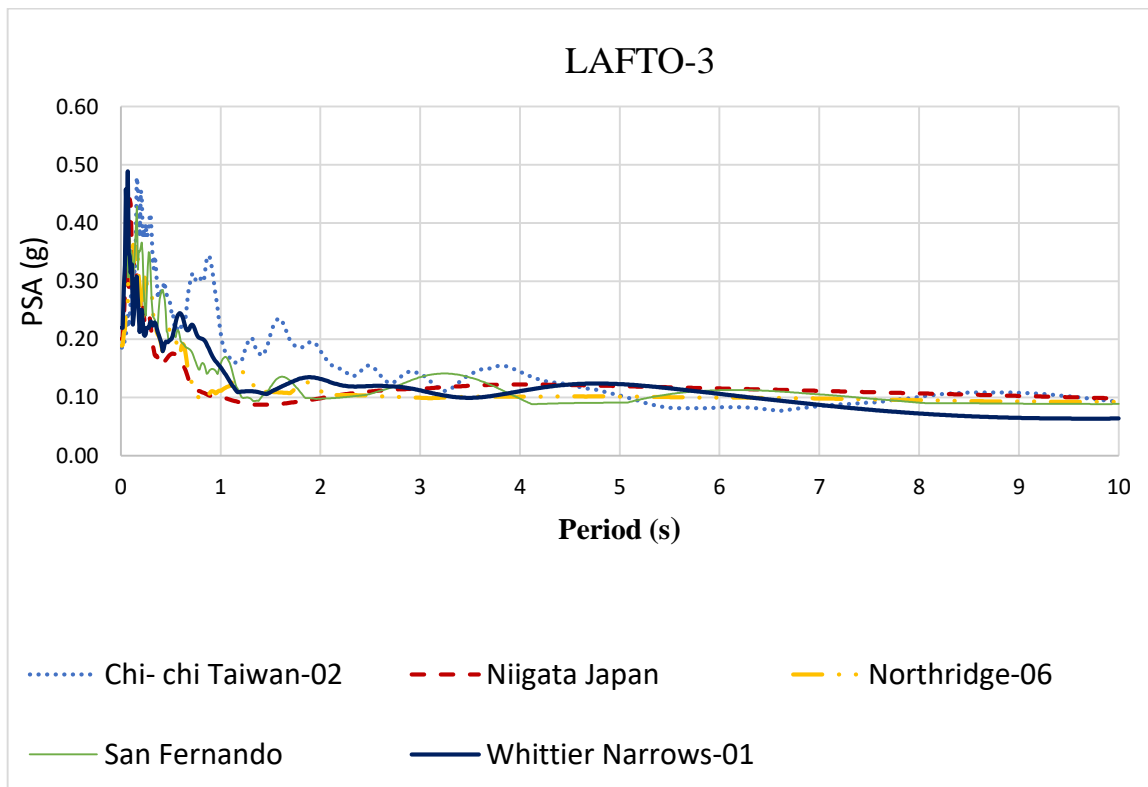


(d)

Figure B- 6: Two dimensional response spectra from SPT data : (c) Kolfe keranyo, and (d) Lafto-1

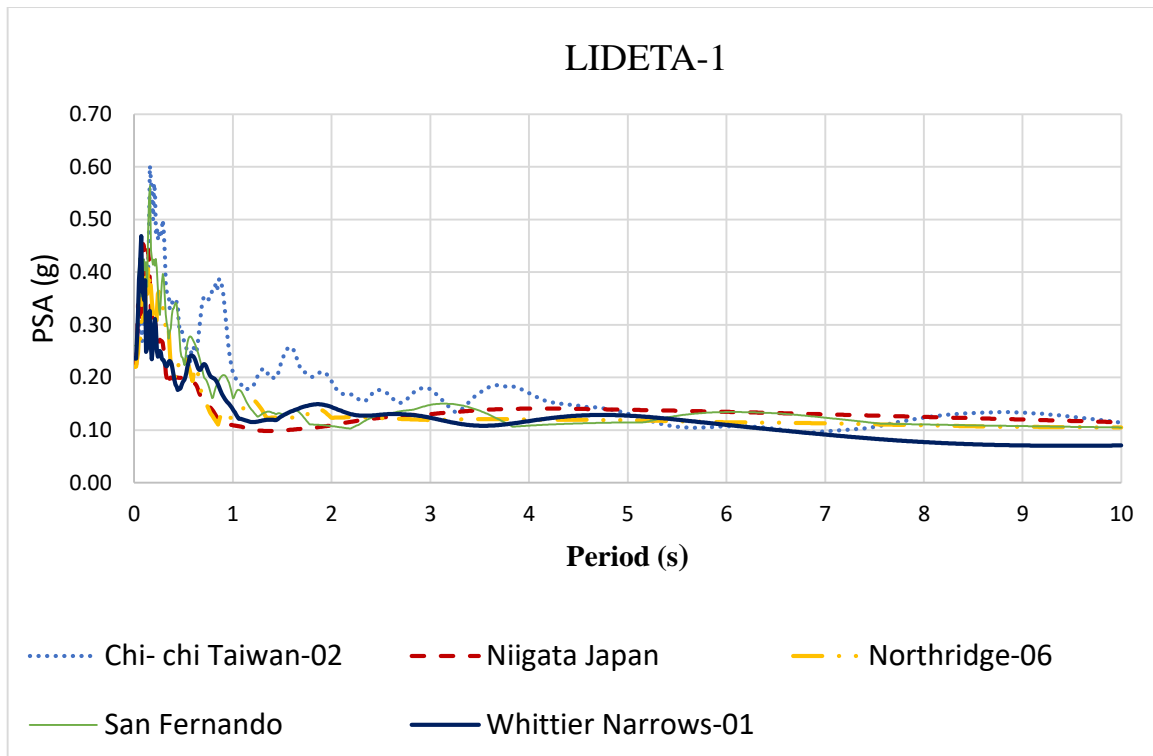


(e)

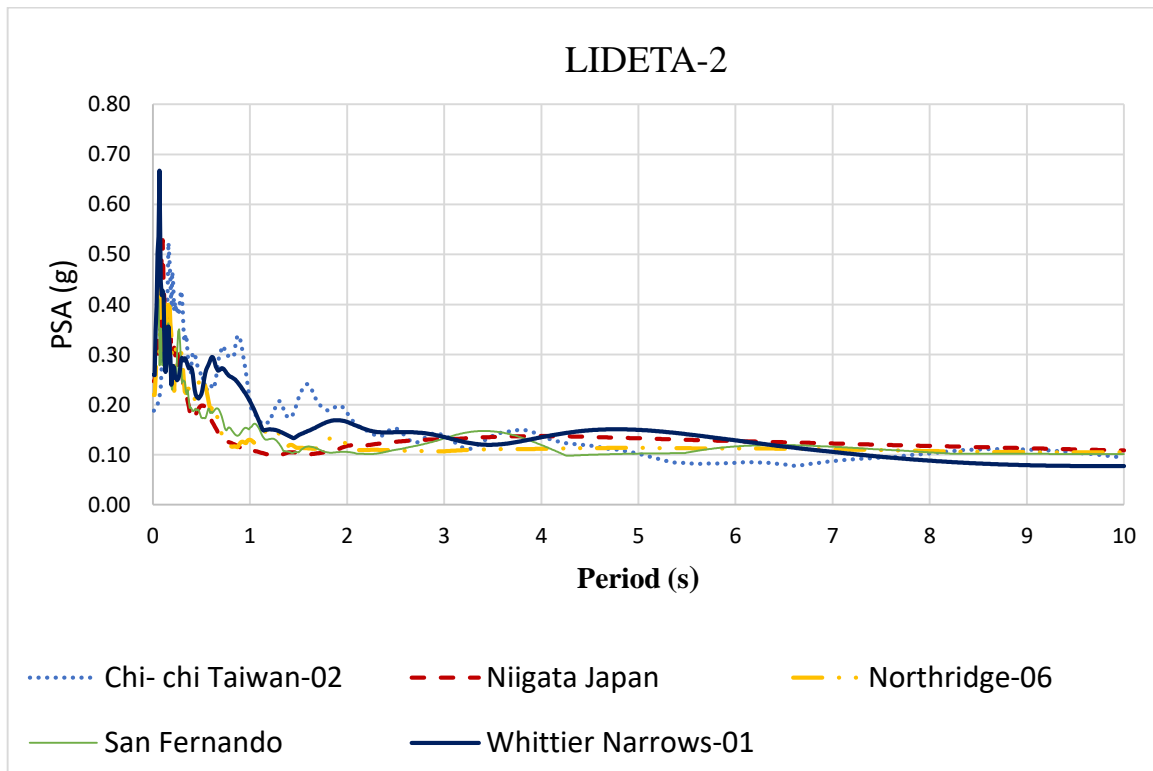


(f)

Figure B- 7: Two dimensional response spectra from SPT data : (e) Lafto-2, and (f) Lafto-3



(g)

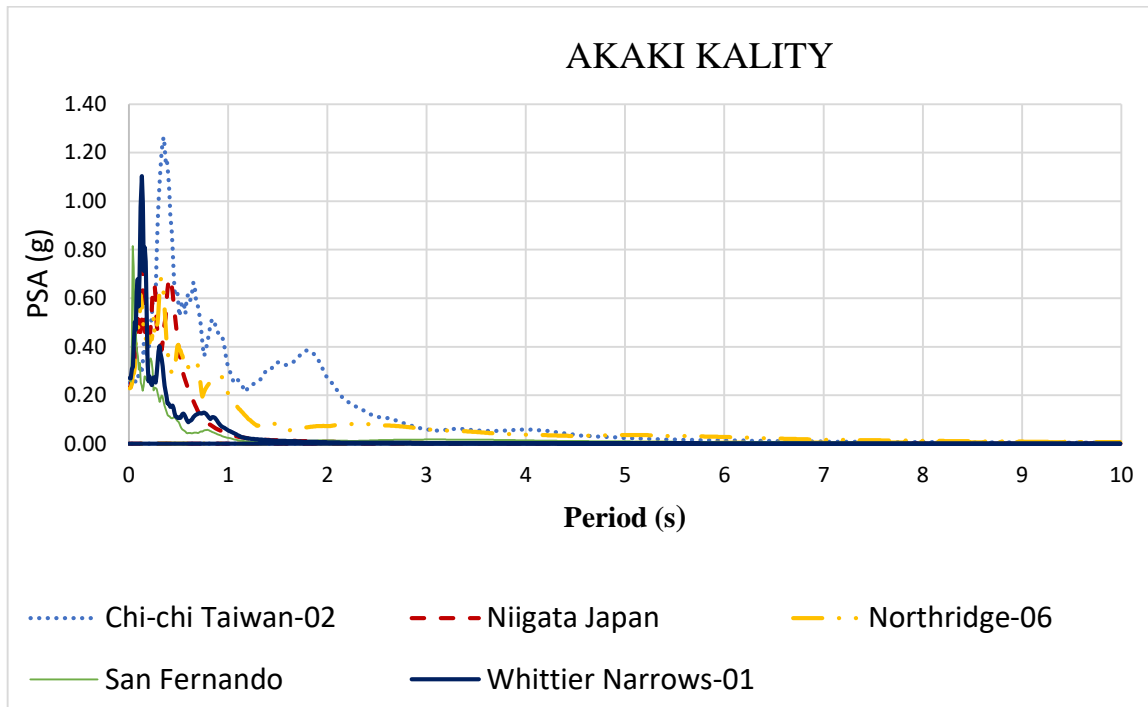


(h)

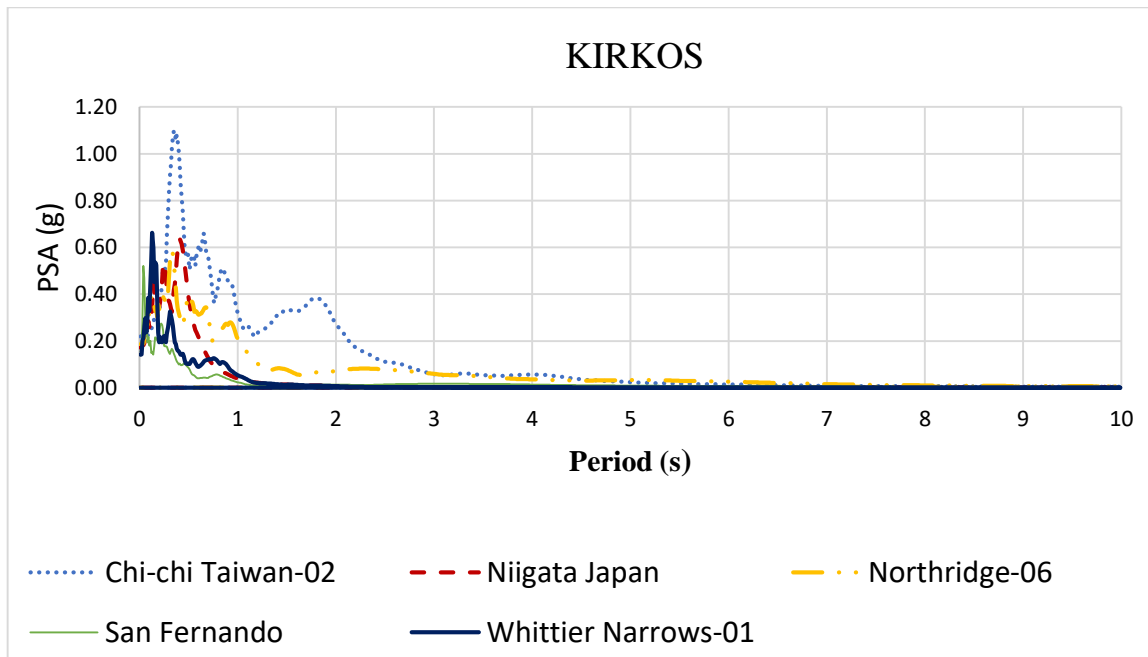
Figure B- 8: Two dimensional response spectra from SPT data : (g) Lideta-1, and (h) Lideta-2

b. Based on Seismic survey

- One dimensional response spectra

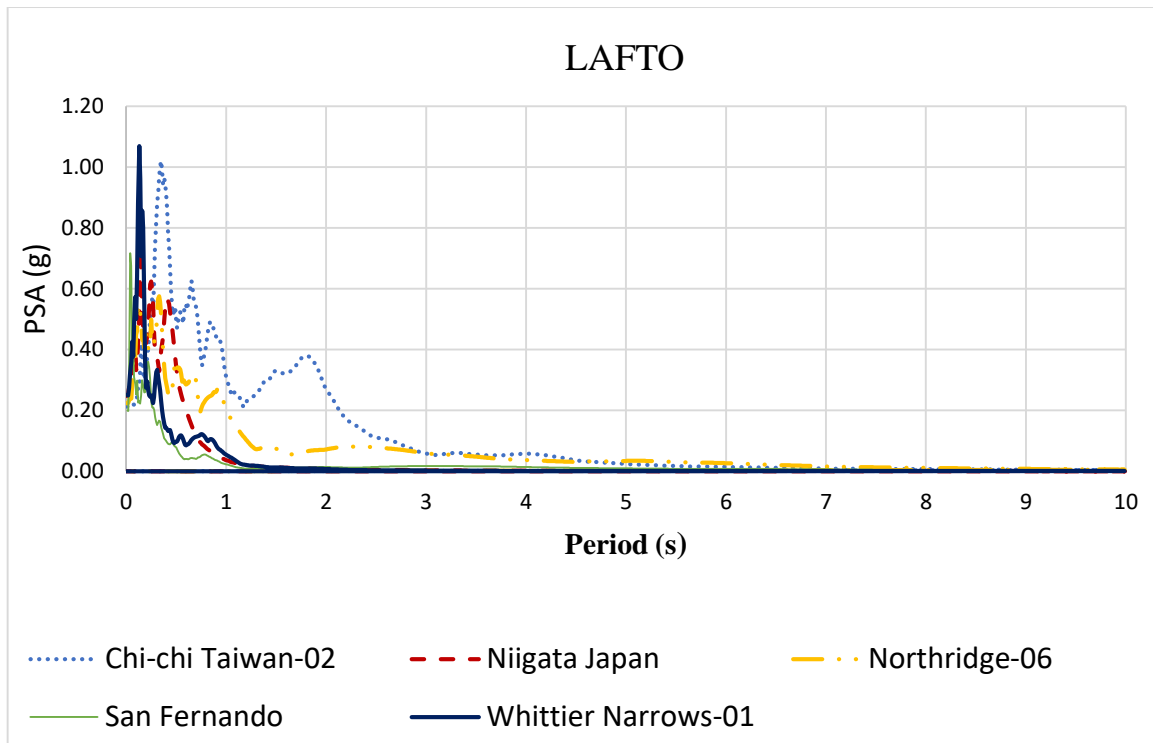


(a)

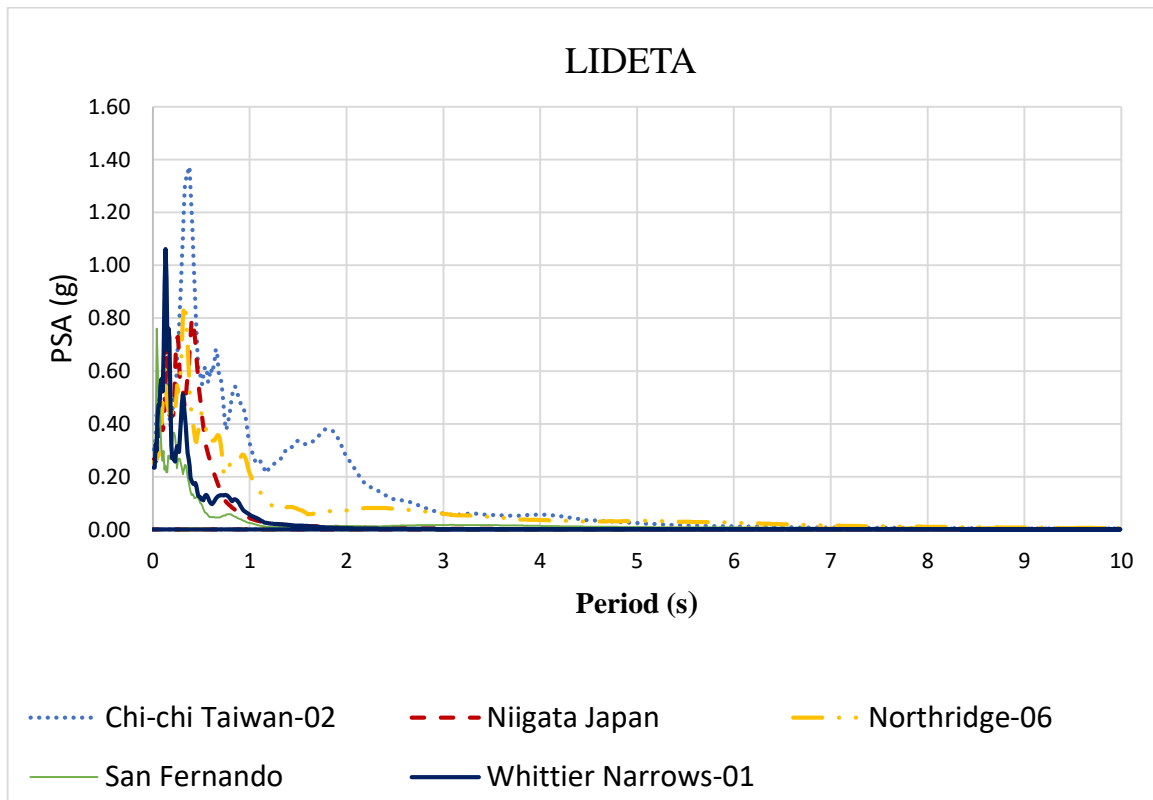


(b)

Figure B- 9: One dimensional response spectra from Seismic survey data : (a) Akaki kality, and (b) Kirkos



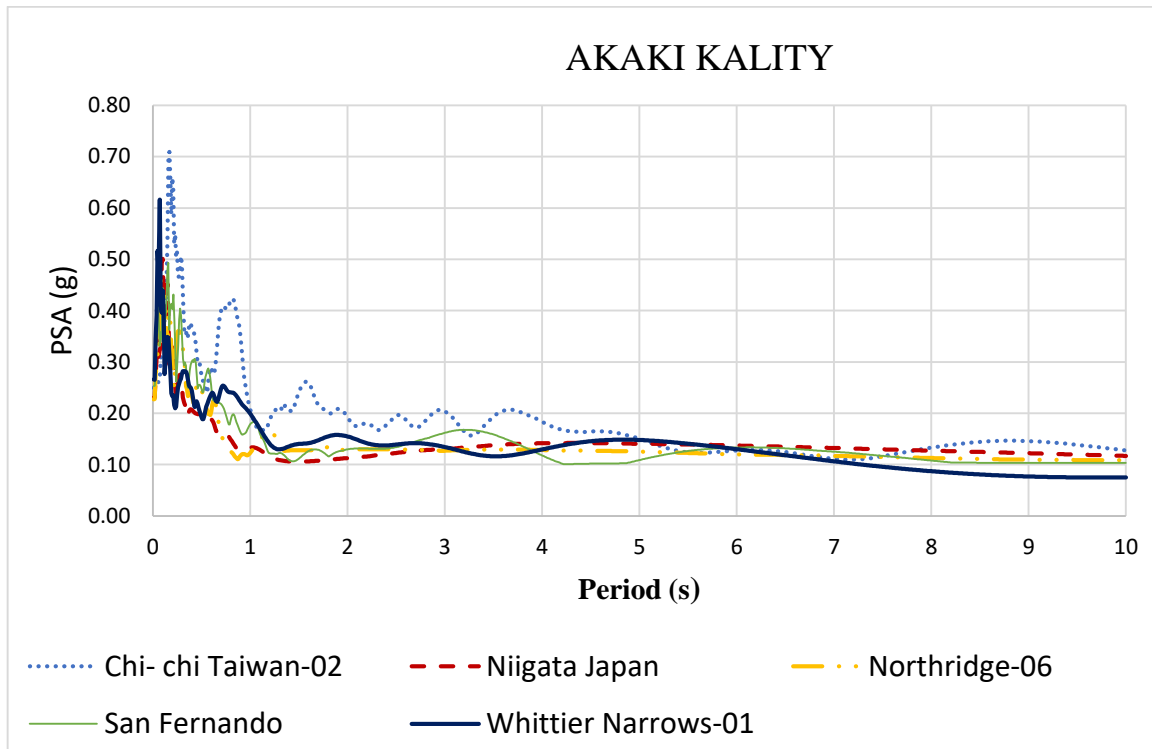
(c)



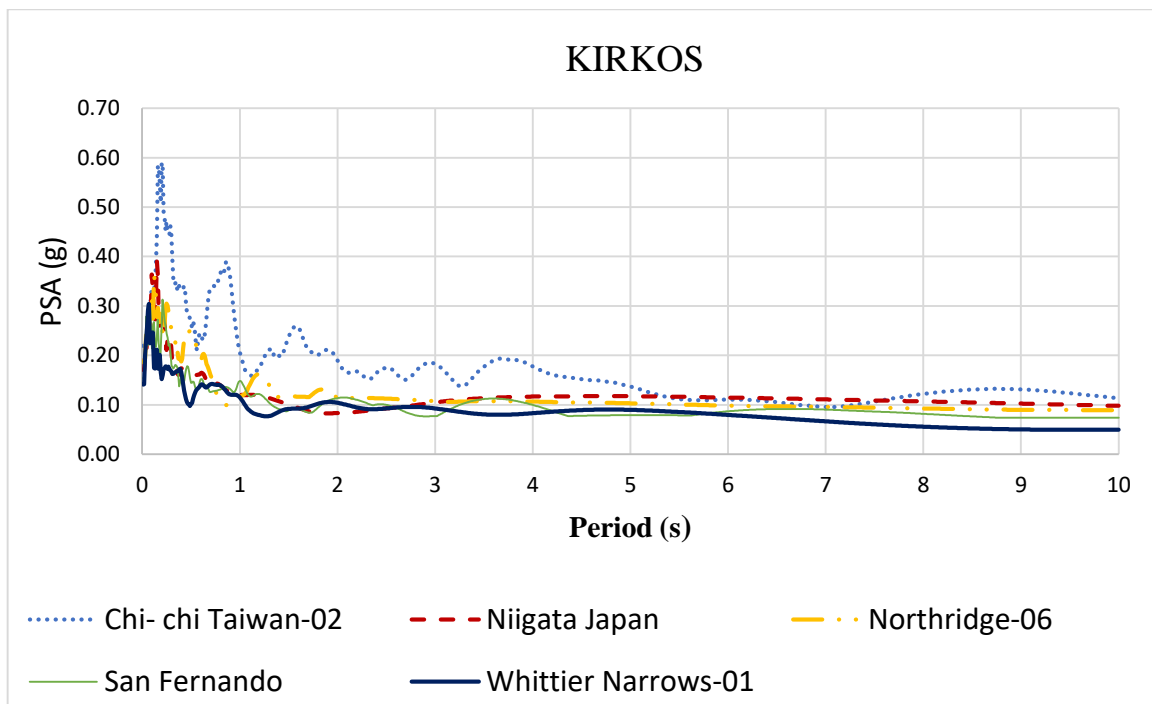
(d)

Figure B- 10: One dimensional response spectra from Seismic survey data : (c) Lafto, and (d) Lideta

- Two dimensional response spectra

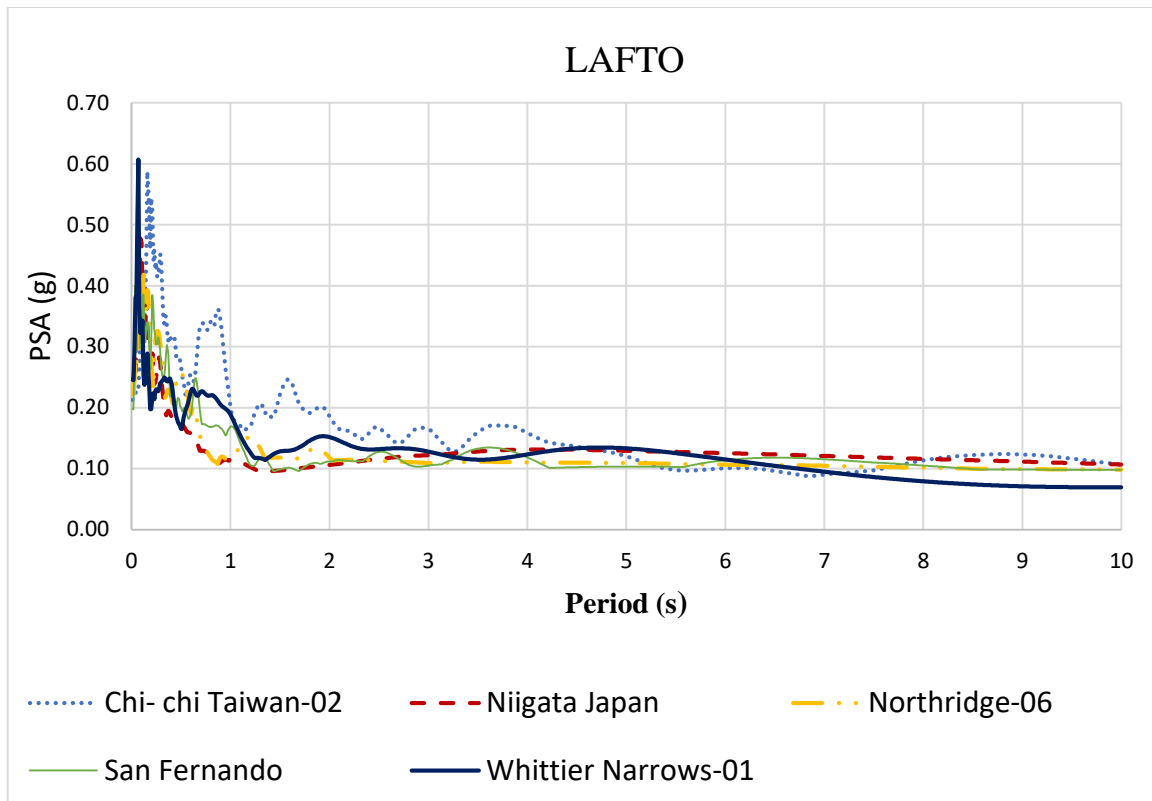


(a)

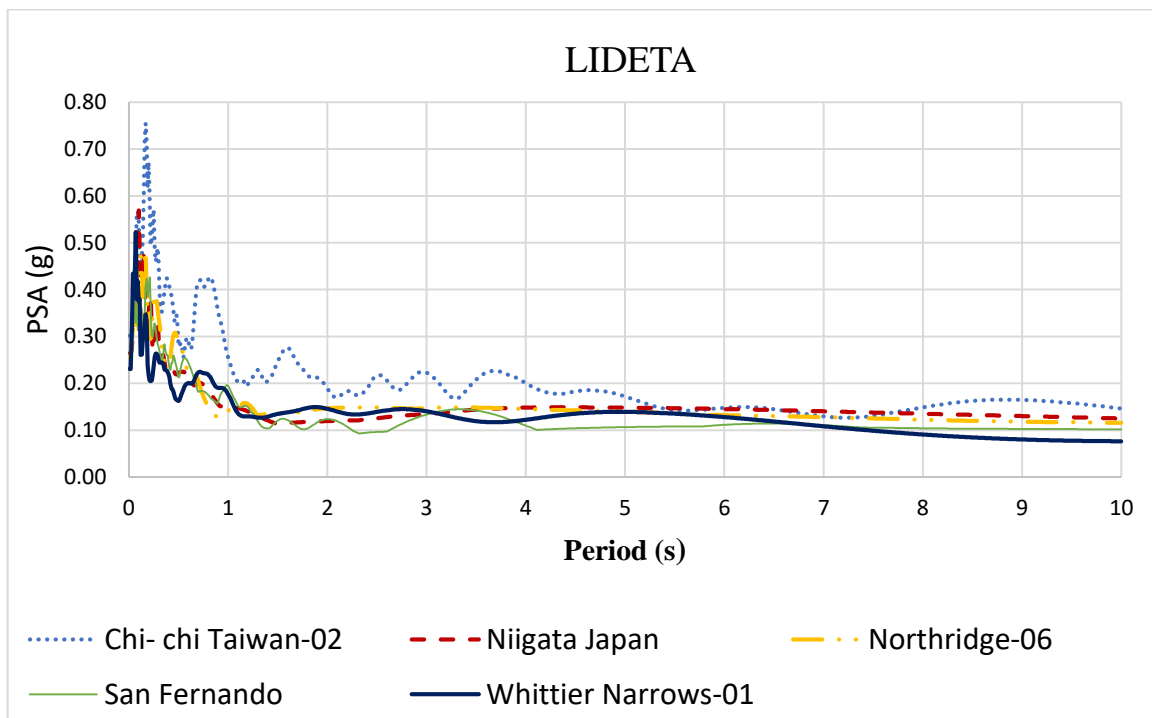


(b)

Figure B- 11: Two dimensional response spectra from Seismic survey data : (a) Akaki kality, and (b) Kirkos



(c)



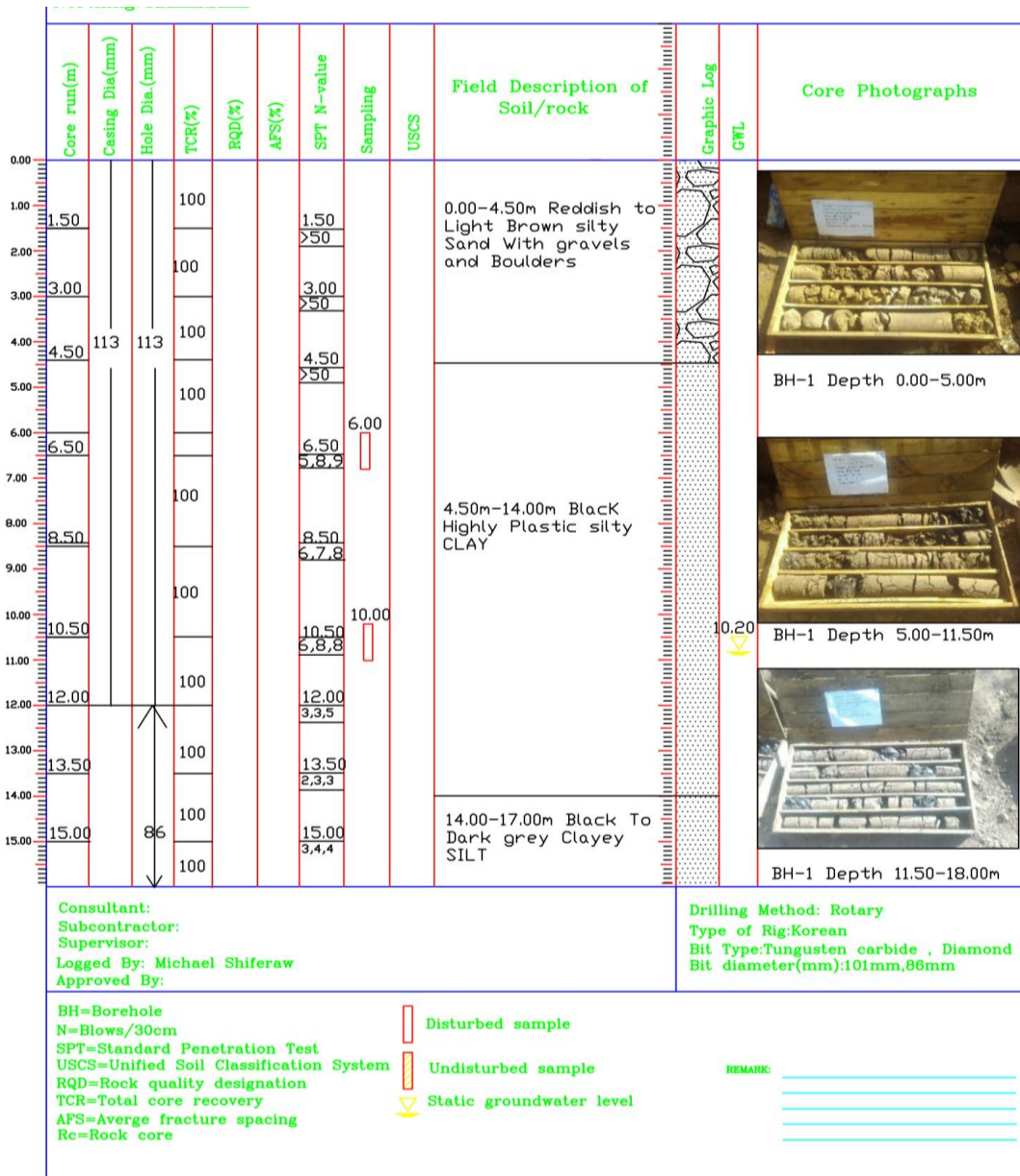
(d)

Figure B- 12: Two dimensional response spectra from Seismic survey data : (c) Lafto, and (d) Lideta

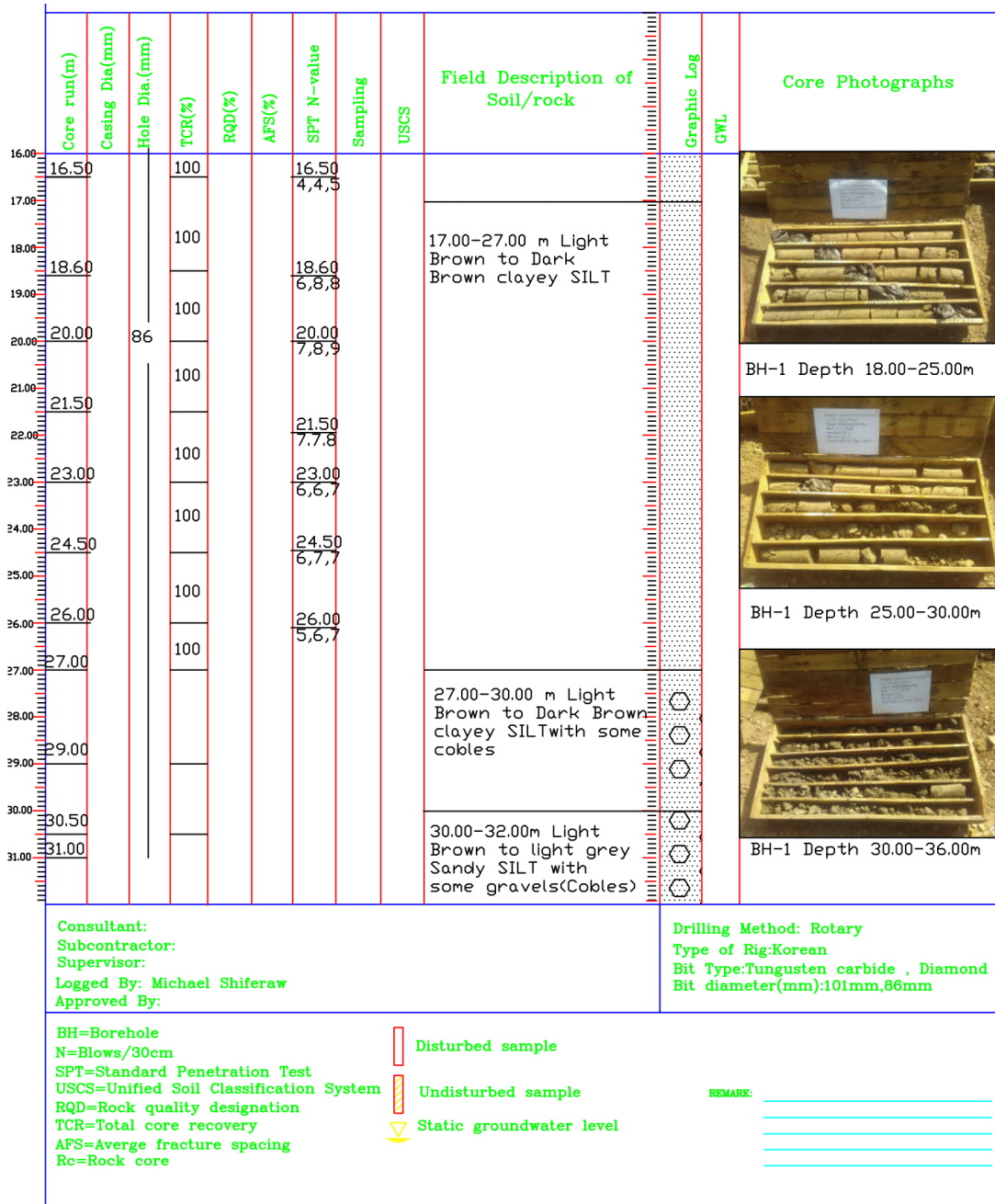
Appendix C

Description of geotechnical layers

a. Akaki kality

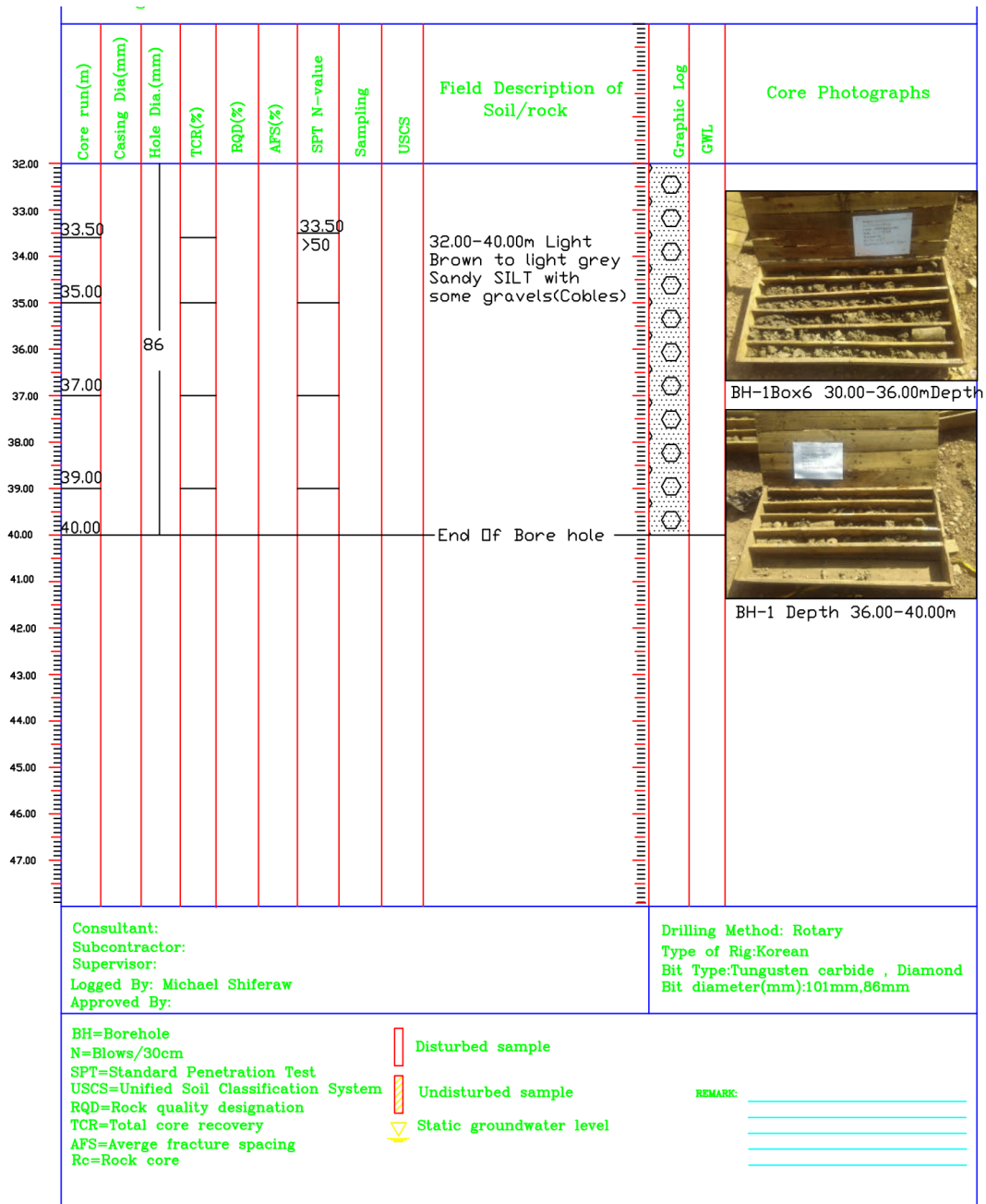


Site specific Ground Response Analysis at South - Western part of Addis Ababa



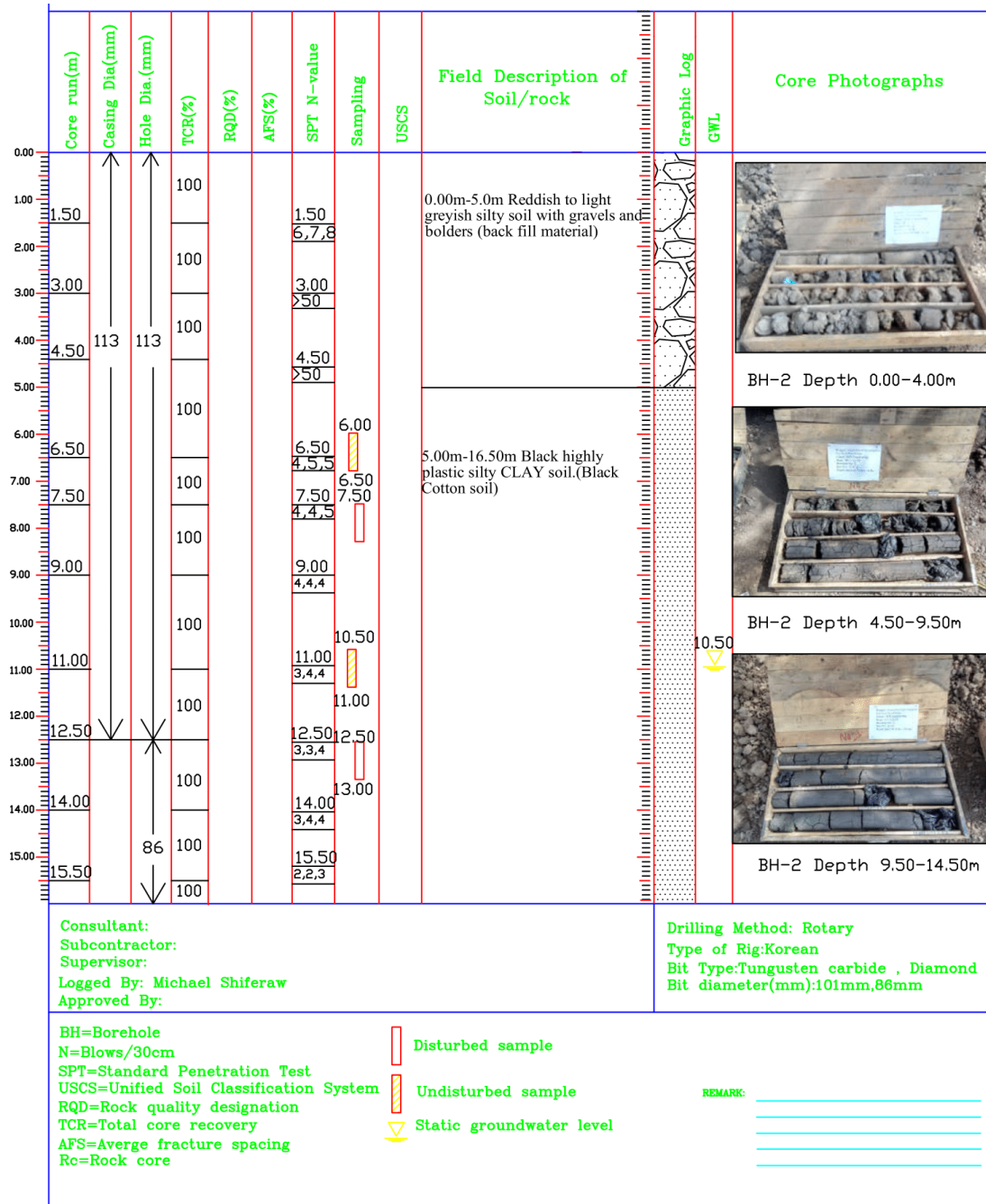
PLEASE MAKE SURE THIS IS THE CORRECT ISSUE BEFORE USE

Site specific Ground Response Analysis at South - Western part of Addis Ababa

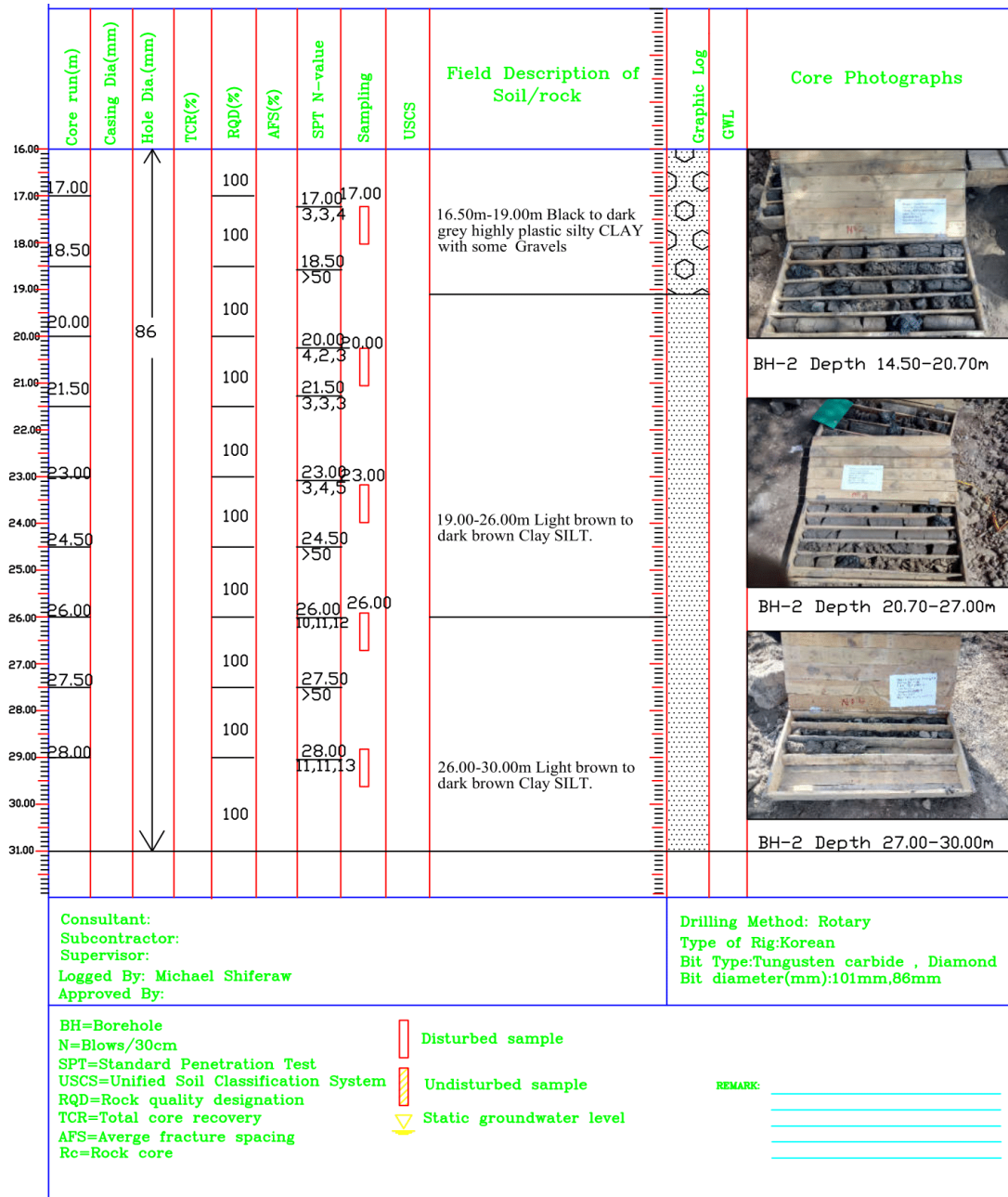


PLEASE MAKE SURE THIS IS THE CORRECT ISSUE BEFORE USE

Site specific Ground Response Analysis at South - Western part of Addis Ababa

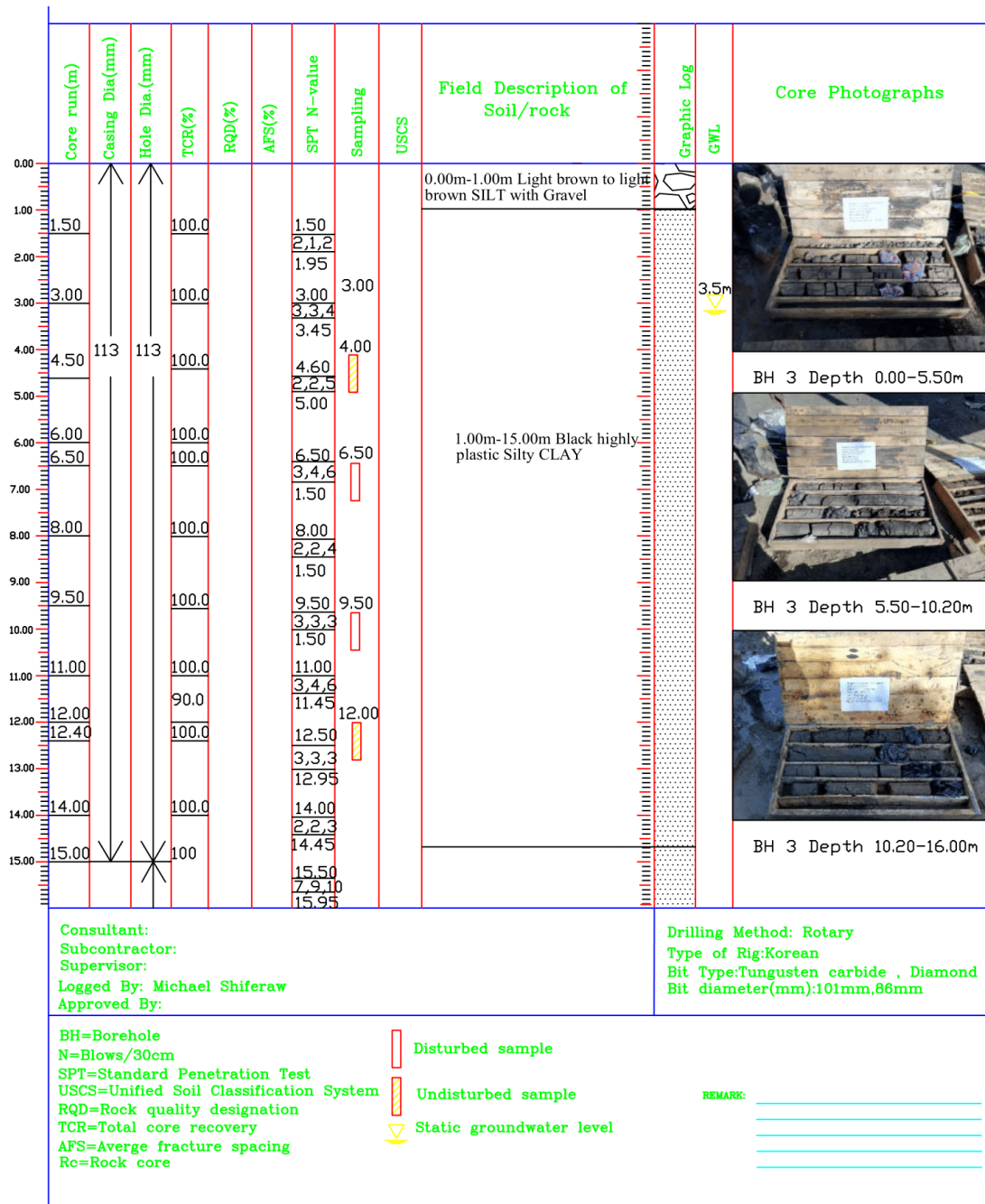


Site specific Ground Response Analysis at South - Western part of Addis Ababa



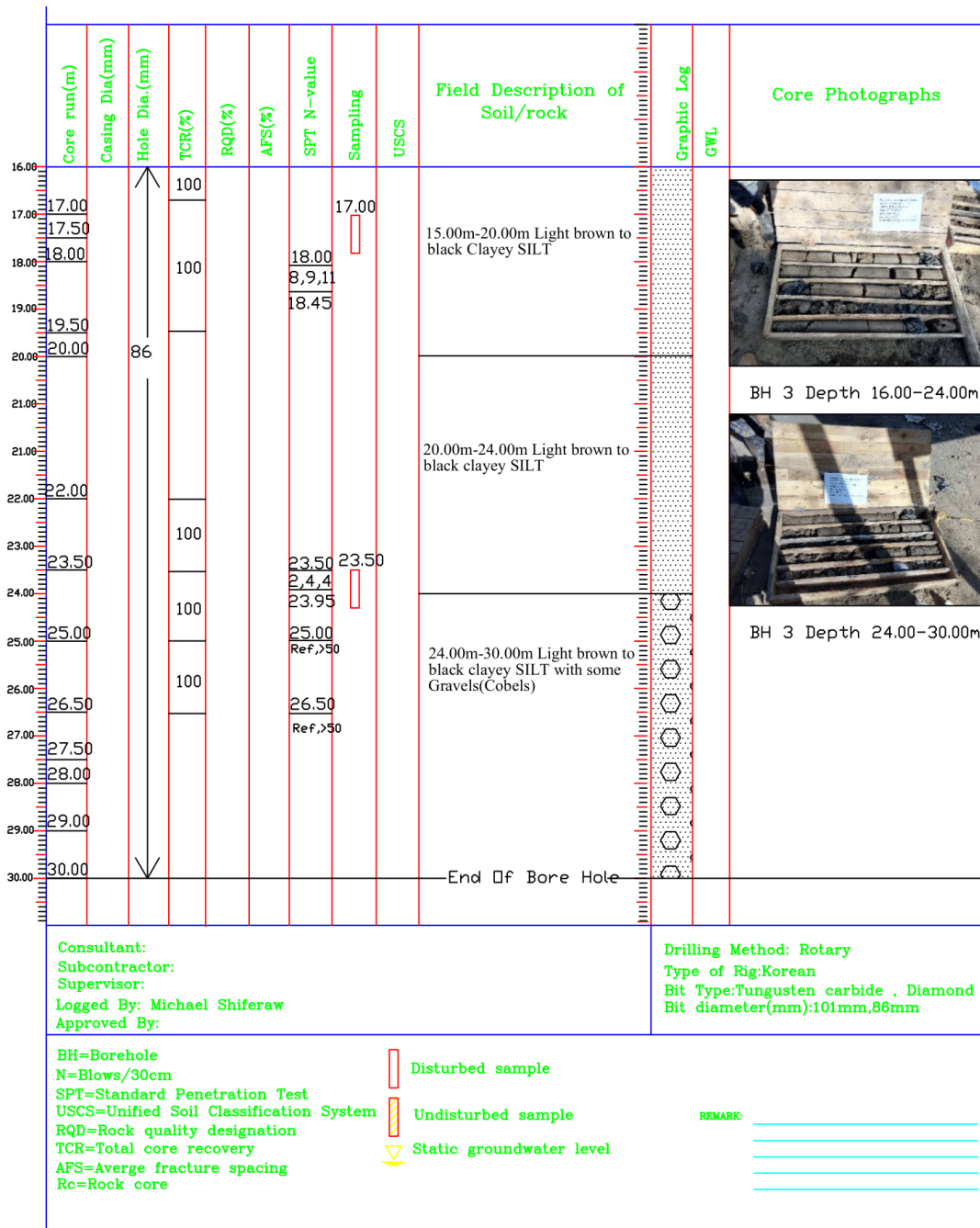
PLEASE MAKE SURE THIS IS THE CORRECT ISSUE BEFORE USE

Site specific Ground Response Analysis at South - Western part of Addis Ababa



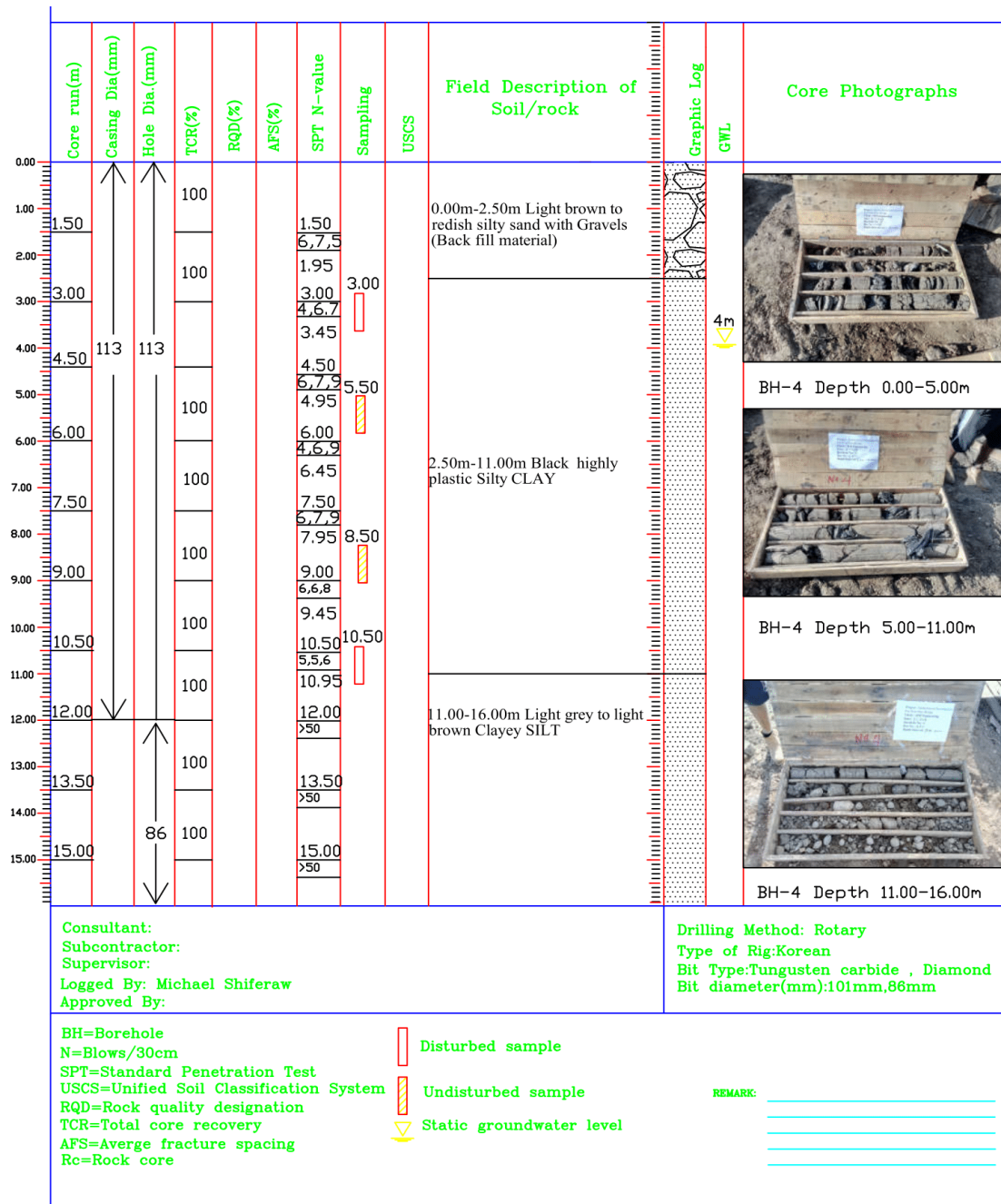
PLEASE MAKE SURE THIS IS THE CORRECT ISSUE BEFORE USE

Site specific Ground Response Analysis at South - Western part of Addis Ababa



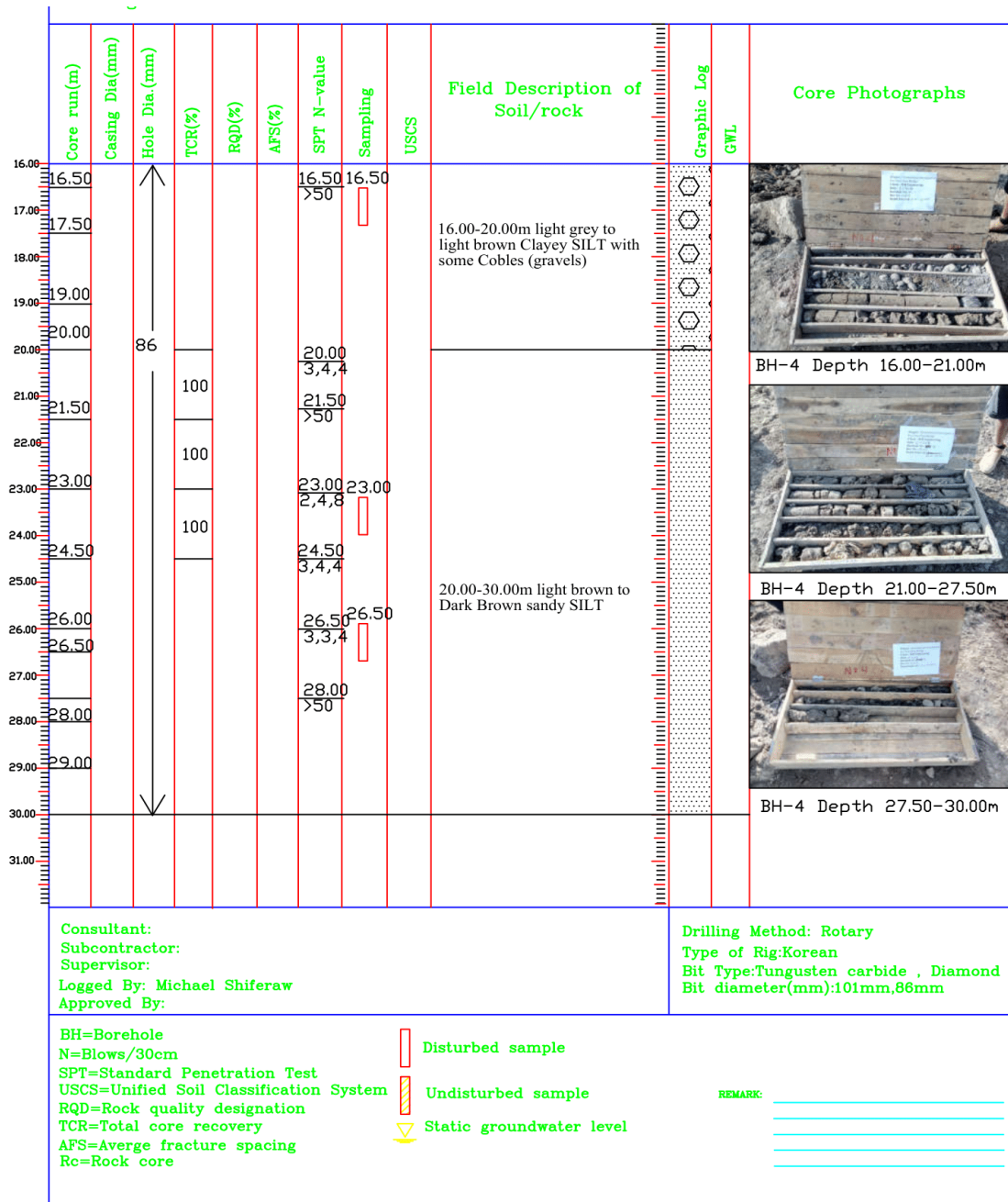
PLEASE MAKE SURE THIS IS THE CORRECT ISSUE BEFORE USE

Site specific Ground Response Analysis at South - Western part of Addis Ababa



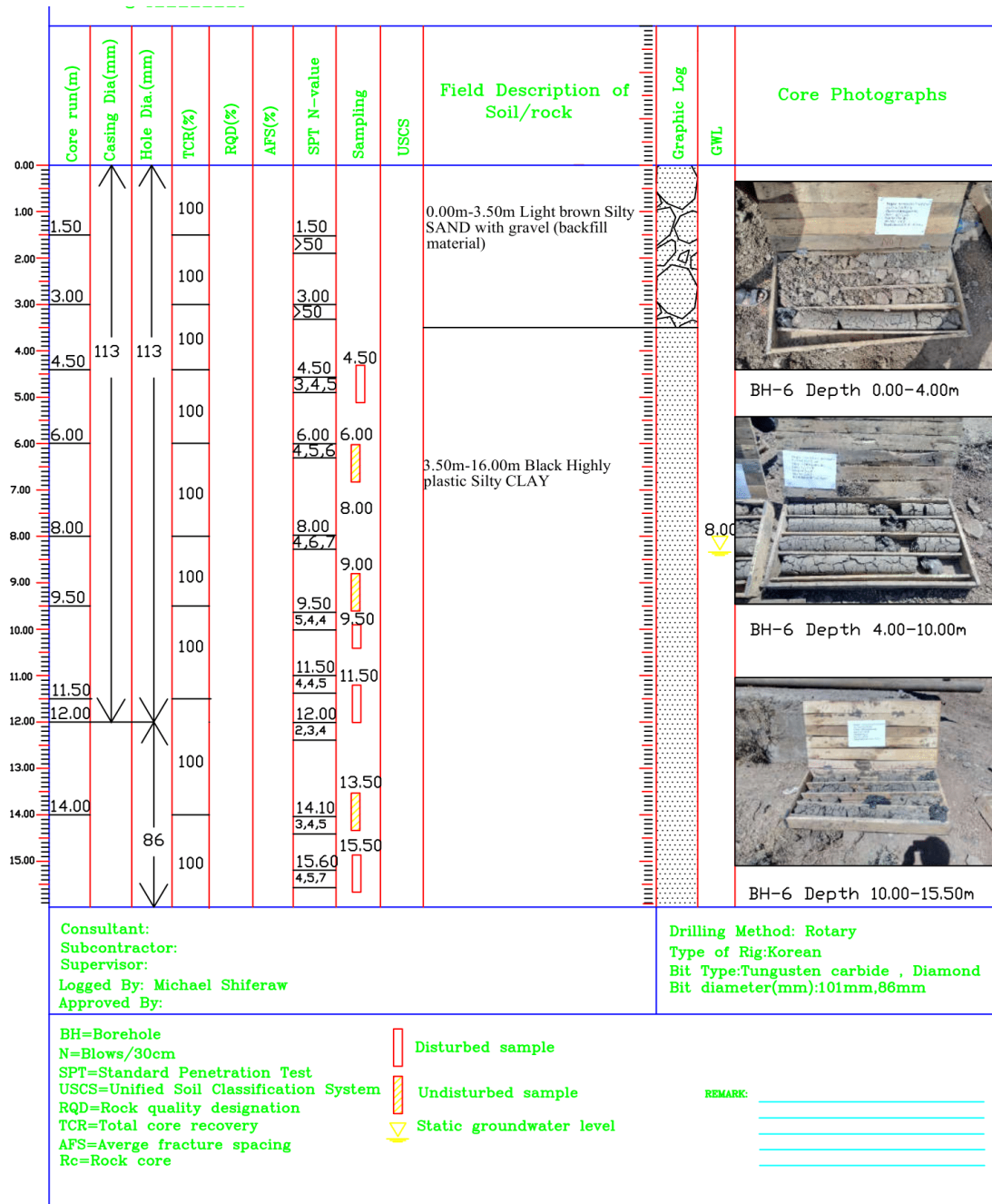
PLEASE MAKE SURE THIS IS THE CORRECT ISSUE BEFORE USE

Site specific Ground Response Analysis at South - Western part of Addis Ababa



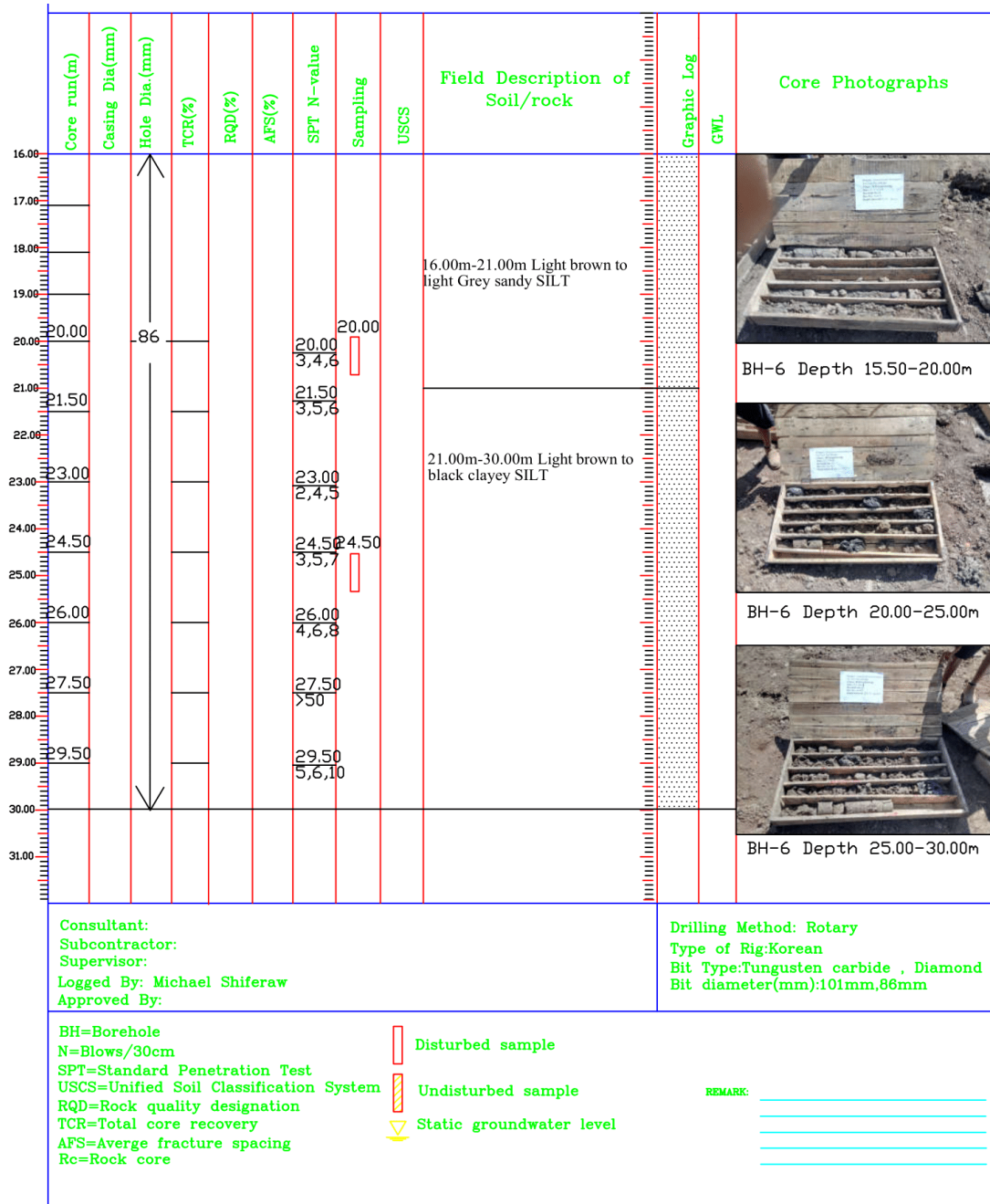
PLEASE MAKE SURE THIS IS THE CORRECT ISSUE BEFORE USE

Site specific Ground Response Analysis at South - Western part of Addis Ababa



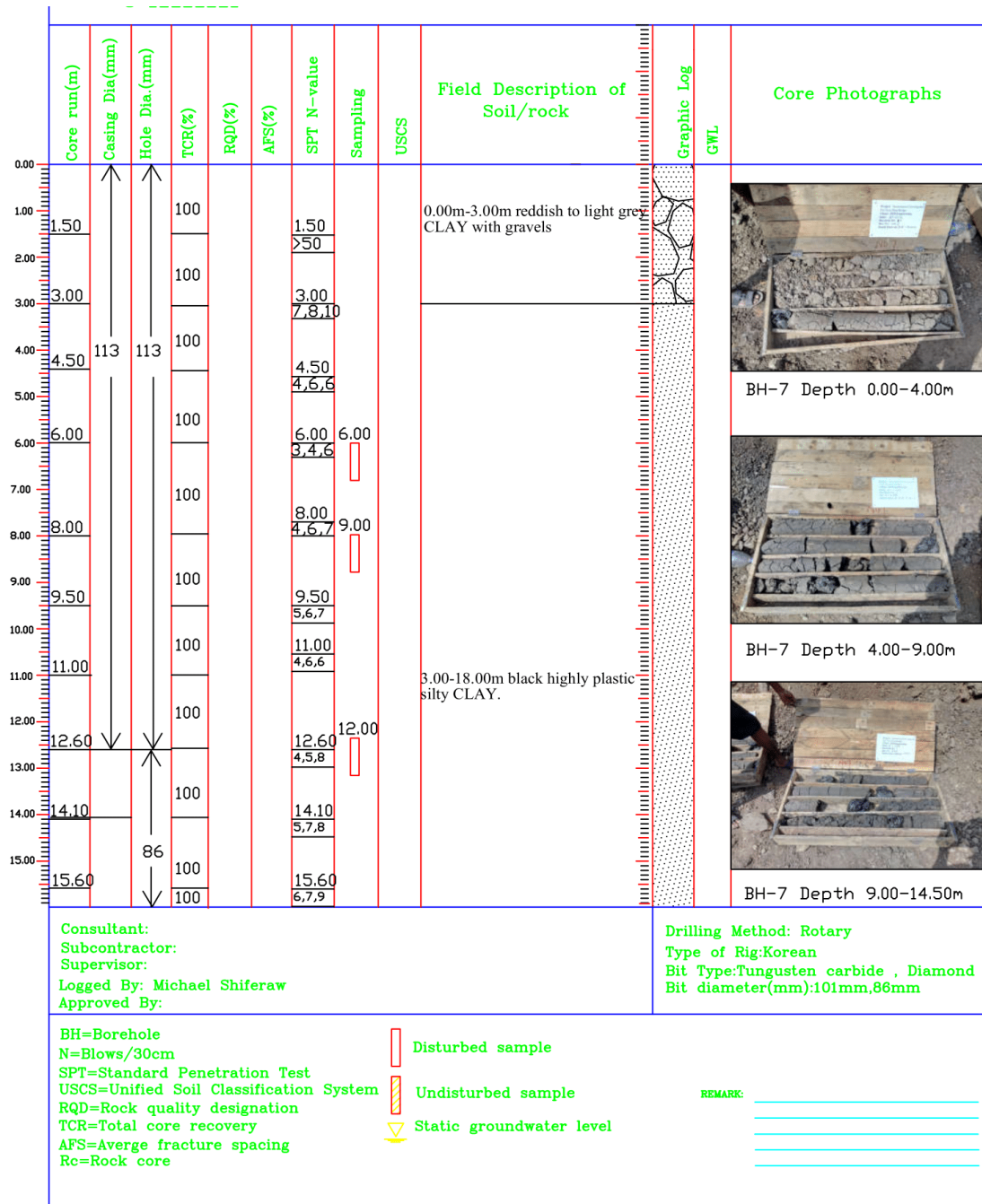
PLEASE MAKE SURE THIS IS THE CORRECT ISSUE BEFORE USE

Site specific Ground Response Analysis at South - Western part of Addis Ababa



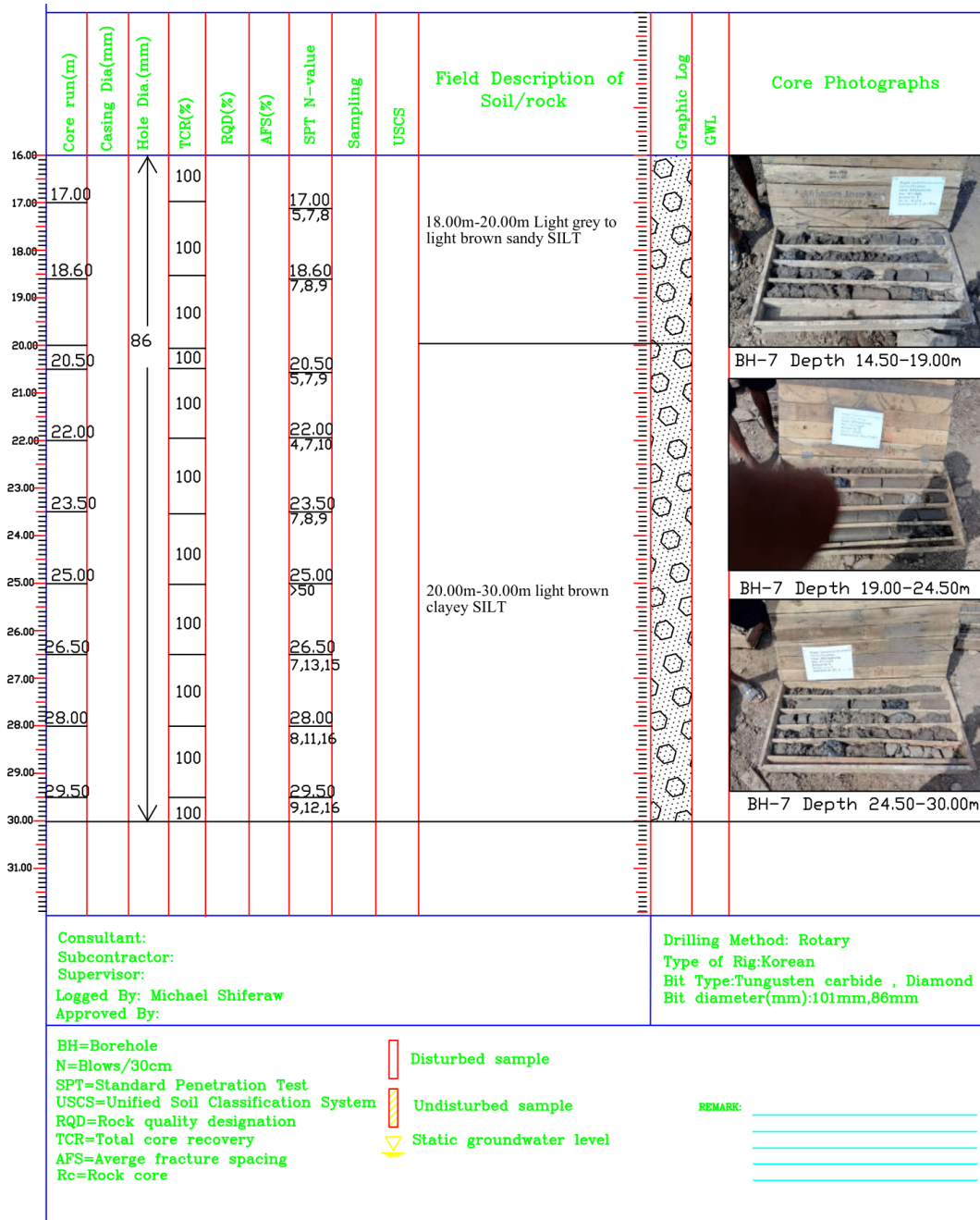
PLEASE MAKE SURE THIS IS THE CORRECT ISSUE BEFORE USE

Site specific Ground Response Analysis at South - Western part of Addis Ababa



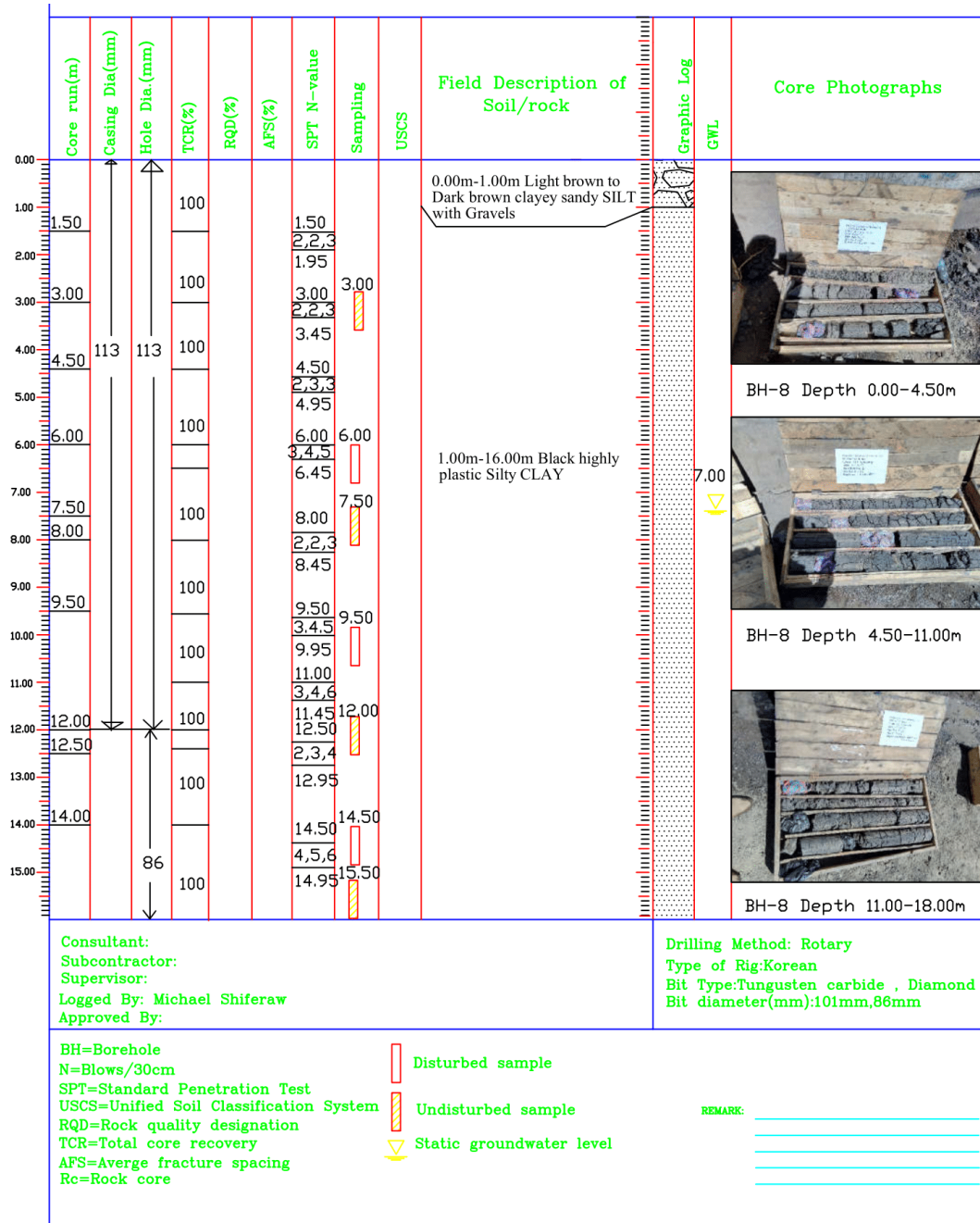
PLEASE MAKE SURE THIS IS THE CORRECT ISSUE BEFORE USE

Site specific Ground Response Analysis at South - Western part of Addis Ababa



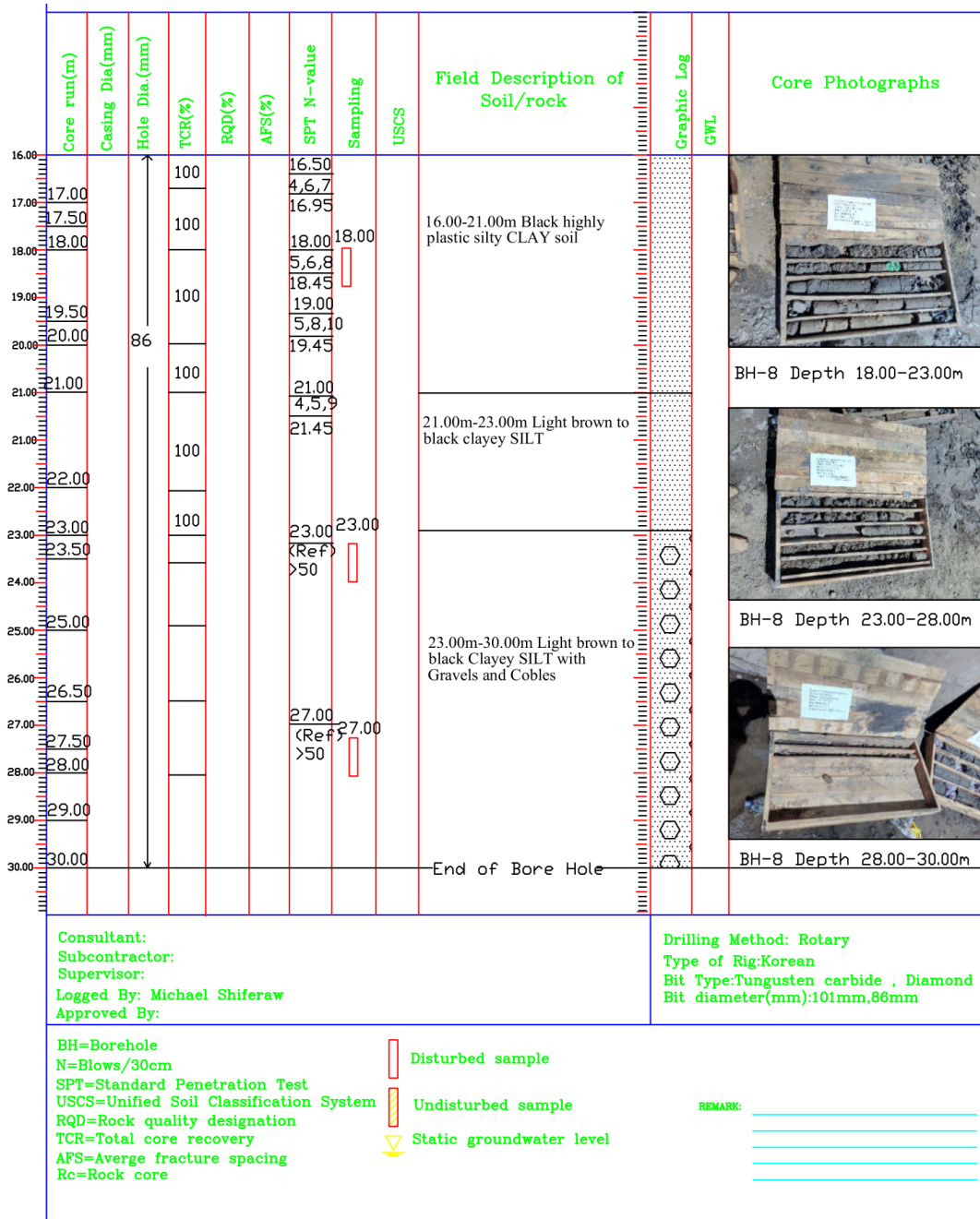
PLEASE MAKE SURE THIS IS THE CORRECT ISSUE BEFORE USE

Site specific Ground Response Analysis at South - Western part of Addis Ababa



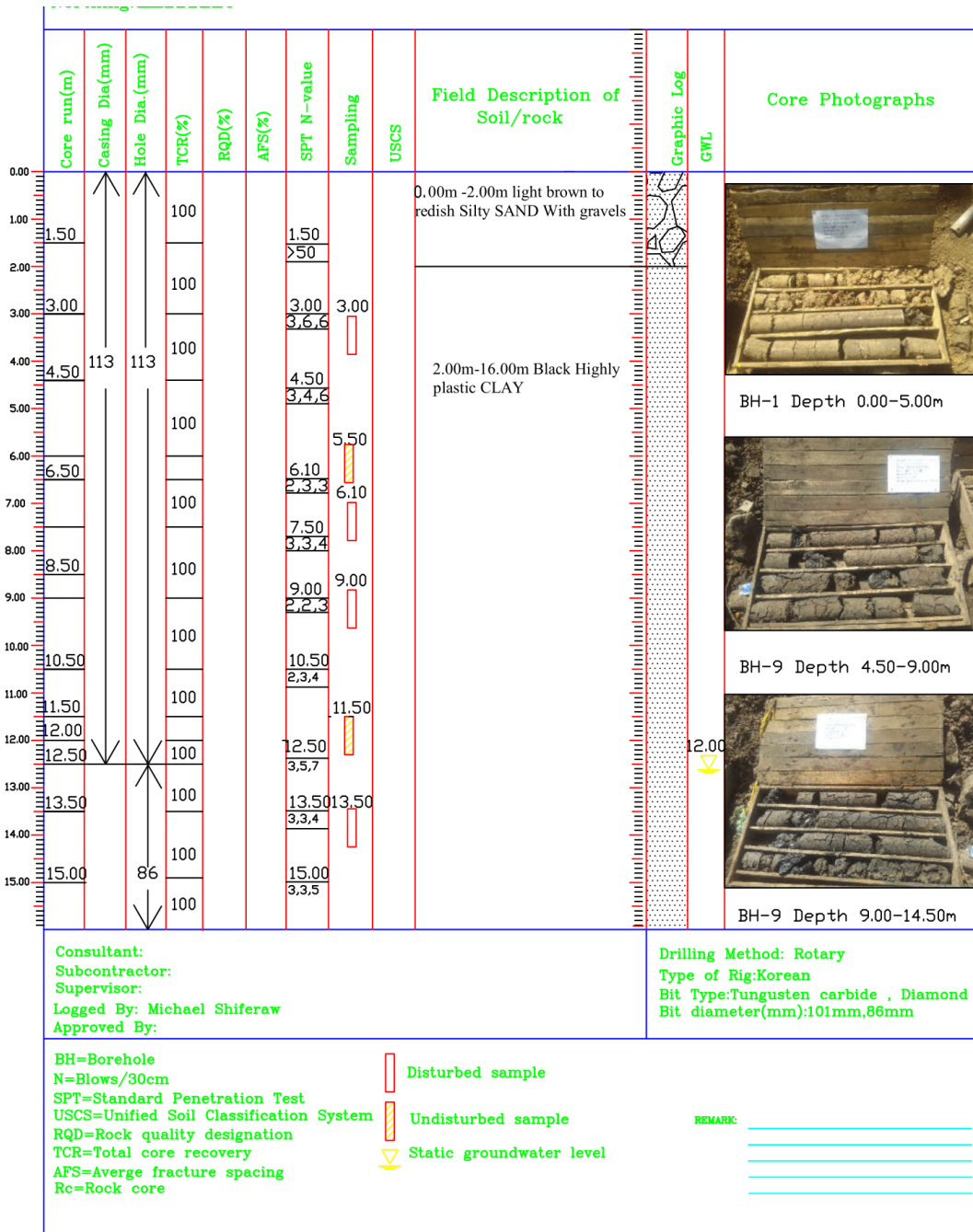
PLEASE MAKE SURE THIS IS THE CORRECT ISSUE BEFORE USE

Site specific Ground Response Analysis at South - Western part of Addis Ababa

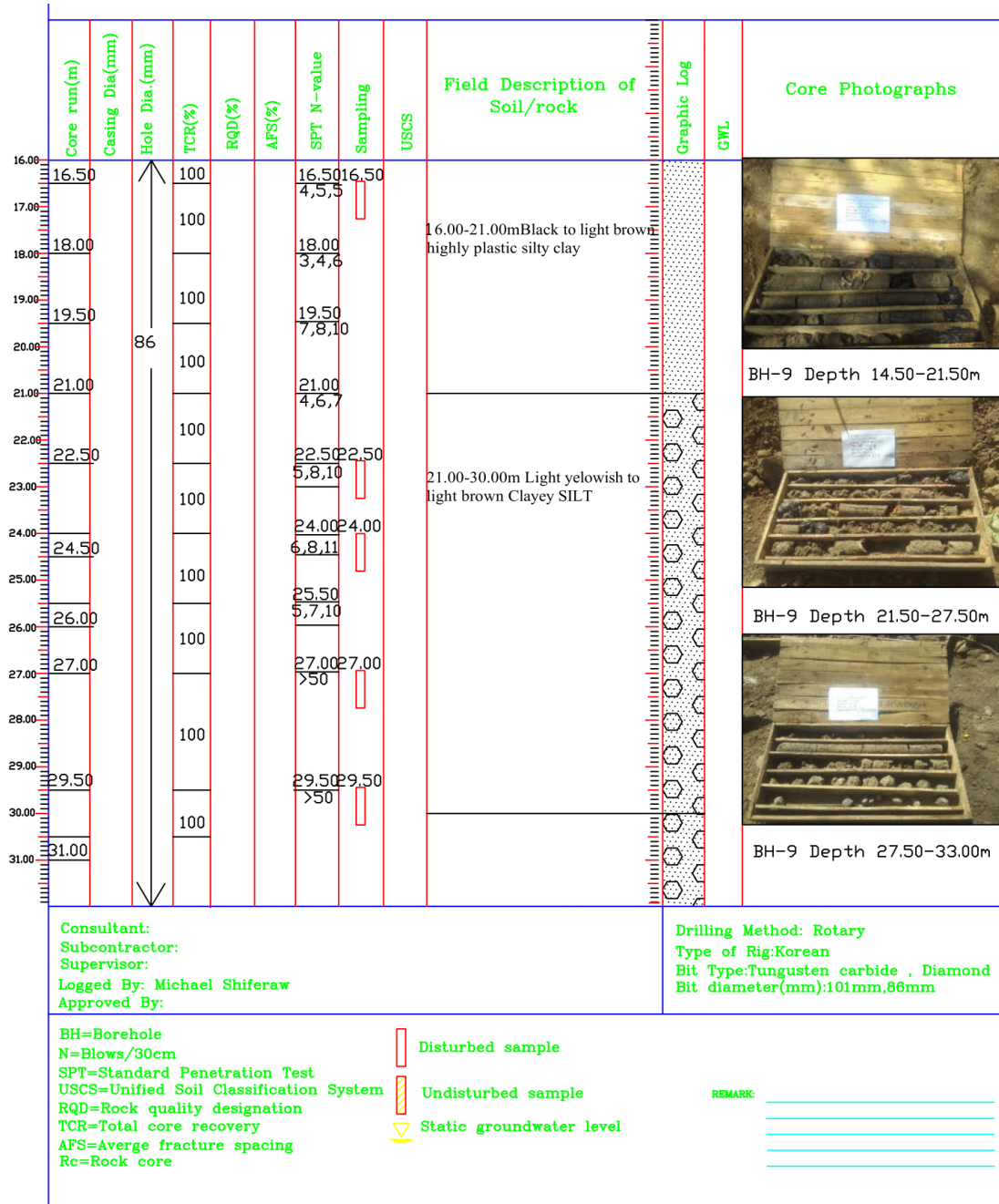


PLEASE MAKE SURE THIS IS THE CORRECT ISSUE BEFORE USE

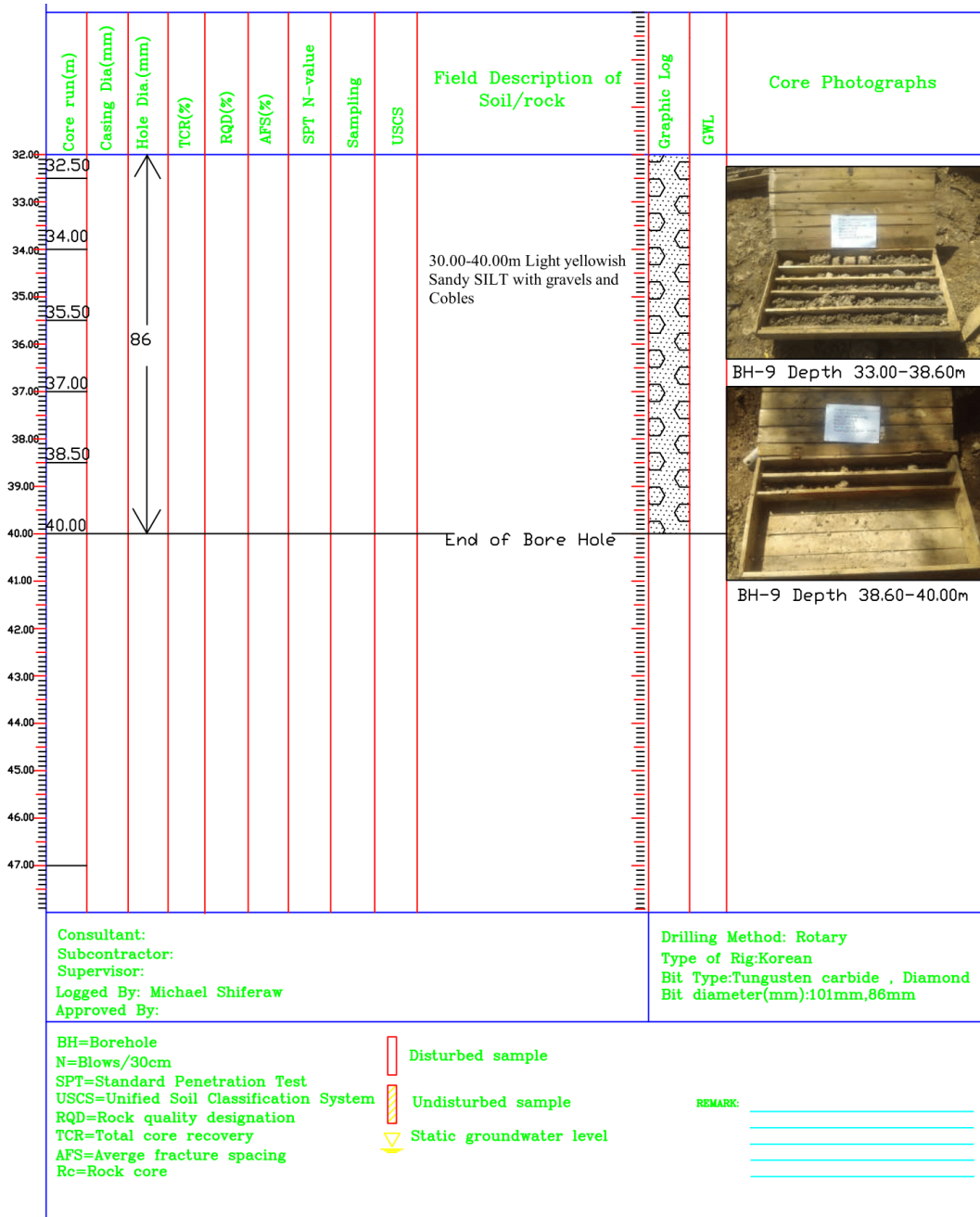
Site specific Ground Response Analysis at South - Western part of Addis Ababa



Site specific Ground Response Analysis at South - Western part of Addis Ababa



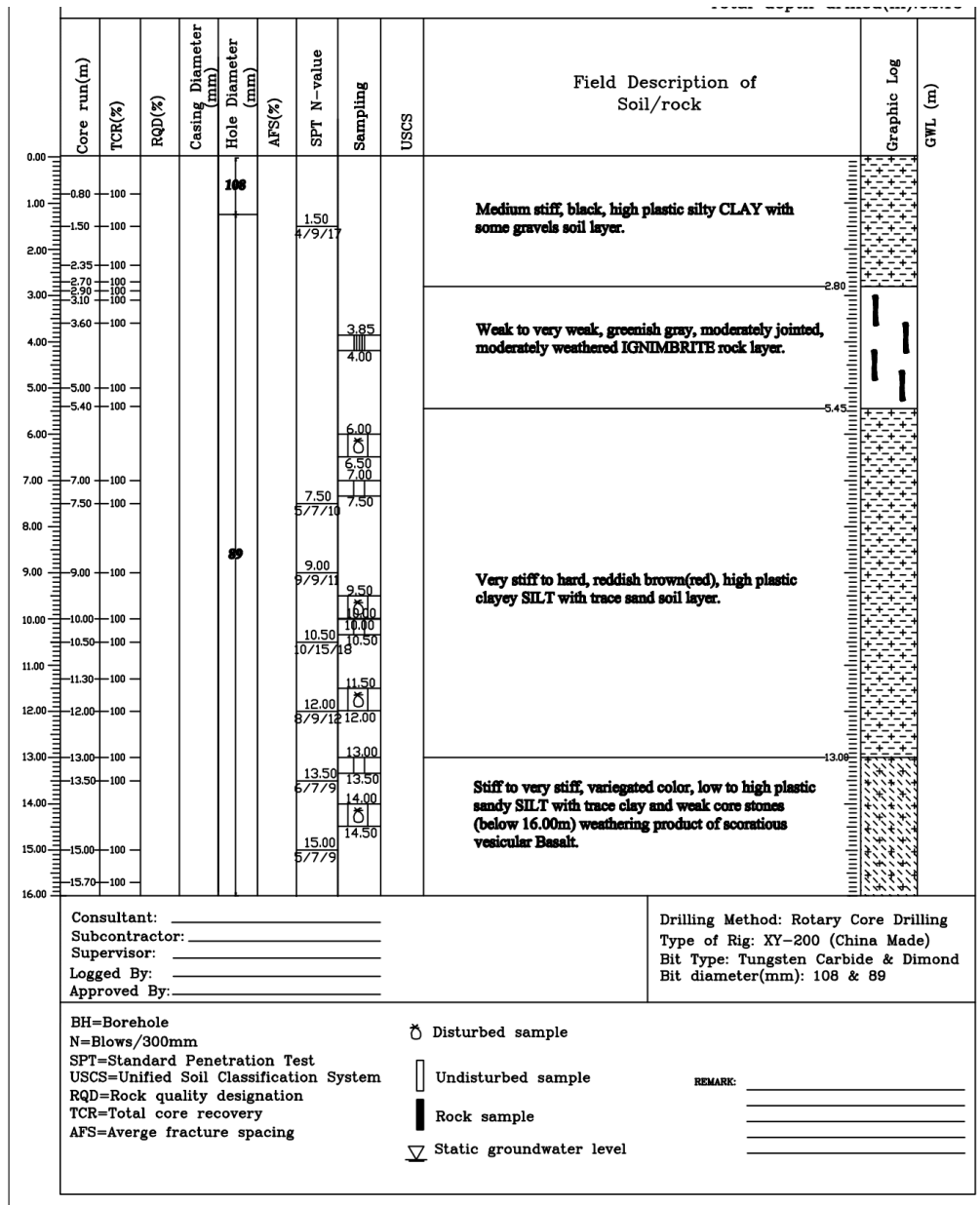
Site specific Ground Response Analysis at South - Western part of Addis Ababa



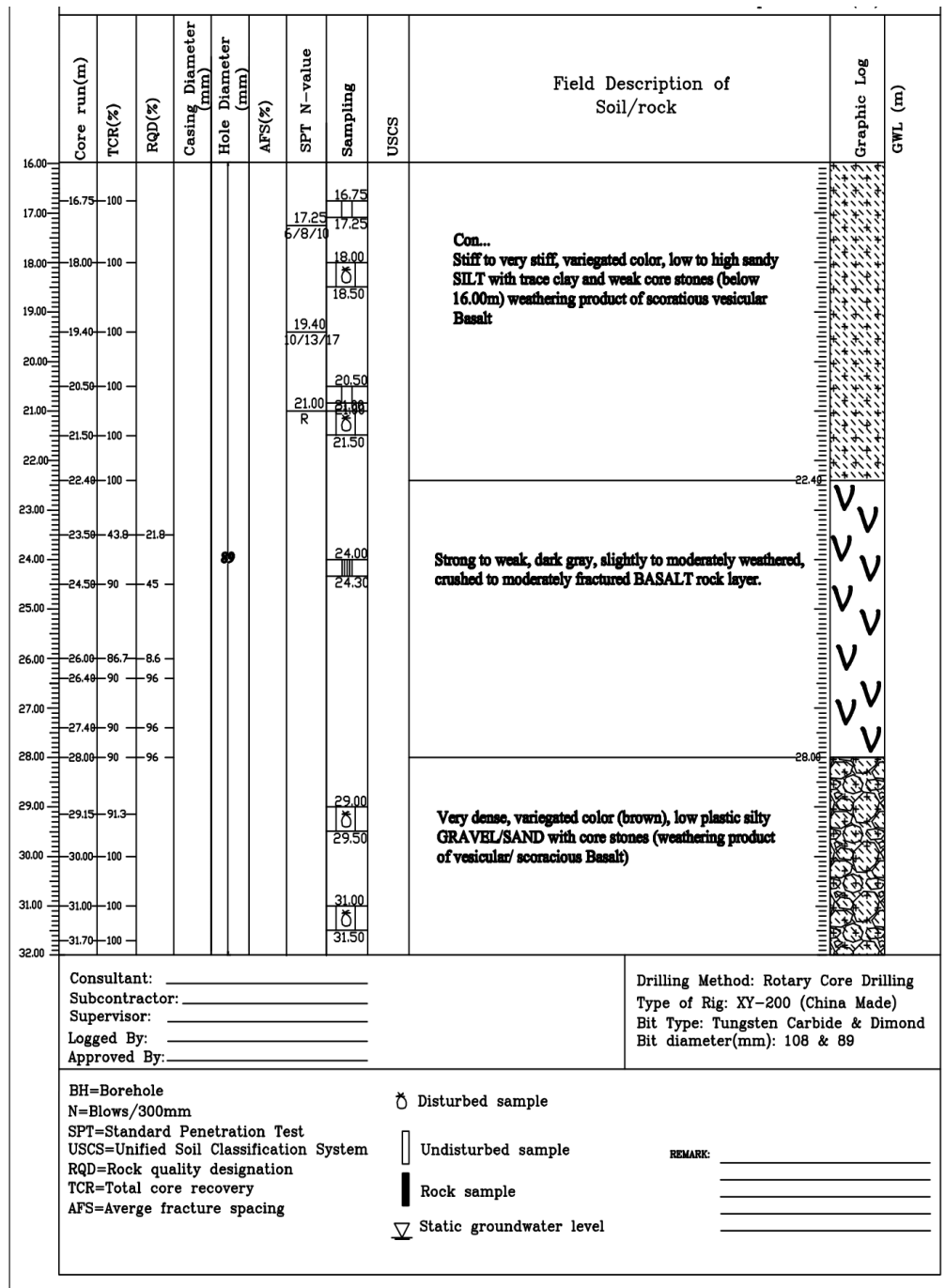
PLEASE MAKE SURE THIS IS THE CORRECT ISSUE BEFORE USE

Figure C- 1: Akaki Kality borehole logs

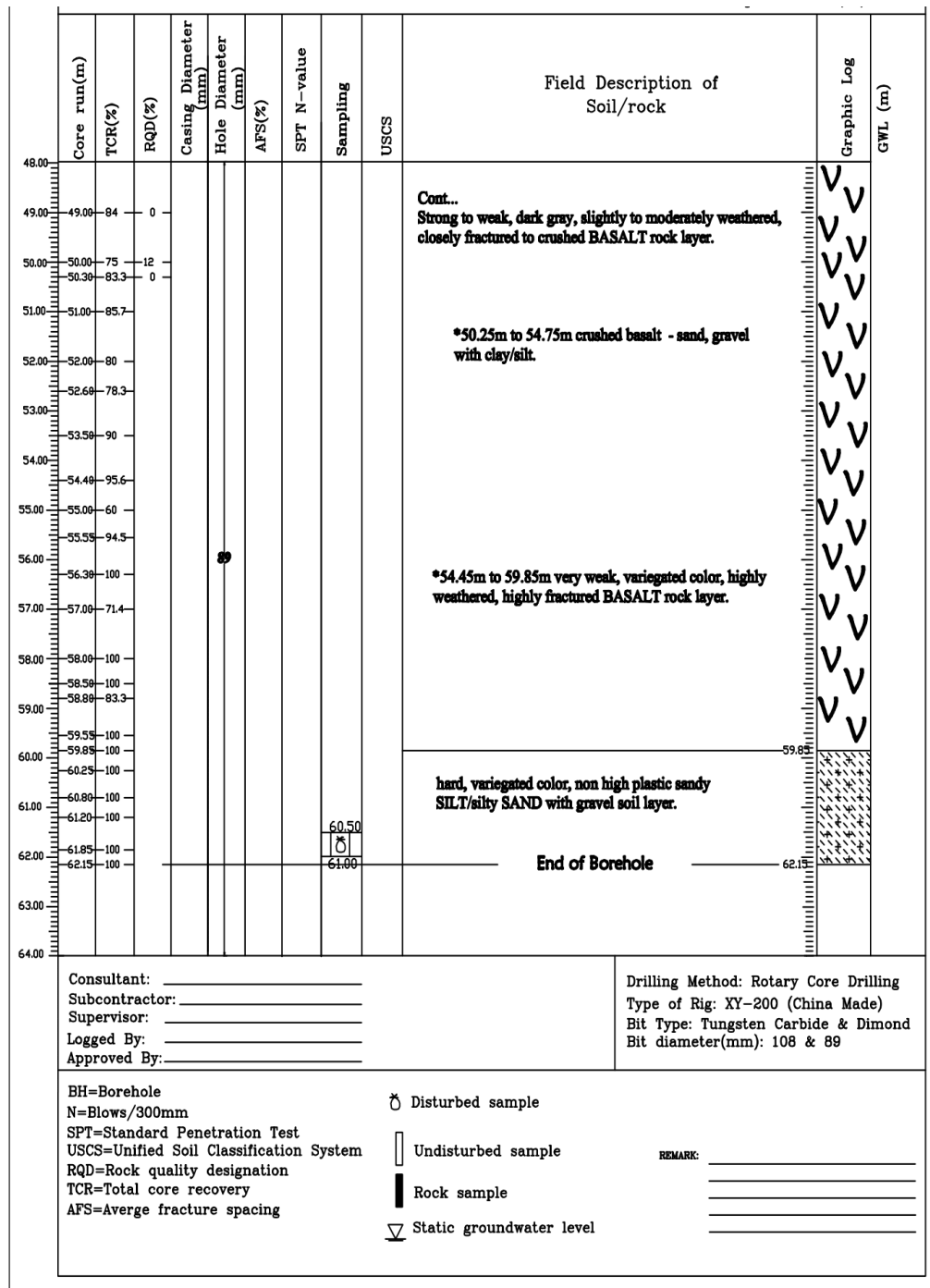
b. Kirkos Sub city



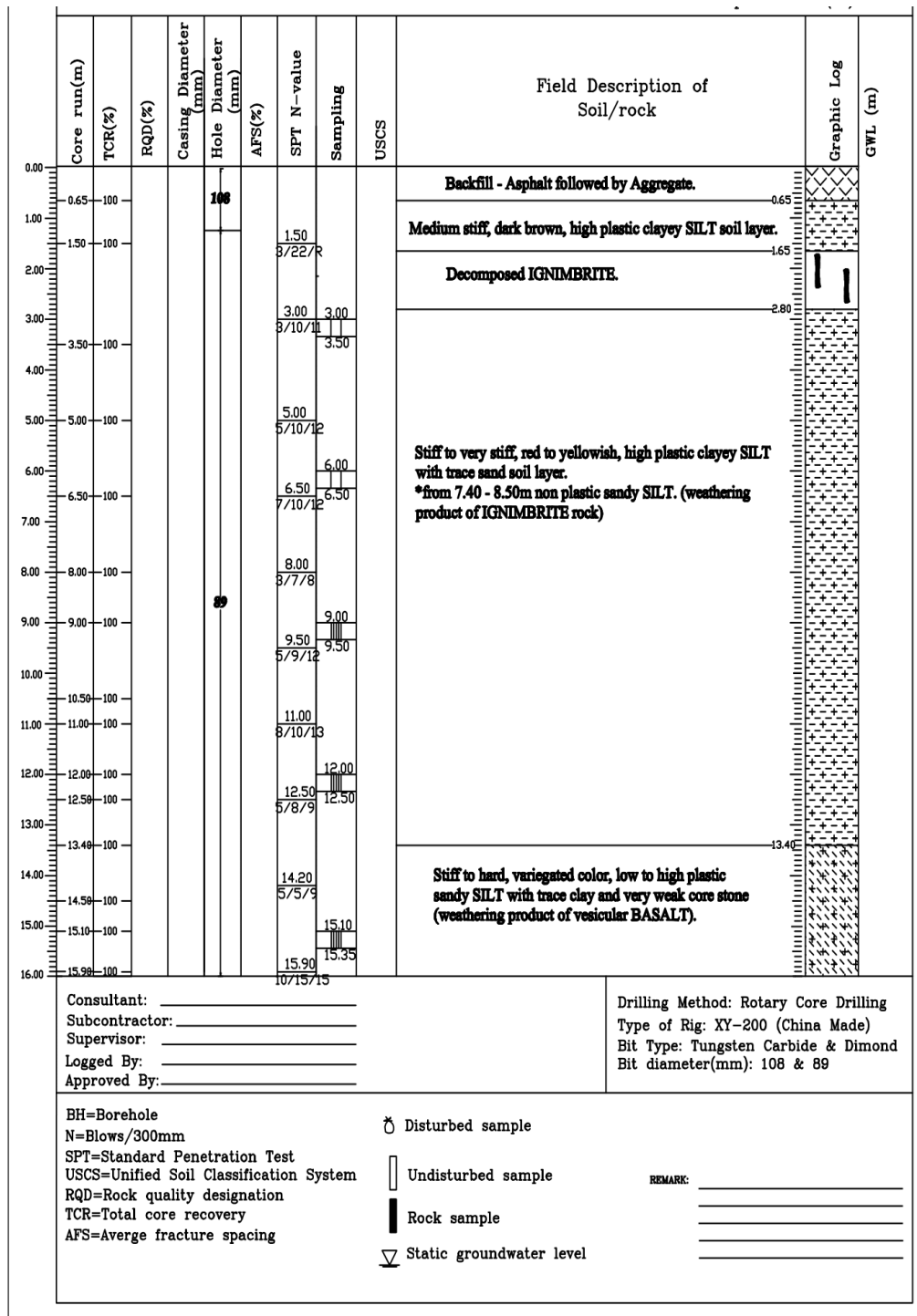
Site specific Ground Response Analysis at South - Western part of Addis Ababa



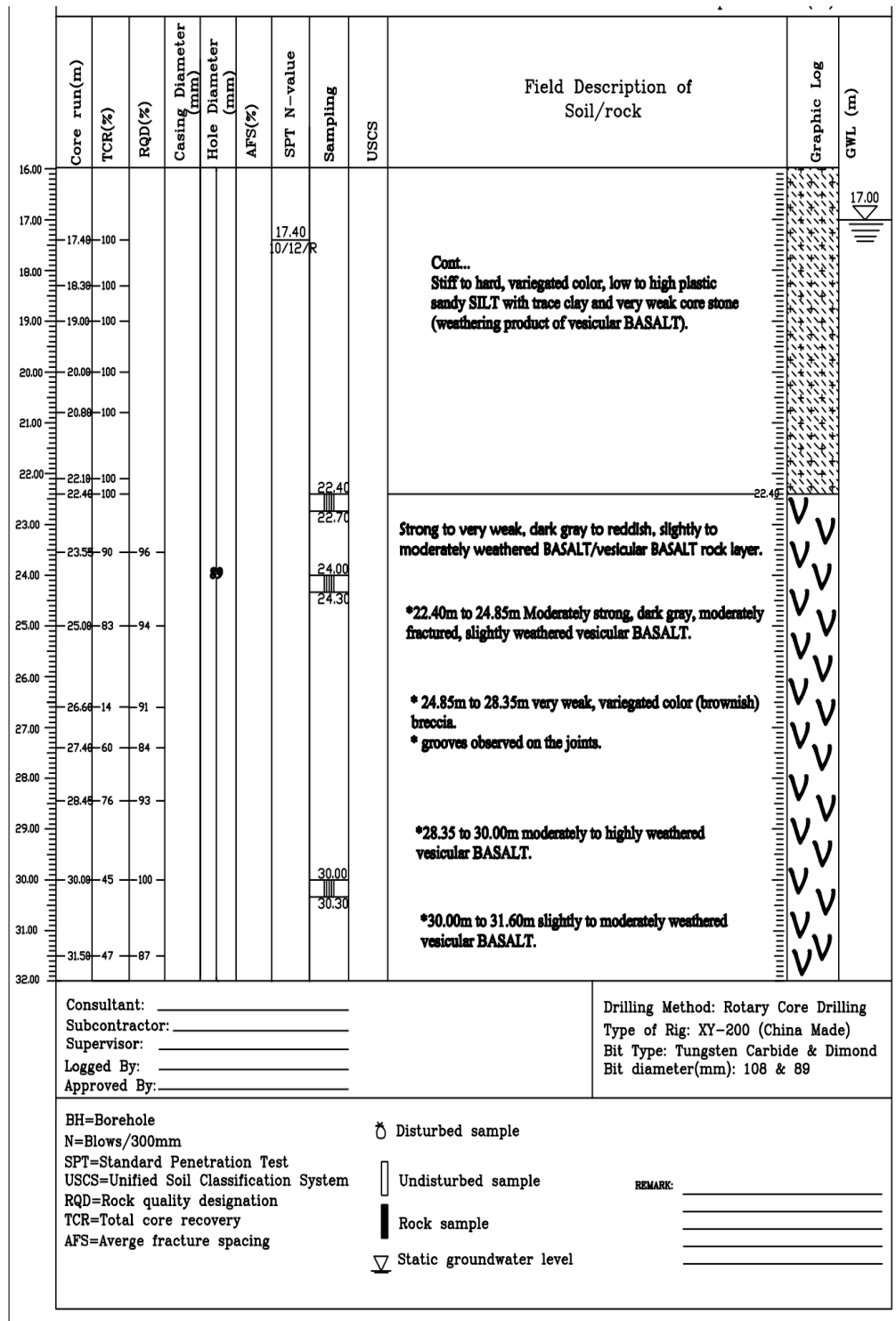
Site specific Ground Response Analysis at South - Western part of Addis Ababa



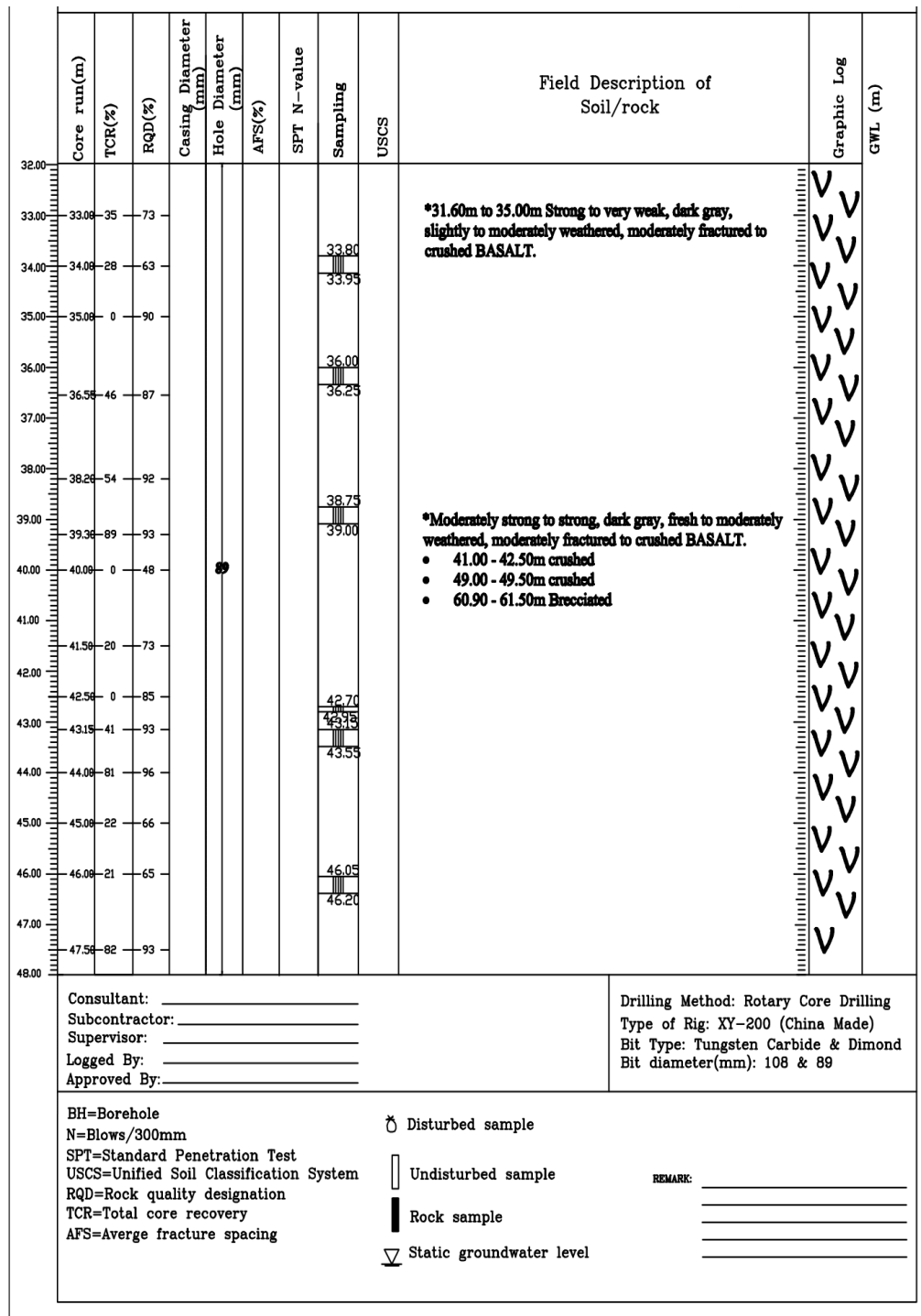
Site specific Ground Response Analysis at South - Western part of Addis Ababa



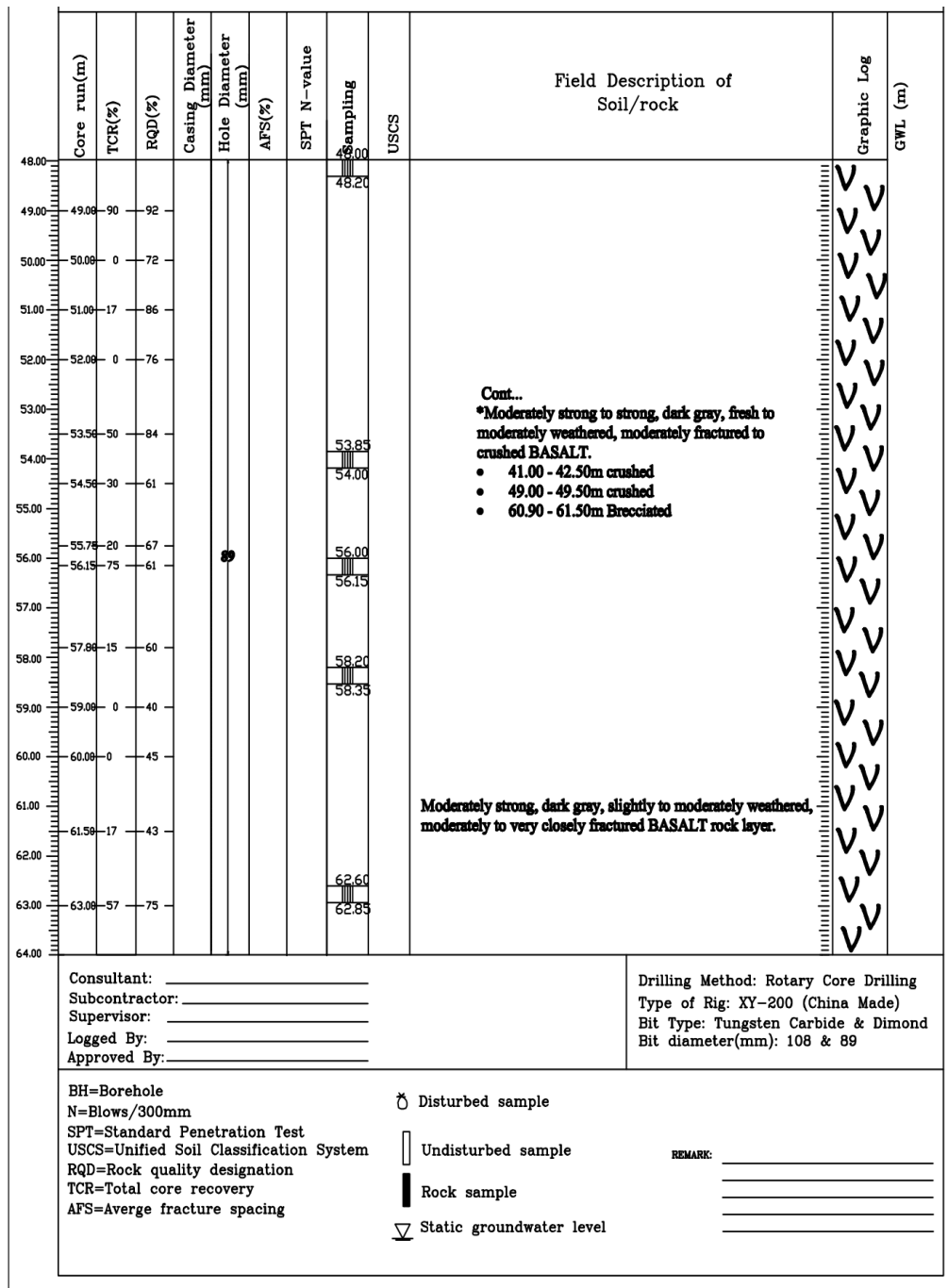
Site specific Ground Response Analysis at South - Western part of Addis Ababa



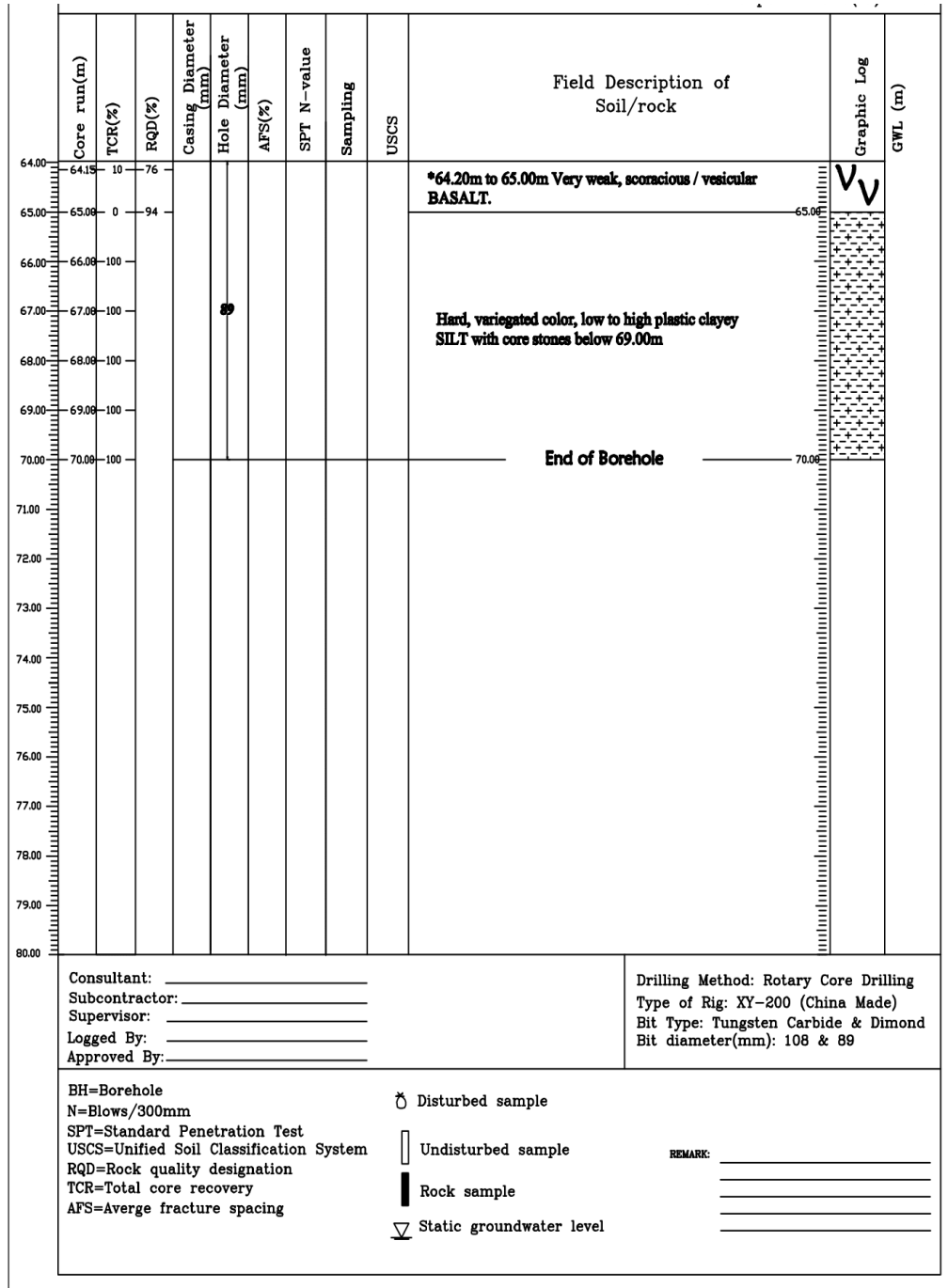
Site specific Ground Response Analysis at South - Western part of Addis Ababa



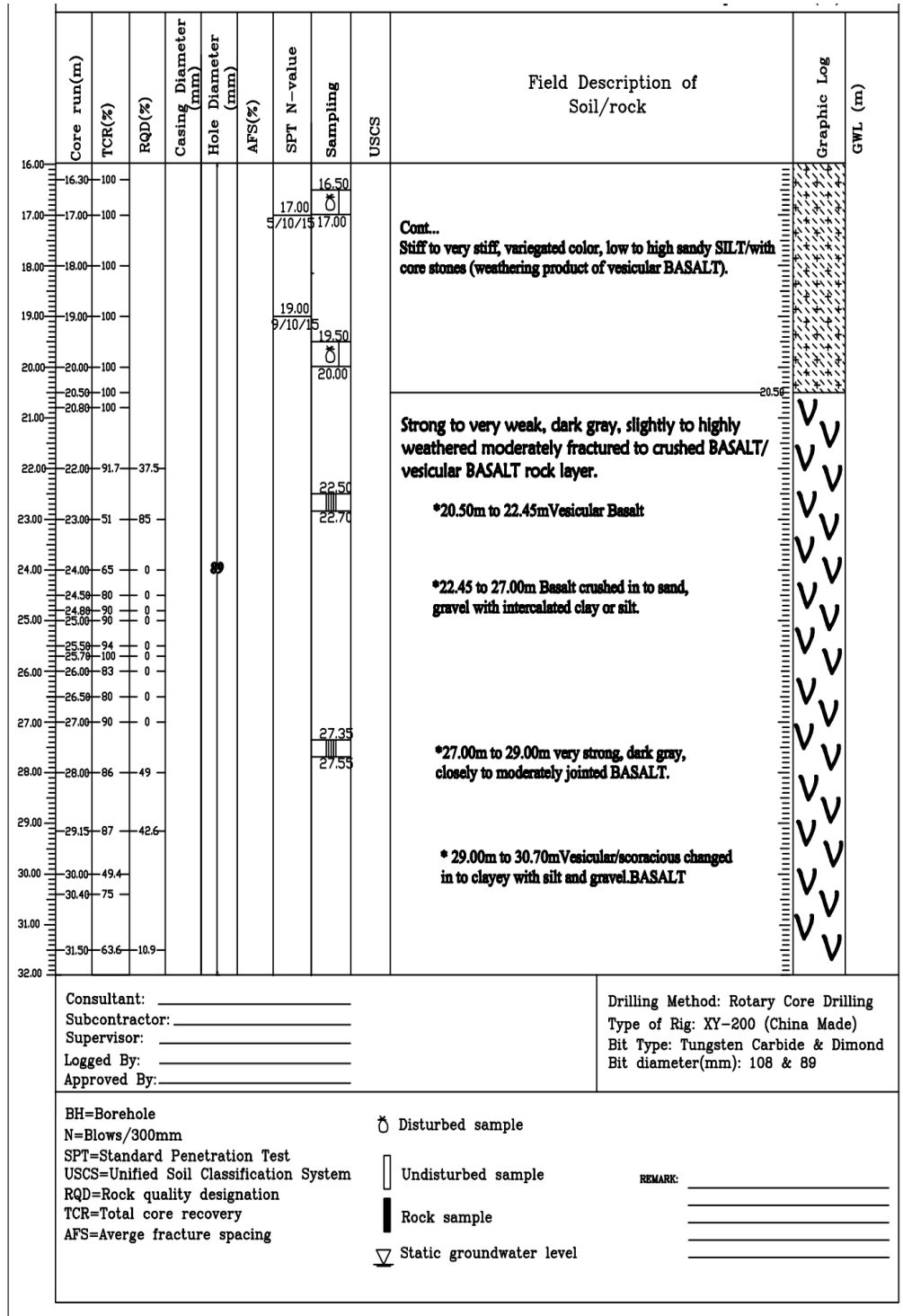
Site specific Ground Response Analysis at South - Western part of Addis Ababa



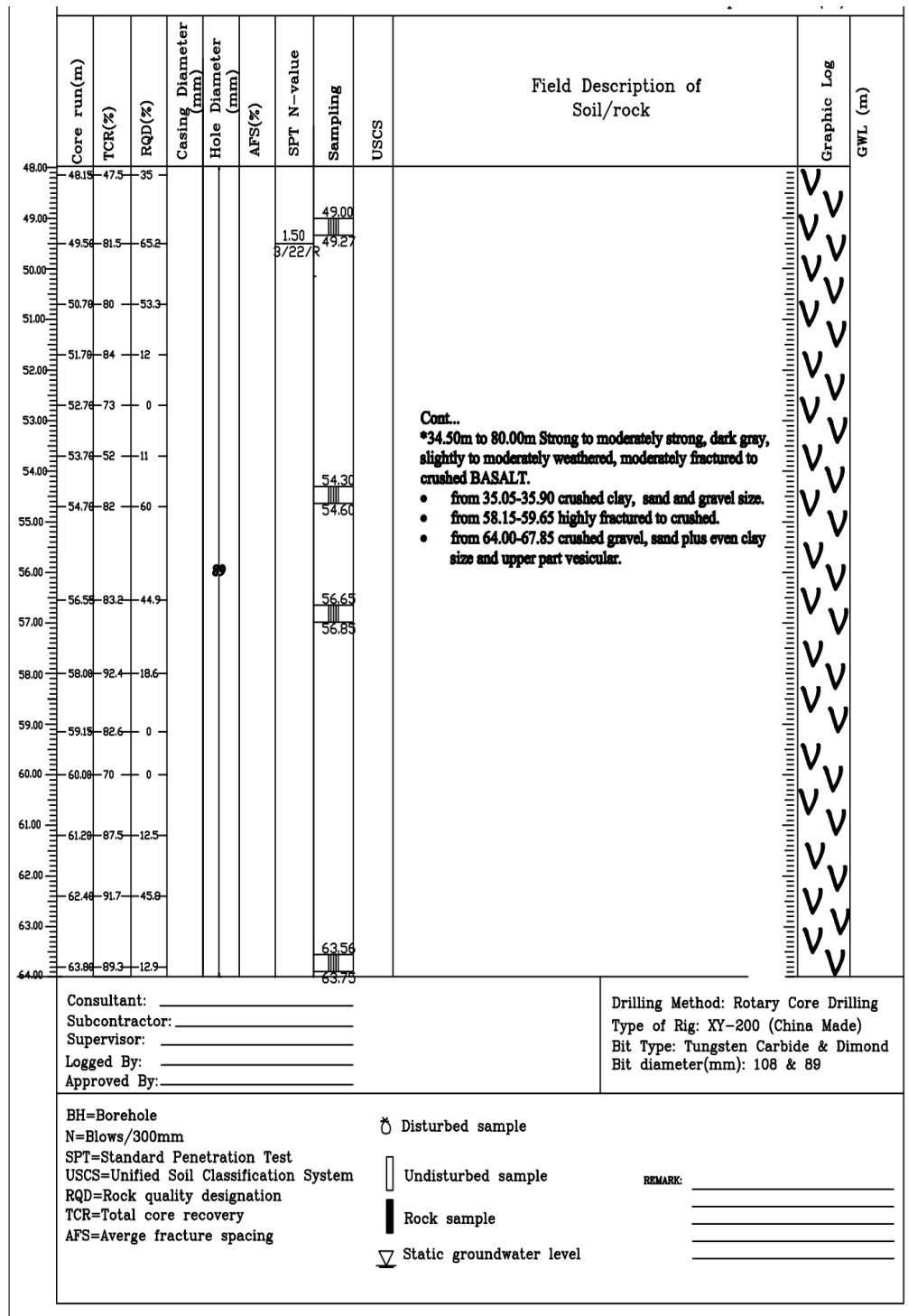
Site specific Ground Response Analysis at South - Western part of Addis Ababa



Site specific Ground Response Analysis at South - Western part of Addis Ababa



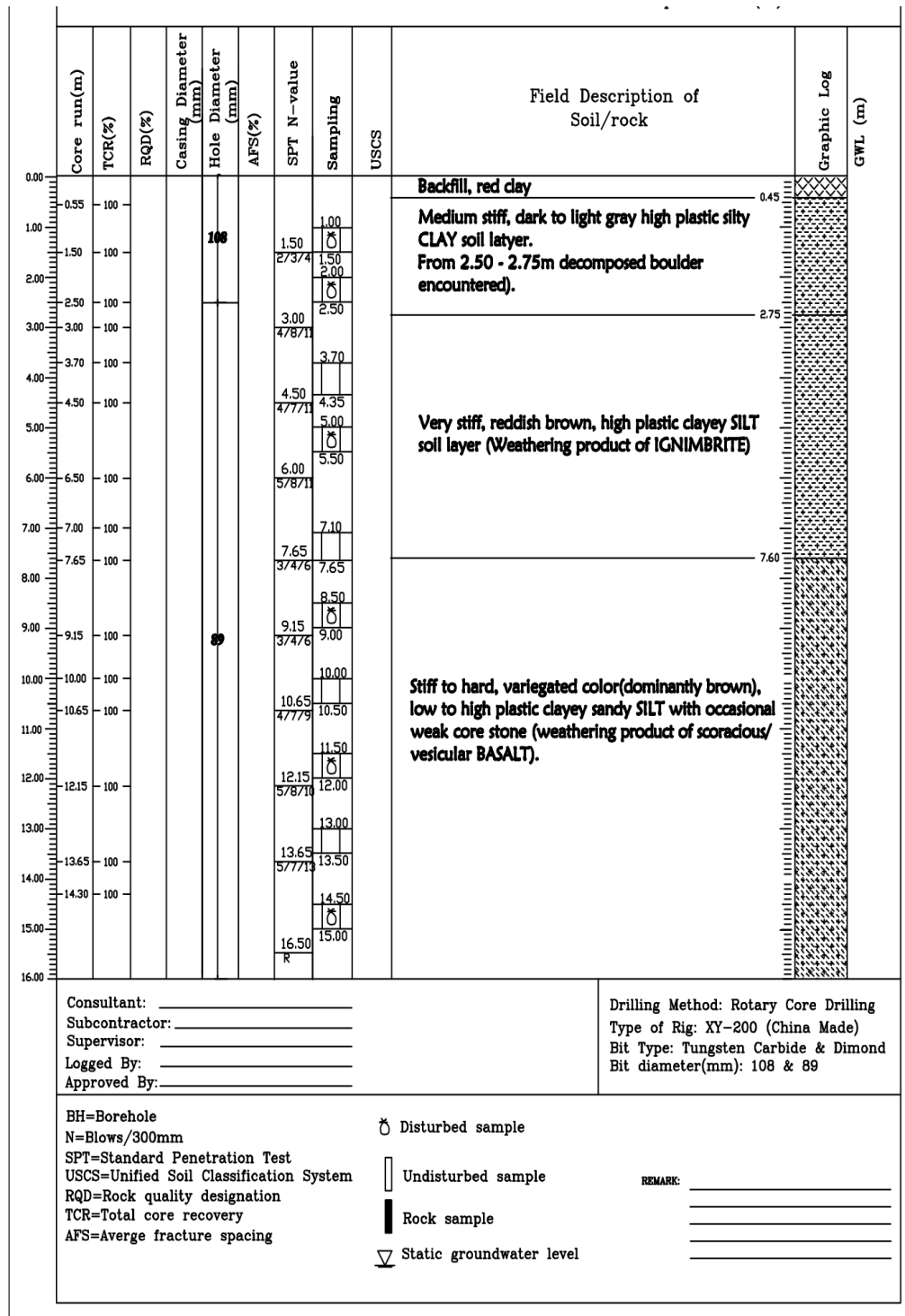
Site specific Ground Response Analysis at South - Western part of Addis Ababa



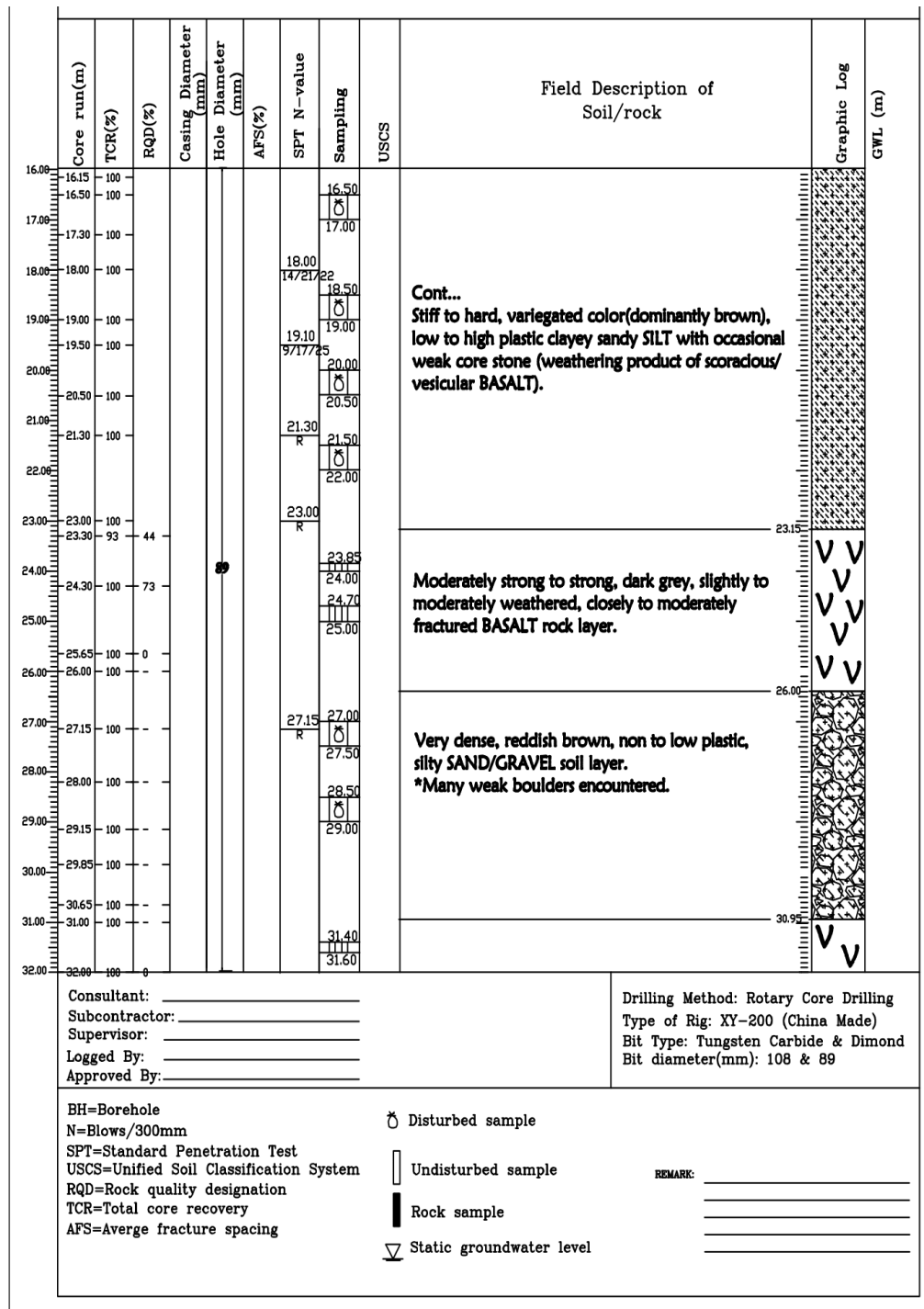
Site specific Ground Response Analysis at South - Western part of Addis Ababa

Core run(m)	TCR(%)	RQD(%)	Casing Diameter (mm)	Hole Diameter (mm)	AFS(%)	SPT N-value	Sampling	USCS	Field Description of Soil/rock	Graphic Log	GWL (m)
64.00									<p>Cont... *34.50m to 80.00m Strong to moderately strong, dark gray, slightly to moderately weathered, moderately fractured to crushed BASALT.</p> <ul style="list-style-type: none"> • from 35.05-35.90 crushed clay, sand and gravel size. • from 58.15-59.65 highly fractured to crushed. • from 64.00-67.85 crushed gravel, sand plus even clay size and upper part vesicular. 		
65.00	82.5	0									
66.00	75										
67.00	62	0									
68.00	70	13									
69.00	65	83									
69.66	93.3	48.3									
70.00											
70.78	86.4	52.7									
71.00											
71.78	67	10	●								
72.00											
73.00	81.5	11.5									
74.00	65	10									
74.58	60	24									
75.00	44	0									
75.58	92	0									
76.00	92	0									
76.58	100										
77.00	92										
78.00	80	0									
78.58	94	0									
79.00											
79.78	93.3	0									
80.00	96	0						End of Borehole			
Consultant: _____ Subcontractor: _____ Supervisor: _____ Logged By: _____ Approved By: _____								Drilling Method: Rotary Core Drilling Type of Rig: XY-200 (China Made) Bit Type: Tungsten Carbide & Dimond Bit diameter(mm): 108 & 89			
BH=Borehole N=Blows/300mm SPT=Standard Penetration Test USCS=Unified Soil Classification System RQD=Rock quality designation TCR=Total core recovery AFS=Average fracture spacing								○ Disturbed sample □ Undisturbed sample ■ Rock sample ▽ Static groundwater level			
								REMARK: _____ _____ _____			

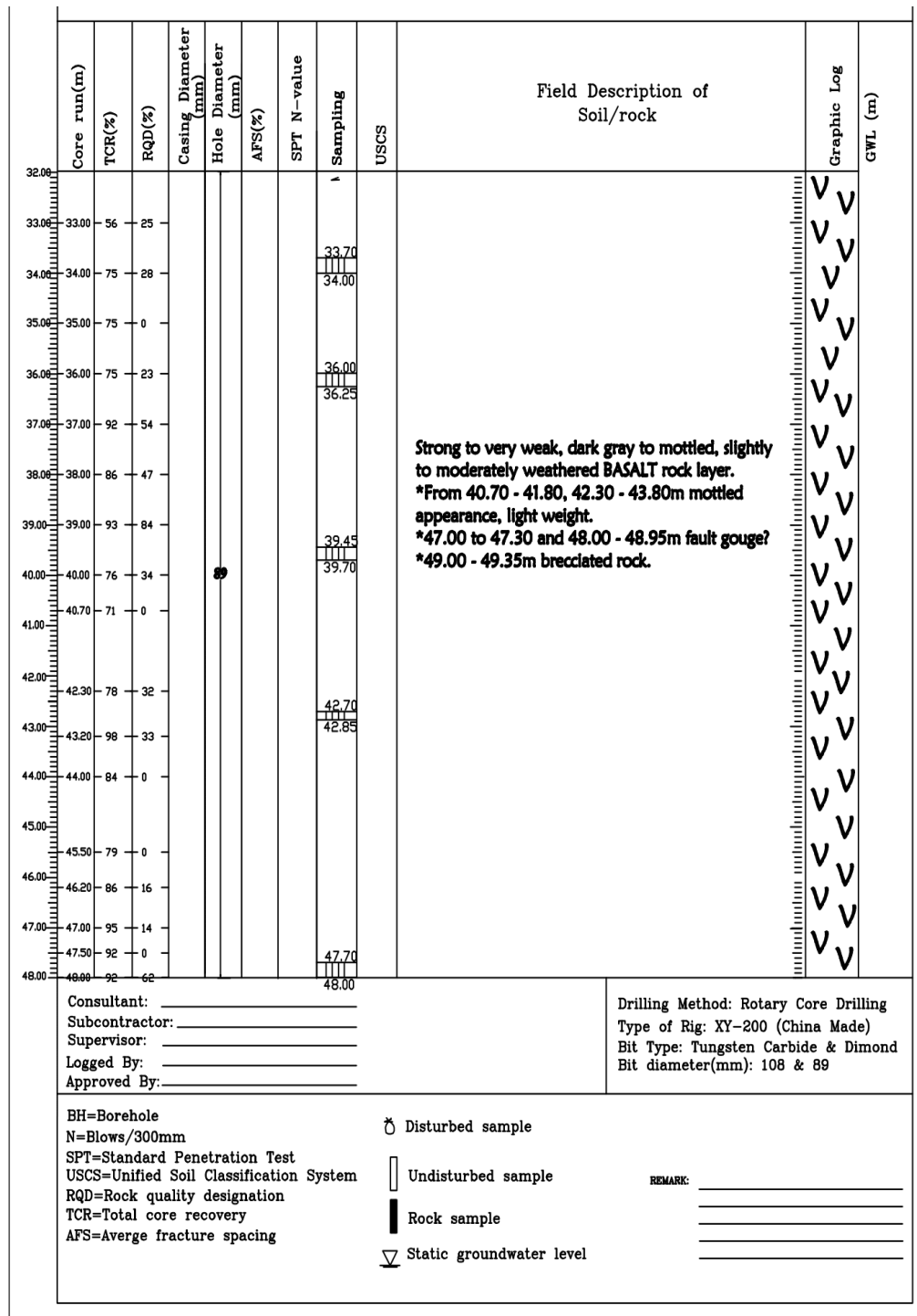
Site specific Ground Response Analysis at South - Western part of Addis Ababa



Site specific Ground Response Analysis at South - Western part of Addis Ababa



Site specific Ground Response Analysis at South - Western part of Addis Ababa



Site specific Ground Response Analysis at South - Western part of Addis Ababa

Core run(m)	TCR(%)	RQD(%)	Casing Diameter (mm)	Hole Diameter (mm)	AFS(%)	SPT N-value	Sampling	USCS	Field Description of Soil/rock	Graphic Log	GWL (m)
48.00							48.00		Ditto.....		
49.00	97	0					48.50				
50.00	92	0									
51.00	90	26									
51.70	79	0									
52.00							52.00				
52.30	94	63					52.25				
53.00											
53.35	92	0									
54.00	92	65									
55.00	73	45									
56.00											
56.30	92	42									
57.00											
57.50	93	67					57.30				
58.00							57.50				
59.00	83	43									
60.00	100										
61.00	83	0									
62.00	79	36					62.30				
63.00	98	36					62.50				
64.00											

Consultant: _____
 Subcontractor: _____
 Supervisor: _____
 Logged By: _____
 Approved By: _____

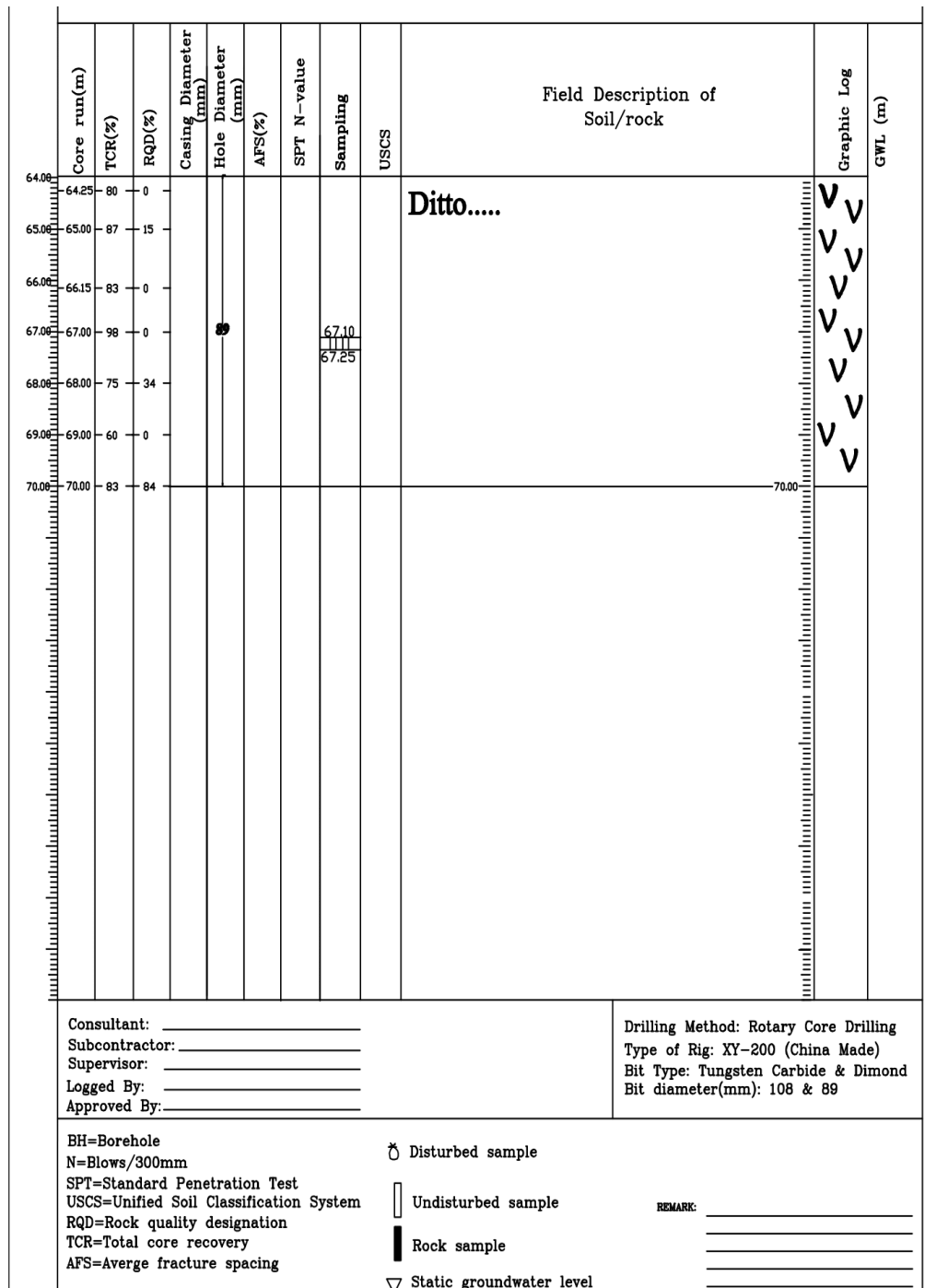
Drilling Method: Rotary Core Drilling
 Type of Rig: XY-200 (China Made)
 Bit Type: Tungsten Carbide & Dimond
 Bit diameter(mm): 108 & 89

BH=Borehole
 N=Blows/300mm
 SPT=Standard Penetration Test
 USCS=Unified Soil Classification System
 RQD=Rock quality designation
 TCR=Total core recovery
 AFS=Average fracture spacing

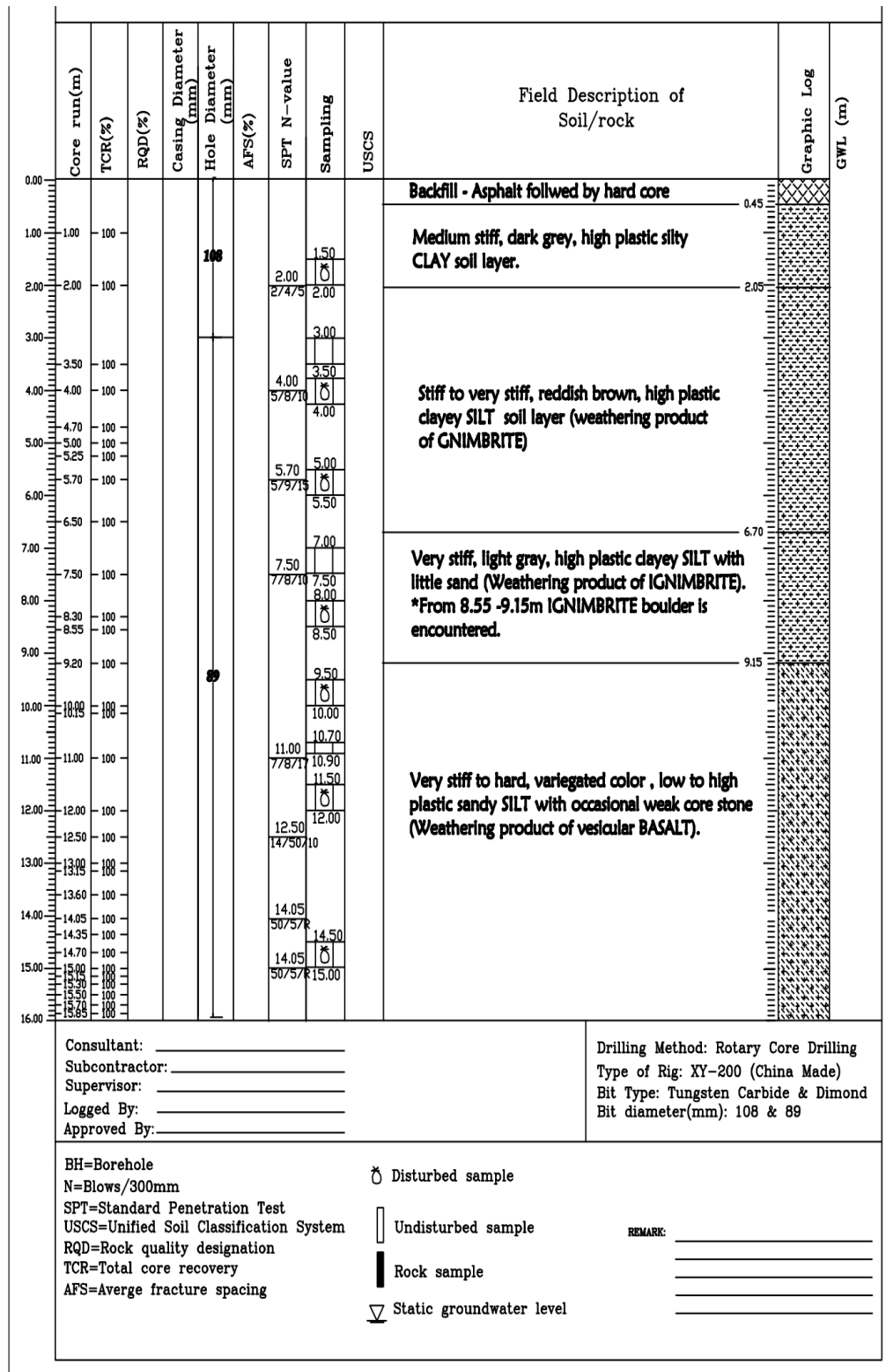
Disturbed sample
 Undisturbed sample
 Rock sample
 Static groundwater level

REMARK: _____

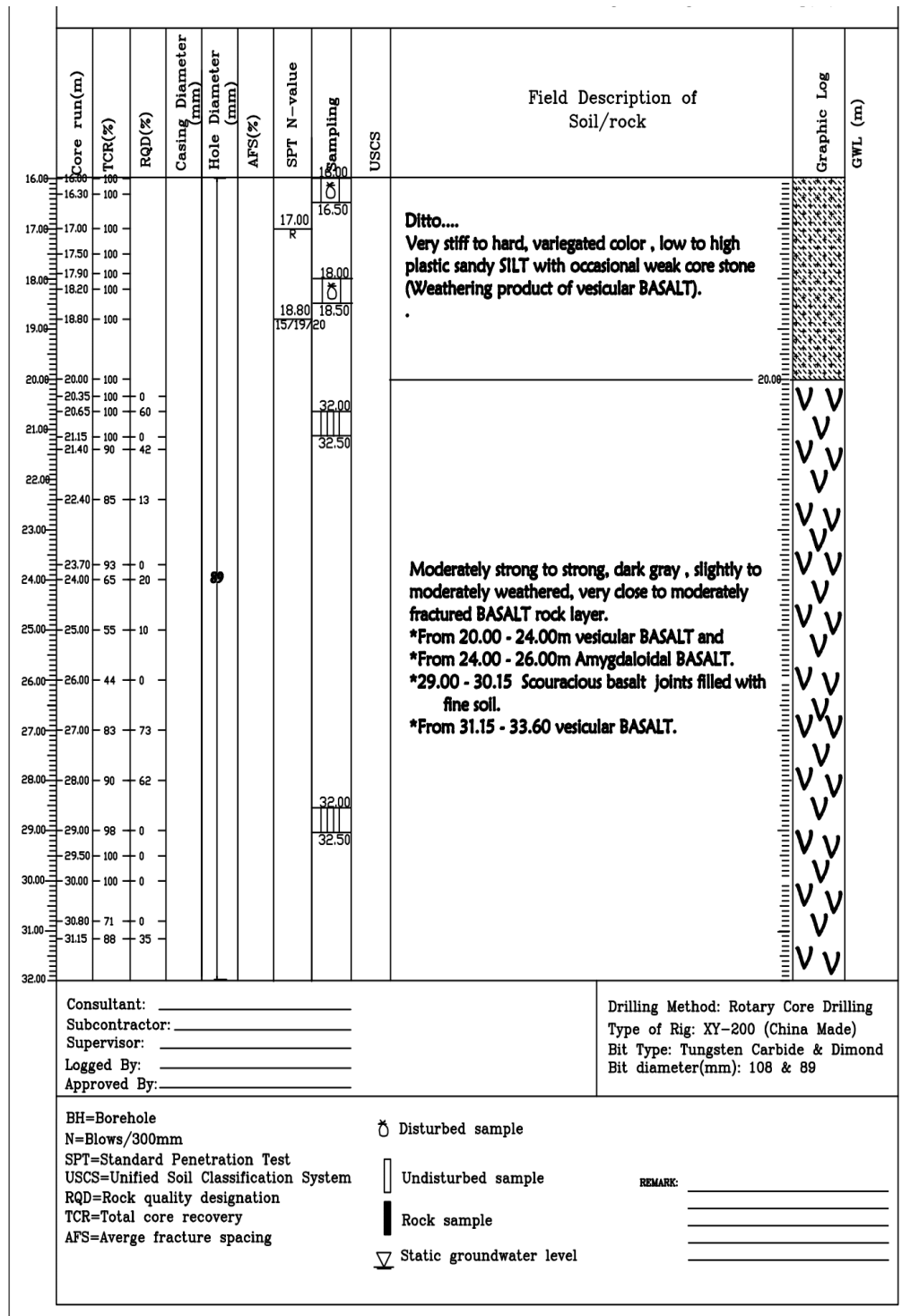
Site specific Ground Response Analysis at South - Western part of Addis Ababa



Site specific Ground Response Analysis at South - Western part of Addis Ababa



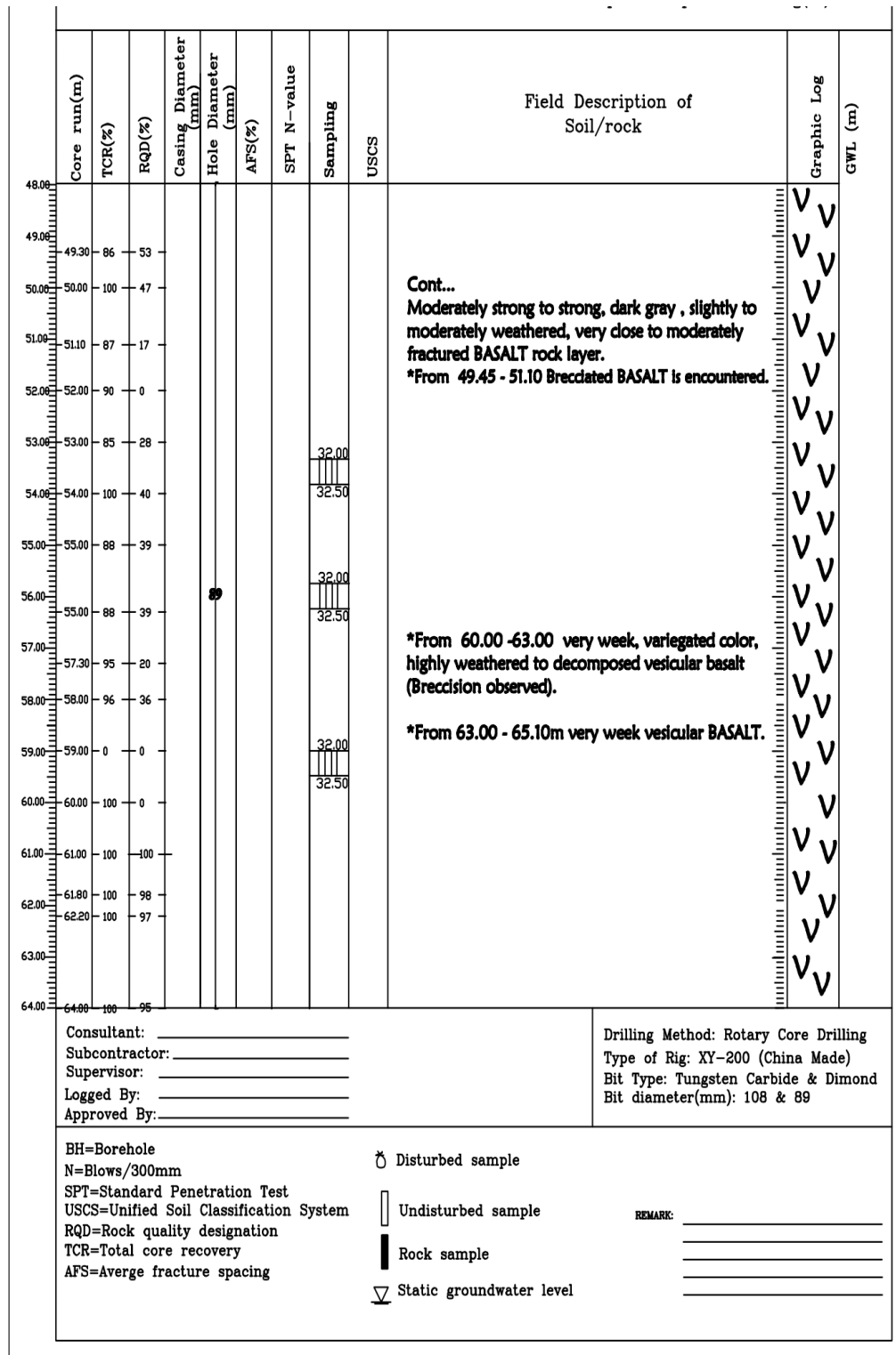
Site specific Ground Response Analysis at South - Western part of Addis Ababa



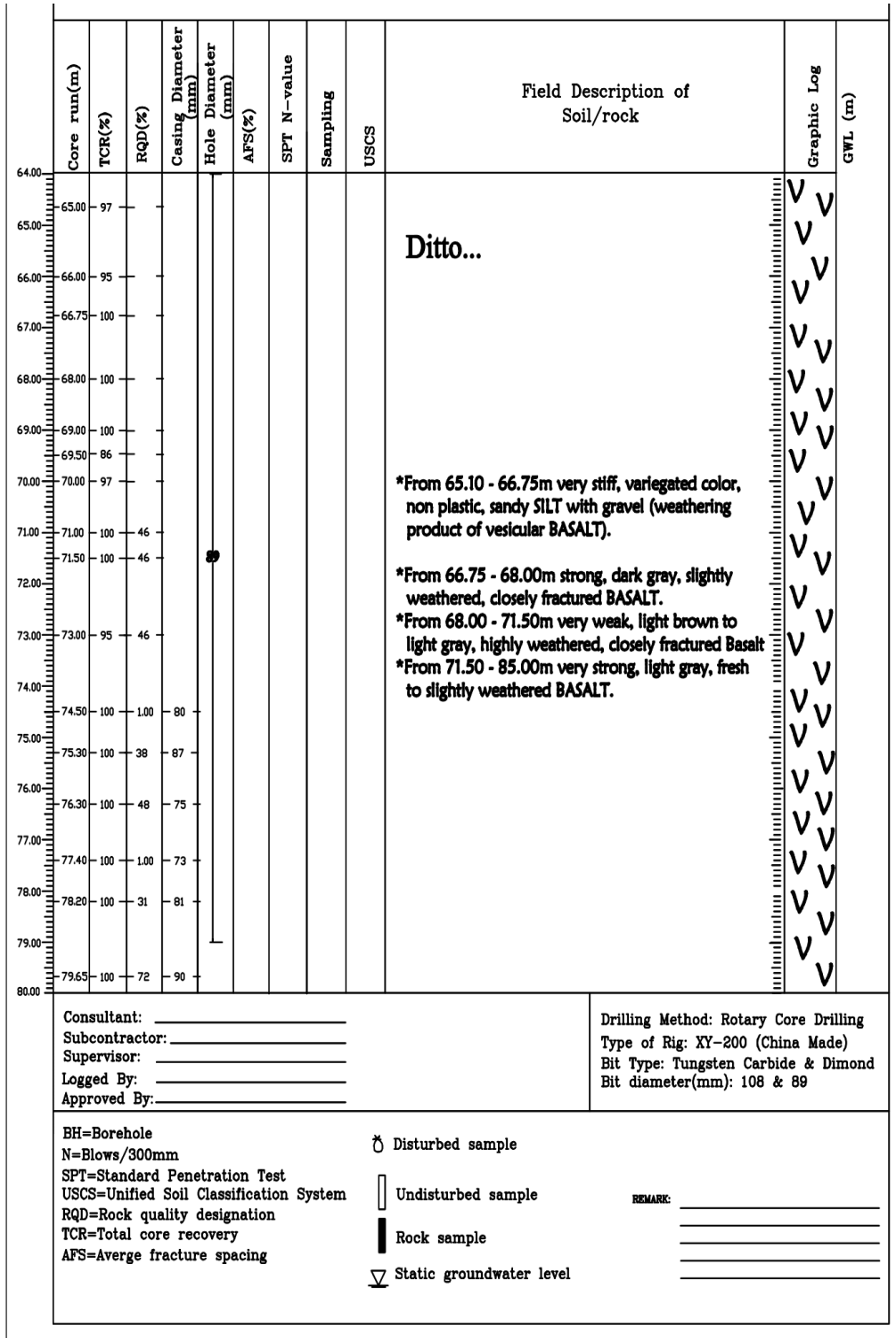
Site specific Ground Response Analysis at South - Western part of Addis Ababa

Core run(m)	TCR(%)	RQD(%)	Casing Diameter (mm)	Hole Diameter (mm)	AFS(%)	SPT N-value	Sampling	USCS	Field Description of Soil/rock	Graphic Log	GWL (m)
32.00	83	57					32.00		<p>Cont... Moderately strong to strong, dark gray , slightly to moderately weathered, very close to moderately fractured BASALT rock layer. *From 31.15 - 33.60 vesicular BASALT. *From 33.60 - 34.00 vesicular Basalt crushed in to sand but binded by clay.</p>		
33.00	85	36				32.50					
34.00	71	0									
35.00	75	0									
36.00	80	47									
37.00	85	54				32.00					
38.00	95	70				32.50					
39.00	100	60				32.00					
40.00	90	53				32.50					
41.00	88	18									
42.00											
43.00	90	57				32.00					
44.00	84	68				32.50					
45.00	58	47				32.00					
46.00	91	54				32.50					
47.00						32.00					
48.00	62	18				32.50					
Consultant: _____ Subcontractor: _____ Supervisor: _____ Logged By: _____ Approved By: _____									Drilling Method: Rotary Core Drilling Type of Rig: XY-200 (China Made) Bit Type: Tungsten Carbide & Dimond Bit diameter(mm): 108 & 89		
BH=Borehole N=Blows/300mm SPT=Standard Penetration Test USCS=Unified Soil Classification System RQD=Rock quality designation TCR=Total core recovery AFS=Average fracture spacing									REMARK: _____ _____ _____		
									○ Disturbed sample □ Undisturbed sample ■ Rock sample ▽ Static groundwater level		

Site specific Ground Response Analysis at South - Western part of Addis Ababa



Site specific Ground Response Analysis at South - Western part of Addis Ababa



Site specific Ground Response Analysis at South - Western part of Addis Ababa

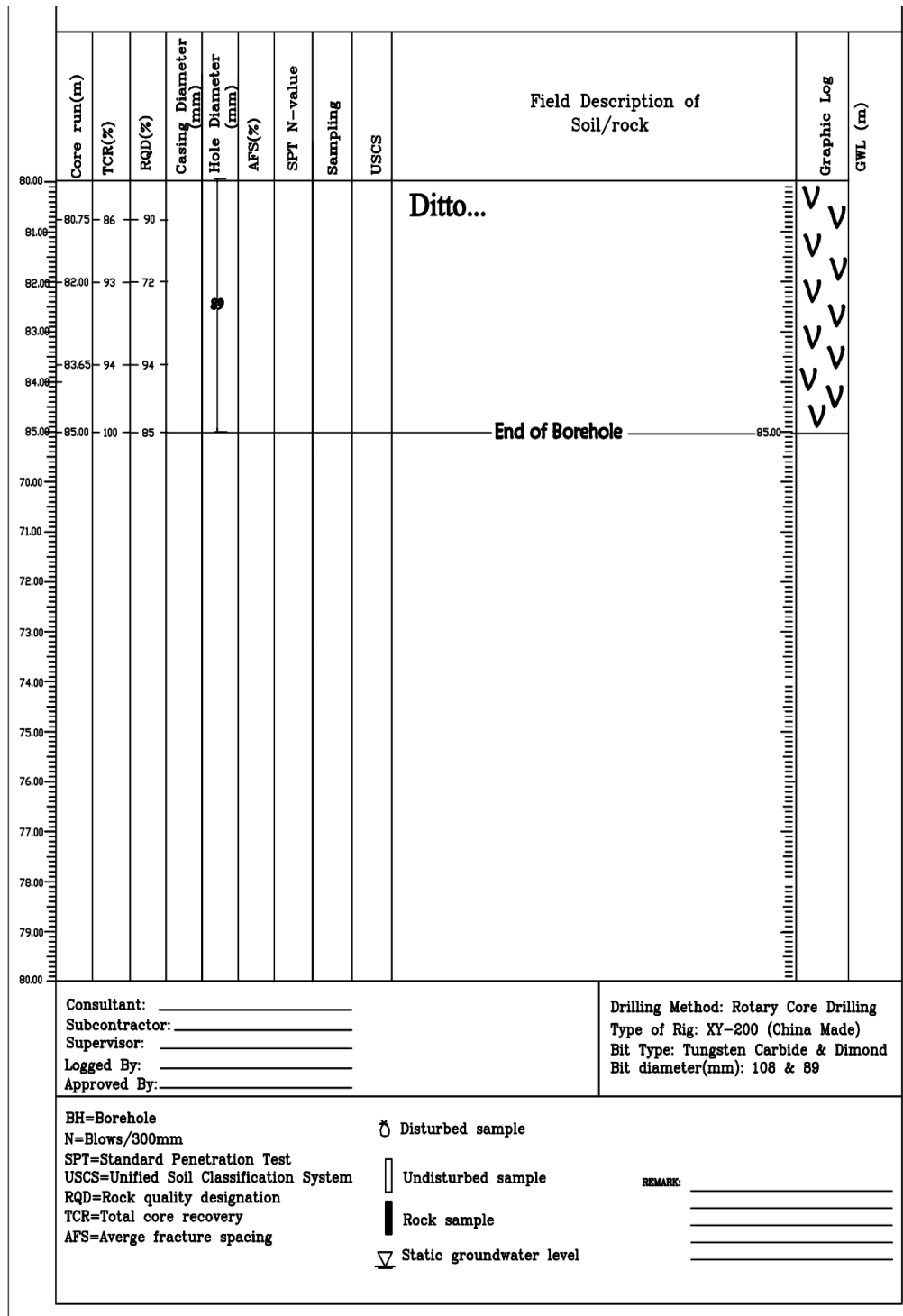
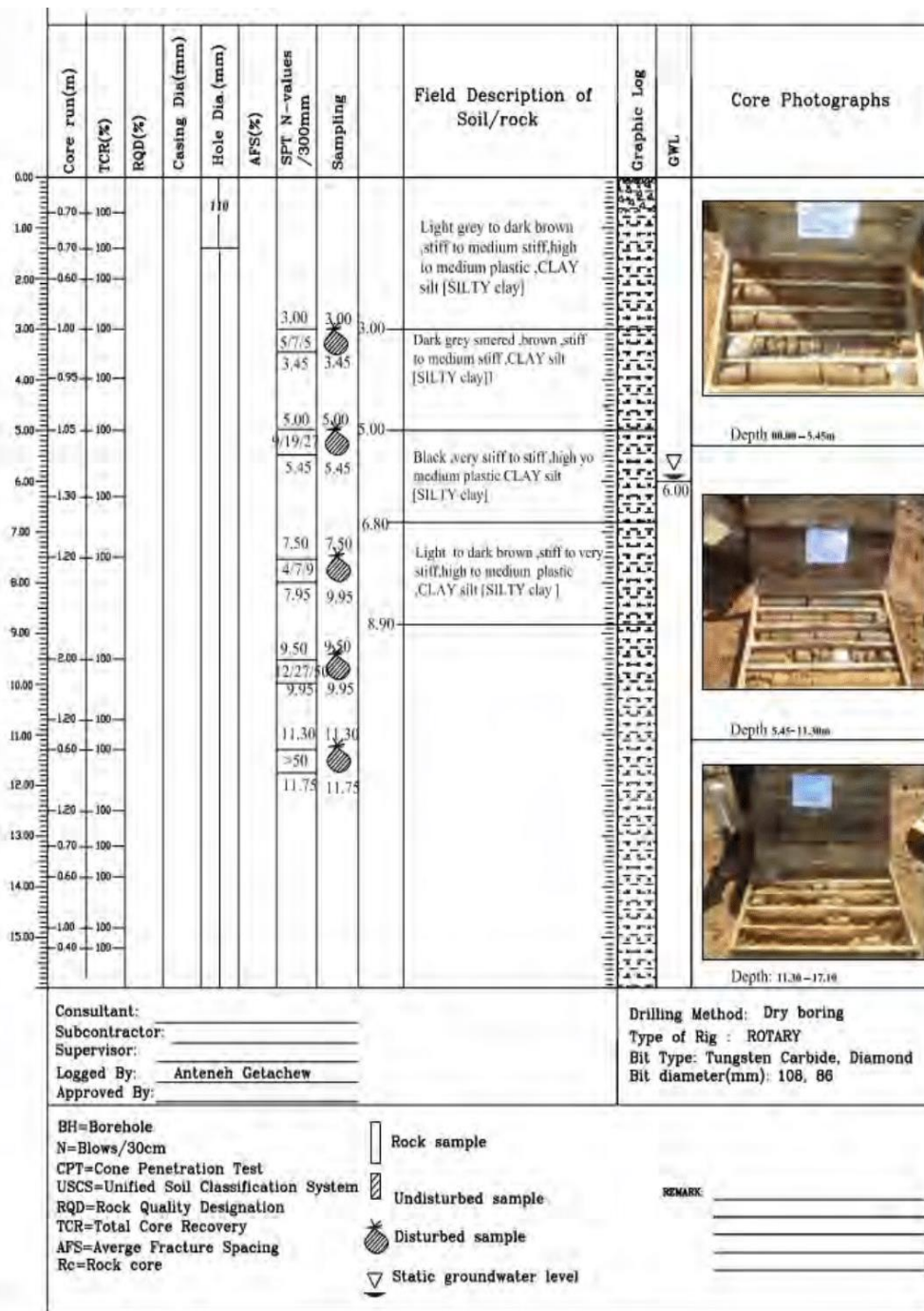
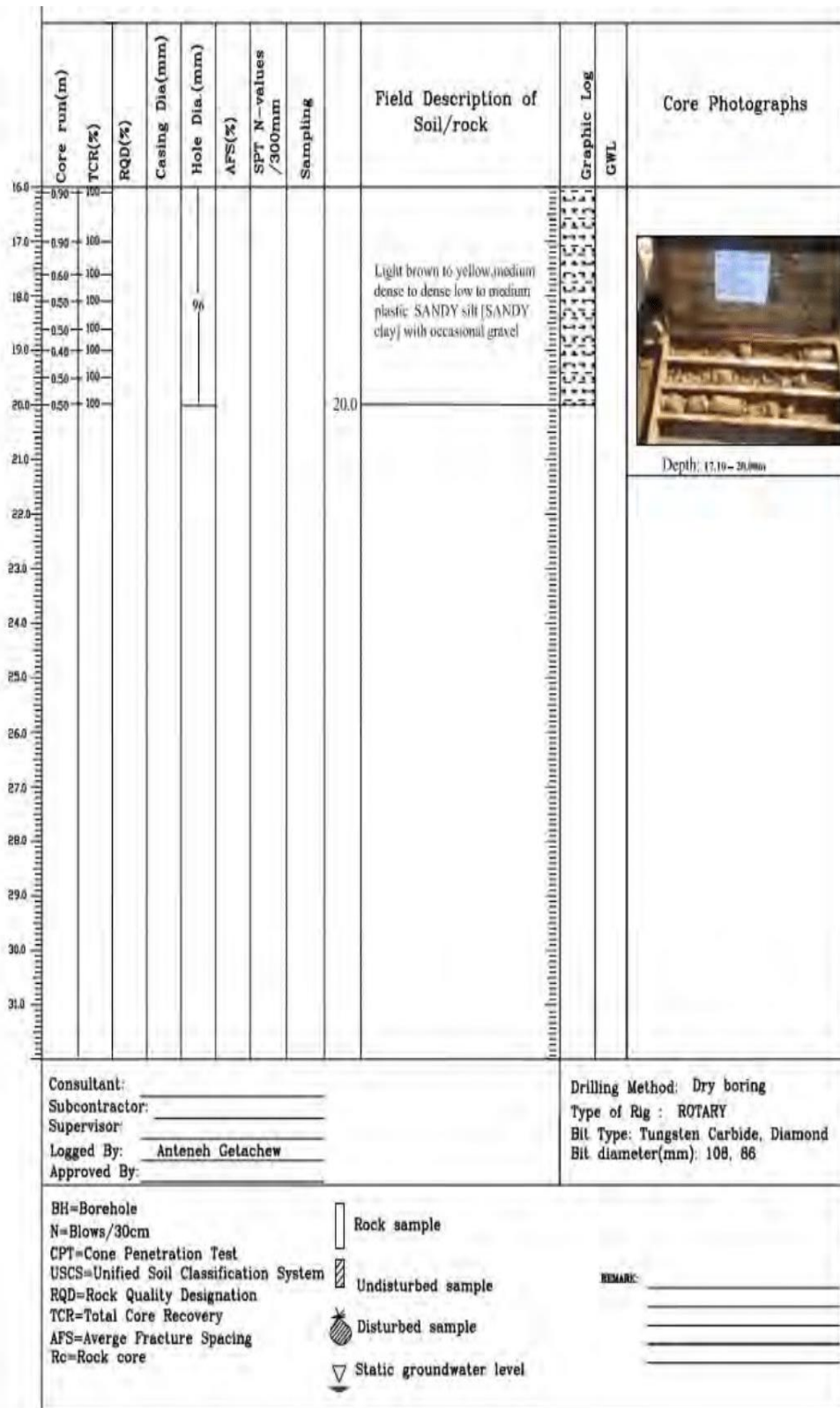


Figure C- 2:Kirkos borehole logs

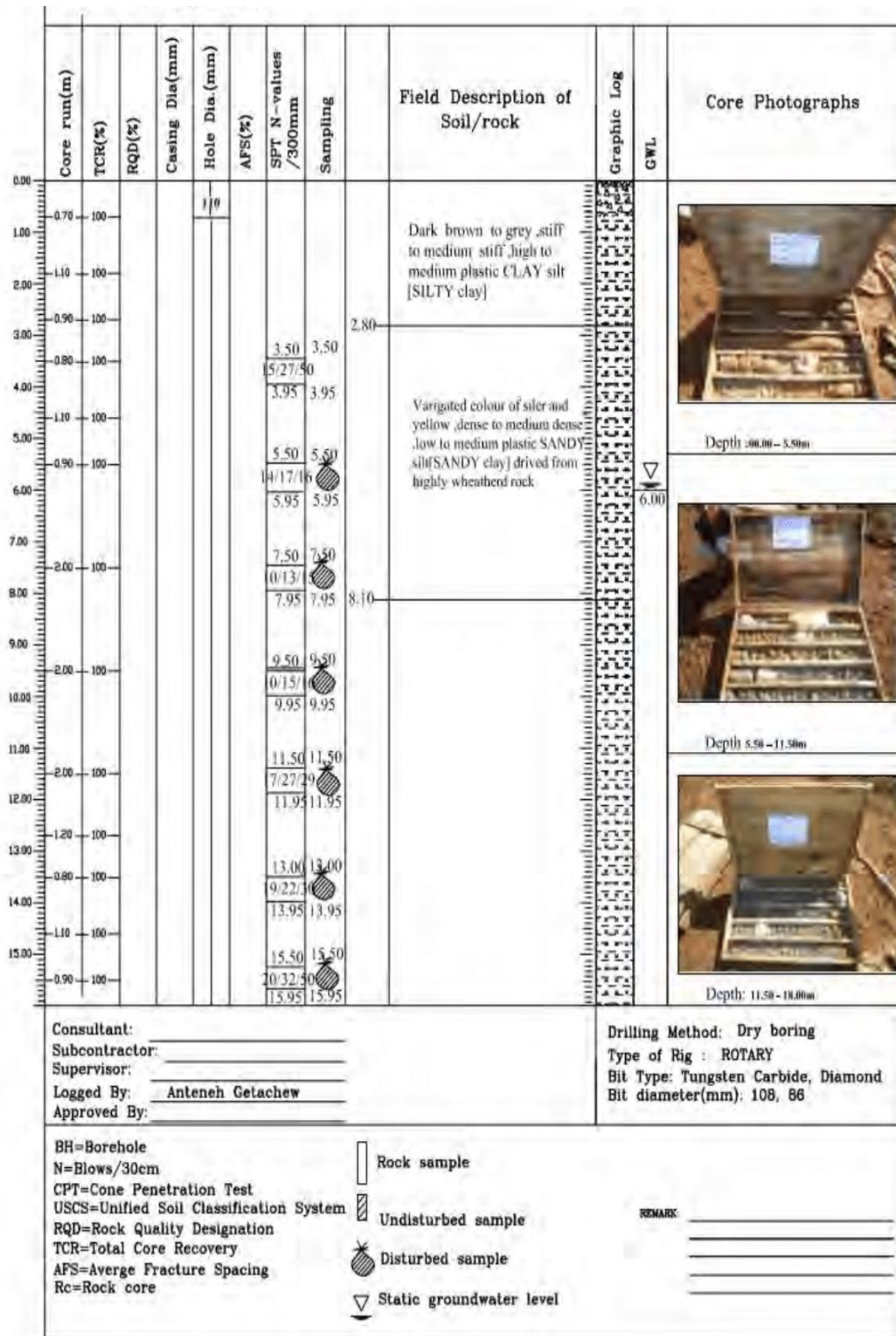
c. Kolfe keranyo



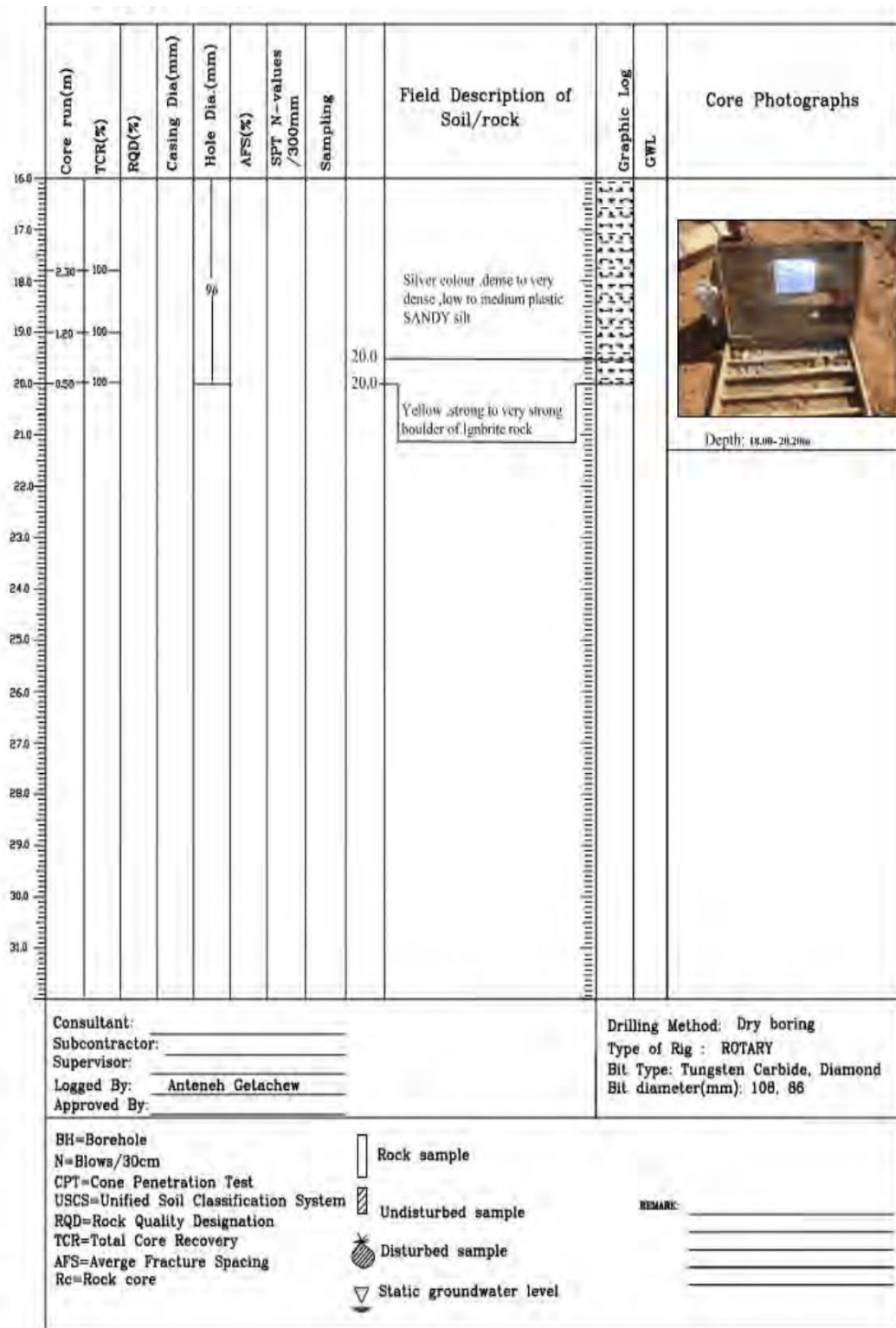
Site specific Ground Response Analysis at South - Western part of Addis Ababa



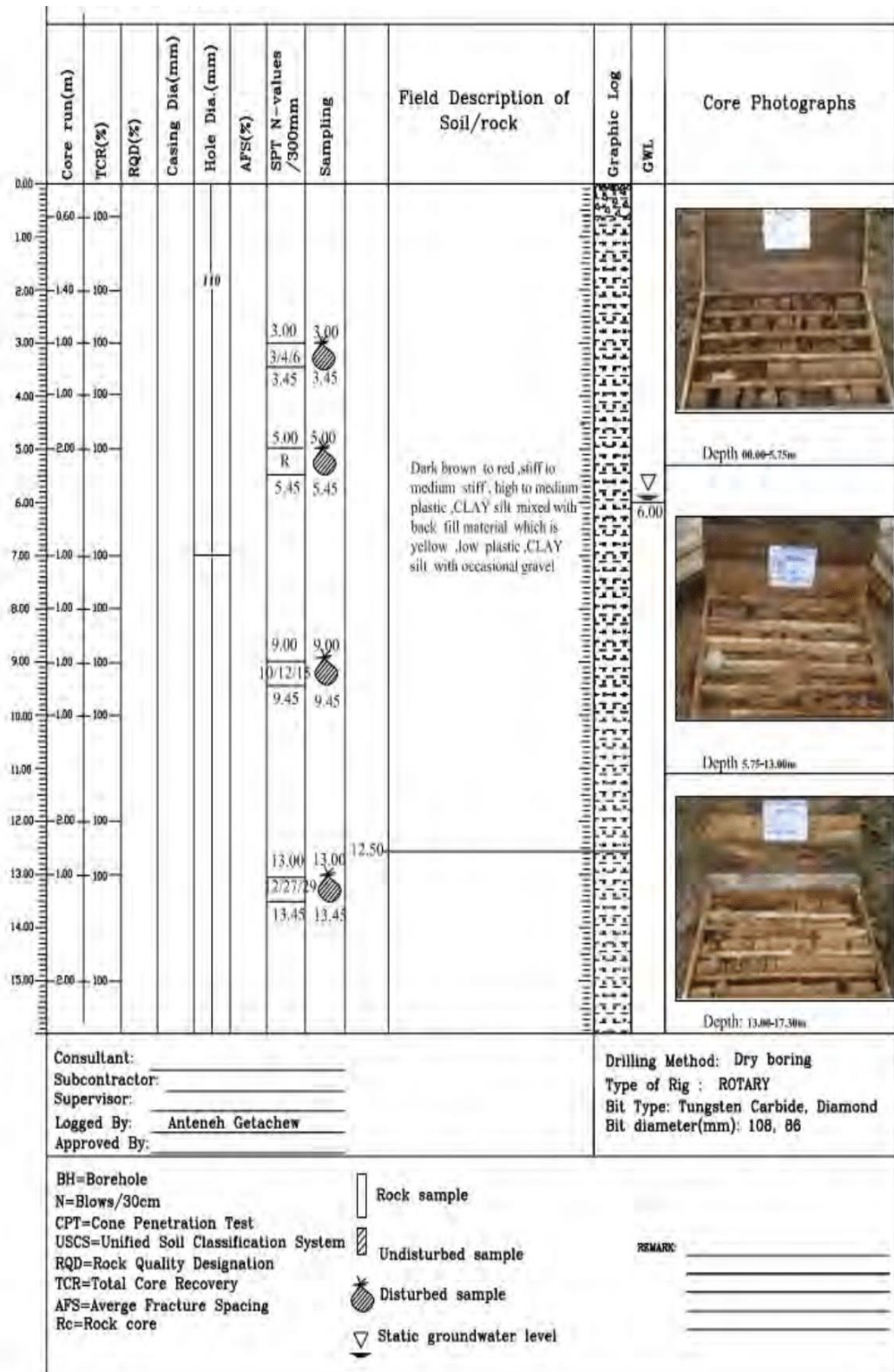
Site specific Ground Response Analysis at South - Western part of Addis Ababa



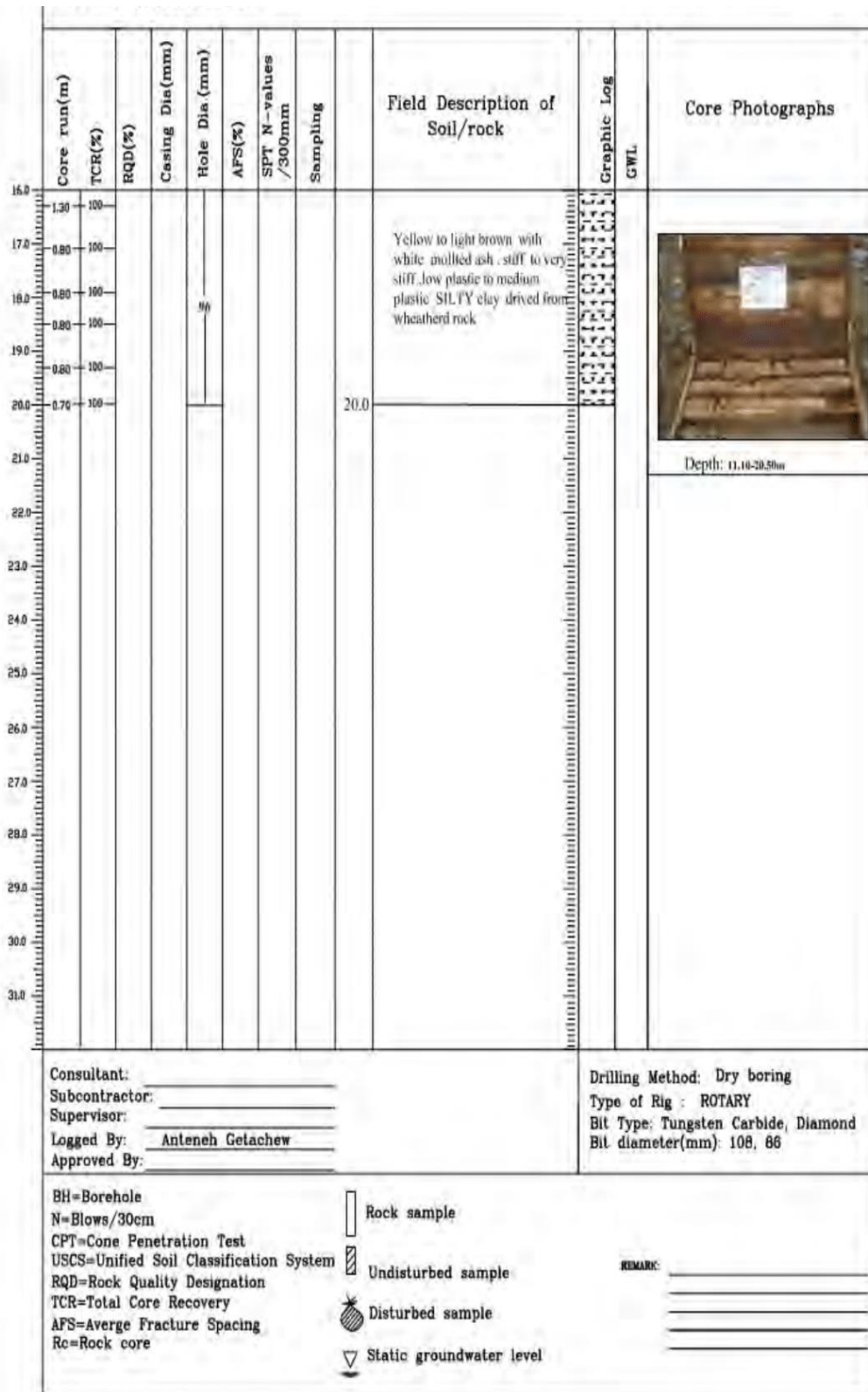
Site specific Ground Response Analysis at South - Western part of Addis Ababa



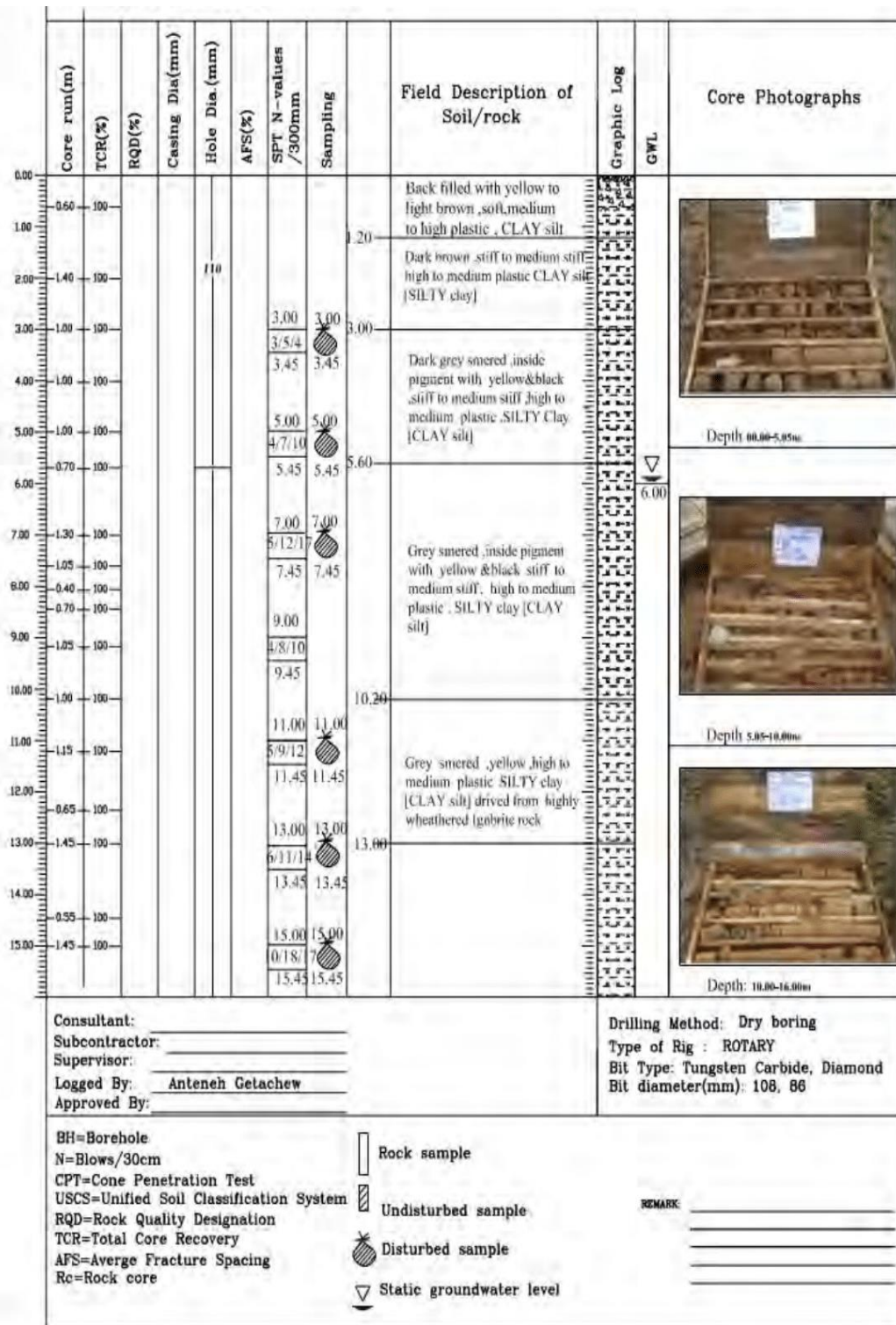
Site specific Ground Response Analysis at South - Western part of Addis Ababa



Site specific Ground Response Analysis at South - Western part of Addis Ababa



Site specific Ground Response Analysis at South - Western part of Addis Ababa



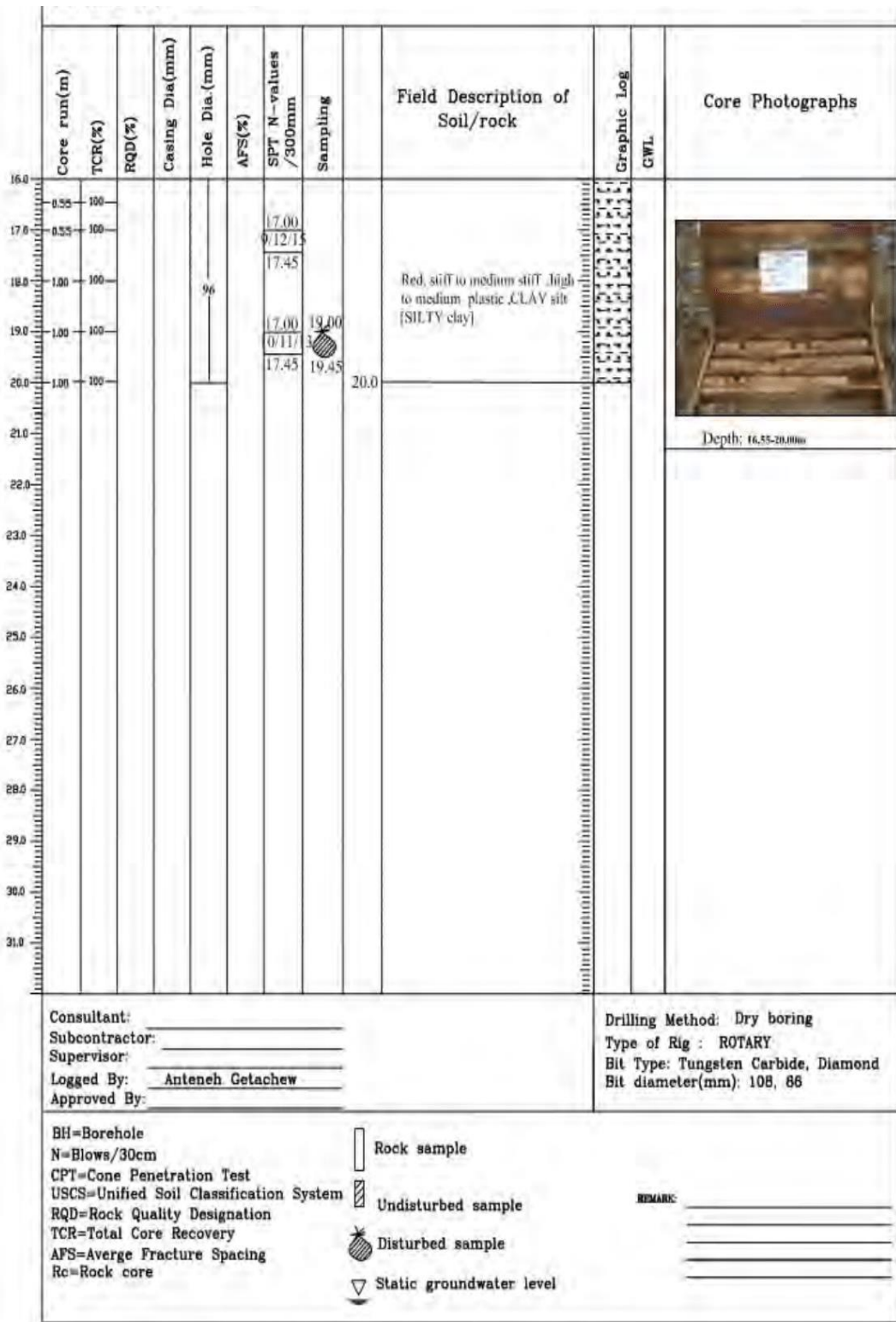
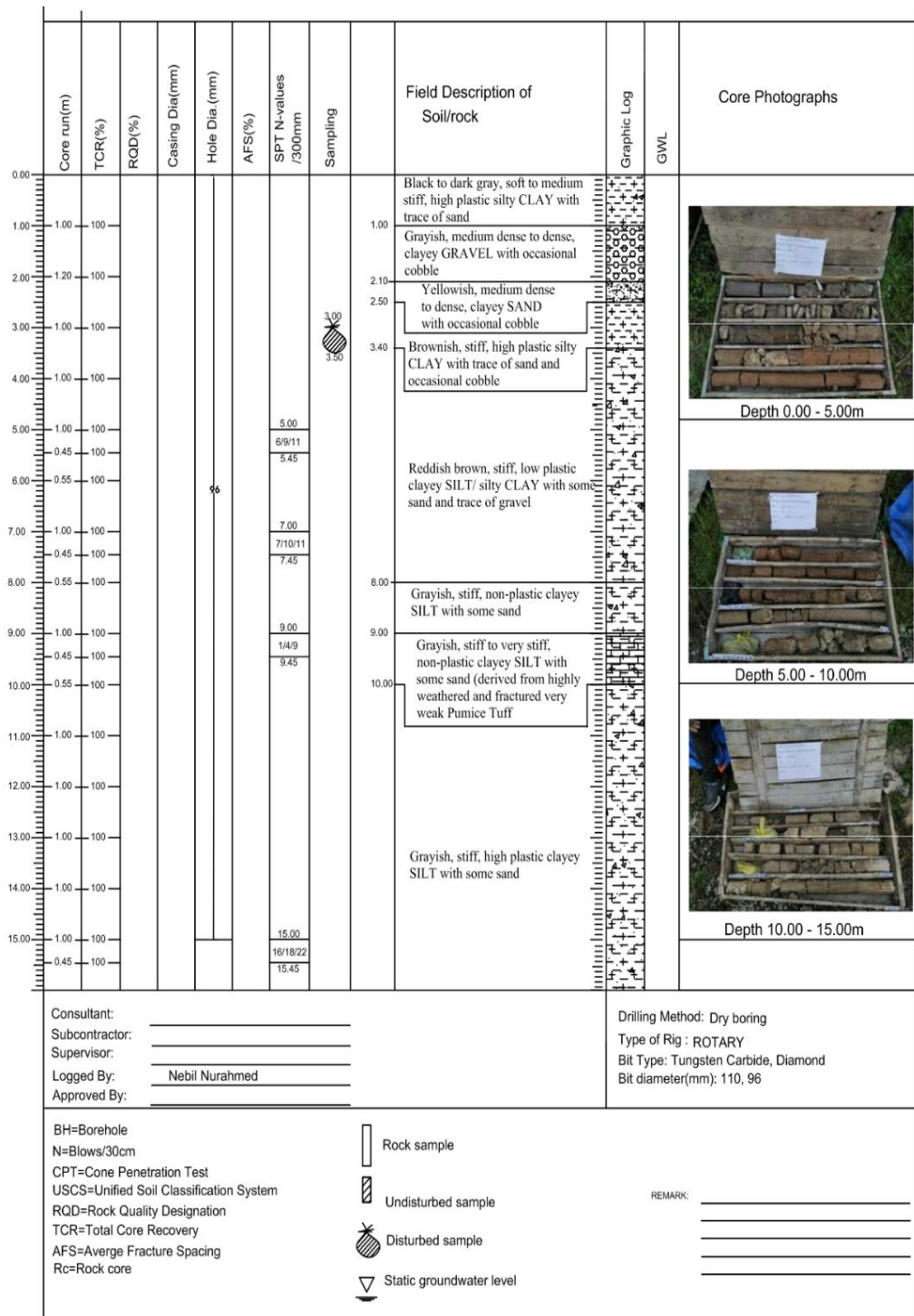


Figure C- 3:Kolfe keranyo borehole logs

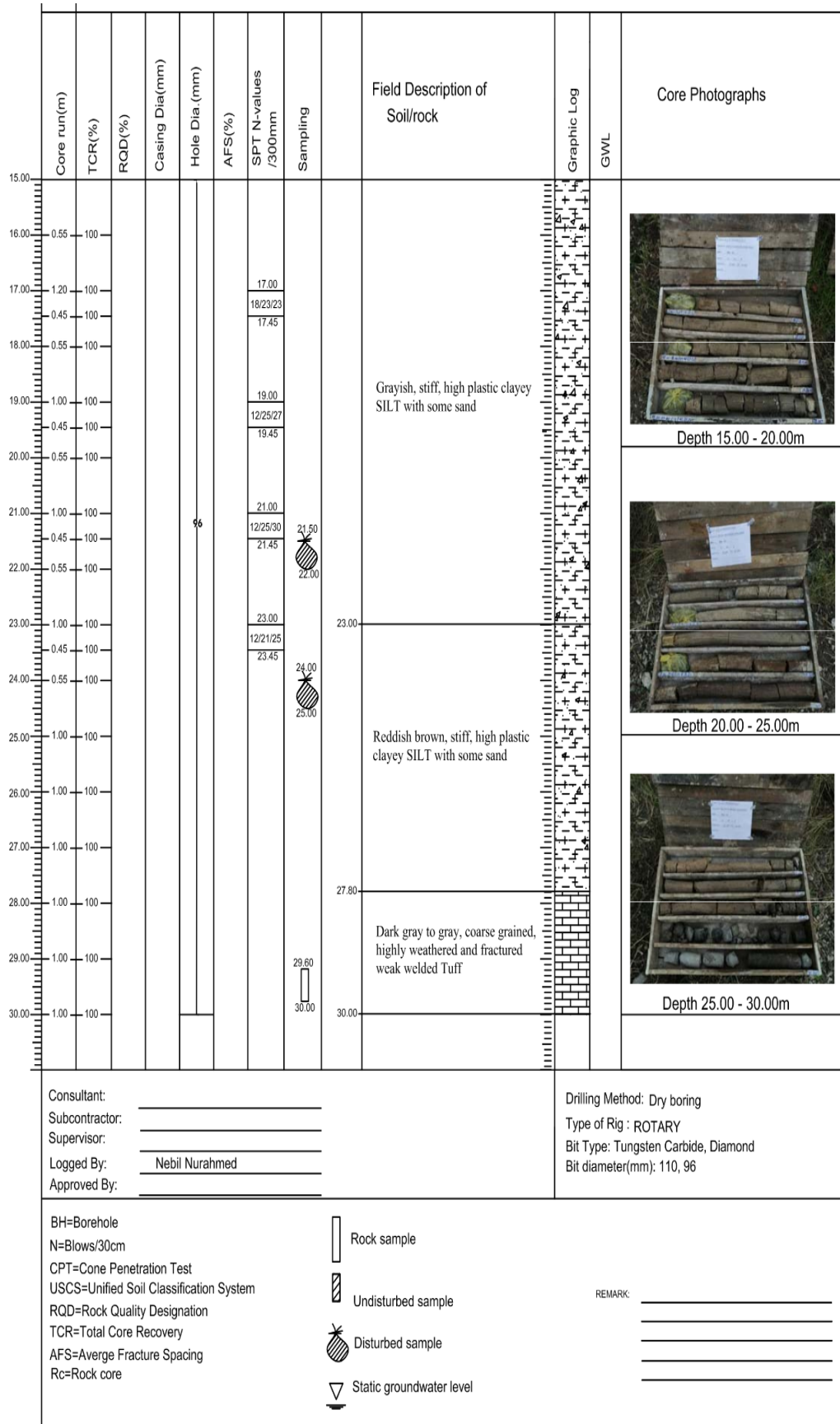
d. Lafto-1

Depth (cm)	Hole Diameter (mm)	Sample Record	SPT/DPT N_value	Legend	Strata Description	Run Length Depth (m)	TCR (%)	RQD (%)	Remark
0	108				Stiff, dark gray, Silty CLAY (Blackcotton soil), with some backfill materials at the top.	0.5	100		
1						1	100		
2						1.6	100		
3		DS	7			2	100		
4						2.45	100		
5						3	100		
6	DS	10	4	100					
7			4.45	100					
8			5.1	100					
9	DS	17	6	100					
10			6.45	100	Soft, light gray to white, Clayey SILT ASH/TUFF.	6.8	100		
11			6.8	100		7.5	100		
12			7.5	100		8	100		
13			8.45	100		8.45	100		
14			9	100		9	100		
15			9.5	100		9.5	100		
16	DS	24	10	100					
17			10.45	100					
18			11	100					
19			11.5	100					
20			12	100					
21			12.45	100					
22			13.5	100					
23	DS	41	14	100					
24			14.45	100					
25			15	100					
26			16	100					
27			16.45	100					
28			17	100					
29			17.6	100					
30			18	100					
31			18.45	100					
32			19	100					
33			19.6	100					
34			20.5	100					
35			21	100					
36			22	100					
37			22.45	100					
38			22.5	100					
39			23	100					
40			23.3	100					
41			24	100					
42			24	100					
43			25	100					
44			25.5	100					
45			26	100					
46			26.4	100					
47			27	100					
48			27.5	100					
49			28	100					
50			28	100					
51			29	100					
52			29	100					
53			30	100					
54			30	100					
55									
56									
57									
58									
59									
60									
61									
62									
63									
64									
65									
66									
67									
68									
69									
70									
71									
72									
73									
74									
75									
76									
77									
78									
79									
80									
81									
82									
83									
84									
85									
86									
87									
88									
89									
90									
91									
92									
93									
94									
95									
96									
97									
98									
99									
100									
101									
102									
103									
104									
105									
106									
107									
108									
109									
110									
111									
112									
113									
114									
115									
116									
117									
118									
119									
120									
121									
122									
123									
124									
125									
126									
127									
128									
129									
130									
131									
132									
133									
134									
135									
136									
137									
138									
139									
140									
141									
142									
143									
144									
145									
146									
147									
148									
149									
150									
151									
152									
153									
154									
155									
156									
157									
158									
159									
160									
161									
162									
163									
164									
165									
166									
167									
168									
169									
170									
171									
172									
173									
174									
175									
176									
177									
178									
179									
180									
181									
182									
183									
184									
185									
186									
187									
188									
189									
190									
191									
192									
193									
194									
195									
196									
197									
198									
199									
200									
201									
202									
203									
204									
205									
206									
207									
208									
209									
210									
211									
212									
213									
214									
215									
216									
217									
218									
219									
220									
221									
222									
223									
224									
225									
226									
227									
228									
229									
230									
231									
232									
233									
234									
235									
236									
237									
238									
239									
240									
241									
242									
243									
244									
245									
246									
247									
248									
249									
250									
251									
252									

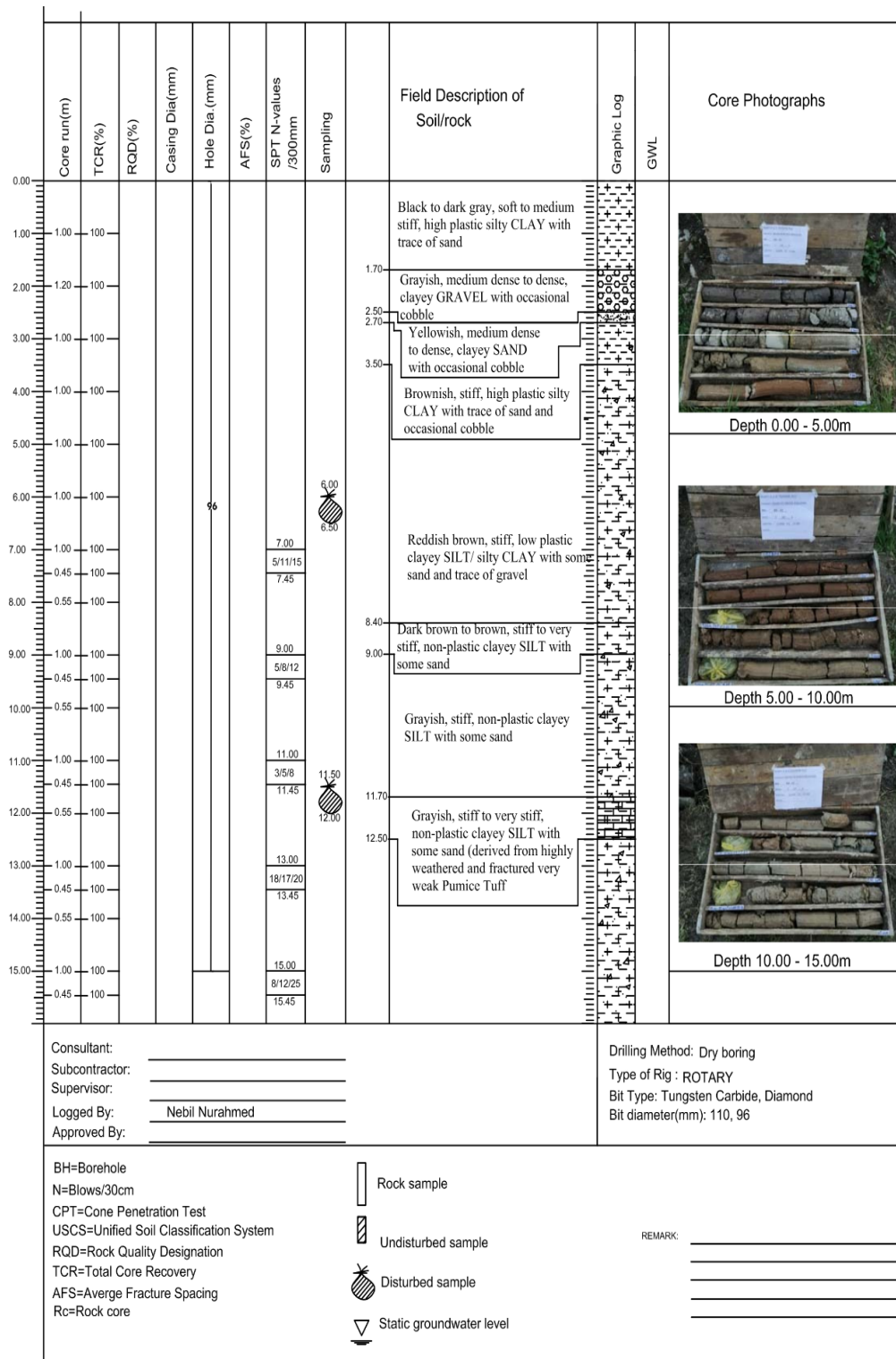
e. Lafto-2






Site specific Ground Response Analysis at South - Western part of Addis Ababa



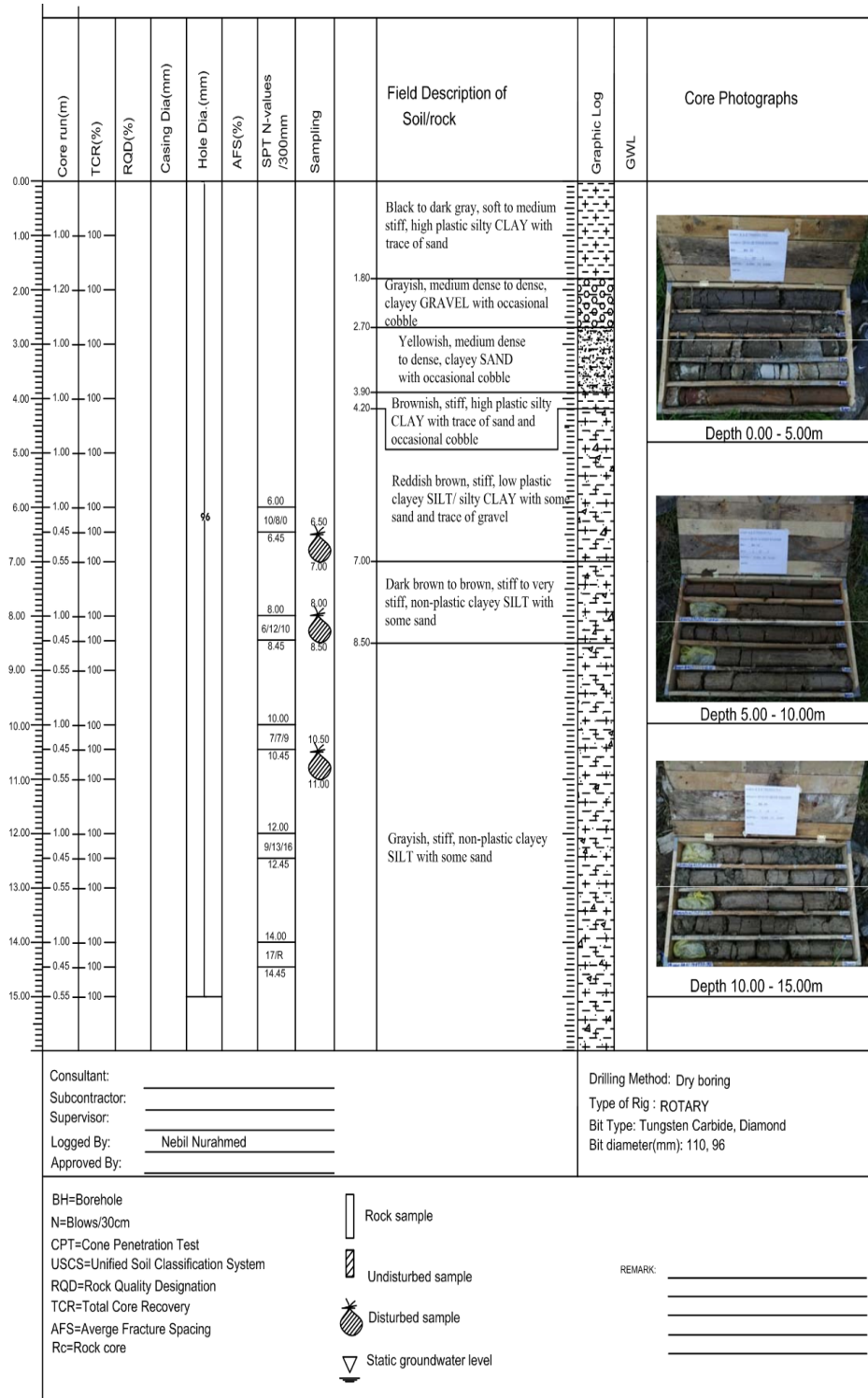
Site specific Ground Response Analysis at South - Western part of Addis Ababa



Site specific Ground Response Analysis at South - Western part of Addis Ababa

Core run(m)	TCR(%)	RQD(%)	Casing Dia(mm)	Hole Dia. (mm)	AFS(%)	SPT N-values /300mm	Sampling	Field Description of Soil/rock	Graphic Log	GWL	Core Photographs
15.00											
16.00	1.00	100						Grayish, stiff, high plastic clayey SILT with some sand			 <p style="text-align: center;">Depth 15.00 - 20.00m</p>
17.00	1.00	100				17.00 5/7/12 17.45					
18.00	0.45	100						Red to Reddish brown, stiff to very stiff, non-plastic clayey SILT with trace of sand			 <p style="text-align: center;">Depth 20.00 - 25.00m</p>
19.00	1.00	100				19.00 10/12/18 19.45					
20.00	0.55	100						Variegated color(yellowish), highly weathered and fractured very weak Pumice Tuff			 <p style="text-align: center;">Depth 25.00 - 30.00m</p>
21.00	1.00	100		96		21.00 19/19/18 21.45					
22.00	0.45	100						Dark gray to gray, coarse grained, highly weathered and fractured weak welded Tuff			
23.00	1.00	100				22.00 22.50 23.00 12/23/26 23.45 23.50 24.00					
24.00	0.55	100									
25.00	1.00	100									
26.00	0.45	100									
27.00	1.00	100									
28.00	0.55	100									
29.00	1.00	100									
30.00	0.45	100									
Consultant: _____ Subcontractor: _____ Supervisor: _____ Logged By: <u>Nebil Nurahmed</u> Approved By: _____										Drilling Method: Dry boring Type of Rig : ROTARY Bit Type: Tungsten Carbide, Diamond Bit diameter(mm): 110, 96	
BH=Borehole N=Blows/30cm CPT=Cone Penetration Test USCS=Unified Soil Classification System RQD=Rock Quality Designation TCR=Total Core Recovery AFS=Average Fracture Spacing Rc=Rock core										REMARK: _____ _____ _____	
Rock sample Undisturbed sample Disturbed sample Static groundwater level											

Site specific Ground Response Analysis at South - Western part of Addis Ababa



Site specific Ground Response Analysis at South - Western part of Addis Ababa

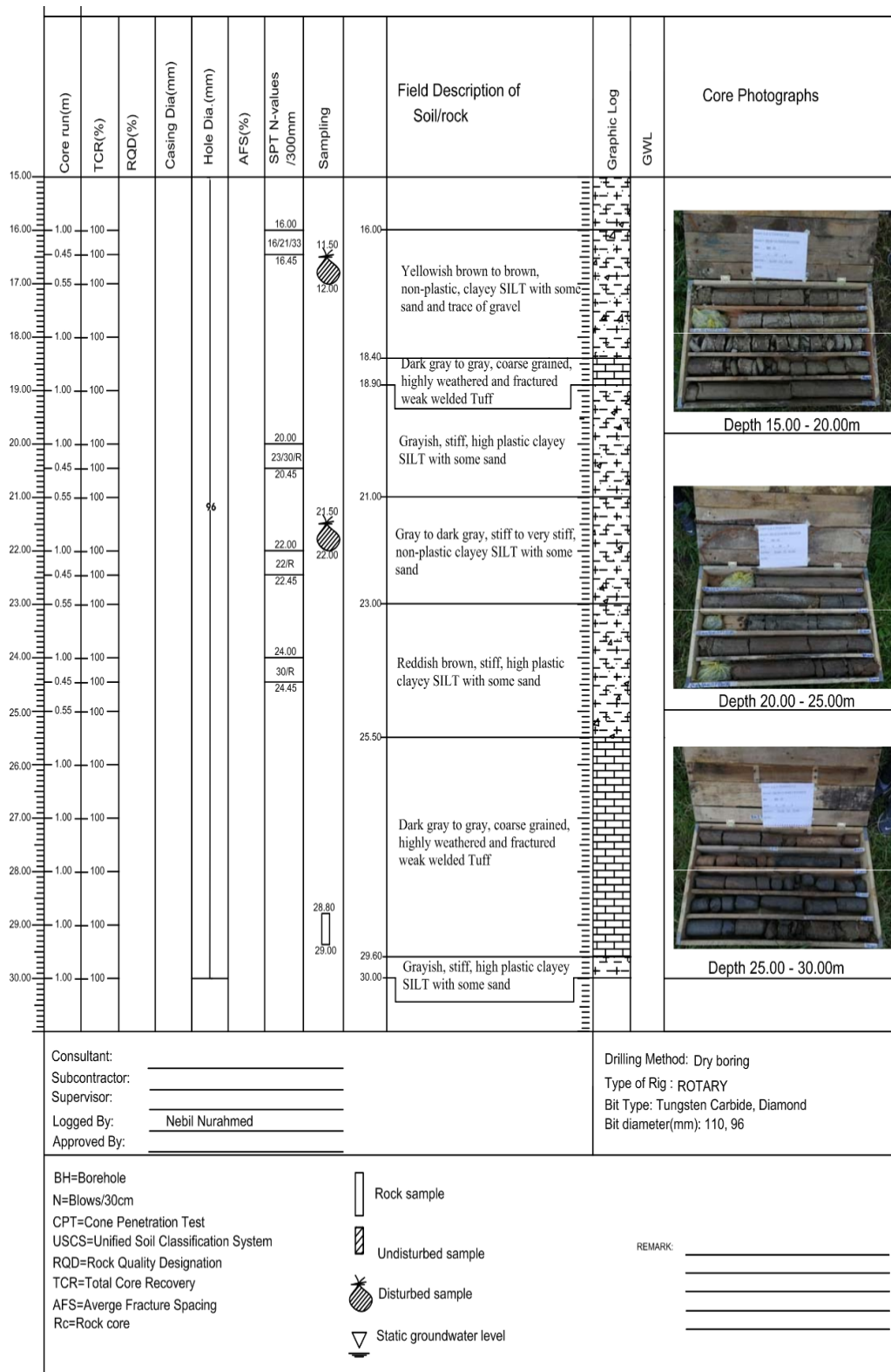
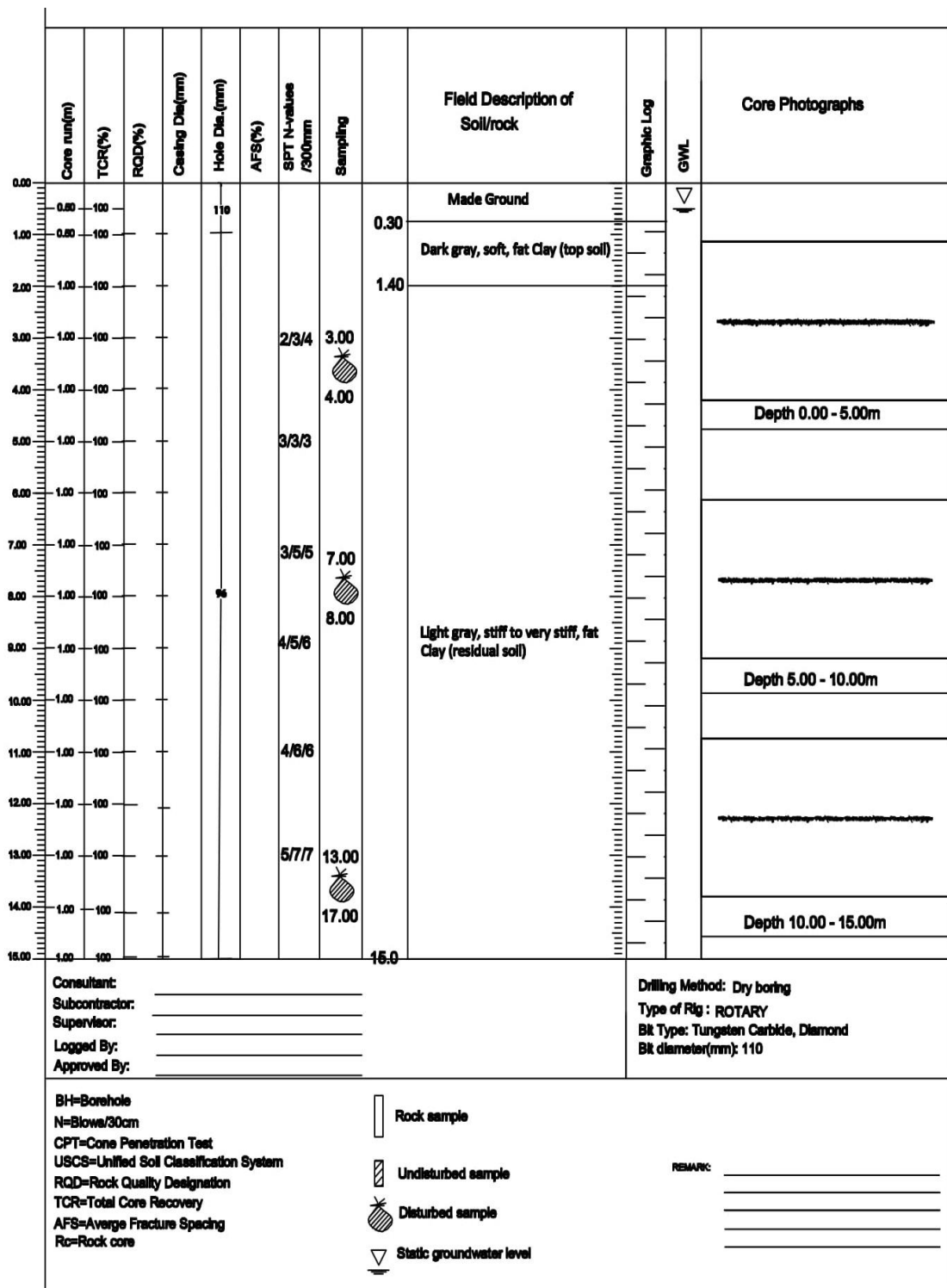


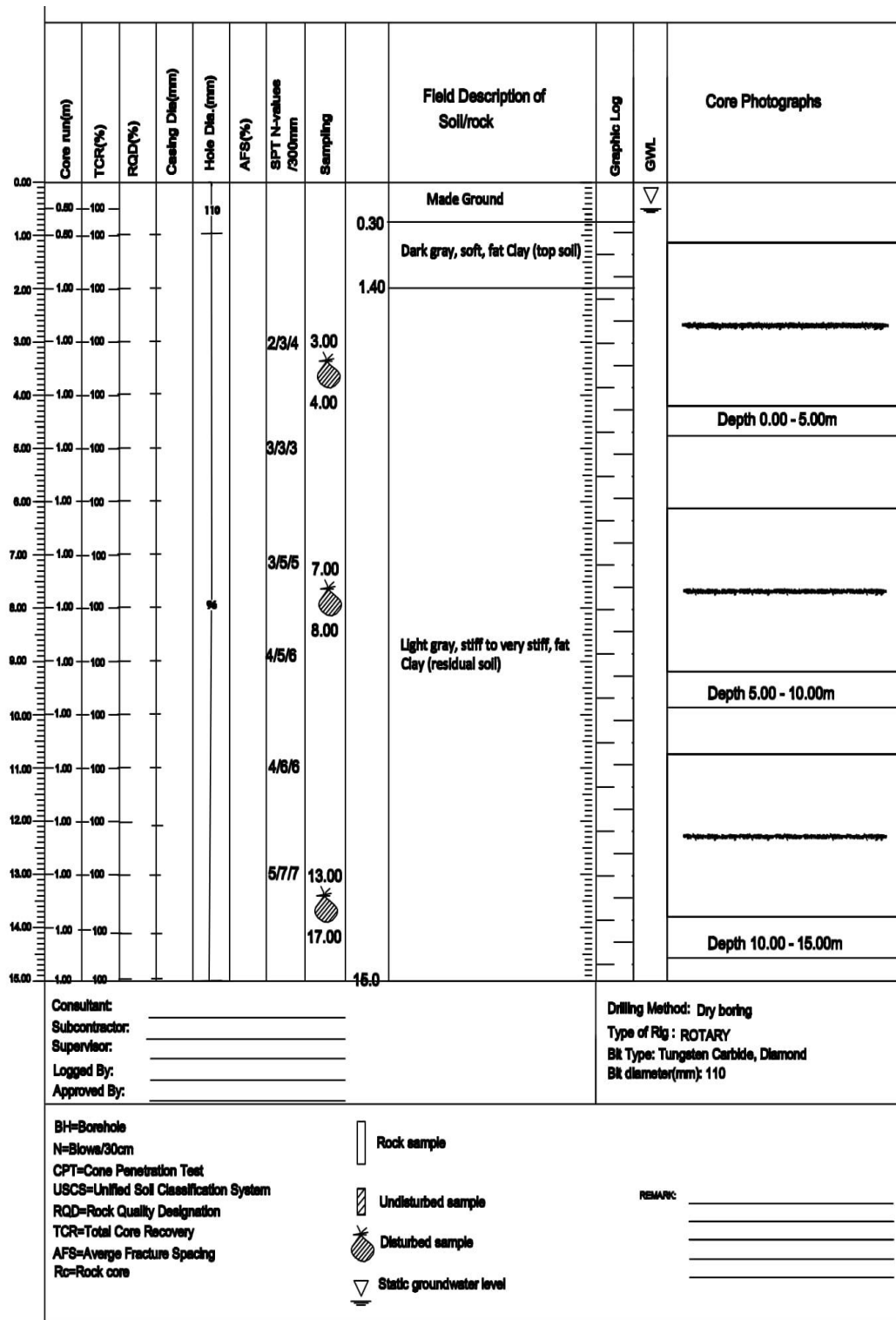
Figure C- 5: Lafto-2 borehole logs

f. Lafto-3



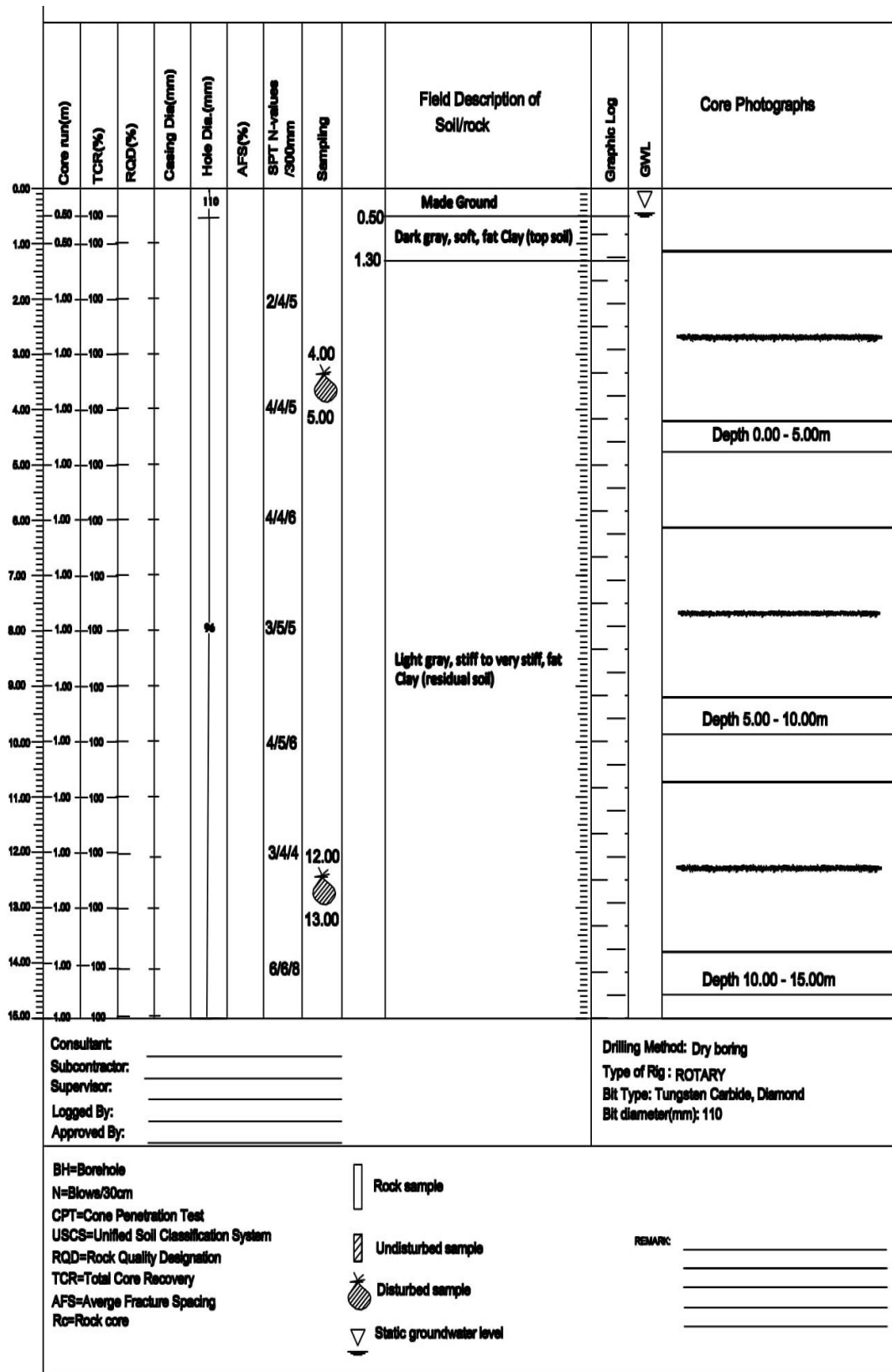
PLEASE MAKE SURE THIS IS THE CORRECT ISSUE BEFORE USE

Site specific Ground Response Analysis at South - Western part of Addis Ababa



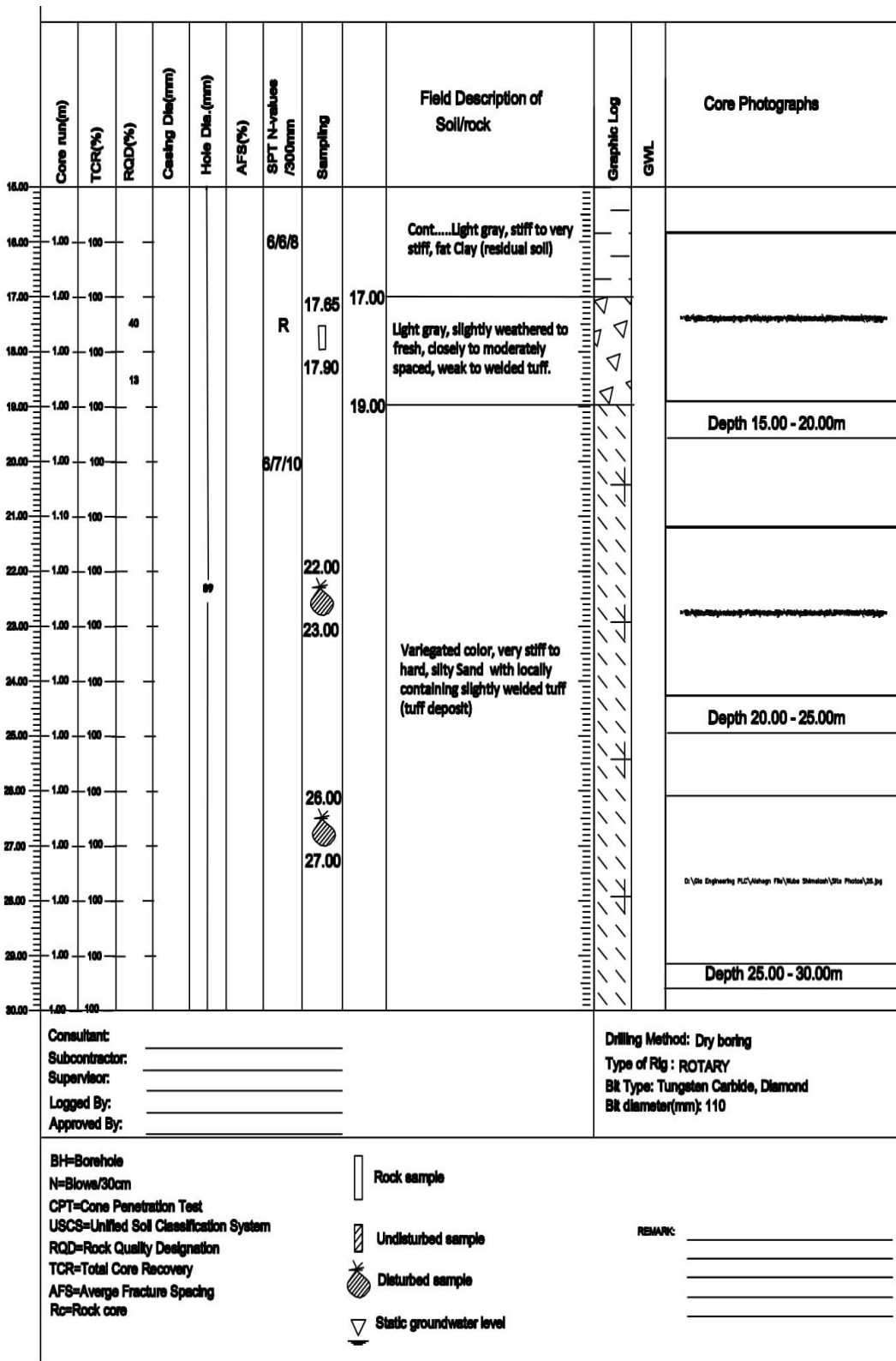
PLEASE MAKE SURE THIS IS THE CORRECT ISSUE BEFORE USE

Site specific Ground Response Analysis at South - Western part of Addis Ababa



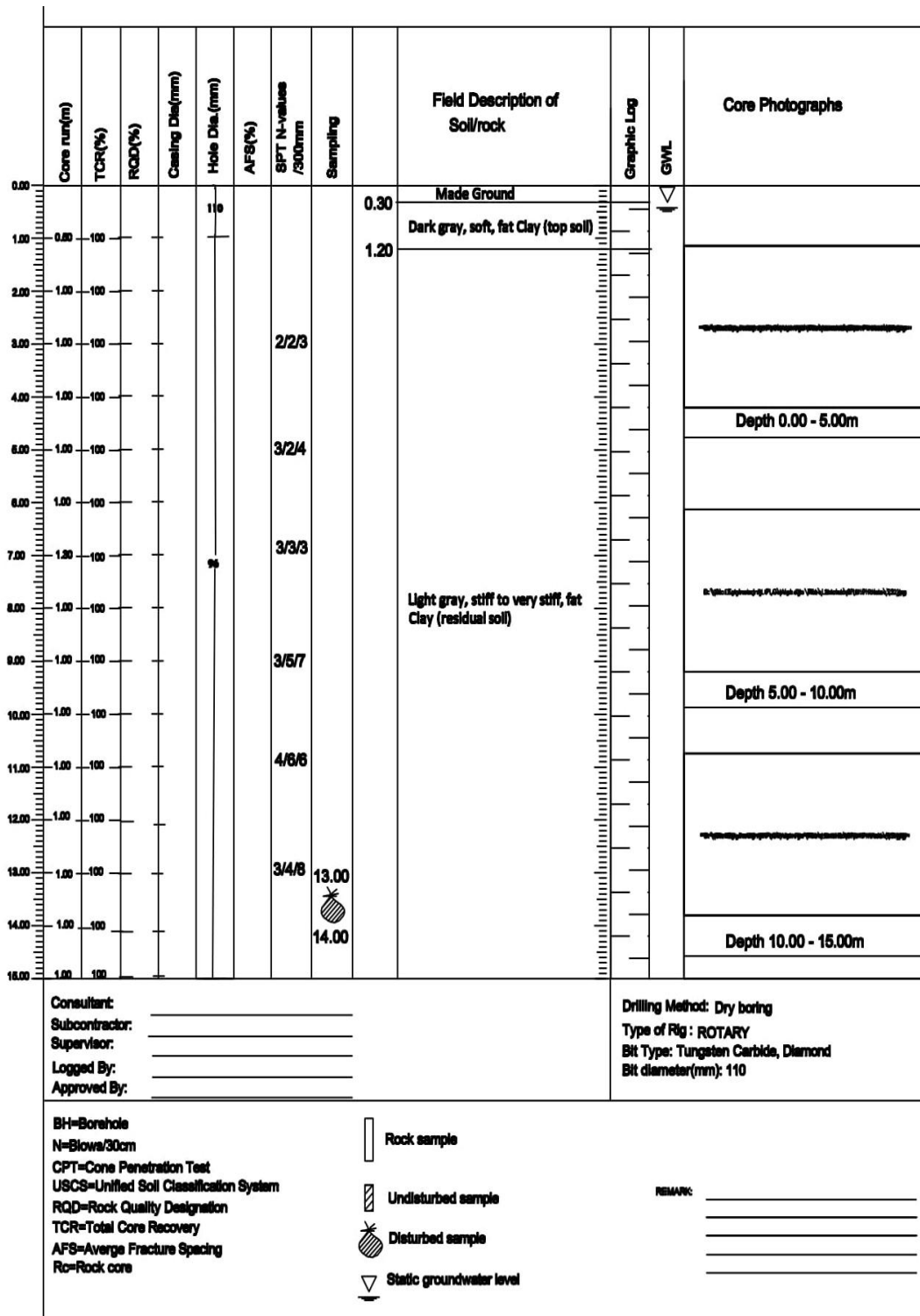
PLEASE MAKE SURE THIS IS THE CORRECT ISSUE BEFORE USE

Site specific Ground Response Analysis at South - Western part of Addis Ababa

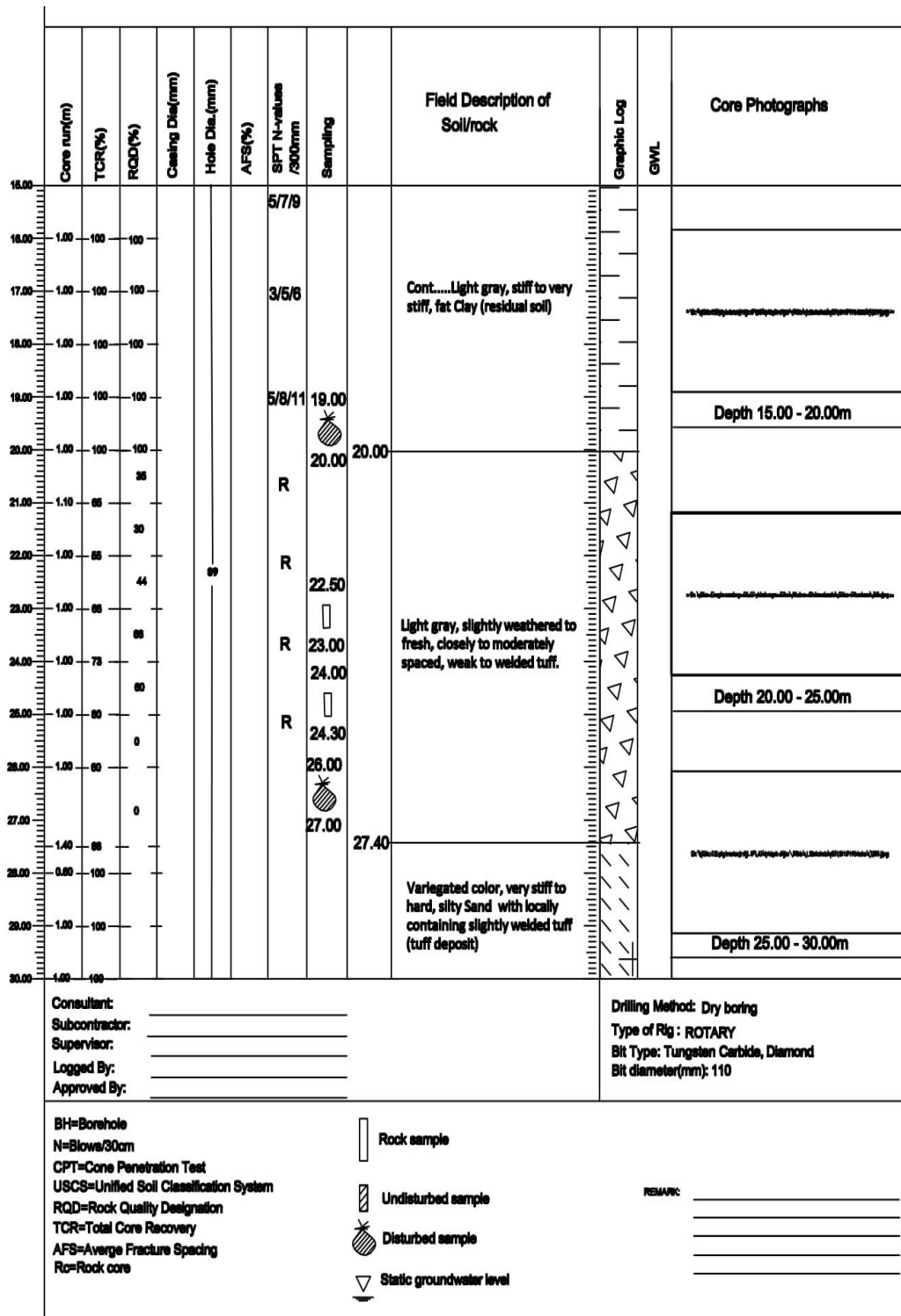


PLEASE MAKE SURE THIS IS THE CORRECT ISSUE BEFORE USE

Site specific Ground Response Analysis at South - Western part of Addis Ababa



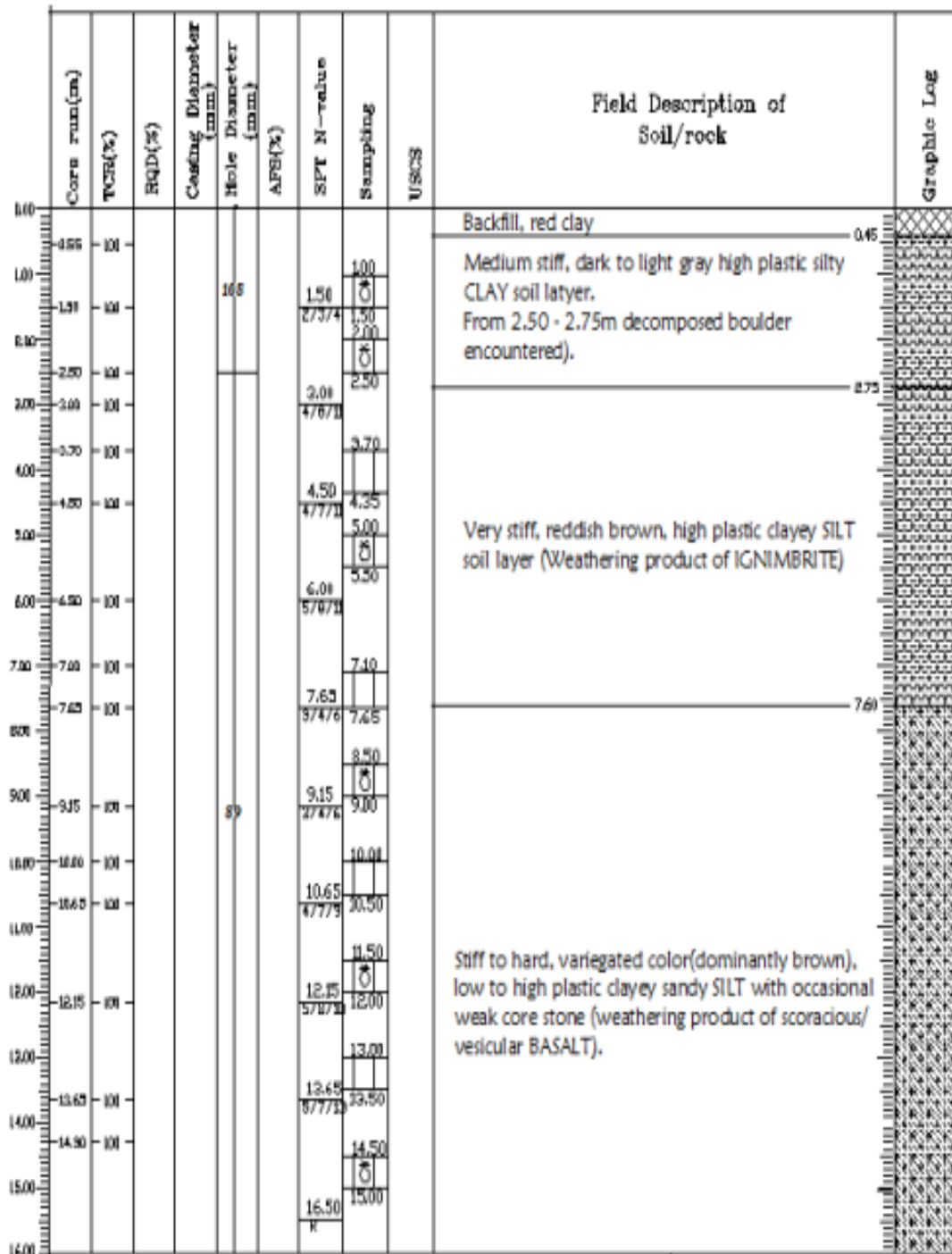
PLEASE MAKE SURE THIS IS THE CORRECT ISSUE BEFORE USE



PLEASE MAKE SURE THIS IS THE CORRECT ISSUE BEFORE USE

Figure C- 6: Lafto-3 borehole logs

g. Lideta-1



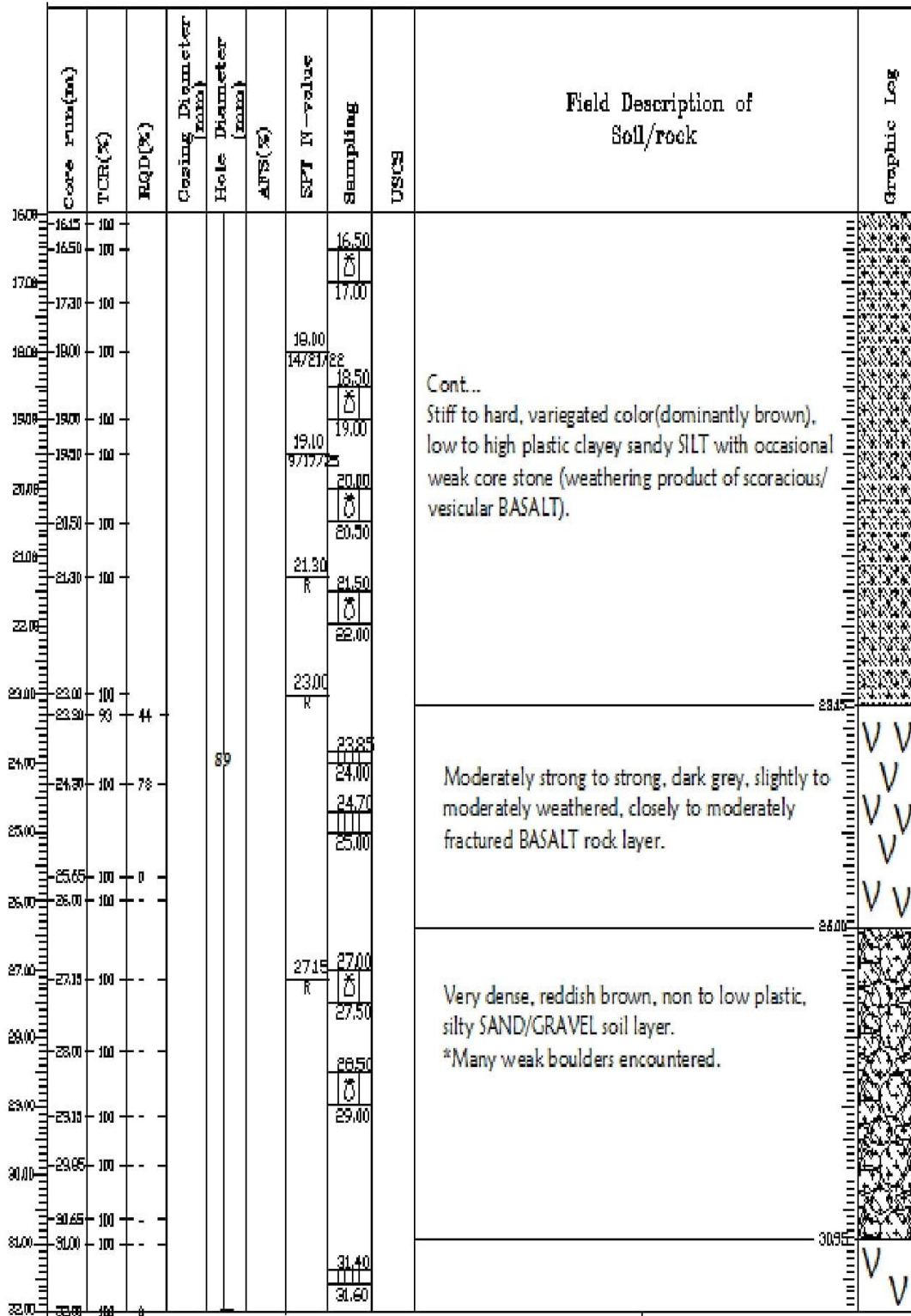
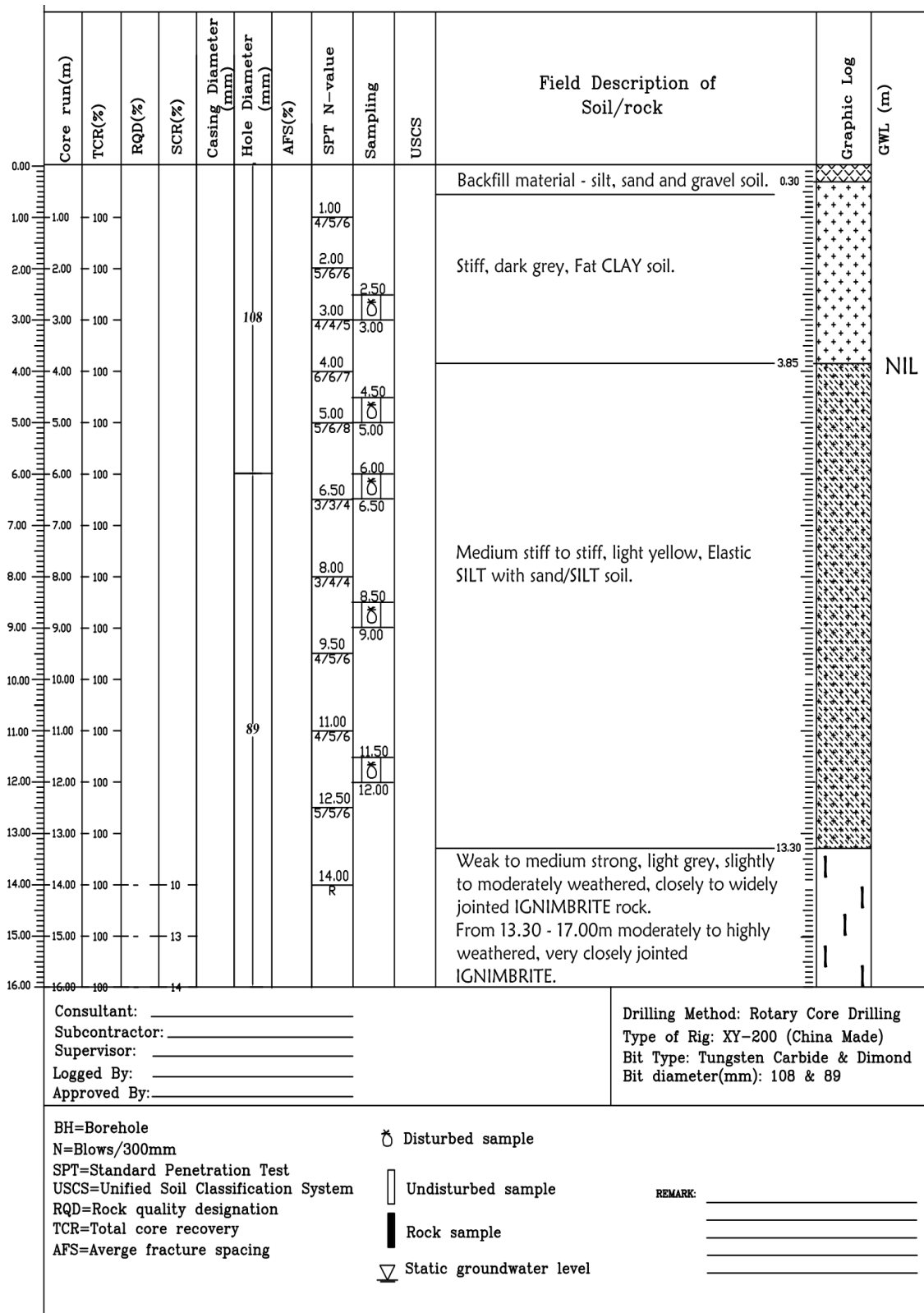
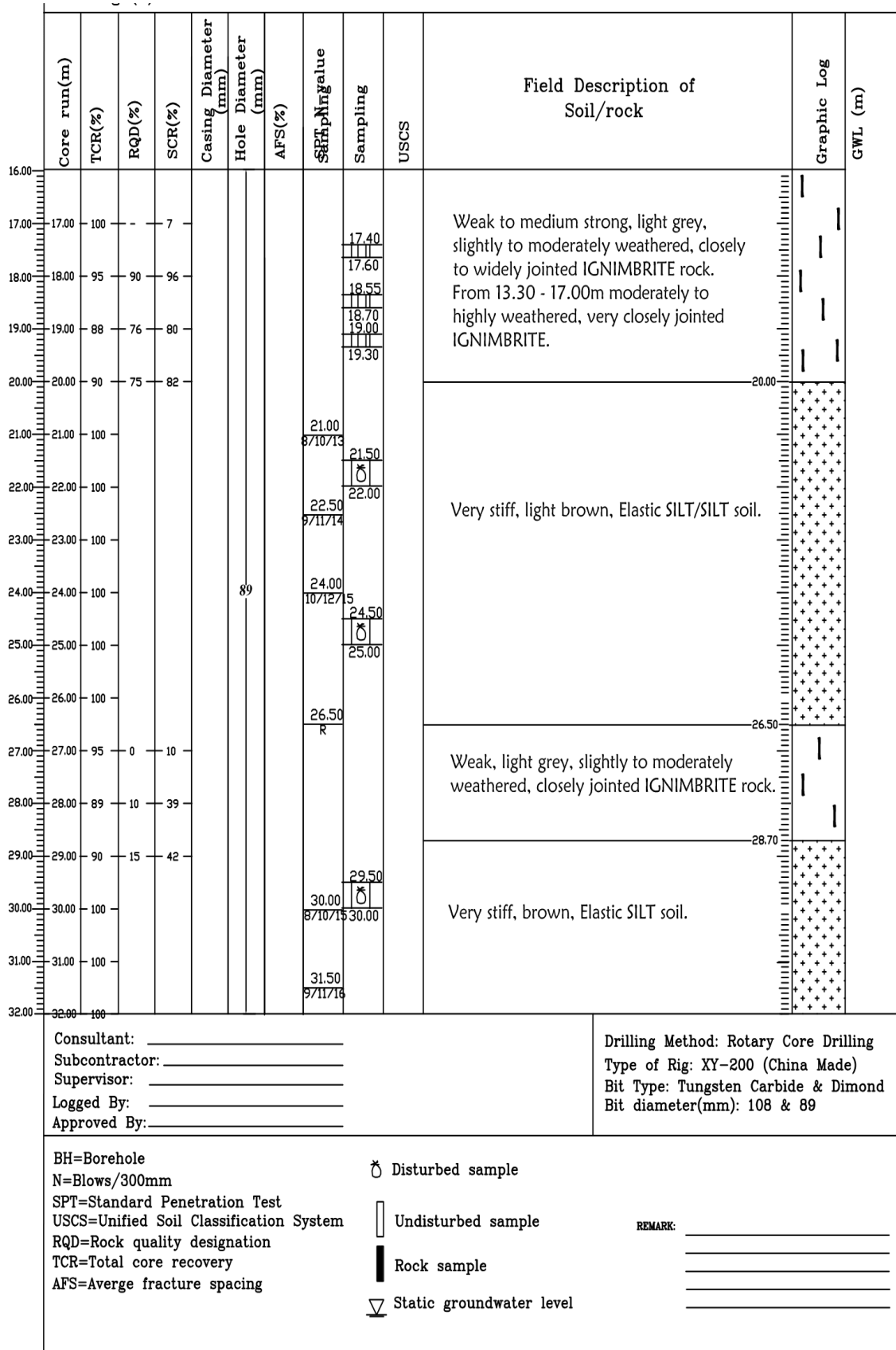


Figure C- 7: Lideta-1 borehole logs

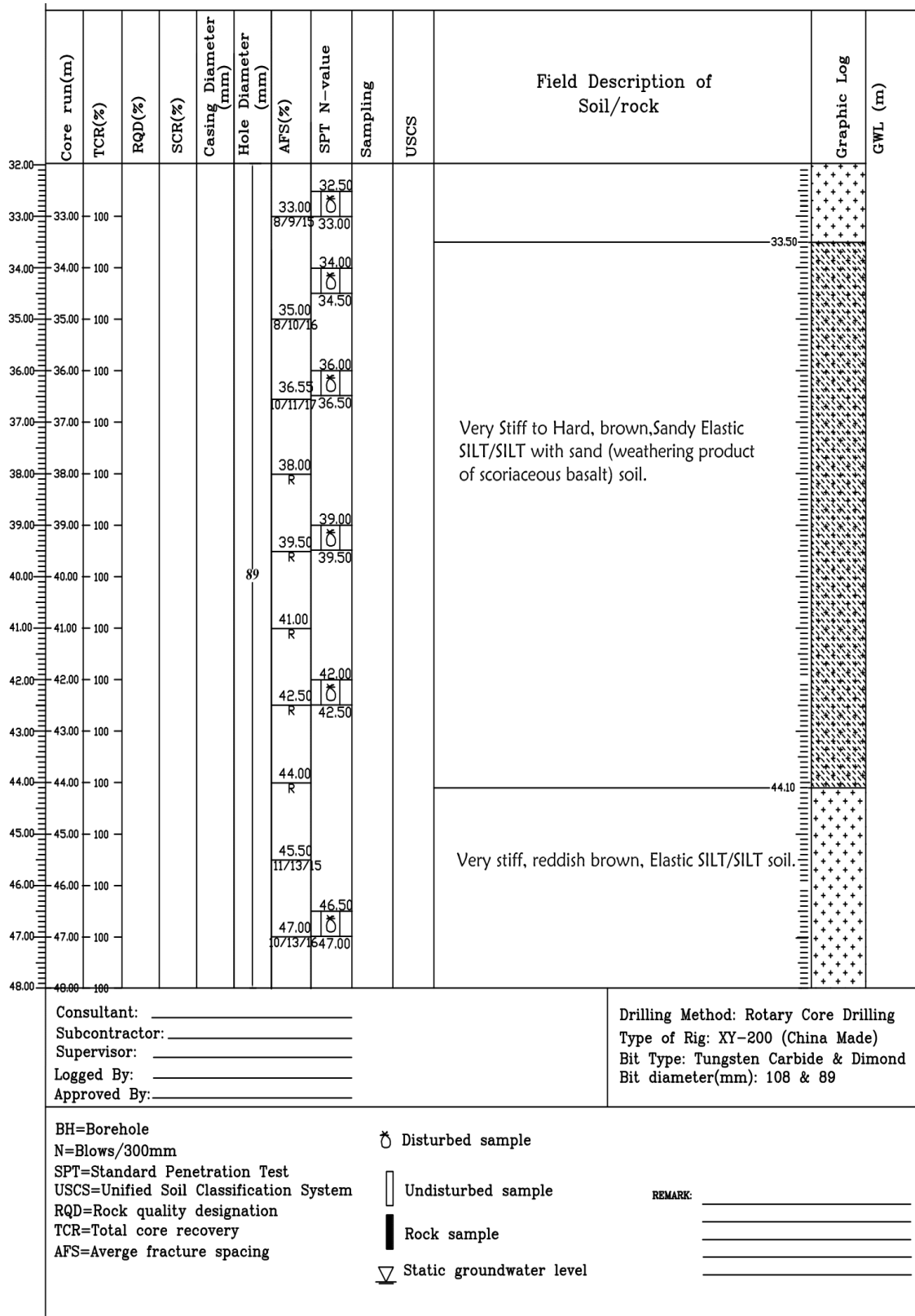
h. Lideta-2



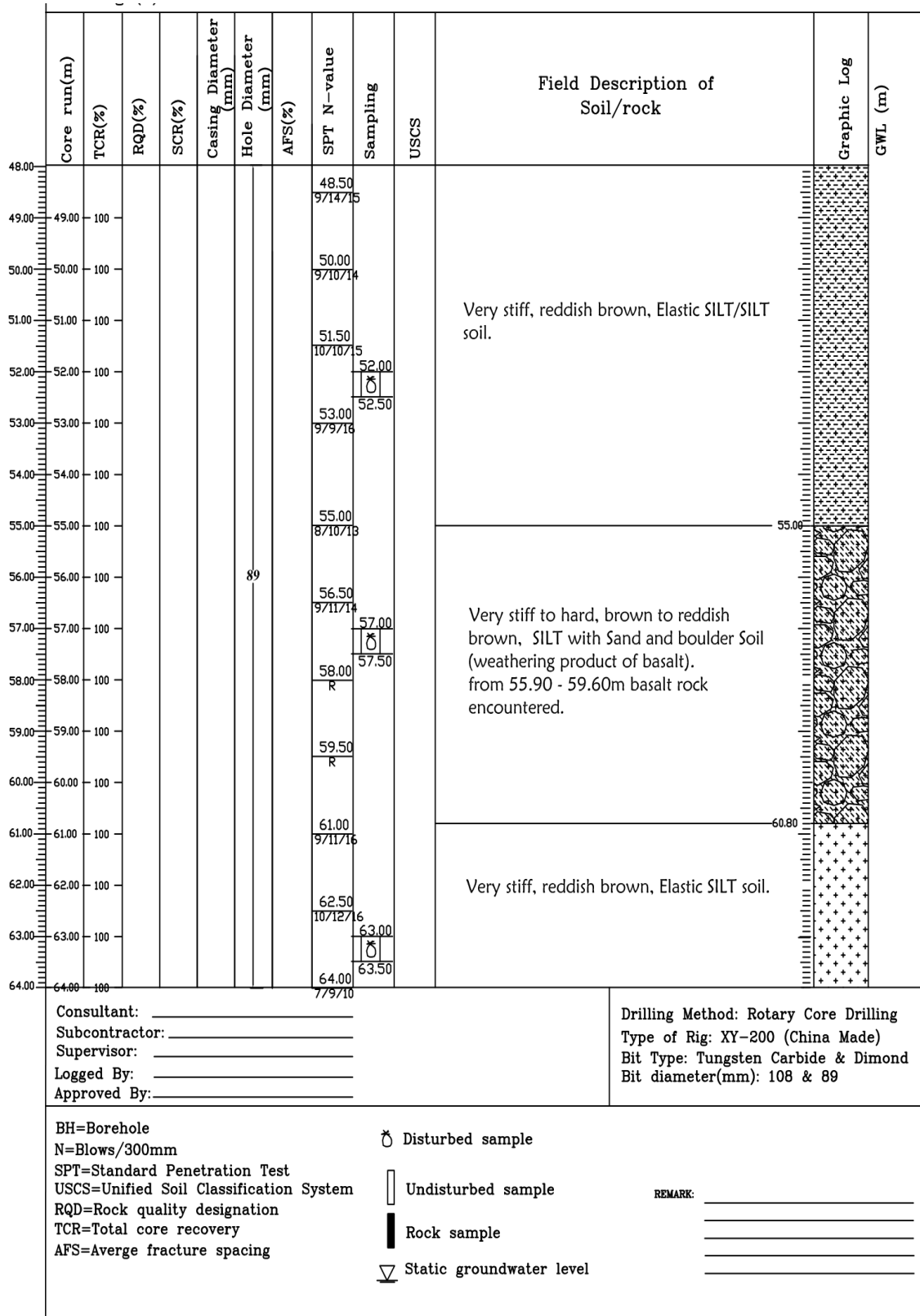
Site specific Ground Response Analysis at South - Western part of Addis Ababa



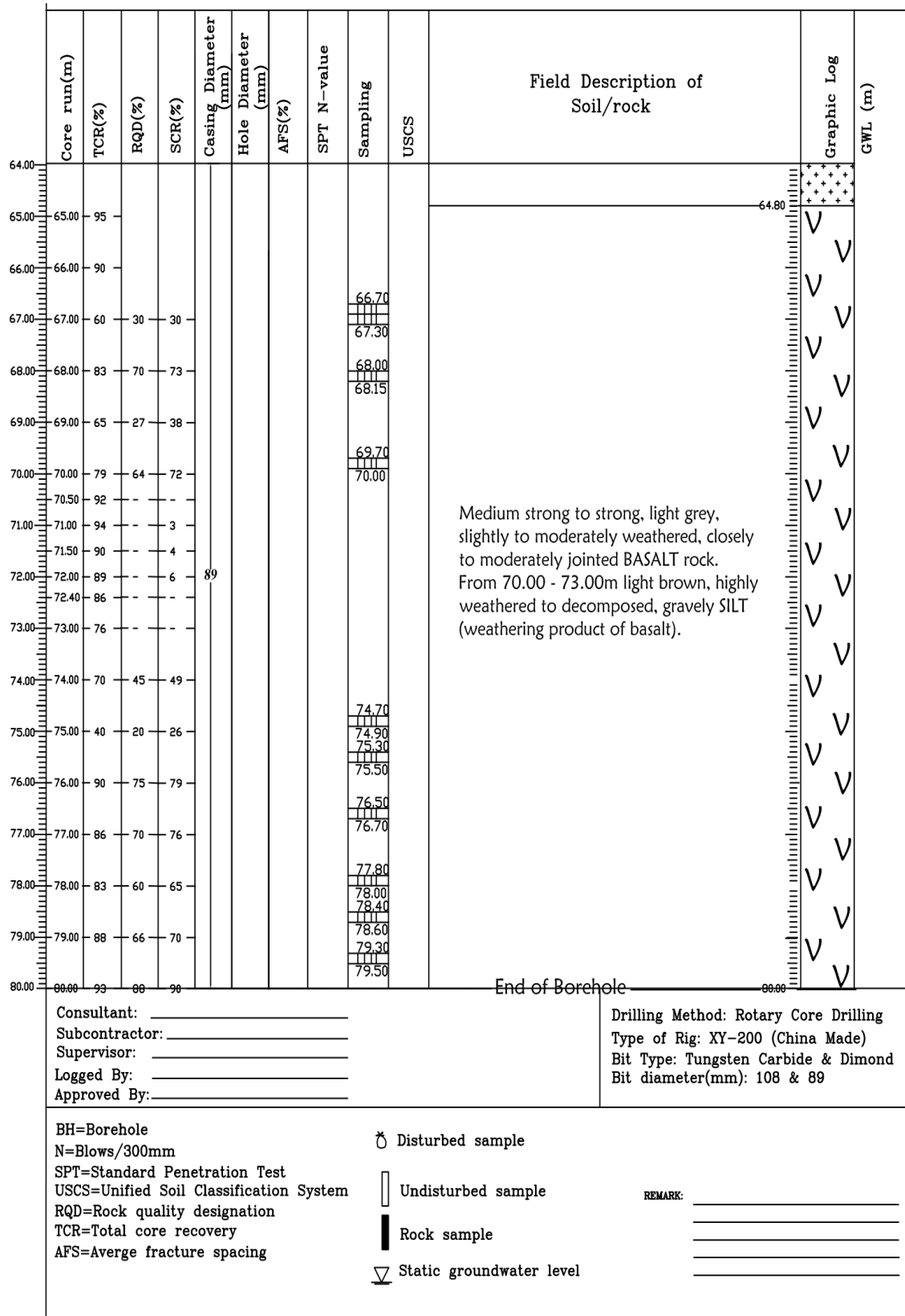
Site specific Ground Response Analysis at South - Western part of Addis Ababa



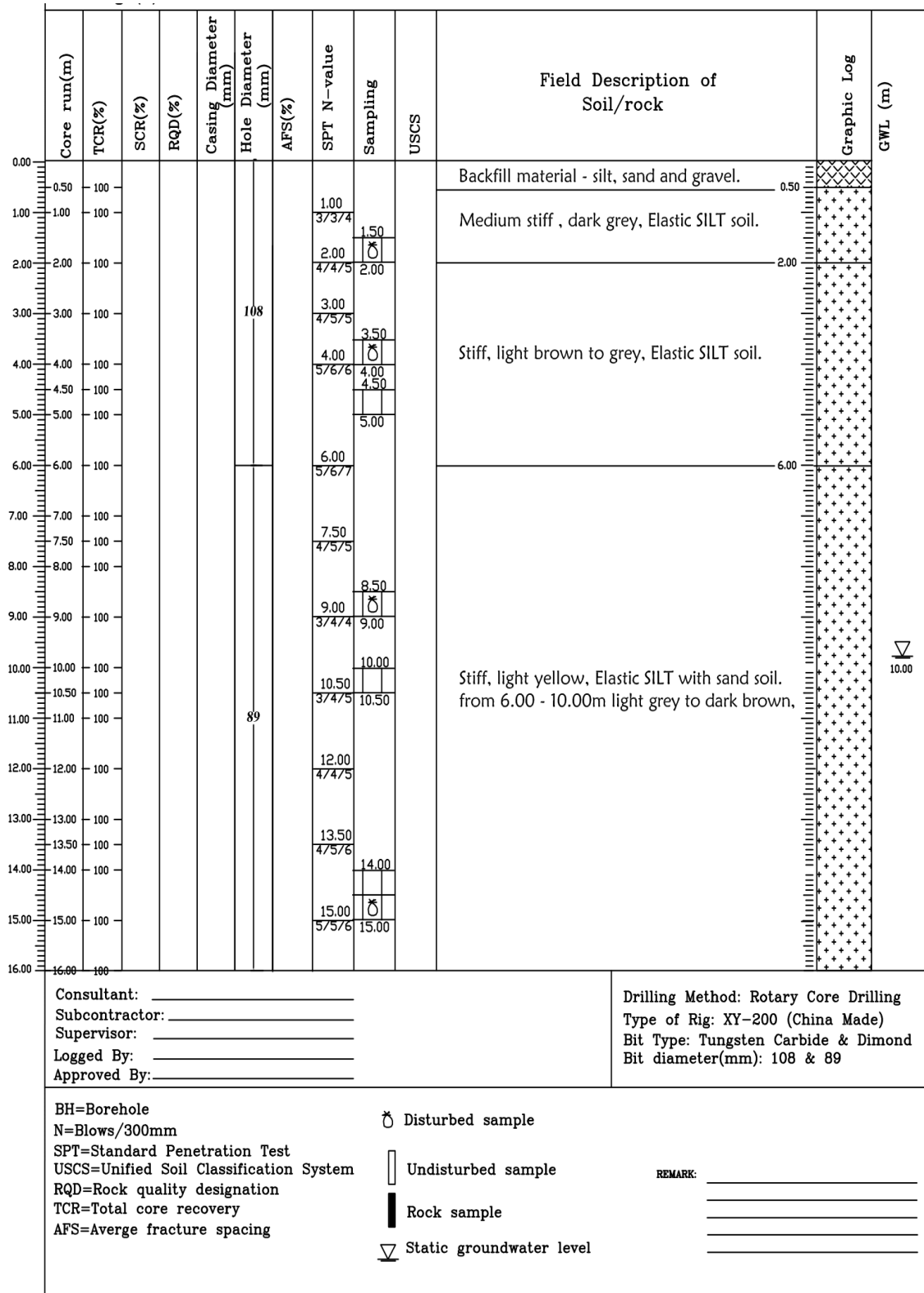
Site specific Ground Response Analysis at South - Western part of Addis Ababa



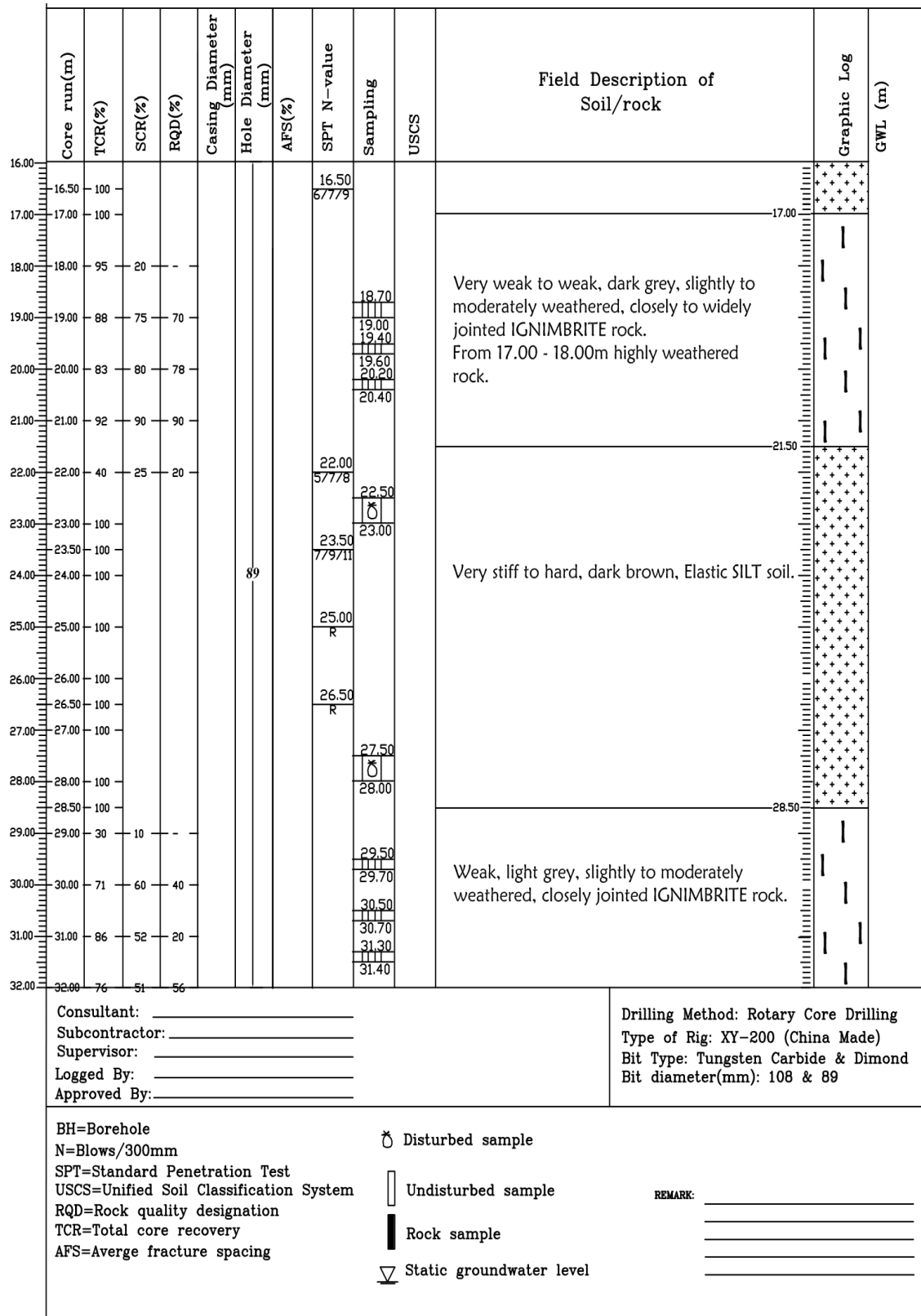
Site specific Ground Response Analysis at South - Western part of Addis Ababa



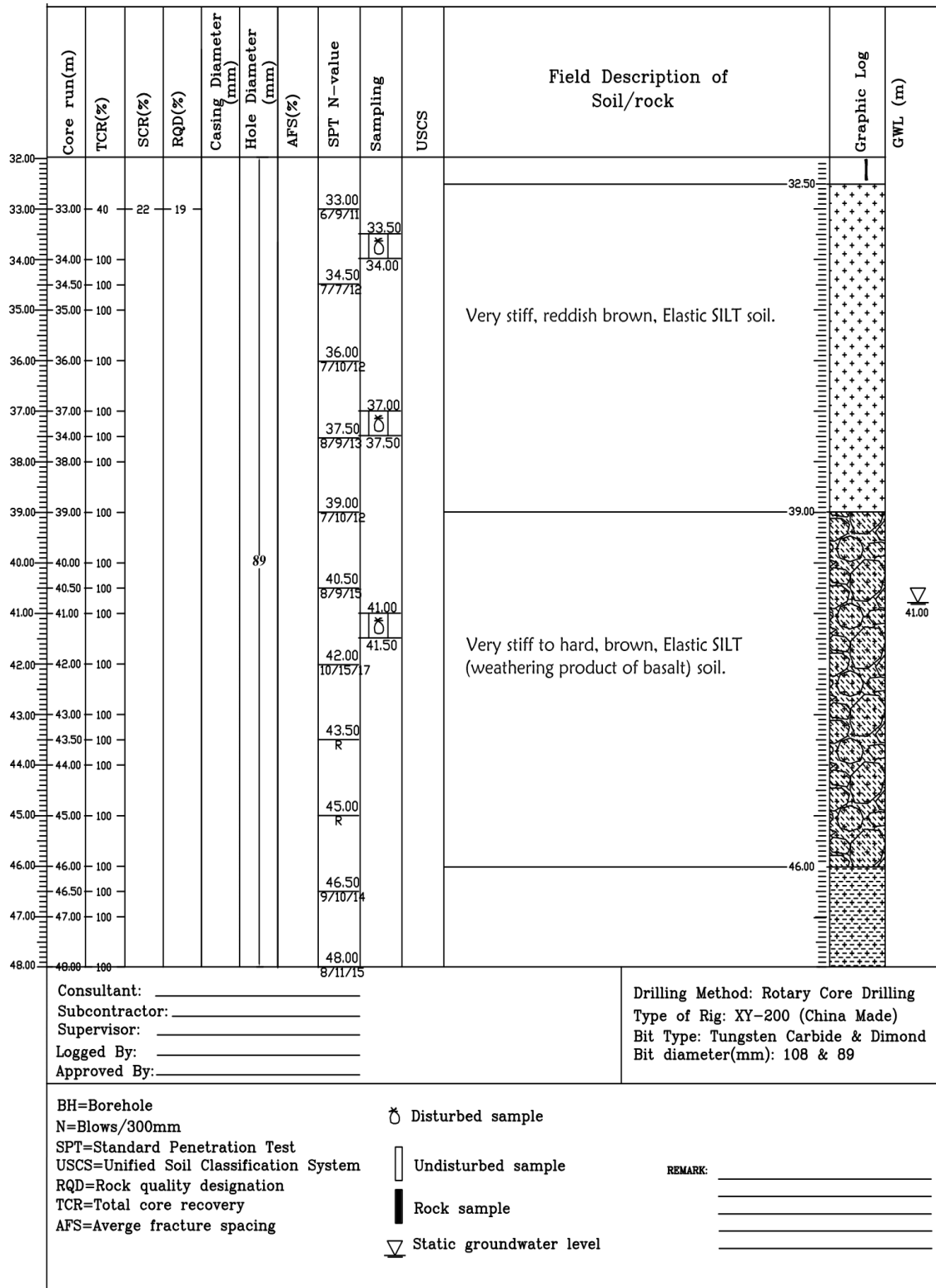
Site specific Ground Response Analysis at South - Western part of Addis Ababa



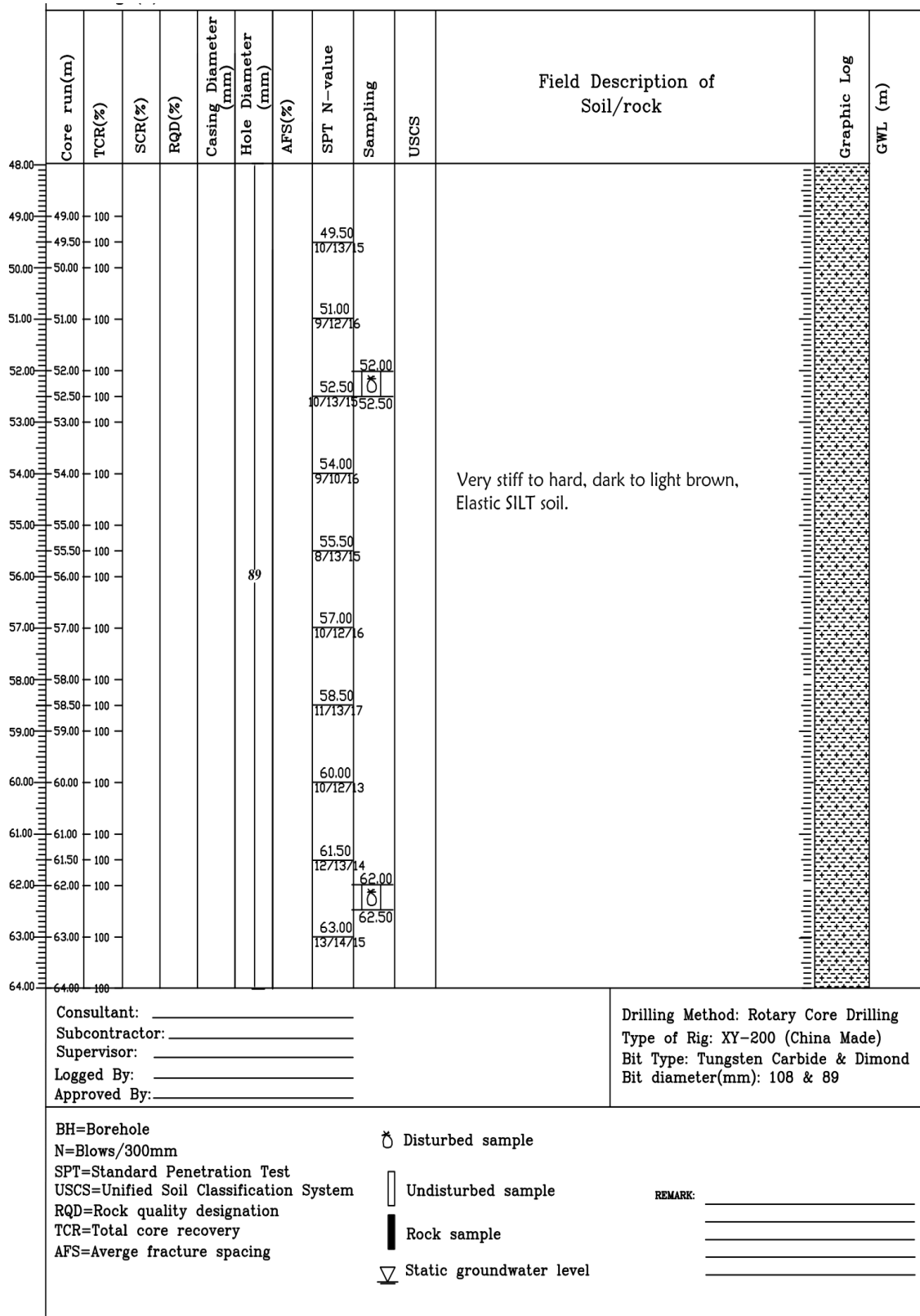
Site specific Ground Response Analysis at South - Western part of Addis Ababa



Site specific Ground Response Analysis at South - Western part of Addis Ababa



Site specific Ground Response Analysis at South - Western part of Addis Ababa



Site specific Ground Response Analysis at South - Western part of Addis Ababa

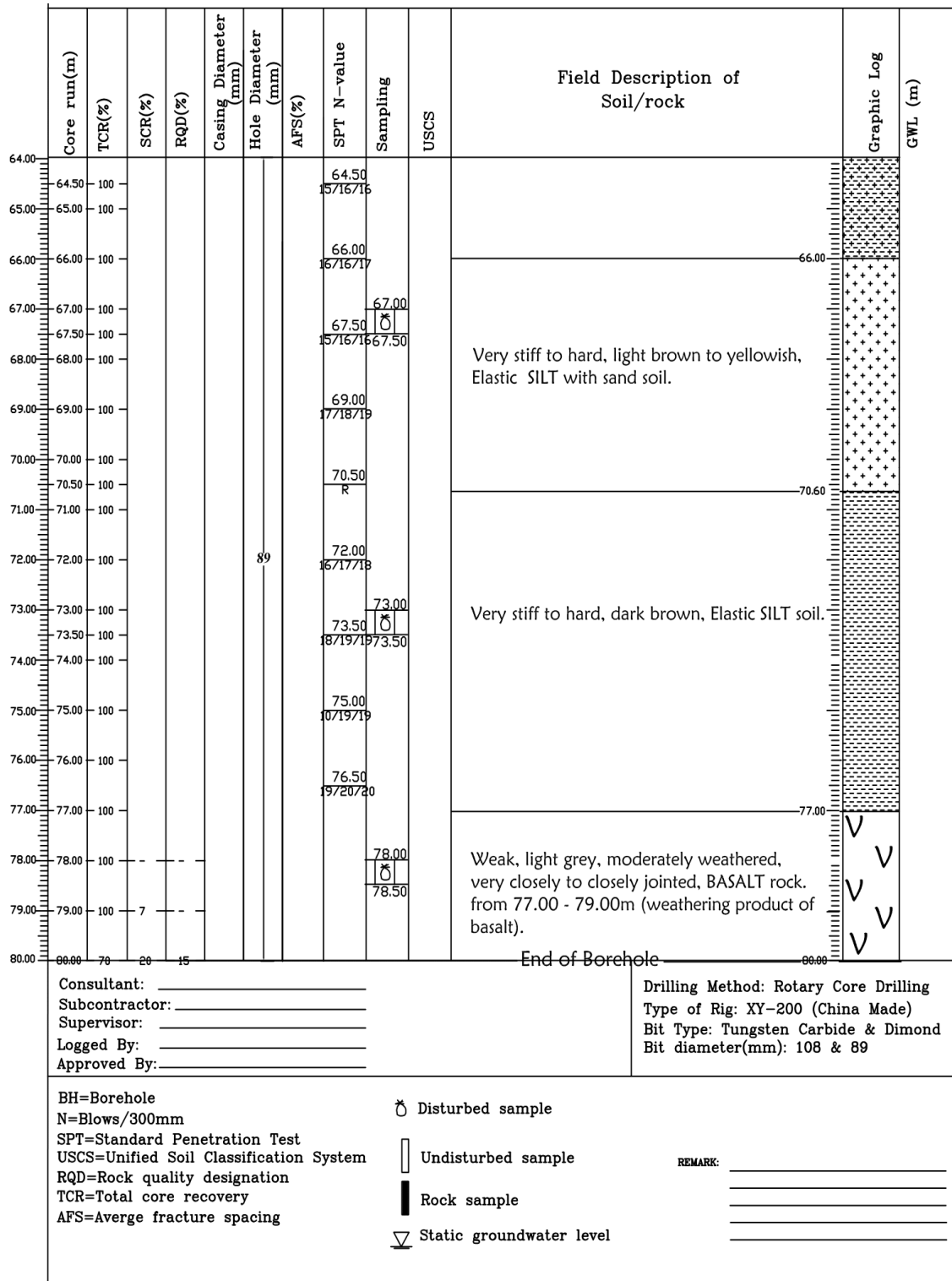


Figure C- 8: Lideta-2 borehole logs

Appendix D

Correction to field SPT-N values

Table D-1: Corrections to Field SPT-N Values (Martin, et al., 1999)

Factor	Equipment Variable	Term	Correction
Overburden Pressure		C_N	$(P_a/\sigma'_{vo})^{0.5}$ $0.4 \leq C_N \leq 2^*$
Energy Ratio	Safety Hammer Donut Hammer Automatic Trip Hammer	C_E	0.60 to 1.17 0.45 to 1.00 0.9 to 1.6
Borehole Diameter	65 mm to 115 mm 150 mm 200 mm	C_B	1.0 1.05 1.15
Rod Length**	3 m to 4 m 4 m to 6 m 6 m to 10 m 10 m to 30 m >30 m	C_R	0.75 0.85 0.95 1.0 < 1.0
Sampling Method	Standard Sampler Sampler without liners	C_S	1.0 1.2

Appendix E

Site Categories

a. ES EN 1998:2015 site categories

Table E-1: ES EN 1998:2015 site categories

Ground type	Description of stratigraphic profile	$V_{s, 30}$ (m/s)	SPT-N (blows/30cm)	Cu (kPa)
A	Rock or other rock-like geological formation, including at most 5 m of weaker material at the surface.	> 800	—	—
B	Deposits of very dense sand, gravel, or very stiff clay, at least several tens of meters in thickness, characterized by a gradual increase of mechanical properties with depth.	360 – 800	> 50	> 250
C	Deep deposits of dense or medium-dense sand, gravel or stiff clay with thickness from several tens to many hundreds of meters.	180 – 360	15 - 50	70 - 250
D	Deposits of loose-to-medium cohesiveness soil (with or without some soft cohesive layers), or predominantly soft-to-firm cohesive soil.	< 180	< 15	< 70
E	A soil profile consisting of a surface alluvium layer with V_s values of type C or D and thickness varying between about 5 m and 20 m, underlain by stiffer material with $V_s > 800$ m/s.	—	—	—
S1	Deposits consisting, or containing a layer at least 10 m thick, of soft clays/silts with a high plasticity index ($PI > 40$) and high water content.	< 100 (indicative)	—	10- 20
S2	Deposits of liquefiable soils, of sensitive clays, or any other soil profile not included in types A - E or S1.	—	—	—

b. NEHRP provisions

Table E-2: Summary of site categories in NEHRP provisions

Site Class or Soil Profile Type	Description	Shear Wave Velocity Vs Top 30m (m/sec)	Standard Pen. Resistance N or N ₆₀ (blows/ft)	Undrained Shear Strength Su (kPa)
S-A / A	Hard Rock	> 1500	---	---
S-A / B	Rock	760 - 1500	---	---
S-A / C and S-B / D	Very dense soil /soft rock	360 - 760	> 50	> 100
S-B / D	Stiff soil	180 - 360	15 - 50	50 - 100
S-E	Soft soil	< 180	< 15	< 50
S-C / F	Special soils requiring site-specific evaluation	---	---	---